International Journal of Cell Biology

Cell Death

Guest Editors: Claudia Giampietri, Alessio Paone, and Alessio D'Alessio

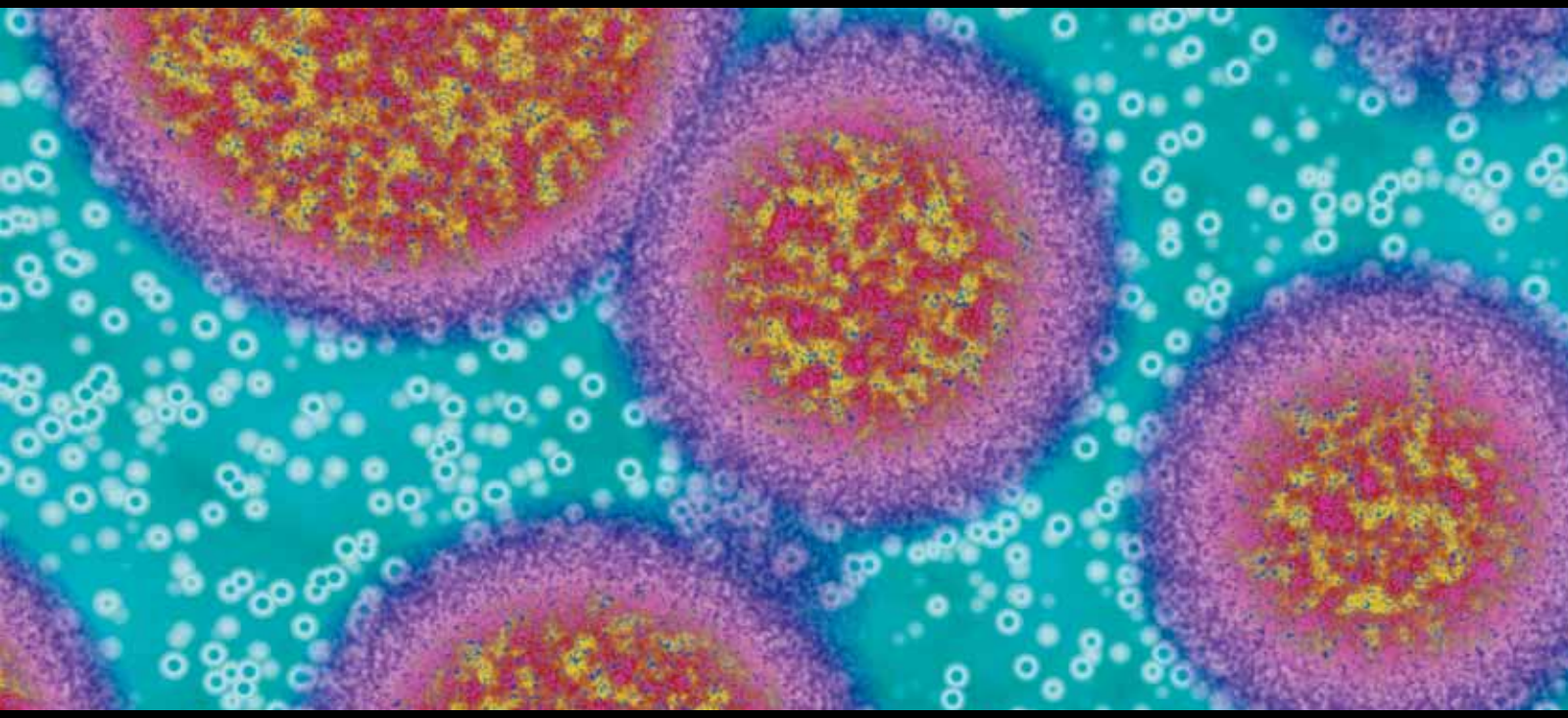

Cell Death

International Journal of Cell Biology

Cell Death

Guest Editors: Claudia Giampietri, Alessio Paone, and Alessio DAlessio

Editorial Board

Contents

Hindawi Publishing Corporation
International Journal of Cell Biology
Volume 2014, Article ID 864062, 2 pages
http://dx.doi.org/10.1155/2014/864062

Editorial
Cell Death

Claudia Giampietri,[1] Alessio Paone,[2] and Alessio D'Alessio[3]

[1] *DAHFMO-Section of Histology and Medical Embryology, Sapienza University of Rome, Via Scarpa 14, 00161 Rome, Italy*
[2] *Department of Biochemical Sciences, Sapienza University of Rome, Piazzale Aldo Moro 5, 00185 Rome, Italy*
[3] *Institute of Histology and Embryology, School of Medicine, Catholic University of the Sacred Heart, Largo Francesco Vito 1, 00168 Rome, Italy*

Correspondence should be addressed to Claudia Giampietri; claudia.giampietri@uniroma1.it

Received 26 March 2014; Accepted 26 March 2014; Published 11 May 2014

Cell death is a crucial process involved in a variety of biological mechanisms controlling development, homeostasis, and immune regulation of multicellular organisms and its imbalance is associated with numerous pathologies. According to the literature, it is undeniable that the field of cell death research has been continuously growing and novel cell death modalities have been also described. Cell death can be classified according to morphological criteria identifying modalities such as apoptosis, necrosis, autophagy, or death associated with mitotic catastrophe. Additionally, cell death can be identified on the basis of biochemical mechanisms which include, for instance, the activation of different class of proteases (proteases, nucleases, and caspases) and according to the presence of specific cell surface molecules or the release of soluble mediators (immunogenic or nonimmunogenic cell death). The field of cell death is so complex that The Nomenclature Committee on Cell Death (NCCD) has recently proposed unified criteria which define the different types of cell death, while providing recommendations facilitating the communication among scientists involved in this field.

The main purpose of this special issue is to cover the field of cell death with themes focusing on pathways and mechanisms that specify active forms of cell death in health and disease. The topics therefore span apoptotic signaling networks (e.g., Bcl-2 family proteins, caspase control, novel molecular players of apoptotic control in immune regulation, and epigenetic regulation of apoptosis) and noncanonical cell death pathways, including necroptosis, pyroptosis, and autophagy, with a particular attention on the relationship between these mechanisms.

More specifically, M. E. Morrison et al. describe a novel role for the proapoptotic protein Bim in modulating cellular functions such as migration and extracellular matrix protein expression in retinal endothelial cells and pericytes. This study therefore provides additional regulatory mechanisms linking apoptosis control to vascular function.

M. Garg et al. focus on the regulation of apoptosis during the immune response. Their work highlights the role of the linker histone H1.2 trafficking in inducing T-effector lymphocytes apoptotic response after cytokine withdrawal. They demonstrate the well-controlled association between H1.2 and the proapoptotic mitochondrial resident Bak following metabolic stress.

M. N. Rossi and F. Antonangeli review our current knowledge of the role of long noncoding RNAs in apoptosis control. The authors highlight the altered expression pattern of specific lncRNAs in cancer cells when compared with normal cells and tissues. They also underline that overexpression or downregulation of different long noncoding RNAs in specific types of tumors may sensitize cancer cells to apoptotic stimuli. The authors discuss the new perspectives of using long noncoding RNAs as tumor biomarkers and as possible therapeutic targets.

M. D. King et al. show the novel role for the necroptosis inhibitor necrostatin-1 in limiting neurovascular injury in hemorrhagic injury models. This study emphasizes the potential clinical utility for necroptosis inhibitors as an adjunct therapy to reduce neurological injury after intracerebral hemorrhage.

C. Fabrizi et al., in the existing debate between pro- and antitumoral role of autophagy, draw attention on its significance in protecting cancer cells from death. The authors in fact demonstrate that pharmacological stimulation of

autophagy may protect pheochromocytoma cells in stressful conditions such as high-density cultures and toxins exposure.

S. W. Ryter et al. give an exhaustive overview of the autophagic process. Furthermore, the authors discuss the impact of autophagy on the different cell death modalities (apoptosis, necroptosis, and pyroptosis). They underline the importance of strategies modulating autophagy for therapeutic interventions in diseases where cell death is deregulated.

A. Micera et al. investigate NGF and Reelin crosstalk in a genetic model of Reelin deprivation, namely, E-Reeler. Their results demonstrate that the loss of normal Reelin expression leads to early retinal impairment and loss of Rod Bipolar Cells in E-Reeler animals, damaging signaling from rod to ganglion cells. Altogether, their data propose Reelin as an important regulator in the retina which can be of great interest for studying mechanisms regulating retinal disorders.

C. Giampietri et al. give an overview of the molecular signalling of necroptosis. The authors focus on FLIP and IAP proteins that regulate the complex balance between apoptosis and necroptosis in particular in the immune system and in other physiological and pathological conditions. Finally, they discuss the deregulation of the necroptotic mechanisms in specific pathological conditions.

J.-R. Hong et al. reviewed the role of reactive oxygen species (ROS) in apoptosis and ROS induction by viral infection. They report how virus-mediated oxidative stress can participate to the etiopathology of several diseases by affecting immune cells and other tissues.

R. McFarland et al. employ the Lurcher animal model, which carries a mutated form of the glutamate receptor (GluRδ2L) in order to show that the over activation of the Na/K pump in response to the chronic Na^+ leak is responsible for ATP consuming, leading to Purkinje cell death.

In summary, though cell death represents a major biological phenomenon, our understanding of its regulation in health and disease is far from being complete. The study of the multiple pathways driving to cell death has become increasingly complex and multidisciplinary, requiring expertise from all fields of the modern biology. Investigating the role of cell death and its regulation in the development of disease demands a constant update of our knowledge and the broadest interplay among both basic and clinical investigators. Therefore, better understanding of molecular signaling taking place during different types of cell death would not only foster the comprehension of disease pathogenesis but might be of crucial interest to develop new therapeutic strategies for treatment of cell death-related conditions. We believe that this special issue, due to the novel data presented and accurate reviews reported, will be appropriate for the broad readership interested in the new progress in the cell death field.

Claudia Giampietri
Alessio Paone
Alessio D'Alessio

Hindawi Publishing Corporation
International Journal of Cell Biology
Volume 2014, Article ID 467452, 16 pages
http://dx.doi.org/10.1155/2014/467452

Review Article

RNA Viruses: ROS-Mediated Cell Death

Mohammad Latif Reshi,[1,2] Yi-Che Su,[1] and Jiann-Ruey Hong[1]

[1] *Laboratory of Molecular Virology and Biotechnology, Institute of Biotechnology, National Cheng Kung University, Tainan 701, Taiwan*
[2] *Department of Life Sciences, College of Bioscience and Biotechnology, National Cheng Kung University, Tainan 701, Taiwan*

Correspondence should be addressed to Jiann-Ruey Hong; jrhong@mail.ncku.edu.tw

Received 10 November 2013; Revised 18 March 2014; Accepted 20 March 2014; Published 8 May 2014

Academic Editor: Alessio D'Alessio

Reactive oxygen species (ROS) are well known for being both beneficial and deleterious. The main thrust of this review is to investigate the role of ROS in ribonucleic acid (RNA) virus pathogenesis. Much evidences has accumulated over the past decade, suggesting that patients infected with RNA viruses are under chronic oxidative stress. Changes to the body's antioxidant defense system, in relation to SOD, ascorbic acid, selenium, carotenoids, and glutathione, have been reported in various tissues of RNA-virus infected patients. This review focuses on RNA viruses and retroviruses, giving particular attention to the human influenza virus, Hepatitis c virus (HCV), human immunodeficiency virus (HIV), and the aquatic Betanodavirus. Oxidative stress via RNA virus infections can contribute to several aspects of viral disease pathogenesis including apoptosis, loss of immune function, viral replication, inflammatory response, and loss of body weight. We focus on how ROS production is correlated with host cell death. Moreover, ROS may play an important role as a signal molecule in the regulation of viral replication and organelle function, potentially providing new insights in the prevention and treatment of RNA viruses and retrovirus infections.

1. Introduction

Cellular metabolisms produce different varieties of reactive oxygen species (ROS) as byproducts. These ROS play an important role in cell signaling and regulate hormone action, growth factors, cytokines, transcription, apoptosis, ion transport, immunomodulation, and neuromodulation [1, 2]. They lend fundamental aid to the normal functioning of the body's immune system and proliferate T-cells that provide immunological defense (adaptive immunity) [3, 4]. However, when the same ROS are produced by activated neutrophiles, macrophages destroy microbes/viruses and neighboring cells via oxidative bursts [5]. Any imbalance in the production of ROS and the body's inability to detoxify these ROS is referred to as oxidative stress [6]. SOD and catalases are the major defense against the ROS produced in cells [7, 8]. The research has shown that children suffering from hepatitis B or C exhibit increased levels of lipid peroxidation, which indicates weak antioxidant defense due to low catalase and SOD activity [9]. Earlier and recent studies have suggested that ROS induces apoptosis [10–12], and that the agents that cause apoptosis are either oxidants or generate the ROS. This hypothesis was later shown to be correct when researchers demonstrated the role of proto-oncogene BCL-2 in preventing apoptosis in an antioxidant way [13].

Peterhan and his coworkers were the first to demonstrate that a virus could generate ROS from phagocytes [14]. Later research showed that many retroviruses, DNA viruses and RNA viruses can cause cell death by generating oxidative stress in infected cells [15–17]. In 1994, the scientific community held its first conference to discuss the possible interaction between viral infection and ROS in detail [18]. RNA viruses generally use RNA as their genetic material, and those that use DNA intermediates in their replication cycle are known as retroviruses. These viruses posses the highest mutation rates among every living creature [19–22]. Therefore, it is not always easy to develop successful and effective vaccines and drugs against these viruses. Oxidative stress always plays a dominant pathogenic role in HIV and hepatitis infections. AIDS is the end phase of HIV infection. This pandemic is

caused by the HIV-1 and HIV-2 groups of cytopathic viruses, wherein the levels of GSH, cystine, vitamin C and SOD are decreased and the MD and HNE levels are elevated in patients infected with HIV-1 [23–25]. A decrease in antioxidants indicates the weakening of the immune system, as immune cells require more antioxidants to maintain their function and integrity. The CD4+ T-helper cells that form important components of the immune system are the main targets of the HIV virus. The virus production decreases to begin with, as about 5% of the T-cells are destroyed and replaced each day via the apoptotic process. This in turn leads to decreases in zinc and vitamin E (antioxidants). The decrease in zinc results in the inhibition of intracellular virus replication [26], and the selenium decrease indicates the progression of HIV toward AIDS. After suffering the primary illness, patients do not show any symptoms for up to more than 10 years, during which the virus load falls but the virus does not stop replicating. This in turn leads to a higher decrease in the CD4+ T-cell count, which ultimately leads to AIDS and the terminal stage of the infection. HIV-2 infection is slow compared with HIV-1 infection. In hepatitis patients, HIV preferentially infects CD4+ T-lymphocytes and macrophages. The hepatitis C virus belongs to the flaviviridae family of RNA with a positive strand RNA genome [27] at a size of 9,400 bp [28]. About 150 million people are infected, and have a higher chance of developing liver cancer/cirrhosis [29]. The World Health Organization reported that 80% of patients with acute hepatitis C progress toward chronic hepatitis, with 2% developing liver cirrhosis and 1–5% developing hepatitis C carcinoma [30, 31]. Researchers first exhibited the occurrence of oxidative stress during chronic hepatitis C in 1990 [32]. This OS is associated with hepatic damage, a decrease in GHS, an increase in serum malondialdrhyde (MDA), 4-hydroxynonenal (HNE) and caspase activity, and decreases in plasma and hepatic zinc concentrations [33–35]. Zinc therapy increases the functioning of surviving liver tissue [35]. However, zinc and selenium deficiencies affect DNA repair and the immune system, increasing the chances of chronicity and malignancy [36]. HCV replication takes place in hepatocytes, which potentially attack and propagate in immune system cells. The infection of different influenza viruses presents different clinical scenarios [37]. The influenza A virus is highly active, causing infection of the upper and lower respiratory tract. It can be divided into 16 different HA and NA combinations, with three HA (HA1, HA2 and HA3) and NA1 and NA2 being prevalent in humans [38]. Studies conducted in 19 different countries have shown that HINA and H3N2 are the most dominant influenza A viruses [39]. Influenza viruses and parmoviruses have been shown to activate monocytes and polymorphonuclar monocytes to generate ROS *in vitro* [15]. Activated phagocytes release not only ROS but also cytokine and TNF. The pro-antioxidant effect of TNF may be relevant to influenza virus infection because children with Rey's syndrome [40] exhibit increased levels of pro-oxidants and lipid peroxides. OS ultimately leads to a decrease in antioxidant levels and indicates a decrease in the functioning of the immune system. Immune system cells generally require a higher concentration of antioxidants than other cells to maintain the system's rodex balance and preserve its integrity and function.

2. Apoptosis

Apoptosis, the process of programmed cell death, involves a sequence of events that lead to various morphological changes in a cell including cell shrinkage, changes to the cell membrane such as the loss of membrane asymmetry and attachment, nuclear fragmentation, chromatin condensation, and genomic DNA fragmentation. Apoptosis has a key role in the pathogenesis of many diseases including cancer, inflammation and neurodegenerative diseases. Different modes of cell death are defined by morphological criteria. The term "apoptosis," which was coined by kerr et al. [41], makes no clear reference to a precise biochemical mechanism, and is rather used to explain a special mode of cell death that is characterized by the rounding-up of cells, reduction in cell volume (pyknosis), condensation of chromatin, fragmentation of the nucleus (karyorrhexis) and maintenance of the intact plasma membrane until the very late stages of the process [42]. The process of programmed cell death is controlled by different ranges of cell signaling pathways originating from either the external surroundings of a cell (extrinsic inducers) or from within the cell itself (intrinsic inducers). Extrinsic inducers include heat, radiations, toxins [43], nitric oxide [44] and hormones. They must either pass into the cell or interact with the specific receptors present on the cell membrane to initiate the specific signal transduction pathway inside. This action leads the cell to undergo apoptosis. Thus, any external or internal disturbance in the signal transduction pathways within a cell, such as heat, radiation, viral infection, lack of nutrients or an increase in calcium concentration [45], leads the cell to undergo continuous proliferation or necrosis. Different kinds of cellular components such as polyADP ribose polymerase may also help regulate apoptosis [46]. Thus, any disturbance in the regulation of the apoptotic process either inside or outside a cell can lead to excessive apoptosis causing hypotrophy, such as in the form of ischemic damage, or result in an unchecked cell proliferation such as cancer. However, more than 139,000 research articles have been published in relation to the molecules involved in the activation of intrinsic and extrinsic apoptotic pathways such as BCL-2, TNF, NF-κB and P53 [43]. Genetic studies related to the nematode *Caenorhabditis elegans* have shown that the molecules Ced-3 and Ced-4 ("Ced" for cell death abnormal) are important for the apoptosis of 131 cells during worm development [47]. These two molecules have been found to be the same as caspases. Caspases are the 30–60 KDa proenzymes inside cells. They are made continuously and activated by proteolytic processing either auto catalytically or in a cascade by enzymes with similar characteristics [48, 49]. This indicates that the apoptosis process is highly conserved. However, in the case of cell injury where an injured cell swells and bursts, the cell leaks its contents and attracts different immune cells such as lymphocytes by engaging in an unwanted inflammatory response [50].

3. Necrotic Cell Death

The term "necrosis" is currently used to describe accidental cell death, which mostly occurs due to cell injury resulting in the early death of cells in the affected area [51]. Therefore, necrosis is always detrimental and can even prove fatal. In the case of cell injury where the injured cell swells and bursts, the cells leaks its contents out and attracts different immune cells such as lymphocytes by engaging in an unwanted inflammatory response [50]. Nearby phagocytes are prevented from engulfing the dead cells [52], which in turn results in the formation of dead tissue. There is often no explanation for how a necrotic cell death occurs [53]. Therefore, necrosis lacks some of the features of apoptosis and autophagy. In addition, the clearance of necrotic cells operates differently from that of apoptotic cells [54].

4. Apoptosis in Virus Infected Cells

The perforin/granzyme pathway is often examined and highly involved in virus infection studies, which have found that CTLs and NK cells can eradicate virus-infected target cells via the apoptosis process [55]. Another important apoptosis-related host defense mechanism involves CTL, and recognizes and kills target cells by sending signals through cell surface death receptors [56]. Death receptors are a special type of receptor belonging to the tumor necrosis family (TNF). They contain specific homologous amino acid sequences in their cytoplasmic tails, referred to as the death domain (DD). The most well-studied death receptors include CD95/FAS and TNFRI, although additional death receptors such as DR3, 4 and 5 have been examined [56, 57]. In addition to killing virus-infected cells, death receptors aid in killing mature T-cells at the end of immune responses.

In the case of FAS-mediated apoptosis, the interaction between the receptor and legend needs the help of adaptor proteins to signal the target cell to undergo the apoptosis process (Figure 1). The interaction between the two cells results in a clustering of intracellular DDs on the target cell. However, to be effective, this in turn activates the FADD adaptor protein within the target cell. In addition to interacting with the receptor [58], the FADD also contains a caspase-recruiting domain (CARD) that is responsible for activating the caspases (caspase-8). Upon oligomerization, the caspase-8 activates itself and the cascade of caspases (caspase-3) to begin the apoptosis process [58].

TNFR1- and DR3-type death receptors require FADD in addition to the TNFR-associated DD (TRADD) adaptor protein. TNFR1- and DR3-mediated cell deaths rarely occur unless and until protein synthesis is inhibited [59]. When the TNF-α pathway is activated, it can also suppress the apoptosis process inside the cell using different signaling pathways, which in turn stimulates the expression of antiapoptotic genes such as IAP, BCL-2, and BCL-XL and TNFR-associated factors that do not allow the activation of caspase family proteins [59–61]. The NF-κB signaling pathway has proved to be important in cell death studies. Although a P53-mediated cell death requires the activation of the NF-κB signaling pathway, the activation of NF-κB by P53 is quite different because it requires MEKi (MEK inhibitor) and pp90rsk [62]. Recent research carried out on the Epstein Bar virus has shown that NF-κB plays an important role in virus-mediated cell death compared with other signaling pathways. The activity of NF-κB can be regulated by a number of viruses such as EBV through latent membrane protein-1 (LMP-1), which in turn enhance cell survival upon virus infection [63–65].

5. ROS Friend and Foe of Cells

There are many different types of free radicals, but those of the greatest concern in biological systems are derived from oxygen. Excessive ROS production in a cell can lead to the oxidation of macromolecules and has been found to be responsible for causing mtDNA mutations, aging, and cell death. Any imbalance in the production of ROS is often referred to as oxidative stress [66, 67]. The effect of ROS on the cellular functions inside a cell depends on the amount of ROS and how much time the cell has been exposed to ROS (Figure 2). It has been confirmed multiple times that ROS act as both friend and foe to a cell. Oxidative stress has been found to play a role in various pathological conditions such as cancer, diabetes, and neurological disorders [68–71]. ROS include both the free radicals and nonradicals produced during various metabolic processes, mostly in the electron transport chains in mitochondria, peroxisomes, and ER stress and in nuclear and plasma membranes in aerobic cell metabolism. ROS are typically also produced during normal metabolic processes inside the cells. They are neutralized by the antioxidant defense system, including enzymes such as SOD, free-radical scavengers, and metal chelates. However, nutrition makes the most significant contribution to the body's antioxidant defense system. It is widely believed that diet-derived antioxidants play a role in the prevention of human diseases. These antioxidants work in a coordinated manner, where a deficiency in one may affect the efficiency of another. Semba and Tang reported that the low plasma or serum levels of vitamins A, E, B6, B12, and C; carotenoids; selenium; and zinc are common in many HIV-infected populations and may contribute to the pathogenesis of the HIV infection via increased oxidative stress and compromised immunity [72, 73]. Another research team showed that a deficiency of vitamin E or selenium allows the conversion of the normal benigh coxsackievirus virus B3 to virulence via a change in the nucleotide sequence in the genome of the benign virus and causes heart damage [74]. However, Evans and Halliwell showed that iron deficiency may serve as protection for malaria or Yersinia infections and that iron overload may make patients susceptible to infection by supplying enough iron for multiplying bacteria [75]. Therefore, the oxidative stress generated by micronutrient deficiencies becomes significant when disease or infection occurs. Any imbalance in the body's antioxidant defense system results in oxidative stress leading to cell damage. ROS and free radicals are generated in various human infectious diseases caused mostly by viruses in addition to bacteria and other parasites [71]. After entering a cell, a virus disturbs

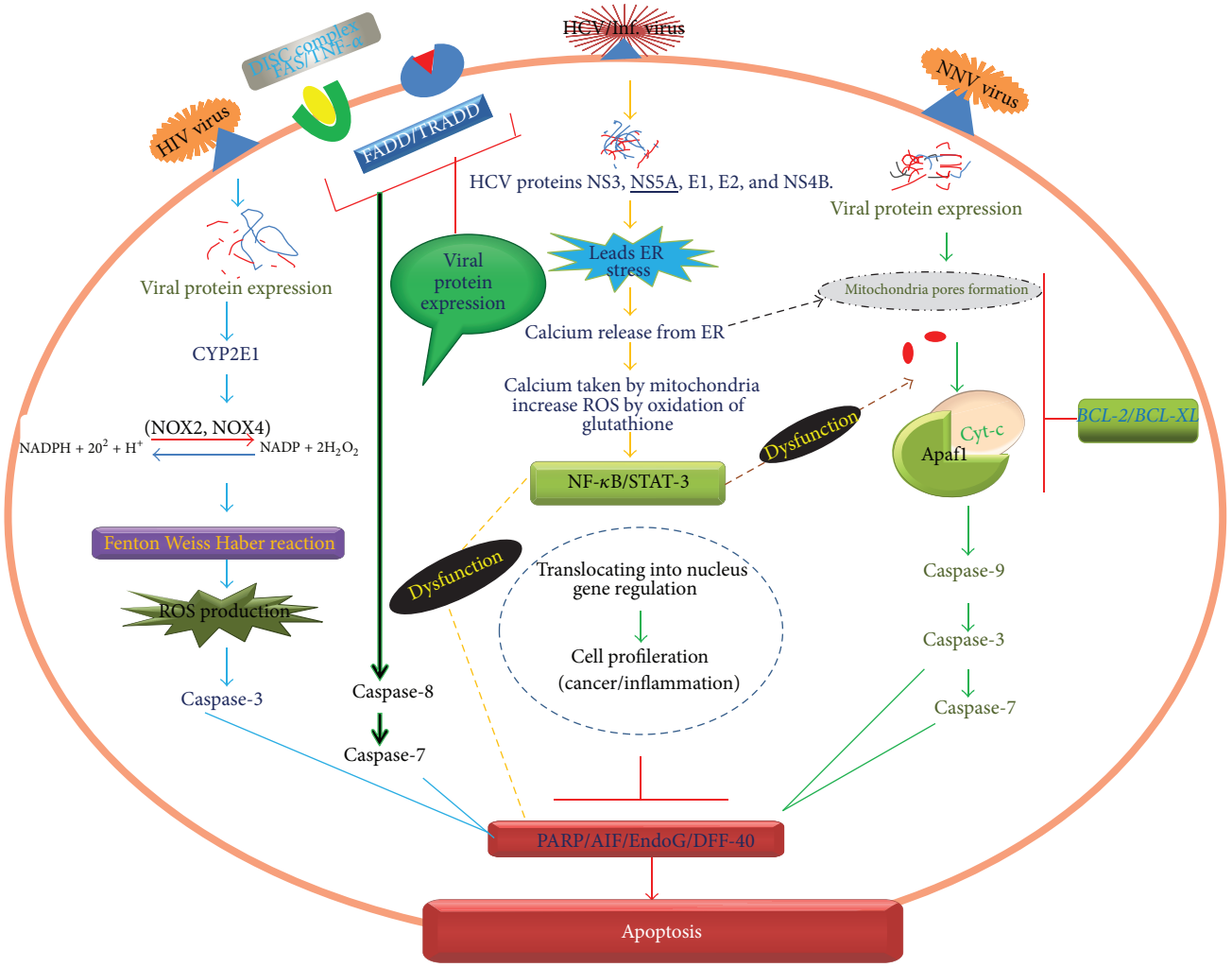

FIGURE 1: Schematic diagram of apoptotic cascade and the sites of action of general and specific caspases. The figure also illustrates how ROS produced during viral infection can affect apoptotic cascades. Abbreviations used in figure: FAS/TNF-α: tumor necrosis factor alpha (death receptors); FADD: Fas associated death domain; TRADD: tumor necrosis factor receptor associated death domain; Cas: caspase; AIF: apoptosis-inducing factor; PARP: poly (ADP) ribose polymerase; EndoG: endonuclease G; DFF-40: DNA fragmentation factor 40 KDa; tBID: truncated BID; DISC: death-inducing signaling complex.

the cell's normal functioning by using the cell's machinery to replicate itself. This in turn leads to an imbalance in the cell's ROS system. Oxidative stress has been found to enhance viral replication in different viral infections [76–78].

ROS are usually generated during allergic and nonallergic inflammation in the body's inflammatory cells [79, 80]. Because they can act on the proteins and lipids in addition to other cell organelles, ROS can be considered part of the defense system against viral/bacterial infections. The ROS produced must be specific and also produced in limited amounts, as they can destroy the cell for which they are generated in addition to the cell's neighboring surroundings during highly inflammatory reactions [81, 82]. However, the ROS produced during the normal metabolic process vanish in the body's antioxidant pools such as catalases and SOD. In the case of bacterial and viral infections, ROS are produced by phagocytes to generate the respiratory burst [83–85] resulting from the NADPH oxidase activity. In addition, ROS can act as chemical messengers. Research has shown that ROS take part in both signaling pathways [86–88] and transcriptional activation [86–88].

5.1. Mitochondria: Source and Target of ROS. Although mitochondria are known as the powerhouses of a cell, they are the most suitable targets of the ROS produced inside a cell. These ROS mostly target the mtDNA, which encodes 13 polypeptides, 2 ribosomal RNA, and 22 tRNA [89]. All of these byproducts of mtDNA are essential components in electron transport chains for the generation of ATP via the oxidative phosphorylation process [90]. ATP generation requires proteins from both the nuclear genome and mitochondria. Therefore, the oxidative production of the ATP required for cellular function also generates ROS that can damage the mtDNA, membrane lipid permeability, release of cytochrome C into the cytosol, and activation of the key effector protease caspase-3 via proteolytic cleavage that

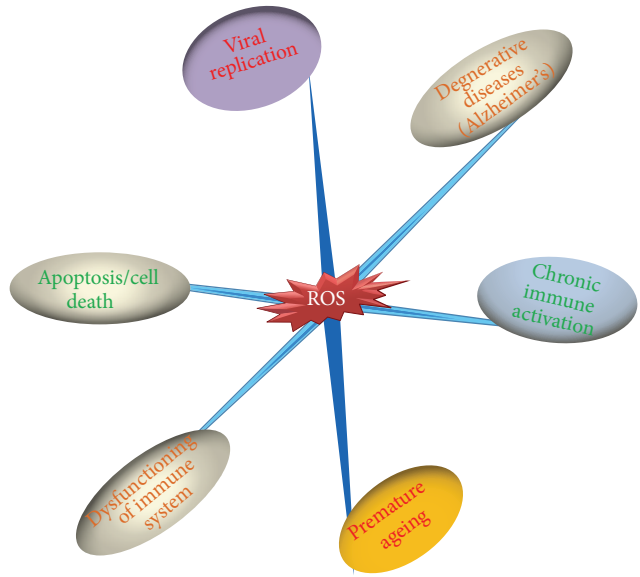

Figure 2: Effects of reactive oxygen species on different areas.

ultimately results in the mitochondrial-mediated apoptosis pathway [91, 92]. Thus, any injury to mitochondria DNA can result in serious cell damage. The mtDNA is more suitable for ROS due to its lack of protective histones and its proximity to the electron transport chain, which is the main center of ATP production in mitochondria. Therefore, mitochondria are the major source of ROS production inside a cell, and Mother Nature has provided them with their own antioxidant defense system, the most important component of which is the glutathione GSH (reduced glutathione). Although there is no proof that glutathione biosynthesis occurs inside mitochondria, these organelles have their own distinct glutathione polls [93].

In the case of mitochondrial dysfunction, when released into cytoplasm, cytochrome C interacts with the apoptotic release factor (Apaf1) to initiate apoptosis (the mitochondrial-mediated apoptosis pathway). The proapoptotic gene Bax from the BCL family can cause mitochondria to release cytochrome C directly [94]. Along with other members of the BCL-2 family, Bax has the ability to create ion channels on the outer membrane of mitochondria, through which cytochrome C is released easily into the cytoplasm. Although how ROS act on mitochondria to release cytochrome C remains unknown, the ROS could cause MMP loss [93, 94], which can allow pore formation and the release of cytochrome C into cytoplasm, activating the cell death mechanism. However, it is unclear how ROS are initially released from mitochondria into the cytoplasm.

5.2. ROS in Endoplasmic Reticulum. Endoplasmic reticulum is mainly responsible for protein folding and assembly. It also acts as a primary storage house of calcium, which is required for the proper folding of proteins [95]. Any change in the normal function of endoplasmic reticulum results in the accumulation of misfolded and unfolded proteins, and changes in calcium homeostasis cause endoplasmic reticulum stress that finally leads to apoptosis [96]. Researchers currently believe that the oxidation of proteins in endoplasmic reticulum, which is associated with protein folding, is responsible for the generation of ROS that cause oxidative stress. This oxidative stress results in the leakage of calcium from endoplasmic reticulum lumen into cytoplasm [97–100]. Therefore rising Ca^{2+} concentration in the cytoplasm causes Ca^{2+} entry into mitochondria and nuclei [96]. In mitochondria Ca^{2+} cause the activation of mitochondrial metabolism that can switch from a physiological beneficial process to a cell death signal whereas in nuclei Ca^{2+} modulate gene transcription and nucleases that control cell death. Moreover Stout et. al. have experimentally shown that increased levels of Ca^{2+} in the cytoplasm are not necessarily toxic if the Ca^{2+} uptake by mitochondria is inhibited. [101]. Therefore this indicates that mitochondria are important targets for switching normal Ca^{2+} signaling to signals for cell death during severe oxidative stress.

6. Antioxidant Defense System

Several defense mechanisms have been developed to protect against exposure to different free radicals [102], such as physical, repair, and preventive mechanisms. The antioxidant defense mechanism comprises two components: (1) enzymatic components including catalases, SOD, and glutathione peroxidase and (2) nonenzymatic components including vitamin C, vitamin E, carotenoids, glutathione, and flavonoids, among others. Various reviews and research papers have indicated the role and mechanism of both enzymatic and nonenzymatic components in protecting against oxidative stress [103–116].

Consider the case of GSH, which acts as a redox buffer inside a cell [117]. GSH is found in almost every cell

compartment, including the cytosol. GSSG represents the oxidized form of GSH inside a cell. Therefore, measuring the ratio of GSH to GSSG can provide a good indication of the oxidative stress [118, 119]. The GSH inside the nucleus helps maintain the redox of sulfhydryl proteins, which are important for repair and expression. When a cell is treated with GSH, it is readily taken by the mitochondria against the concentration gradient. GSH also plays an important role [117] in activating vitamin C and vitamin E and transporting amino acids through the plasma membrane. It scavenges singlet oxygen and hydroxyl radicals, detoxifies hydrogen, and lipid peroxide and is a cofactor in several detoxifying enzymes.

7. Oxidative Stress in Human Immunodeficiency Virus (HIV)

Oxidative stress has been found to occur in various viral infections [120–123] that may enhance viral replication. In an *in vitro* condition, oxidative stress has been found to enhance HIV replication [124–126]. The nuclear transcription factor NF-κB, which is necessary for viral replication, is activated when oxidative stress is present [124, 127]. The other role of NF-κB is to activate many of the immune system's inflammatory cytokines [128, 129]. Many antioxidants have been examined to determine their antiviral activities. However, due to unknown reasons, they have been shown to have varying effects in different cell culture systems and have shown no improvement even when examined *in vitro* at higher concentrations. HIV-infected and AIDS patients have exhibited elevated serum levels of hydroperoxides and malondialdehyde, which are the byproducts of lipid peroxidation [130–133], in addition to membrane damage. They have also exhibited an increase in resting oxygen consumption, as free-radical formation is linked to oxygen metabolism [133]. This information is supported by the production of ROS in the neutrophiles of HIV-infected patients [134], whose antioxidant defense systems undergo dramatic changes. Children suffering from HIV infection have exhibited decreased SOD levels and activity [135]. Antioxidant enzyme catalase activity increases as AIDS progresses in HIV-infected patients [136]. The level of glutathione peroxidase in RBCs and plasma also decreases. This clearly shows that the body antioxidant system becomes weaker as HIV progresses. The imbalances inside and outside the cell influence the cell to undergo a programmed cell death. The weakening of the body's antioxidant components such as catalase and glutathione leads to an excess storage of H_2O_2, which further increases the hydroxyl radicals and lipid peroxide that signal the cell to undergo a programmed cell death [137]. In *in vitro* conditions, the additions of H_2O_2 and antioxidants result in a respective increase and decrease in apoptosis in the cell culture system. AIDS, which is characterized by a decrease in the CD4 lymphocytes, is currently believed to be the main culprit of this apoptosis [138, 139]. The imbalance in the ROS seems to contribute to the progression of AIDS in different ways, including the apoptosis of CD4 cells and the functioning of other immune system components [140].

7.1. Envelop Glycoprotein "Gp120" of Human Immunodeficiency Virus-1 in ROS Production. HIV-1 uses glycoprotein (gp120) to enter host cells (T-cells and monocytes). Infected monocytes can cross the blood-brain barrier (BBB) and finally replicate in astrocytes and microglia [141, 142]. Recent work has shown that HIV-1 induces ROS production (oxidative stress) in astrocytes and microglia [143, 144] and that gp120 can directly induce apoptosis in neurons [145]. It has also been shown recently that the involvement of P450 (CYP) in neurotoxicity may be due to the generation of ROS or other reactive metabolites [146]. Furthermore, gp120 along with the drug methamphetamine (MA) involves CYP and NOX pathways in apoptotic cell death. Both gp120 and MA have been found to cause oxidative stress due to the production of ROS concentrations in a time-dependent manner [147]. The ROS-mediated BBB damage in the HIV-1 infection has been shown to cause a loss of cell tight junction proteins and lipid per oxidation [148, 149]. MA and gp120 together cause a loss of tight junction proteins in BBB and make it leaky, facilitating the entry of infected monocytes [149]. MA increases oxidative stress through dopaminergic and glutamatergic mechanisms [150], and gp120 increases oxidative stress through glutathione and lipid per oxidation [144, 151]. A combination of cocaine and gp120 results in an excess production of ROS that in turn activate caspase-3 and NF-κB to force the astrocytes to undergo apoptosis [152]. In addition to considering the role of ROS in different diseases [153], recent reports have shown that oxidative stress is involved in the pathology of HIV-associated neurocognitive disorders [154]. The role that CYPs play in different tissues/organs including the brain [155] has also been confirmed. Astrocytes have been shown to express many CYPs at variable levels, and the roles of CYP2E1 and CYP2A6 in alcohol- and nicotine-mediated oxidative stress have been demonstrated [147, 156, 157]. MA has been shown to cause increased expressions of CYP2A6, 2B6, and 2D6; gp120 has been shown to cause increased expressions of CYP2E1, 2B6, and 2D6 [158]. These overall additive increases suggest that CYP may be involved in oxidative stress. The interaction between CYPs and NADPH is tightly regulated by NOX enzymes [159], which are currently being used as therapeutics in various CNS disorders such as Alzheimer's disease and strokes [159, 160]. Studies have shown that NOX 2 and NOX 4 increase oxidative stress in astrocytes [161, 162]. Others have shown that when NOX2 and NOX4 expression is blocked in astrocytes, the level of oxidative stress decreases, indicating that NOX could be used as a therapeutic agent in the treatment of neuro-AIDS. Such studies of oxidative stress in astrocytes caused by MA/gp120 have examined the use of antioxidants in HIV-1 pathogenesis and considered the potential of CYP pathways to be a target of new drugs.

8. ROS in the Hepatitis C Virus (HCV)

HCV infection cases have been reported around the world and are increasing at an alarming rate, especially in developing nations. Reports have shown that 3% of the world's population is infected with HCV [163]. Although acute

hepatitis caused by HCV is naturally cleared in 20–30% of patients [164], 70–80% of cases involve chronic hepatitis. No effective vaccine was available until recently, and the current treatment is not very effective [165, 166]. Reports have shown that HCV gene expression in the host cell increases the level of ROS through the mediation of calcium signaling [167]. This release of calcium from the ER results in ER stress. The released calcium is taken by the mitochondria, resulting in increased ROS production and oxidative stress. Oxidative stress is the main contributor to a number of diseases such as cancer [168], diabetes, and even viral infections [169]. The livers of patients with HCV infections show elevated levels of ROS and decreased antioxidant levels [170]. It has been reported that the two core proteins of HCV, NS3 and NS5A, are responsible for oxidative stress in culture cells [171]. However, the host cell Cox-2 gene, which is the main regulator of prostaglandins, is activated by the excess ROS produced [172]. This activation involves NF-κB, which is present in cells in an inactive form but becomes activated and migrates to the nucleus in HCV-infected cells due to ER stress and ROS [173]. NF-κB controls the expression of the genes responsible for apoptosis and inflammation. This elevated level of ROS activates another transcriptional factor (STAT-3) that is responsible for cell proliferation, survival, and ontogenesis [174]. This coactivation of both NF-κB and STAT-3 as a result of the oxidative stress created by excessive ROS in HCV-infected cells has an equal role in both acute and chronic liver diseases [169, 173, 175].

8.1. HCV Genome in ROS Production. The liver plays an important role in the detoxification and metabolism of harmful substances and is the main target of HCV. HCV replicates in cytoplasm, causing hepatitis cirrhosis and hepatocellular carcinoma [176, 177]. ROS-induced viral genome heterogeneity has been considered in terms of viral escape from the immune system [178]. The core nucleocapsid protein of HCV is responsible for increasing oxidative stress in the liver [179]. Although this core protein is considered the main contributor of oxidative stress [180, 181], other proteins such as NS3 and NS5A are also involved in generating oxidative stress [182–184]. Recent studies have shown that many other proteins such as E1 [180], E2 [185, 186], and NS4B [182, 187] are also involved in generating oxidative stress. The nonstructural protein NS5A is a membrane integral protein that is important not only for viral replication but also for apoptosis and immune responses such as interferon resistance [188] and changes in calcium levels. NS5A and NS3 increase the calcium uptake and cause glutathione oxidation in mitochondria, thereby increasing the ROS production [189–191]. The mitochondria thereby activate and translocate the transcriptional factors NF-κB and STAT3 to the nucleus, leading to oxidative stress. The NS5A activation of NF-κB and STAT3 is opposed by antioxidants [192, 193]. NS4B also translocates NF-κB to the nucleus in a PTK-mediated pathway. ROS and $NO^{\bullet}$ not only cause oxidative damage but also affect the DNA repair machinery [194–196] that leads to cell apoptosis. ROS are believed to be the main culprits of liver inflammation in HCV infections [197, 198].

9. ROS in Influenza Virus

The influenza virus induces the production of ROS in host cells that can damage the virus genome [199]. ROS enhance the pathogenesis ability of infections such as influenza [200, 201]. One study of mice infected with the influenza virus showed that although the spread of infection remained confined to the airways and lungs [201], systematic effects such as weight loss and a decrease in body temperature were clearly visible. The mice used in the experiment died after 5 or 6 days. The cells taken from the dead mice showed elevated levels of O_2^- and xanthine oxidase (an enzyme synthesizing O_2^-), indicating enhanced ROS production [202]. Furthermore, analysis of the antioxidant content revealed an overall decrease in the concentration of antioxidants during infection. The study suggested that influenza infection is associated with oxidative stress. In another study, influenza intravenously injected into mice with pyran-copolymer-conjugated SOD was found to protect the mice from the effects of influenza. This observation was not immediately apparent because pyran copolymers are well-known antiviral agents [203]. The localized effects of the influenza virus make it difficult to detect the redox content of tissues because the analysis methods are based on whole-tissue homogenates. The infected mice released cytokines and lipid mediators that could have caused the systematic symptoms [204]. To determine the cause of the systematic symptoms, the mice injected with the influenza virus were given cytokine injections (mostly interferon) and showed symptoms resembling influenza [205]. ROS are known for their antiviral activity [206] and can also increase the titer of the influenza virus. Influnza virus carrying glycoprotein on its surface is know as hemagglutinin which is responsible for binding the virus to cells with sialic acid on their membranes, like cells in the upper respiratory tract or erythrocytes [207]. The hemagglutinin protein is synthesized in an inactive form (HOA) and activated by specific proteases into HA1 and HA2. The cleavage of HOA into HA1 and HA2 is an important determinant of influenza virulence [207, 208]. If the influenza virus released from the cell contains inactive HOA, it may still be activated by some of the proteases present in the pulmonary surfactants [209]. However, these antiproteases can be inactivated by the ROS, converting a noninfectious influenza virus into an infectious one. Further studies have shown that an oxidant-treated antiprotease is unable to prevent trypsin from converting HOA to HA1 and HA2, resulting in a 10,000-fold increase in virus infection [207]. However, how the influenza virus induces apoptosis is still not clearly understood.

ROS production enhances the molecular pathogenesis of the influenza virus infection. Previous research has proved that although ROS are involved in damaging lung parenchyma, that damage can be repaired by taking an appropriate dose of antioxidants [209, 210]. ROS are important in the overall normal development of whole organisms [211, 212], are important components of adaptive immune responses, and are involved in the normal function of many transcription factors. The production of ROS (superoxide's) is an important defense against microbial infections. However,

the excess production of superoxide's in the influenza A virus infection is detrimental. The downregulation of the superoxide achieved by targeting specific enzymes such as NADPH oxidase-2 markedly alleviates lung injuries caused by the influenza virus and viral replication, irrespective of the infected viral strain [213]. One study showed that influenza infection leads to the thymus-specific elevation of the mitochondrial superoxide, which interferes with the normal functioning of T-cell lymphocyte damage in influenza A virus infections [214]. A further knockdown of SOD2 indicates that T-cells begin the apoptosis process and take on many developmental defects, resulting in overall weakening of the adaptive immune system and an increased susceptibility to the influenza A virus (H1N1). Keeping the use of ROS as specific targets in mind, ROS inhibitors and other therapeutic agents may prove useful in controlling such a disease [215].

10. ROS Production in Fish Virus Infections

10.1. Betanodavirus (Mitochondria as the ROS Production Houses in Infected Cells). The Betanodavirus is an RNA virus belonging to the Nodaviridae family, which mostly infects fish. The virus causes virus nervous necrosis (VNN) disease, which is characterized by the necrosis of the central nervous system, including the brain and retina. The common symptoms shown by infected fish are abnormal swimming behavior, darkening of the skin, and weight loss [216]. The viral capsid protein [217] is involved in the postapoptotic necrotic cell death via a cytochrome C release-dependent pathway [218]. Research has shown that the majority of RNA viruses, DNA viruses, and retroviruses cause ROS-mediated cell death. The Betanodavirus genome encodes protein alpha and B2, both of which are death inducers. Protein alpha causes mitochondria-mediated cell death involving caspase-3 [219], and B2 does the same via a Bax-mediated pathway [220]. Another protein, B1, acts as an antinecrotic death gene [221]. Our research shows that the production of ROS partly causes mitochondria-mediated cell death in RGNNV-infected cells [94]. This supports previous research related to the involvement of oxidative stress in cell deaths caused during RNA virus infection. It opens doors for the development of new drugs by making the enzymes or other key factors involved in ROS production the main targets. Mitochondria are the main production houses of ROS during RGNNV infection, which ultimately leads to mitochondria-mediated cell death [94, 222]. Mitochondria complexes I and II of the electron transport chains are the major sites of ROS production [222, 223]. The inhibition of complexes I (rotenone) and II (antimycin) and the oxidation of either complex both lead to increased ROS production [222, 224–226]. However, ROS are also important in the activation of the body's antioxidant enzymes such as SOD and glutathione peroxidase [127, 227]. RGNNV-infected cells were found to produce ROS at 24 h after infection, with a gradual regulation of catalase and Nrf2 transcription factors [228] and autophagy (unpublished data). However, it remains unclear whether Nrf2 upregulates ROS production. We used antioxidants such as NAC and DPI and overexpressed zfcatalase to further explore our hypothesis and found a decrease in RGNNV-induced ROS production and an increase in cell viability. The cell death mechanism influenced by the novel antinecrotic cell death protein B1 remains unknown. To determine which cell death mechanism is influenced by B1, we examined how the Betanodavirus nonstructural protein B1 regulates oxidative stress and p53 expression in fish cell lines [94].

11. Conclusion and Future Perspective

Viral infections are becoming more common daily around the world. People living in the poorest countries represent the most infected population due to their unhygienic food conditions, illiteracy, and lack of basic health care. Identifying the main culprit of new epidemics is the most important factor in controlling the outbreak of disease. Many host mechanisms have been shown or are suspected to contribute to the pathogenesis of viral infections, such as ROS and cytokines. Current studies of ROS are based on the lethal effects of ROS in various diseases such as cancer, HIV, hepatitis, and diabetes. The discovery of *"respiratory bursts"* revealed that ROS are only produced by phagocyte cells to protect against microbial invasions and are thus considered toxic molecules. However, recent cellular ROS studies have shown that ROS are produced in all types of cells and serve as important messengers in cell signaling and various signal transduction pathways. The ROS produced inside cells are maintained by complex intracellular regulatory systems. Cells respond to the ROS they produce according to different parameters such as intensity, duration, and amount. Therefore, the combination of several mechanisms described in this review could be exploited to find new solutions for combating oxidative stress in different viral infections. However, the role of oxidants in viral diseases is more complex because it includes metabolic regulations for both host metabolisms and viral replication. A number of different additional host mechanisms have been shown or are suspected to contribute to the pathogenesis of viral infections, including excessive cytokine, lipid peroxidation, lipid mediator release, and compliment activation [15, 229]. Therefore, more deep and detailed research is needed to interfere with the activation or stop the undesired effects of these pathways. The limitations of interfering with such viral disease mechanisms are similar to those involved in interfering with oxidant generation, as these pathways are associated with normal host physiology and pathology. It is clear that any useful approach to solving this problem will require a variety of drugs rather than two or three drugs according to modern pharmacotherapy. Clarifying the role of oxidation stress in apoptosis could lead to a discovery of novel therapeutic strategies and pathogenetic insights into different viral diseases, particularly given that ROS-mediated mechanisms are responsible for apoptosis during viral infections. ROS were initially detected based on simple absorbance measurements. Due to the discovery that ROS act as intracellular messengers and regulators, the absorbance-based detection was replaced by fluorescence- and luminescence-based forms of detection that are more specific and accurate and less time consuming. The present-day cellular ROS research faces

great difficulty in detecting ROS due to the lack of reporter agents against these molecules. Because ROS molecules are highly reactive with most other molecules, designing reporter agents has been difficult. Some of the challenges involved in researching cellular ROS in different diseases include the following.

(i) Although much of the available evidence supports the involvement of ROS in lung injuries caused by the influenza A virus, the molecular mechanism and enzymes for ROS production remain unclear. Thus, knowing the enzymes and other key factors could be the main aim in designing new drugs against the influenza infection.

(ii) Studying the oxidative stress in HIV-infected patients has opened new doors for cellular ROS researchers to use antioxidants as novel drugs to decrease HIV-1 pathogenesis in humans.

(iii) The current cellular ROS research does not provide enough proof to show the exact relationships among mitochondria functions, ROS production, ROS damage, and the development of clinical phenotypes.

(iv) Research has shown that ROS are the main regulatory factors in a number of molecular pathways, especially those linked to the development and spreading of tumors. Thus, studying ROS as the main therapeutic targets could be made a focus for controlling disease.

(v) The role of ROS and mitochondria in neurodegenerative diseases and aging is also a matter of interest, as the oxidative stress generated by an ROS imbalance can be a consequence rather than a cause of the disease process.

(vi) Studying the detailed mechanisms of $N0^{\bullet}$/redox-mediated signaling will help in the development of novel therapeutic approaches to addressing heart failure.

(vii) It remains unknown how much of the mitochondrial damage in Parkinson's disease cases is of genetic origin and how much is caused by the H_2O_2 generated in the dopamine produced by neurons.

As discussed previously, much of the available evidence indicates that free radicals play a complex role in different viral diseases, beginning with their influence on the host cell's metabolism and viral replication and extending to their desired inactivation effects on viruses and less-desired toxic effects on host tissues. The use of antioxidants in viral disease therapy could therefore be applied at many levels and replace the old symptomatic therapy, which would not alter the viral replication. The new therapy should also target additional mechanisms that contribute to the symptoms and pathology of viral diseases such as cytokines, lipid peroxidation, and $NO^{\bullet}$. Most virus-induced ROS generation is linked to the activation of different signaling molecules and transcription factors such as NF-κB, STAT (STAT1, STAT3), and JAK (JAK2). However, the intracellular signaling events that lead the viral-induced gene expression are mostly unknown. Some ROS researchers have described ROS as secondary messengers that influence a number of different molecular processes, including the apoptotic, antiapoptotic, and proapoptotic expression of a number of genes. The physiological role played by ROS is important because viruses depend on the biosynthetic mechanisms of their host cells as intracellular parasites. The activation of ROS production in viral infections in the absence of antiviral antibodies could play a role in the generation of symptoms and pathologies such as the induction of fever in the influenza virus and could also lead to internal organ hemorrhages. Therefore, the main challenge for present-day molecular virologists is to understand the pathophysiological functions of ROS, which would provide deep understanding of the many aspects of viral infectious diseases. The effect of ROS on the host's immune response is another important factor of viral pathogenesis and mutation. The toxicity and reactivity of ROS, which are produced in excess amounts by the overreactions of immune responses against the organs or tissues in which viruses replicate, may explain the tissue injury mechanisms observed in the different viral diseases involving immunological interactions. Understanding of the host pathogen interactions at the molecular level requires the characterization of host-derived small radical molecules, which appear to play an important role in the pathogenesis of viral infection. An energizing concept related to free radicals would contribute to the insights into the molecular mechanisms of pathological events that occur as a result of the interaction between viruses and their hosts. Therefore, more deep and detailed research must be conducted to better understand the molecular mechanism and specific apoptotic pathways involved in ROS-mediated cell death. The growing interest shown by cellular ROS researchers should provide answers for many of these unsolved questions.

Conflict of Interests

The authors declare that there is no conflict of interests regarding the publication of this paper.

Acknowledgments

Due to space limitations, the authors are unable to cite the work of every author who contributed to their cellular ROS research. This work was supported by a Grant (NSC 98-2313-B-006-004-MY3) awarded to Dr. Jainn-Ruey Hong by the National Science Council of Taiwan.

References

[1] G. Gloire, S. Legrand-Poels, and J. Piette, "NF-κB activation by reactive oxygen species: fifteen years later," *Biochemical Pharmacology*, vol. 72, no. 11, pp. 1493–1505, 2006.

[2] H. M. Lander, "An essential role for free radicals and derived species in signal transduction," *FASEB Journal*, vol. 11, no. 2, pp. 118–124, 1997.

[3] S. Devadas, L. Zaritskaya, S. G. Rhee, L. Oberley, and M. S. Williams, "Discrete generation of superoxide and hydrogen peroxide by T cell receptor stimulation: selective regulation

of mitogen-activated protein kinase activation and Fas ligand expression," *Journal of Experimental Medicine*, vol. 195, no. 1, pp. 59–70, 2002.

[4] D. A. Hildeman, "Regulation of T-cell apoptosis by reactive oxygen species," *Free Radical Biology and Medicine*, vol. 36, no. 12, pp. 1496–1504, 2004.

[5] F. C. Fang, "Antimicrobial actions of reactive oxygen species," *mBio*, vol. 2, no. 5, 2011.

[6] K. Krapfenbauer, E. Engidawork, N. Cairns, M. Fountoulakis, and G. Lubec, "Aberrant expression of peroxiredoxin subtypes in neurodegenerative disorders," *Brain Research*, vol. 967, no. 1-2, pp. 152–160, 2003.

[7] S. Desagher, J. Glowinski, and J. Premont, "Astrocytes protect neurons from hydrogen peroxide toxicity," *Journal of Neuroscience*, vol. 16, no. 8, pp. 2553–2562, 1996.

[8] R. Dringen and B. Hamprecht, "Involvement of glutathione peroxidase and catalase in the disposal of exogenous hydrogen peroxide by cultured astroglial cells," *Brain Research*, vol. 759, no. 1, pp. 67–75, 1997.

[9] A. M. Chrobot, A. Szaflarska-Szczepanik, and G. Drewa, "Antioxidant defense in children with chronic viral hepatitis B and C," *Medical Science Monitor*, vol. 6, no. 4, pp. 713–718, 2000.

[10] M.-L. Gougeon and L. Montagnier, "Apoptosis in AIDS," *Science*, vol. 260, no. 5112, pp. 1269–1270, 1993.

[11] G. W. Pace and C. D. Leaf, "The role of oxidative stress in HIV disease," *Free Radical Biology and Medicine*, vol. 19, no. 4, pp. 523–528, 1995.

[12] U. Z. Paracha, K. Fatima, M. Alqahtani et al., "Oxidative stress and hepatitis C virus," *Virology Journal*, vol. 10, article 251, 2013.

[13] D. M. Hockenbery, Z. N. Oltvai, X.-M. Yin, C. L. Milliman, and S. J. Korsmeyer, "Bcl-2 functions in an antioxidant pathway to prevent apoptosis," *Cell*, vol. 75, no. 2, pp. 241–251, 1993.

[14] E. Peterhans, "Sendal virus stimulates chemiluminescence in mouse spleen cells," *Biochemical and Biophysical Research Communications*, vol. 91, no. 1, pp. 383–392, 1979.

[15] E. Peterhans, M. Grob, T. Bürge, and R. Zanoni, "Virus-induced formation of reactive oxygen intermediates in phagocytic cells," *Free Radical Research Communications*, vol. 3, no. 1–5, pp. 39–46, 1987.

[16] A. Vierucci, M. De Martino, and E. Graziani, "A mechanism for liver cell injury in viral hepatitis: effects of hepatitis B virus on neutrophil function in vitro and in children with chronic active hepatitis," *Pediatric Research*, vol. 17, no. 10, pp. 814–820, 1983.

[17] F. Muller, "Reactive oxygen intermediates and Human Immunodeficiency Virus (HIV) infection," *Free Radical Biology and Medicine*, vol. 13, no. 6, pp. 651–657, 1992.

[18] C. Pasquier, R. Y. Olivier, C. Auclair, and L. Packer, *Oxidative Stress, Cell Activation and Viral Infection*, 1994.

[19] J. W. Drake, "Rates of spontaneous mutation among RNA viruses," *Proceedings of the National Academy of Sciences of the United States of America*, vol. 90, no. 9, pp. 4171–4175, 1993.

[20] J. W. Drake and J. J. Holland, "Mutation rates among RNA viruses," *Proceedings of the National Academy of Sciences of the United States of America*, vol. 96, no. 24, pp. 13910–13913, 1999.

[21] S. Duffy, L. A. Shackelton, and E. C. Holmes, "Rates of evolutionary change in viruses: patterns and determinants," *Nature Reviews Genetics*, vol. 9, no. 4, pp. 267–276, 2008.

[22] L. García-Villada and J. W. Drake, "The three faces of riboviral spontaneous mutation: spectrum, mode of genome replication, and mutation rate," *PLOS Genetics*, vol. 8, Article ID e1002832, 2012.

[23] D. J.-M. Malvy, M.-J. Richard, J. Arnaud, A. Favier, and O. Amédée-Manesme, "Relationship of plasma malondialdehyde, vitamin E and antioxidant micronutrients to human immunodeficiency virus-1 seropositivity," *Clinica Chimica Acta*, vol. 224, no. 1, pp. 89–94, 1994.

[24] J. Fuchs, I. Emerit, A. Levy, L. Cernajvski, H. Schofer, and R. Milbradt, "Clastogenic factors in plasma of HIV-1 infected patients," *Free Radical Biology and Medicine*, vol. 19, no. 6, pp. 843–848, 1995.

[25] E. Peterhans, "Reactive oxygen species and nitric oxide in viral diseases," *Biological Trace Element Research*, vol. 56, no. 1, pp. 107–116, 1997.

[26] J. E. Sprietsma, "Zinc-controlled Th1/Th2 switch significantly determines development of diseases," *Medical Hypotheses*, vol. 49, no. 1, pp. 1–14, 1997.

[27] Q.-L. Choo, G. Kuo, A. J. Weiner, L. R. Overby, D. W. Bradley, and M. Houghton, "Isolation of a cDNA clone derived from a blood-borne non-A, non-B viral hepatitis genome," *Science*, vol. 244, no. 4902, pp. 359–362, 1989.

[28] P. Simmonds, "Genetic diversity and evolution of hepatitis C virus—15 years on," *Journal of General Virology*, vol. 85, no. 11, pp. 3173–3188, 2004.

[29] F. V. Chisari and C. Ferrari, "Hepatitis B virus immunopathogenesis," *Annual Review of Immunology*, vol. 13, pp. 29–60, 1995.

[30] G. L. Davis, "Treatment of chronic hepatitis C," *British Medical Journal*, vol. 323, no. 7322, pp. 1141–1142, 2001.

[31] A. V. Ivanov, B. Bartosch, O. A. Smirnova, M. G. Isaguliants, and S. N. Kochetkov, "HCV and oxidative stress in the liver," *Viruses*, vol. 5, no. 2, pp. 439–469, 2013.

[32] H. Bantel, A. Lügering, C. Poremba et al., "Caspase activation correlates with the degree of inflammatory liver injury in chronic Hepatitis C virus infection," *Hepatology*, vol. 34, no. 4, pp. 758–767, 2001.

[33] P. Boya, A. D. L. Peña, O. Beloqui et al., "Antioxidant status and glutathione metabolism in peripheral blood mononuclear cells from patients with chronic hepatitis C," *Journal of Hepatology*, vol. 31, no. 5, pp. 808–814, 1999.

[34] N. De Maria, A. Colantoni, S. Fagiuoli et al., "Association between reactive oxygen species and disease activity in chronic hepatitis C," *Free Radical Biology and Medicine*, vol. 21, no. 3, pp. 291–295, 1996.

[35] G. P. Bianchi, G. Marchesini, M. Brizi et al., "Nutritional effects of oral zinc supplementation in cirrhosis," *Nutrition Research*, vol. 20, no. 8, pp. 1079–1089, 2000.

[36] P. M. Newberne, S. Broitman, and T. F. Schrager, "Esophageal carcinogenesis in the rat: zinc deficiency, DNA methylation and alkyltransferase activity," *Pathobiology*, vol. 65, no. 5, pp. 253–263, 1997.

[37] M. Kaji, A. Watanabe, and H. Aizawa, "Differences in clinical features between influenza A H1N1, A H3N2, and B in adult patients," *Respirology*, vol. 8, no. 2, pp. 231–233, 2003.

[38] Y.-C. Hsieh, T.-Z. Wu, D.-P. Liu et al., "Influenza pandemics: past, present and future," *Journal of the Formosan Medical Association*, vol. 105, no. 1, pp. 1–6, 2006.

[39] B. S. Finkelman, C. Viboud, K. Koelle, M. J. Ferrari, N. Bharti, and B. T. Grenfell, "Global patterns in seasonal activity of influenza A/H3N2, A/H1N1, and B from 1997 to 2005: viral coexistence and latitudinal gradients," *PLoS ONE*, vol. 2, no. 12, Article ID e1296, 2007.

[40] M. S. Cooperstock, R. P. Tucker, and J. V. Baublis, "Possible pathogenic role of endotoxin in Reye's syndrome," *The Lancet*, vol. 1, no. 7919, pp. 1272–1274, 1975.

[41] J. F. Kerr, A. H. Wyllie, and A. R. Currie, "Apoptosis: a basic biological phenomenon with wide-ranging implications in tissue kinetics," *British Journal of Cancer*, vol. 26, no. 4, pp. 239–257, 1972.

[42] E. C. Borden, H. Kluger, and J. Crowley, "Apoptosis: a clinical perspective," *Nature Reviews Drug Discovery*, vol. 7, no. 12, p. 959, 2008.

[43] S. G. Popov, R. Villasmil, J. Bernardi et al., "Lethal toxin of Bacillus anthracis causes apoptosis of macrophages," *Biochemical and Biophysical Research Communications*, vol. 293, no. 1, pp. 349–355, 2002.

[44] B. Brüne, "Nitric oxide: NO apoptosis or turning it ON?" *Cell Death and Differentiation*, vol. 10, no. 8, pp. 864–869, 2003.

[45] R. S. Cotran and C. Kumar, *Robbins Pathologic Basis of Disease*, WB Saunders, Philadelphia, Pa, USA, 1998.

[46] A. Chiarugi and M. A. Moskowitz, "Cell biology: PARP-1—a perpetrator of apoptotic cell death?" *Science*, vol. 297, no. 5579, pp. 259–263, 2002.

[47] H. R. Horvitz, "Genetic control of programmed cell death in the nematode Caenorhabditis elegans," *Cancer Research*, vol. 59, no. 7, pp. 1701s–1706s, 1999.

[48] G. S. Salvesen, "Programmed cell death and the caspases," *APMIS*, vol. 107, no. 1, pp. 73–79, 1999.

[49] G. N. Barber, "Host defense, viruses and apoptosis," *Cell Death and Differentiation*, vol. 8, no. 2, pp. 113–126, 2001.

[50] S. Y. Proskuryakov, A. G. Konoplyannikov, and V. L. Gabai, "Necrosis: a specific form of programmed cell death?" *Experimental Cell Research*, vol. 283, no. 1, pp. 1–16, 2003.

[51] D. L. Kasper and D. F. Zaleznik, "Gas gangrene, antibiotic associated colitis, and other clostridial infections," in *Harrisons's Principles of Internal Medicine*, E. Kasper and D. L. Braunwald, Eds., McGraw Hill, New York, NY, USA, 2001.

[52] S. M. Schwarz and M. R. Bennett, "Death by any other name," *American Journal of Pathology*, vol. 147, no. 2, pp. 229–234, 1995.

[53] J. Savill and V. Fadok, "Corpse clearance defines the meaning of cell death," *Nature*, vol. 407, no. 6805, pp. 784–788, 2000.

[54] C. J. Froelich, V. M. Dixit, and X. Yang, "Lymphocyte granule-mediated apoptosis: matters of viral mimicry and deadly proteases," *Immunology Today*, vol. 19, no. 1, pp. 30–36, 1998.

[55] A. Ashkenazi and V. M. Dixit, "Death receptors: signaling and modulation," *Science*, vol. 281, no. 5381, pp. 1305–1308, 1998.

[56] N. Itoh, S. Yonehara, A. Ishii et al., "The polypeptide encoded by the cDNA for human cell surface antigen fas can mediate apoptosis," *Cell*, vol. 66, no. 2, pp. 233–243, 1991.

[57] A. M. Chinnalyan, K. O'Rourke, M. Tewari, and V. M. Dixit, "FADD, a novel death domain-containing protein, interacts with the death domain of Fas and initiates apoptosis," *Cell*, vol. 81, no. 4, pp. 505–512, 1995.

[58] C.-Y. Wang, M. W. Mayo, R. G. Korneluk, D. V. Goeddel, and A. S. Baldwin Jr., "NFkappaB antiapoptosis: induction of TRAF1 and TRAF2 and c-IAP1 and c-IAP2 to suppress caspase-8 activation," *Science*, vol. 281, no. 5383, pp. 1680–1683, 1998.

[59] S. J. Baker and E. P. Reddy, "Modulation of life and death by the TNF receptor superfamily," *Oncogene*, vol. 17, no. 25, pp. 3261–3270, 1998.

[60] R. H. Arch, R. W. Gedrich, and C. B. Thompson, "Tumor necrosis factor receptor-associated factors (TRAFs)—a family of adapter proteins that regulates life and death," *Genes and Development*, vol. 12, no. 18, pp. 2821–2830, 1998.

[61] Q. L. Deveraux and J. C. Reed, "IAP family proteins—suppressors of apoptosis," *Genes and Development*, vol. 13, no. 3, pp. 239–252, 1999.

[62] K. M. Ryan, M. K. Ernst, N. R. Rice, and K. H. Vousden, "Role of NF-κB in p53-mediated programmed cell death," *Nature*, vol. 404, no. 6780, pp. 892–897, 2000.

[63] J. Feuillard, M. Schuhmacher, S. Kohanna et al., "Inducible loss of NF-κB activity is associated with apoptosis and Bcl-2 down-regulation in Epstein-Barr virus-transformed B lymphocytes," *Blood*, vol. 95, no. 6, pp. 2068–2075, 2000.

[64] E. D. Cahir-McFarland, D. M. Davidson, S. L. Schauer, J. Duong, and E. Kieff, "NF-κB inhibition causes spontaneous apoptosis in Epstein-Barr virus-transformed lymphoblastoid cells," *Proceedings of the National Academy of Sciences of the United States of America*, vol. 97, no. 11, pp. 6055–6060, 2000.

[65] M. Repetto, C. Reides, M. L. Gomez Carretero, M. Costa, G. Griemberg, and S. Llesuy, "Oxidative stress in blood of HIV infected patients," *Clinica Chimica Acta*, vol. 255, no. 2, pp. 107–117, 1996.

[66] N. Israël and M.-A. Gougerot-Pocidalo, "Oxidative stress in human immunodeficiency virus infection," *Cellular and Molecular Life Sciences*, vol. 53, no. 11-12, pp. 864–870, 1997.

[67] I. Dalle-Donne, R. Rossi, R. Colombo, D. Giustarini, and A. Milzani, "Biomarkers of oxidative damage in human disease," *Clinical Chemistry*, vol. 52, no. 4, pp. 601–623, 2006.

[68] N. S. Dhalla, R. M. Temsah, and T. Netticadan, "Role of oxidative stress in cardiovascular diseases," *Journal of Hypertension*, vol. 18, no. 6, pp. 655–673, 2000.

[69] P. Jenner, "Oxidative stress in Parkinson's disease," *Annals of Neurology*, vol. 53, pp. S26–S36, 2003.

[70] L. M. Sayre, M. A. Smith, and G. Perry, "Chemistry and biochemistry of oxidative stress in neurodegenerative disease," *Current Medicinal Chemistry*, vol. 8, no. 7, pp. 721–738, 2001.

[71] G. Nabel and D. Baltimore, "An inducible transcription factor activates expression of human immunodeficiency virus in T cells," *Nature*, vol. 326, no. 6114, pp. 711–713, 1987.

[72] R. D. Semba and A. M. Tang, "Micronutrients and the pathogenesis of human immunodeficiency virus infection," *British Journal of Nutrition*, vol. 81, no. 3, pp. 181–189, 1999.

[73] G. T. Keusch, "Micronutrients and susceptibility to infection," *Annals of the New York Academy of Sciences*, vol. 587, pp. 181–188, 1990.

[74] M. A. Beck, Q. Shi, V. C. Morris, and O. A. Levander, "Rapid genomic evolution of a non-virulent coxsackievirus B3 in selenium- deficient mice results in selection of identical virulent isolates," *Nature Medicine*, vol. 1, no. 5, pp. 433–436, 1995.

[75] P. Evans and B. Halliwell, "Micronutrients: oxidant/antioxidant status," *British Journal of Nutrition*, vol. 85, no. 2, pp. S67–S74, 2001.

[76] P. A. Baeuerle and D. Baltimore, "Activation of DNA-binding activity in an apparently cytoplasmic precursor of the NF-κB transcription factor," *Cell*, vol. 53, no. 2, pp. 211–217, 1988.

[77] F. J. T. Staal, M. Roederer, L. A. Herzenberg, and L. A. Herzenberg, "Intracellular thiols regulate activation of nuclear factor κB and transcription of human immunodeficiency virus," *Proceedings of the National Academy of Sciences of the United States of America*, vol. 87, no. 24, pp. 9943–9947, 1990.

[78] H.-U. Simon, S. Yousefi, C. Schranz, A. Schapowal, C. Bachert, and K. Blaser, "Direct demonstration of delayed eosinophil apoptosis as a mechanism causing tissue eosinophilia," *Journal of Immunology*, vol. 158, no. 8, pp. 3902–3908, 1997.

[79] B. Dibbert, M. Weber, W. H. Nikolaizik et al., "Cytokine-mediated Bax deficiency and consequent delayed neutrophil apoptosis: a general mechanism to accumulate effector cells in inflammation," *Proceedings of the National Academy of Sciences of the United States of America*, vol. 96, no. 23, pp. 13330–13335, 1999.

[80] J. A. Smith, "Neutrophils, host defense, and inflammation: a double-edged sword," *Journal of Leukocyte Biology*, vol. 56, no. 6, pp. 672–686, 1994.

[81] I. Vachier, P. Chanez, C. Le Doucen, M. Damon, B. Descomps, and P. Godard, "Enhancement of reactive oxygen species formation in stable and unstable asthmatic patients," *European Respiratory Journal*, vol. 7, no. 9, pp. 1585–1592, 1994.

[82] S. J. Chanock, J. El Benna, R. M. Smith, and B. M. Babior, "The respiratory burst oxidase," *Journal of Biological Chemistry*, vol. 269, no. 40, pp. 24519–24522, 1994.

[83] D. A. Bass, J. W. Parce, and L. R. Dechatelet, "Flow cytometric studies of oxidative product formation by neutrophils: a graded response to membrane stimulation," *Journal of Immunology*, vol. 130, no. 4, pp. 1910–1917, 1983.

[84] S. Dusi, V. Della Bianca, M. Donini, K. A. Nadalini, and F. Rossi, "Mechanisms of stimulation of the respiratory burst by TNF in nonadherent neutrophils," *Journal of Immunology*, vol. 157, no. 10, pp. 4615–4623, 1996.

[85] P. J. Coffer, B. M. T. Burgering, M. P. Peppelenbosch, J. L. Bos, and W. Kruijer, "UV activation of receptor tyrosine kinase activity," *Oncogene*, vol. 11, no. 3, pp. 561–569, 1995.

[86] A. Knebel, H. J. Rahmsdorf, A. Ullrich, and P. Herrlich, "Dephosphorylation of receptor tyrosine kinases as target of regulation by radiation, oxidants or alkylating agents," *EMBO Journal*, vol. 15, no. 19, pp. 5314–5325, 1996.

[87] R.-P. Huang, J.-X. Wu, Y. Fan, and E. D. Adamson, "UV activates growth factor receptors via reactive oxygen intermediates," *Journal of Cell Biology*, vol. 133, no. 1, pp. 211–220, 1996.

[88] R. Schreck, P. Rieber, and P. A. Baeuerle, "Reactive oxygen intermediates as apparently widely used messengers in the activation of the NF-κB transcription factor and HIV-1," *EMBO Journal*, vol. 10, no. 8, pp. 2247–2258, 1991.

[89] S. Anderson, A. T. Bankier, and B. G. Barrell, "Sequence and organization of the human mitochondrial genome," *Nature*, vol. 290, no. 5806, pp. 457–465, 1981.

[90] S. Papa, "Mitochondrial oxidative phosphorylation changes in the life span. Molecular aspects and physiopathological implications," *Biochimica et Biophysica Acta: Bioenergetics*, vol. 1276, no. 2, pp. 87–105, 1996.

[91] O. W. Griffith and A. Meister, "Origin and turnover of mitochondrial glutathione," *Proceedings of the National Academy of Sciences of the United States of America*, vol. 82, no. 14, pp. 4668–4672, 1985.

[92] D. R. Green and G. Kroemer, "The pathophysiology of mitochondrial cell death," *Science*, vol. 305, no. 5684, pp. 626–629, 2004.

[93] M. O. Hengartner, "The biochemistry of apoptosis," *Nature*, vol. 407, no. 6805, pp. 770–776, 2000.

[94] D. J. Reed, "Mitochondrial glutathione and chemically induced stress including ethanol," *Drug Metabolism Reviews*, vol. 36, no. 3-4, pp. 569–582, 2004.

[95] J. R. Hong, "Betanodavirus: mitochondrial disruption and necrotic cell death," *World Journal of Virology*, vol. 2, no. 1, pp. 1–5, 2013.

[96] J. D. Malhotra and R. J. Kaufman, "Endoplasmic reticulum stress and oxidative stress: a vicious cycle or a double-edged sword?" *Antioxidants and Redox Signaling*, vol. 9, no. 12, pp. 2277–2293, 2007.

[97] G. Ermak and K. J. A. Davies, "Calcium and oxidative stress: from cell signaling to cell death," *Molecular Immunology*, vol. 38, no. 10, pp. 713–721, 2002.

[98] M. J. Berridge, M. D. Bootman, and H. L. Roderick, "Calcium signalling: dynamics, homeostasis and remodelling," *Nature Reviews Molecular Cell Biology*, vol. 4, no. 7, pp. 517–529, 2003.

[99] A. Görlach, P. Klappa, and T. Kietzmann, "The endoplasmic reticulum: folding, calcium homeostasis, signaling, and redox control," *Antioxidants and Redox Signaling*, vol. 8, no. 9-10, pp. 1391–1418, 2006.

[100] B. Lizák, I. Czegle, M. Csala, A. Benedetti, J. Mandl, and G. Bánhegyi, "Translocon pores in the endoplasmic reticulum are permeable to small anions," *American Journal of Physiology: Cell Physiology*, vol. 291, no. 3, pp. C511–C517, 2006.

[101] E. Cadenas, "Basic mechanisms of antioxidant activity," *BioFactors*, vol. 6, no. 4, pp. 391–397, 1997.

[102] A. K. Stout, H. M. Raphael, B. I. Kanterewicz, E. Klann, and I. J. Reynolds, "Glutamate-induced neuron death requires mitochondrial calcium uptake," *Nature Neuroscience*, vol. 1, no. 5, pp. 366–373, 1998.

[103] E. White, J. S. Shannon, and R. E. Patterson, "Relationship between vitamin and calcium supplement use and colon cancer," *Cancer Epidemiology Biomarkers and Prevention*, vol. 6, no. 10, pp. 769–774, 1997.

[104] A. R. Smith, S. V. Shenvi, M. Widlansky, J. H. Suh, and T. M. Hagen, "Lipoic acid as a potential therapy for chronic diseases associated with oxidative stress," *Current Medicinal Chemistry*, vol. 11, no. 9, pp. 1135–1146, 2004.

[105] Y. Sharoni, M. Danilenko, N. Dubi, A. Ben-Dor, and J. Levy, "Carotenoids and transcription," *Archives of Biochemistry and Biophysics*, vol. 430, no. 1, pp. 89–96, 2004.

[106] G. N. Schrauzer, "Interactive effects of selenium and chromium on mammary tumor development and growth in MMTV-infected female mice and their relevance to human cancer," *Biological Trace Element Research*, vol. 109, no. 3, pp. 281–292, 2006.

[107] L. Packer and Y. J. Suzuki, "Vitamin E and alpha-lipoate: role in antioxidant recycling and activation of the NF-κB transcription factor," *Molecular Aspects of Medicine*, vol. 14, no. 3, pp. 229–239, 1993.

[108] W. A. Pryor, "Vitamin E and heart disease: basic science to clinical intervention trials," *Free Radical Biology and Medicine*, vol. 28, no. 1, pp. 141–164, 2000.

[109] H. Nakamura, K. Nakamura, and J. Yodoi, "Redox regulation of cellular activation," *Annual Review of Immunology*, vol. 15, pp. 351–369, 1997.

[110] E. R. Miller III, R. Pastor-Barriuso, D. Dalal, R. A. Riemersma, L. J. Appel, and E. Guallar, "Meta-analysis: high-dosage vitamin E supplementation may increase all-cause mortality," *Annals of Internal Medicine*, vol. 142, no. 1, pp. 37–46, 2005.

[111] G. N. Landis and J. Tower, "Superoxide dismutase evolution and life span regulation," *Mechanisms of Ageing and Development*, vol. 126, no. 3, pp. 365–379, 2005.

[112] S. Kojo, "Vitamin C: basic metabolism and its function as an index of oxidative stress," *Current Medicinal Chemistry*, vol. 11, no. 8, pp. 1041–1064, 2004.

[113] M. V. Catani, A. Rossi, A. Costanzo et al., "Induction of gene expression via activator protein-1 in the ascorbate protection against UV-induced damage," *Biochemical Journal*, vol. 356, no. 1, pp. 77–85, 2001.

[114] G. W. Burton and K. U. Ingold, "β-Carotene: an unusual type of lipid antioxidant," *Science*, vol. 224, no. 4649, pp. 569–573, 1984.

[115] A. Carr and B. Frei, "Does vitamin C act as a pro-oxidant under physiological conditions?" *FASEB Journal*, vol. 13, no. 9, pp. 1007–1024, 1999.

[116] A. El-Agamey, G. M. Lowe, D. J. McGarvey et al., "Carotenoid radical chemistry and antioxidant/pro-oxidant properties," *Archives of Biochemistry and Biophysics*, vol. 430, no. 1, pp. 37–48, 2004.

[117] R. Masella, R. Di Benedetto, R. Varì, C. Filesi, and C. Giovannini, "Novel mechanisms of natural antioxidant compounds in biological systems: involvement of glutathione and glutathione-related enzymes," *Journal of Nutritional Biochemistry*, vol. 16, no. 10, pp. 577–586, 2005.

[118] C. W. Nogueira, G. Zeni, and J. B. T. Rocha, "Organoselenium and organotellurium compounds: toxicology and pharmacology," *Chemical Reviews*, vol. 104, no. 12, pp. 6255–6285, 2004.

[119] D. P. Jones, J. L. Carlson, V. C. Mody Jr., J. Cai, M. J. Lynn, and P. Sternberg Jr., "Redox state of glutathione in human plasma," *Free Radical Biology and Medicine*, vol. 28, no. 4, pp. 625–635, 2000.

[120] W. C. L. Ford and A. Harrison, "The role of oxidative phosphorylation in the generation of ATP in human spermatozoa," *Journal of Reproduction and Fertility*, vol. 63, no. 1, pp. 271–278, 1981.

[121] J. Fuchs, F. Ochsendorf, H. Schofer, R. Milbradt, and H. Rubsamen-Waigmann, "Oxidative imbalance in HIV infected patients," *Medical Hypotheses*, vol. 36, no. 1, pp. 60–64, 1991.

[122] T. Oda, T. Akaike, T. Hamamoto, F. Suzuki, T. Hirano, and H. Maeda, "Oxygen radicals in influenza-induced pathogenesis and treatment with pyran polymer-conjugated SOD," *Science*, vol. 244, no. 4907, pp. 974–976, 1989.

[123] T. Akaike, M. Ando, T. Oda et al., "Dependence on O2-generation by xanthine oxidase of pathogenesis of influenza virus infection in mice," *Journal of Clinical Investigation*, vol. 85, no. 3, pp. 739–745, 1990.

[124] E. Peterhans, T. W. Jungi, and R. Stocker, "Autotoxicity and reactive oxygen in viral disease," in *Oxy-Radicals in Molecular Biology and Pathology*, pp. 543–562, Alan R. Liss, New York, NY, USA, 1988.

[125] G. Nabel and D. Baltimore, "An inducible transcription factor activates expression of human immunodeficiency virus in T cells," *Nature*, vol. 326, no. 6114, pp. 711–713, 1987.

[126] P. A. Baeuerle and D. Baltimore, "Activation of DNA-binding activity in an apparently cytoplasmic precursor of the NF-κB transcription factor," *Cell*, vol. 53, no. 2, pp. 211–217, 1988.

[127] F. J. T. Staal, M. Roederer, L. A. Herzenberg, and L. A. Herzenberg, "Intracellular thiols regulate activation of nuclear factor κB and transcription of human immunodeficiency virus," *Proceedings of the National Academy of Sciences of the United States of America*, vol. 87, no. 24, pp. 9943–9947, 1990.

[128] M. J. Lenardo and D. Baltimore, "NK-κB: a pleiotropic mediator of inducible and tissue-specific gene control," *Cell*, vol. 58, no. 2, pp. 227–229, 1989.

[129] M. A. Brach, S. de Vos, C. Arnold, H.-J. Gruss, R. Mertelsmann, and F. Herrmann, "Leukotriene B4 transcriptionally activates interleukin-6 expression involving NK-κB and NF-IL6," *European Journal of Immunology*, vol. 22, no. 10, pp. 2705–2711, 1992.

[130] M. Meyer, H. L. Pahl, and P. A. Baeuerle, "Regulation of the transcription factors NF-κB and AP-1 by redox changes," *Chemico-Biological Interactions*, vol. 91, no. 2-3, pp. 91–100, 1994.

[131] A. Favier, C. Sappey, P. Leclerc, P. Faure, and M. Micoud, "Antioxidant status and lipid peroxidation in patients infected with HIV," *Chemico-Biological Interactions*, vol. 91, no. 2-3, pp. 165–180, 1994.

[132] J.-P. Revillard, C. M. A. Vincent, A. E. Favier, M.-J. Richard, M. Zittoun, and M. D. Kazatchkine, "Lipid peroxidation in human immunodeficiency virus infection," *Journal of Acquired Immune Deficiency Syndromes*, vol. 5, no. 6, pp. 637–638, 1992.

[133] A. Sonnerborg, G. Carlin, B. Akerlund, and C. Jarstrand, "Increased production of malondialdehyde in patients with HIV infection," *Scandinavian Journal of Infectious Diseases*, vol. 20, no. 3, pp. 287–290, 1988.

[134] C. Jarstrand and B. Akerlund, "Oxygen radical release by neutrophils of HIV-infected patients," *Chemico-Biological Interactions*, vol. 91, no. 2-3, pp. 141–146, 1994.

[135] B. Halliwell and J. M. C. Gutteridge, "Role of free radicals and catalytic metal ions in human disease: an overview," *Methods in Enzymology*, vol. 186, pp. 1–85, 1990.

[136] V. M. Polyakov, A. P. Shepelev, O. E. Kokovkina, and I. V. Vtornikova, "Superoxide anion (02-) production and enzymatic disbalance in peripheral blood cells isolated from HIV-infected children," *Free Radical Biology & Medicine*, vol. 16, article 15, 1994.

[137] J. A. Leff, M. A. Oppegard, T. J. Curiel, K. S. Brown, R. T. Schooley, and J. E. Repine, "Progressive increases in serum catalase activity in advancing human immunodeficiency virus infection," *Free Radical Biology and Medicine*, vol. 13, no. 2, pp. 143–149, 1992.

[138] D. M. Hockenbery, Z. N. Oltvai, X.-M. Yin, C. L. Milliman, and S. J. Korsmeyer, "Bcl-2 functions in an antioxidant pathway to prevent apoptosis," *Cell*, vol. 75, no. 2, pp. 241–251, 1993.

[139] A. G. Laurent-Crawford, B. Krust, S. Muller et al., "The cytopathic effect of HIV is associated with apoptosis," *Virology*, vol. 185, no. 2, pp. 829–839, 1991.

[140] H. C. Greenspan and O. I. Aruoma, "Oxidative stress and apoptosis in HIV infection: a role for plant-derived metabolites with synergistic antioxidant activity," *Immunology Today*, vol. 15, no. 5, pp. 209–213, 1994.

[141] W. Dröge, H. P. Eck, and S. Mihm, "Oxidant-antioxidant status in human immunodeficiency virus infection," in *Oxygen Radicals in Biological Systems*, L. Packer, Ed., pp. 594–601, Academic Press, San Diego, Calif, USA, 1994.

[142] M. Kaul, J. Zheng, S. Okamoto, H. E. Gendelman, and S. A. Lipton, "HIV-1 infection and AIDS: consequences for the central nervous system," *Cell Death and Differentiation*, vol. 12, no. 1, pp. 878–892, 2005.

[143] D. Carroll-Anzinger, A. Kumar, V. Adarichev, F. Kashanchi, and L. Al-Harthi, "Human immunodeficiency virus-restricted replication in astrocytes and the ability of gamma interferon to modulate this restriction are regulated by a downstream effector of the Wnt signaling pathway," *Journal of Virology*, vol. 81, no. 11, pp. 5864–5871, 2007.

[144] P. V. B. Reddy, N. Gandhi, T. Samikkannu et al., "HIV-1 gp120 induces antioxidant response element-mediated expression in primary astrocytes: role in HIV associated neurocognitive disorder," *Neurochemistry International*, vol. 61, pp. 807–814, 2012.

[145] P. T. Ronaldson and R. Bendayan, "HIV-1 viral envelope glycoprotein gp120 produces oxidative stress and regulates the

functional expression of multidrug resistance protein-1 (Mrp1) in glial cells," *Journal of Neurochemistry*, vol. 106, no. 3, pp. 1298–1313, 2008.

[146] P. S. Silverstein, A. Shah, J. Weemhoff, S. Kumar, D. P. Singh, and A. Kumar, "HIV-1 gp120 and drugs of abuse: interactions in the central nervous system," *Current HIV Research*, vol. 10, pp. 369–383, 2012.

[147] J. Brown III, C. Theisler, S. Silberman et al., "Differential expression of cholesterol hydroxylases in Alzheimer's disease," *Journal of Biological Chemistry*, vol. 279, no. 33, pp. 34674–34681, 2004.

[148] A. Shah, S. Kumar, S. D. Simon et al., "HIV gp120-and methamphetamine-mediated oxidative stress induces astrocyte apoptosis via cytochrome P450 2E1," *Cell Death & Disease*, vol. 4, no. 10, article e850, 2013.

[149] M. Park, B. Hennig, and M. Toborek, "Methamphetamine alters occludin expression via NADPH oxidase-induced oxidative insult and intact caveolae," *Journal of Cellular and Molecular Medicine*, vol. 16, no. 2, pp. 362–375, 2012.

[150] A. Banerjee, X. Zhang, K. R. Manda, W. A. Banks, and N. Ercal, "HIV proteins (gp120 and Tat) and methamphetamine in oxidative stress-induced damage in the brain: potential role of the thiol antioxidant N-acetylcysteine amide," *Free Radical Biology and Medicine*, vol. 48, no. 10, pp. 1388–1398, 2010.

[151] P. S. Silverstein, A. Shah, R. Gupte et al., "Methamphetamine toxicity and its implications during HIV-1 infection," *Journal of NeuroVirology*, vol. 17, no. 5, pp. 401–415, 2011.

[152] J.-P. Louboutin and D. S. Strayer, "Blood-brain barrier abnormalities caused by HIV-1 gp120: mechanistic and therapeutic implications," *The Scientific World Journal*, vol. 2012, Article ID 482575, 15 pages, 2012.

[153] H. Yao, J. E. Allen, X. Zhu, S. Callen, and S. Buch, "Cocaine and human immunodeficiency virus type 1 gp120 mediate neurotoxicity through overlapping signaling pathways," *Journal of NeuroVirology*, vol. 15, no. 2, pp. 164–175, 2009.

[154] K. Dasuri, L. Zhang, and J. N. Keller, "Oxidative stress, neurodegeneration, and the balance of protein degradation and protein synthesis," *Free Radical Biology and Medicine*, vol. 62, pp. 170–185, 2012.

[155] V. Mollace, H. S. L. M. Nottet, P. Clayette et al., "Oxidative stress and neuroAIDS: triggers, modulators and novel antioxidants," *Trends in Neurosciences*, vol. 24, no. 7, pp. 411–416, 2001.

[156] M. Jin, A. Ande, A. Kumar, and S. Kumar, "Regulation of cytochrome P450 2e1 expression by ethanol: role of oxidative stress-mediated pkc/jnk/sp1 pathway," *Cell Death & Disease*, vol. 4, article e554, 2013.

[157] A. Ande, R. Earla, M. Jin et al., "An LC-MS/MS method for concurrent determination of nicotine metabolites and the role of CYP2A6 in nicotine metabolite-mediated oxidative stress in SVGA astrocytes," *Drug and Alcohol Dependence*, vol. 125, pp. 49–59, 2012.

[158] R. P. Meyer, M. Gehlhaus, R. Knoth, and B. Volk, "Expression and function of cytochrome P450 in brain drug metabolism," *Current Drug Metabolism*, vol. 8, no. 4, pp. 297–306, 2007.

[159] A. A. Eid, Y. Gorin, B. M. Fagg et al., "Mechanisms of podocyte injury in diabetes role of cytochrome P450 and NADPH oxidases," *Diabetes*, vol. 58, no. 5, pp. 1201–1211, 2009.

[160] S. Sorce, K. H. Krause, and V. Jaquet, "Targeting NOX enzymes in the central nervous system: therapeutic opportunities," *Cellular and Molecular Life Sciences*, vol. 69, pp. 2387–2407, 2012.

[161] B. Cairns, J. Y. Kim, X. N. Tang, and M. A. Yenari, "NOX inhibitors as a therapeutic strategy for stroke and neurodegenerative disease," *Current Drug Targets*, vol. 13, no. 2, pp. 199–206, 2012.

[162] K. Bedard and K.-H. Krause, "The NOX family of ROS-generating NADPH oxidases: physiology and pathophysiology," *Physiological Reviews*, vol. 87, no. 1, pp. 245–313, 2007.

[163] R. F. van Golen, T. M. van Gulik, and M. Heger, "Mechanistic overview of reactive species-induced degradation of the endothelial glycocalyx during hepatic ischemia/reperfusion injury," *Free Radical Biology and Medicine*, vol. 52, no. 8, pp. 1382–1402, 2012.

[164] Anonymous, "World health organization—hepatitis C: global prevalence," *Weekly Epidemiological Record*, vol. 72, pp. 341–344, 1997.

[165] H. J. Alter and L. B. Seeff, "Recovery, persistence, and sequelae in hepatitis C virus infection: a perspective on long-term outcome," *Seminars in Liver Disease*, vol. 20, no. 1, pp. 17–35, 2000.

[166] M. W. Fried, M. L. Shiffman, K. Rajender Reddy et al., "Peginterferon alfa-2a plus ribavirin for chronic hepatitis C virus infection," *The New England Journal of Medicine*, vol. 347, no. 13, pp. 975–982, 2002.

[167] S. J. Hadziyannis, H. Sette Jr., T. R. Morgan et al., "Peginterferon-α2a and ribavirin combination therapy in chronic hepatitis C: a randomized study of treatment duration and ribavirin dose," *Annals of Internal Medicine*, vol. 140, no. 5, pp. 346–355, 2004.

[168] G. Gong, G. Waris, R. Tanveer, and A. Siddiqui, "Human hepatitis C virus NS5A protein alters intracellular calcium levels, induces oxidative stress, and activates STAT-3 and NF-κB," *Proceedings of the National Academy of Sciences of the United States of America*, vol. 98, no. 17, pp. 9599–9604, 2001.

[169] H. E. Poulsen, H. Prieme, and S. Loft, "Role of oxidative DNA damage in cancer initiation and promotion," *European Journal of Cancer Prevention*, vol. 7, no. 1, pp. 9–16, 1998.

[170] K. B. Schwarz, "Oxidative stress during viral infection: a review," *Free Radical Biology and Medicine*, vol. 21, no. 5, pp. 641–649, 1996.

[171] D. Yadav, H. I. Hertan, P. Schweitzer, E. P. Norkus, and C. S. Pitchumoni, "Serum and liver micronutrient antioxidants and serum oxidative stress in patients with chronic hepatitis C," *American Journal of Gastroenterology*, vol. 97, no. 10, pp. 2634–2639, 2002.

[172] J. Choi, K. J. Lee, Y. Zheng, A. K. Yamaga, M. M. C. Lai, and J.-H. Ou, "Reactive oxygen species suppress hepatitis C virus RNA replication in human hepatoma cells," *Hepatology*, vol. 39, no. 1, pp. 81–89, 2004.

[173] G. Waris and A. Siddiqui, "Hepatitis C virus stimulates the expression of cyclooxygenase-2 via oxidative stress: role of prostaglandin E2 in RNA replication," *Journal of Virology*, vol. 79, no. 15, pp. 9725–9734, 2005.

[174] G. Waris, A. Livolsi, V. Imbert, J.-F. Peyron, and A. Siddiqui, "Hepatitis C virus NS5A and subgenomic replicon activate NF-κB via tyrosine phosphorylation of IκBα and its degradation by calpain protease," *Journal of Biological Chemistry*, vol. 278, no. 42, pp. 40778–40787, 2003.

[175] T. Bowman, R. Garcia, J. Turkson, and R. Jove, "STATs in oncogenesis," *Oncogene*, vol. 19, no. 21, pp. 2474–2488, 2000.

[176] G. Waris, A. Livolsi, V. Imbert, J.-F. Peyron, and A. Siddiqui, "Hepatitis C virus NS5A and subgenomic replicon activate NF-κB via tyrosine phosphorylation of IκBα and its degradation by

calpain protease," *Journal of Biological Chemistry*, vol. 278, no. 42, pp. 40778–40787, 2003.

[177] E. R. Jenny-Avital, "Hepatitis C," *Current Opinion in Infectious Diseases*, vol. 11, no. 3, pp. 293–299, 1998.

[178] I. Saito, T. Miyamura, A. Ohbayashi et al., "Hepatitis C virus infection is associated with the development of hepatocellular carcinoma," *Proceedings of the National Academy of Sciences of the United States of America*, vol. 87, no. 17, pp. 6547–6549, 1990.

[179] X. Forns, R. H. Purcell, and J. Bukh, "Quasispecies in viral persistence and pathogenesis of hepatitis C virus," *Trends in Microbiology*, vol. 7, no. 10, pp. 402–410, 1999.

[180] K. Koike, "Hepatitis C virus contributes to hepatocarcinogenesis by modulating metabolic and intracellular signaling pathways," *Journal of Gastroenterology and Hepatology*, vol. 22, no. 1, pp. S108–S111, 2007.

[181] A. V. Ivanov, O. A. Smirnova, O. N. Ivanova, O. V. Masalova, S. N. Kochetkov, and M. G. Isaguliants, "Hepatitis C virus proteins activate NRF2/ARE pathway by distinct ROS-dependent and independent mechanisms in HUH7 cells," *PLoS ONE*, vol. 6, no. 9, Article ID e24957, 2011.

[182] S. Pal, S. J. Polyak, N. Bano et al., "Hepatitis C virus induces oxidative stress, DNA damage and modulates the DNA repair enzyme NEIL1," *Journal of Gastroenterology and Hepatology*, vol. 25, no. 3, pp. 627–634, 2010.

[183] C. Bureau, J. Bernad, N. Chaouche et al., "Nonstructural 3 protein of hepatitis C virus triggers an oxidative burst in human monocytes via activation of NADPH oxidase," *Journal of Biological Chemistry*, vol. 276, no. 25, pp. 23077–23083, 2001.

[184] M. V. García-Mediavilla, S. Sánchez-Campos, P. González-Pérez et al., "Differential contribution of hepatitis C virus NS5A and core proteins to the induction of oxidative and nitrosative stress in human hepatocyte-derived cells," *Journal of Hepatology*, vol. 43, no. 4, pp. 606–613, 2005.

[185] F. Thorén, A. Romero, M. Lindh, C. Dahlgren, and K. Hellstrand, "A hepatitis C virus-encoded, nonstructural protein (NS3) triggers dysfunction and apoptosis in lymphocytes: role of NADPH oxidase-derived oxygen radicals," *Journal of Leukocyte Biology*, vol. 76, no. 6, pp. 1180–1186, 2004.

[186] C. García-Monzón, P. L. Majano, I. Zubia, P. Sanz, A. Apolinario, and R. Moreno-Otero, "Intrahepatic accumulation of nitrotyrosine in chronic viral hepatitis is associated with histological severity of liver disease," *Journal of Hepatology*, vol. 32, no. 2, pp. 331–338, 2000.

[187] H. Ming-Ju, H. Yih-Shou, C. Tzy-Yen, and C. Hui-Ling, "Hepatitis C virus E2 protein induce reactive oxygen species (ROS)-related fibrogenesis in the HSC-T6 hepatic stellate cell line," *Journal of Cellular Biochemistry*, vol. 112, no. 1, pp. 233–243, 2011.

[188] S. Li, L. Ye, X. Yu et al., "Hepatitis C virus NS4B induces unfolded protein response and endoplasmic reticulum overload response-dependent NF-κB activation," *Virology*, vol. 391, no. 2, pp. 257–264, 2009.

[189] Y. Liang, H. Ye, B. K. Cong, and S. Y. Ho, "Domain 2 of nonstructural protein 5A (NS5A) of hepatitis C virus is natively unfolded," *Biochemistry*, vol. 46, no. 41, pp. 11550–11558, 2007.

[190] H. H. Yen, K. L. Shih, T. T. Lin, W. W. Su, M. S. Soon, and C. S. Liu, "Decreased mitochondrial deoxyribonucleic acid and increased oxidative damage in chronic hepatitis C," *World Journal of Gastroenterology*, vol. 18, no. 36, pp. 5084–5089, 2012.

[191] C. Piccoli, G. Quarato, M. Ripoli et al., "HCV infection induces mitochondrial bioenergetic unbalance: causes and effects," *Biochimica et Biophysica Acta*, vol. 1787, no. 5, pp. 539–546, 2009.

[192] C. Piccoli, R. Scrima, A. D'Aprile et al., "Mitochondrial dysfunction in hepatitis C virus infection," *Biochimica et Biophysica Acta*, vol. 1757, no. 9-10, pp. 1429–1437, 2006.

[193] G. Gong, G. Waris, R. Tanveer, and A. Siddiqui, "Human hepatitis C virus NS5A protein alters intracellular calcium levels, induces oxidative stress, and activates STAT-3 and NF-κB," *Proceedings of the National Academy of Sciences of the United States of America*, vol. 98, no. 17, pp. 9599–9604, 2001.

[194] M. Okuda, K. Li, M. R. Beard et al., "Mitochondrial injury, oxidative stress, and antioxidant gene expression are induced by hepatitis C virus core protein," *Gastroenterology*, vol. 122, no. 2, pp. 366–375, 2002.

[195] M. Jaiswal, N. F. LaRusso, R. A. Shapiro, T. R. Billiar, and G. J. Gores, "Nitric oxide-mediated inhibition of DNA repair potentiates oxidative DNA damage in cholangiocytes," *Gastroenterology*, vol. 120, no. 1, pp. 190–199, 2001.

[196] K. Machida, G. Mcnamara, K. T.-H. Cheng et al., "Hepatitis C virus inhibits DNA damage repair through reactive oxygen and nitrogen species and by interfering with the ATM-NBS1/Mre11/Rad50 DNA repair pathway in monocytes and hepatocytes," *Journal of Immunology*, vol. 185, no. 11, pp. 6985–6998, 2010.

[197] K. Machida, H. Tsukamoto, J.-C. Liu et al., "c-Jun mediates hepatitis C virus hepatocarcinogenesis through signal transducer and activator of transcription 3 and nitric oxide-dependent impairment of oxidative DNA repair," *Hepatology*, vol. 52, no. 2, pp. 480–492, 2010.

[198] J. Choi and J.-H. J. Ou, "Mechanisms of liver injury. III. Oxidative stress in the pathogenesis of hepatitis C virus," *American Journal of Physiology: Gastrointestinal and Liver Physiology*, vol. 290, no. 5, pp. G847–G851, 2006.

[199] S. K. Jain, P. W. Pemberton, A. Smith et al., "Oxidative stress in chronic hepatitis C: not just a feature of late stage disease," *Journal of Hepatology*, vol. 36, no. 6, pp. 805–811, 2002.

[200] E. Peterhans, "Oxidants and antioxidants in viral diseases: disease mechanisms and metabolic regulation," *Journal of Nutrition*, vol. 127, no. 5, pp. 962S–965S, 1997.

[201] O. A. Levander, "Nutrition and newly emerging viral diseases: an overview," *Journal of Nutrition*, vol. 127, no. 5, pp. 948S–950S, 1997.

[202] T. Hennet, H. J. Ziltener, K. Frei, and E. Peterhans, "A kinetic study of immune mediators in the lungs of mice infected with influenza A virus," *Journal of Immunology*, vol. 149, no. 3, pp. 932–939, 1992.

[203] T. Akaike, M. Ando, T. Oda et al., "Dependence on O2-generation by xanthine oxidase of pathogenesis of influenza virus infection in mice," *Journal of Clinical Investigation*, vol. 85, no. 3, pp. 739–745, 1990.

[204] T. Oda, T. Akaike, T. Hamamoto, F. Suzuki, T. Hirano, and H. Maeda, "Oxygen radicals in influenza-induced pathogenesis and treatment with pyran polymer-conjugated SOD," *Science*, vol. 244, no. 4907, pp. 974–976, 1989.

[205] S. C. Kunder, L. Wu, and P. S. Morahan, "Protection against murine cytomegalovirus infection in aged mice and mice with severe combined immunodeficiency disease with the biological response modifiers polyribosinic-polycytidylic acid stabilized with L-lysine and carboxymethylcellulose, maleic anhydride divinyl ether and colony stimulating factor I," *Antiviral Research*, vol. 21, no. 3, pp. 233–245, 1993.

[206] I. Dvoretzky, "Flulike symptoms with interferon," *Journal of the American Academy of Dermatology*, vol. 22, no. 2, pp. 321–322, 1990.

[207] M. E. Belding, S. J. Klebanoff, and C. G. Ray, "Peroxidase-mediated virucidal systems," *Science*, vol. 167, no. 3915, pp. 195–196, 1970.

[208] R. J. Russell, P. S. Kerry, D. J. Stevens et al., "Structure of influenza hemagglutinin in complex with an inhibitor of membrane fusion," *Proceedings of the National Academy of Sciences of the United States of America*, vol. 105, no. 46, pp. 17736–17741, 2008.

[209] R. Rott, H.-D. Klenk, Y. Nagai, and M. Tashiro, "Influenza viruses, cell enzymes, and pathogenicity," *American Journal of Respiratory and Critical Care Medicine*, vol. 152, no. 4, pp. S16–S19, 1995.

[210] H. Kido, K. Sakai, Y. Kishino, and M. Tashiro, "Pulmonary surfactant is a potential endogenous inhibitor of proteolytic activation of Sendai virus and influenza A virus," *FEBS Letters*, vol. 322, no. 2, pp. 115–119, 1993.

[211] T. Hennet, E. Peterhans, and R. Stocker, "Alterations in antioxidant defences in lung and liver of mice infected with influenza A virus," *Journal of General Virology*, vol. 73, no. 1, pp. 39–46, 1992.

[212] J. Geiler, M. Michaelis, P. Naczk et al., "N-acetyl-l-cysteine (NAC) inhibits virus replication and expression of pro-inflammatory molecules in A549 cells infected with highly pathogenic H5N1 influenza A virus," *Biochemical Pharmacology*, vol. 79, no. 3, pp. 413–420, 2010.

[213] H. B. Suliman, L. K. Ryan, L. Bishop, and R. J. Folz, "Prevention of influenza-induced lung injury in mice overexpressing extracellular superoxide dismutase," *American Journal of Physiology: Lung Cellular and Molecular Physiology*, vol. 280, no. 1, pp. L69–L78, 2001.

[214] R. G. Allen and A. K. Balin, "Oxidative influence on development and differentiation: an overview of a free radical theory of development," *Free Radical Biology and Medicine*, vol. 6, no. 6, pp. 631–661, 1989.

[215] M. J. Hitchler and F. E. Domann, "An epigenetic perspective on the free radical theory of development," *Free Radical Biology and Medicine*, vol. 43, no. 7, pp. 1023–1036, 2007.

[216] R. Vlahos, J. Stambas, and S. Selemidis, "Suppressing production of Reactive Oxygen Species (ROS) for influenza A virus therapy," *Trends in Pharmacological Sciences*, vol. 33, no. 1, pp. 3–8, 2012.

[217] B. L. Munday, J. Kwang, and N. Moody, "Betanodavirus infections of teleost fish: a review," *Journal of Fish Diseases*, vol. 25, no. 3, pp. 127–142, 2002.

[218] C. Delsert, N. Morin, and M. Comps, "A fish encephalitis virus that differs from other nodaviruses by its capsid protein processing," *Archives of Virology*, vol. 142, no. 12, pp. 2359–2371, 1997.

[219] H.-C. Wu, C.-S. Chiu, J.-L. Wu et al., "Zebrafish anti-apoptotic protein zfBcl-xL can block betanodavirus protein α-induced mitochondria-mediated secondary necrosis cell death," *Fish and Shellfish Immunology*, vol. 24, no. 4, pp. 436–449, 2008.

[220] D. Gou, N. Jin, and L. Liu, "Gene silencing in mammalian cells by PCR-based short hairpin RNA," *FEBS Letters*, vol. 548, no. 1–3, pp. 113–118, 2003.

[221] Y.-C. Su, J.-L. Wu, and J.-R. Hong, "Betanodavirus nonstructural protein B2: a novel necrotic death factor that induces mitochondria-mediated cell death in fish cells," *Virology*, vol. 385, no. 1, pp. 143–154, 2009.

[222] L.-J. Chen, Y.-C. Su, and J.-R. Hong, "Betanodavirus nonstructural protein B1: a novel anti-necrotic death factor that modulates cell death in early replication cycle in fish cells," *Virology*, vol. 385, no. 2, pp. 444–454, 2009.

[223] C.-W. Chang, Y.-C. Su, G.-M. Her, C.-F. Ken, and J.-R. Hong, "Betanodavirus induces oxidative Stress-Mediated cell death that prevented by Anti-Oxidants and zfcatalase in fish cells," *PLoS ONE*, vol. 6, no. 10, Article ID e25853, 2011.

[224] K. Sugioka, M. Nakano, H. Totsune-Nakano, H. Minakami, S. Tero-Kubota, and Y. Ikegami, "Mechanism of O2- generation in reduction and oxidation cycle of ubiquinones in a model of mitochondrial electron transport systems," *Biochimica et Biophysica Acta: Bioenergetics*, vol. 936, no. 3, pp. 377–385, 1988.

[225] J. F. Turrens and A. Boveris, "Generation of superoxide anion by the NADH dehydrogenase of bovine heart mitochondria," *Biochemical Journal*, vol. 191, no. 2, pp. 421–427, 1980.

[226] J. F. Turrens, A. Alexandre, and A. L. Lehninger, "Ubisemiquinone is the electron donor for superoxide formation by complex III of heart mitochondria," *Archives of Biochemistry and Biophysics*, vol. 237, no. 2, pp. 408–414, 1985.

[227] J. St-Pierre, J. A. Buckingham, S. J. Roebuck, and M. D. Brand, "Topology of superoxide production from different sites in the mitochondrial electron transport chain," *The Journal of Biological Chemistry*, vol. 277, no. 47, pp. 44784–44790, 2002.

[228] M. Ott, V. Gogvadze, and S. Orrenius, "Mitochondria, oxidative stress and cell death," *Apoptosis*, vol. 12, no. 5, pp. 913–922, 2007.

[229] E. Peterhans, "Oxidants and antioxidants in viral diseases: disease mechanisms and metabolic regulation," *The Journal of Nutrition*, vol. 127, no. 5, pp. 962S–965S, 1997.

Hindawi Publishing Corporation
International Journal of Cell Biology
Volume 2014, Article ID 495817, 10 pages
http://dx.doi.org/10.1155/2014/495817

Research Article

Necrostatin-1 Reduces Neurovascular Injury after Intracerebral Hemorrhage

Melanie D. King, Wittstatt A. Whitaker-Lea, James M. Campbell, Cargill H. Alleyne Jr., and Krishnan M. Dhandapani

Department of Neurosurgery, Medical College of Georgia, Georgia Regents University, 1120 15th Street, Augusta, GA 30912, USA

Correspondence should be addressed to Krishnan M. Dhandapani; kdhandapani@gru.edu

Received 11 November 2013; Revised 24 January 2014; Accepted 27 January 2014; Published 6 March 2014

Academic Editor: Claudia Giampietri

Intracerebral hemorrhage (ICH) is the most common form of hemorrhagic stroke, accounting for 15% of all strokes. ICH has the highest acute mortality and the worst long-term prognosis of all stroke subtypes. Unfortunately, the dearth of clinically effective treatment options makes ICH the least treatable form of stroke, emphasizing the need for novel therapeutic targets. Recent work by our laboratory identified a novel role for the necroptosis inhibitor, necrostatin-1, in limiting neurovascular injury in tissue culture models of hemorrhagic injury. In the present study, we tested the hypothesis that necrostatin-1 reduces neurovascular injury after collagenase-induced ICH in mice. Necrostatin-1 significantly reduced hematoma volume by 54% at 72 h after-ICH, as compared to either sham-injured mice or mice administered an inactive, structural analogue of necrostatin-1. Necrostatin-1 also limited cell death by 48%, reduced blood-brain barrier opening by 51%, attenuated edema development to sham levels, and improved neurobehavioral outcomes after ICH. These data suggest a potential clinical utility for necrostatin-1 and/or novel necroptosis inhibitors as an adjunct therapy to reduce neurological injury and improve patient outcomes after ICH.

1. Introduction

Spontaneous intracerebral hemorrhage (ICH) accounts for ~15% of all strokes and induces a 30-day mortality rate of ~40% [1–5]. The rupture of small vessels damaged by chronic hypertension or amyloid angiopathy induces primary ICH, creating a space-occupying hematoma within the brain parenchyma. Hematoma volume directly correlates with neurological deterioration and patient mortality [2, 6–9] and neurosurgical clot evacuation produces more favorable outcomes in subsets of ICH patients; however, many patients are not amenable to surgical intervention due to hematoma location or concurrent intraventricular hemorrhage [10]. As such, conservative management remains a clinical mainstay, reinforcing the notion that ICH is the least treatable form of strokes and stressing the need for novel therapeutic approaches.

Vascular injury and inflammatory activation are predictive markers of hematoma enlargement, development of vasogenic edema, and acute neurological deterioration [11, 12]. Apoptosis of cerebral endothelial cells increased blood-brain barrier (BBB) permeability, vasogenic edema, and neurological impairment after hemorrhagic stroke [13, 14]. Furthermore, activation of the proinflammatory transcription factor, NFκB, correlated with apoptotic cell death within perihematomal blood vessels after ICH [15]. Thus, a reduction in neurovascular injury may improve outcomes after ICH; however, the underlying mechanisms remain poorly defined and contribute to the lack of medical treatment options after ICH.

Inflammation is a conserved immune response to tissue injury. Hemolysis of extravasated erythrocytes triggers the release of proinflammatory mediators in and around the hematoma core. Along these lines, inflammatory activation correlates with increased hematoma expansion, neurological deterioration, and a poor functional recovery after ICH [12, 15–17]. Notably, elevated plasma concentrations of the proinflammatory mediator, tumor necrosis factor-α (TNF-α), clinically correlated with acute hematoma enlargement, edema development, and patient outcome following ICH [18–22].

Similarly, TNF-α expression was acutely increased within the perihematoma tissue using multiple species and models of experimental ICH [23–28]. Coupled with our finding that neurovascular injury directly correlated with TNF-α expression after ICH in mice, TNF-α may induce acute neurological injury after ICH; however, the mechanisms underlying TNF-α-induced neurovascular injury after ICH remain poorly defined.

Recent evidence suggests that TNF-α induces necroptosis, a novel form of cell death that exhibits features of apoptosis, necrosis, and type 2 autophagic death [29–32]. Although the role of necroptotic cell death after ICH remains unexplored, we first reported that hemin, a hemoglobin oxidation byproduct that accumulates within intracranial hematomas [33], induced TNF-α expression and promoted necroptotic cell death in cultured astrocytes [34]. Receptor interacting protein kinase 1 (RIPK1) is a multifunctional protein kinase that interacts with TNF-α receptor (TNFR) to promote NFκB and to activate necroptotic cell death [35–37]. Thus, RIPK1 may represent a novel therapeutic target after ICH. Herein, we hypothesized that necrostatin-1 (Nec-1), a novel and highly selective RIPK1 inhibitor, improves neurological outcomes following ICH.

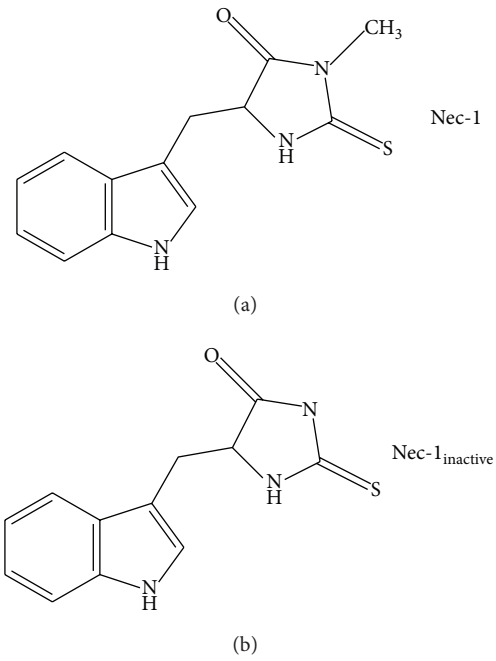

Figure 1: Chemical structures of Nec-1 and Nec-$1_{inactive}$.

2. Materials and Methods

2.1. ICH Model. Animal studies were reviewed and approved by the Committee on Animal Use for Research and Education at Georgia Regents University (Protocol number 2008-0166), in compliance with NIH guidelines. Male CD-1 mice (8–10 weeks old; Charles River, Wilmington, MA, USA) were anesthetized with a cocktail of 8 mg/kg xylazine and 60 mg/kg ketamine. Throughout all surgical procedures, body temperature was maintained at 37°C by using a small-animal temperature controller (David Kopf Instruments, Tujunga, CA, USA). Mice were placed into a stereotactic frame and a 0.5 mm diameter burr hole was drilled over the parietal cortex, 2.2 mm lateral to the bregma. A 26-gauge Hamilton syringe, loaded with 0.04 U of bacterial type IV collagenase in 0.5 μL saline, was lowered 3 mm deep from the skull surface directly into the left striatum. The syringe was depressed at a rate of 450 nL/min and left in place for 10 minutes after the procedure to prevent solution reflux and excess diffusion. Sham animals underwent the same surgical procedure, except that saline was stereotactically injected rather than collagenase. After the syringe was removed, bone wax was used to close the burr hole, the incision was surgically stapled, and mice were kept warm until recovery of the righting reflex. This entire procedure was detailed previously by our structural analog (Nec-$1_{inactive}$) (Tocris, Ballwin, MO, USA; see Figure 1), or saline (placebo) was administered via the intracerebroventricular (icv) route at the time of injury. This dose of Nec-1 and route of administration were based on previous studies showing efficacy in preclinical models of stroke and traumatic brain injury [37, 38].

2.2. Hematoma Volume. Hematoma volume was spectrophotometrically quantified by the QuantiChrom Hemoglobin Assay Kit (Bioassay Systems, Hayward, CA, USA), as per the manufacturer's recommendations and as routine to our laboratory [39]. The amount of hemoglobin in each hemisphere was calculated using the following: [(optical density of sample/optical density of calibrator)$*$100].

2.3. BBB Permeability. BBB permeability was quantified following administration of Evans blue (20 mg/mL in PBS, i.v.) 2 h prior to sacrifice. Blood (100 μL) was obtained by cardiac puncture and centrifuged, and then the plasma was diluted in N,N-Dimethylformamide (1 : 1000). Following perfusion with saline, brains were weighed, solubilized in N,N-Dimethylformamide, and then incubated at 78°C for 18 h. Absorbance was then determined in brain and blood samples at 620 nm using a Synergy HT plate reader (Bio-Tek, Winooski, VT, USA). The concentration of Evans blue (μg/μL) in each sample, a measure of BBB permeability, was calculated using a standard curve, and permeability was equal to [(Evans blue concentration of brain/weight of brain)/(Evans blue concentration of plasma/circulation time)], as reported previously by our group [39, 40].

2.4. Assessment of Cerebral Edema. Brain water content, an established measure of cerebral edema, was quantified in 2 mm coronal tissue sections of the ipsilateral or corresponding contralateral striatum, as routine to our laboratory [39–42]. Tissue was immediately weighed (wet weight) and then dehydrated at 65°C. Samples were reweighed 48 h later to obtain a dry weight. The percentage of water content in each sample was calculated as follows: % Brain water content = [((wet weight−dry weight)/wet weight)$*$100].

2.5. RNA Isolation and qRT-PCR. Total RNA was isolated (SV RNA Isolation kit, Promega, Madison, WI, USA) and qRT-PCR was performed on a Cepheid SmartCycler II (Cepheid, Sunnyvale, CA, USA) using a Superscript III Platinum SYBR Green One-Step qRT-PCR kit (Invitrogen, Carlsbad, CA, USA), as per our laboratory [34, 39, 41–43]. Product specificity was confirmed by melting curve analysis and visualization of a single, appropriately sized band on a 2% agarose gel. Gene expression levels were quantified using a cDNA standard curve and data was normalized to RPS3, a housekeeping gene that is unaffected by the experimental manipulations. Data is expressed as fold change versus sham.

2.6. Immunohistochemistry. Deeply anesthetized mice were perfused with saline followed by 4% paraformaldehyde in PBS. Brains were removed and postfixed in 4% paraformaldehyde overnight at 4°C and then transferred into 30% sucrose. Tissue sections (20 μm) were direct-mounted onto glass slides and stained using a primary antibody against glial fibrillary acidic protein (GFAP; Dako, 1 : 200), as detailed by our laboratory [41, 44]. After labeling with an Alexa-Fluor tagged secondary antibody, immunoreactivity was determined using a Zeiss LSM510 confocal microscope.

2.7. Propidium Iodide Staining. Propidium iodide (PI, 150 ng) was administered via tail vein five hours prior to sacrifice. Following tissue sectioning, brain sections were imaged by confocal microscopy. The number of PI positive cells was quantified by cell counts in three specified regions within the perihematomal regions. Counts were normalized to placebo-treated mice after ICH.

2.8. Neurological Outcomes. Neurological injury was determined using a modified 24-point scale, as detailed previously by our laboratory and others [39, 40, 45, 46]. This scale comprised six behavioral tests, each of which was graded from 0 (performs with no impairment) to 4 (severe impairment). A composite score was calculated as the sum of the grades on all six tests.

2.9. Statistical Analysis. One-way analysis of variance (ANOVA) followed by Student-Newman-Keuls or two-way ANOVA followed by Tukey's post hoc test was used for multiple group comparisons. Data are expressed as mean +/− SEM. A P value of <0.05 was considered to be significant.

3. Results

3.1. Necrostatin-1 Reduces Hematoma Volume after ICH. Administration of Nec-1 significantly reduced hematoma volume within the ipsilateral hemisphere at 72 h after ICH (Figure 2). Specifically, hemoglobin content was increased within the injured hemisphere from 26.5 ± 2.6 mg/dL in sham-operated mice to 80.8 ± 9.9 mg/dL following ICH ($P <$ 0.001 versus sham). Intrastriatal delivery of Nec-1 at the time of ICH reduced hemispheric hemoglobin content to 37.3 ± 8.1 mg/dL ($P < 0.001$ versus ICH, not significantly different from sham). Administration of Nec-1_{inactive} also reduced hemoglobin content after ICH (48.6 ± 7.2 mg/dL; $P < 0.05$ versus sham-, ICH-, and Nec-1-treated mice).

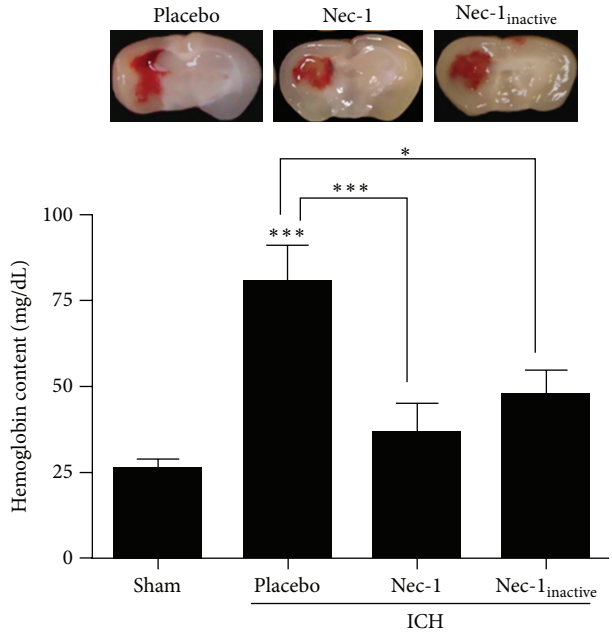

Figure 2: Nec-1 attenuates hematoma size after ICH. Nec-1 administration at the time of injury reduced hematoma size at 72 h after ICH. Coronal brain images were prepared and digitally captured to visualize hematoma size (top panels). Hematoma volume was quantified by determining the hemoglobin content of each hemisphere at 72 hours after ICH (bottom panel). Data are expressed as mean ± SEM ($^{*}P < 0.05$, $^{***}P < 0.001$; n = 10–14 per group). Nec-1 and Nec-1_{inactive} were not significantly different from sham group.

3.2. Cell Death Is Attenuated by Necrostatin-1 after ICH. The effect of Nec-1 on hematoma volume was mirrored by brain lesion volume, as assessed by hematoxylin and eosin staining (data not shown). Consistent with this finding, Nec-1 reduced the number of propidium iodide positive (PI^{+}) cells within the perihematomal tissue by 48%, as compared to ICH only mice ($P < 0.01$) (Figure 3). In contrast, Nec-1_{inactive} reduced the number of PI^{+} cells by 6.3% (not significantly different from placebo treated after ICH). Astrogliosis, a conserved response to brain injury [47, 48], was similarly reduced by Nec-1 treatment. Administration of Nec-1 reduced GFAP expression after ICH, as assessed by Western blotting and by immunohistochemistry, consistent with the attenuation of cellular injury (Figure 4). Coupled with our observation that Nec-1 attenuated proinflammatory gene expression, including reduced TNF-α expression (MEK and KMD, unpublished observations), these findings suggest that necroptosis contributes to glial reactivity after ICH.

3.3. Necrostatin-1 Reduces Neurovascular Injury after ICH. Cerebral edema is a major cause of patient deterioration after ICH. Over the first 24 h after ICH, a significant increase in Evans blue extravasation, a sensitive measure of blood-brain

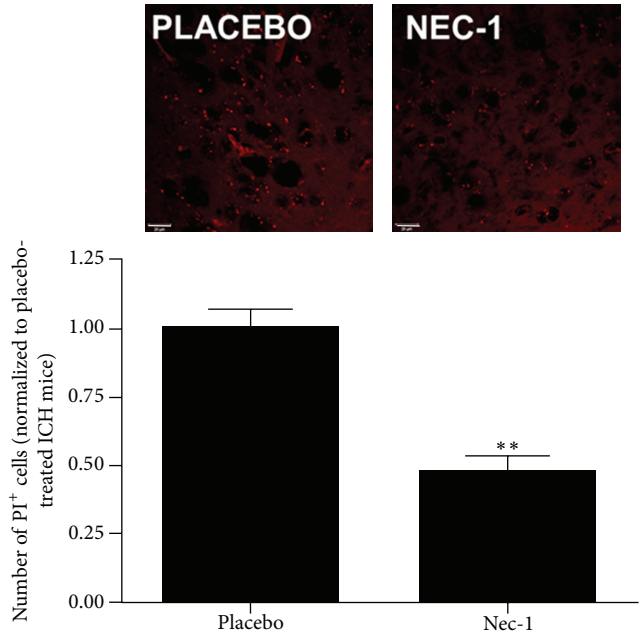

Figure 3: Nec-1 reduces cell death after ICH. Nec-1 administration at the time of ICH reduced perihematomal cell death, as assessed by PI staining. Top panels are representative images from placebo- or Nec-1-treated mice following ICH. Bottom panel depicts the quantification of PI staining following treatment with Nec-1 or Nec-$1_{inactive}$. Cell counts were normalized to placebo-treated ICH mice. Data are expressed as mean ± SEM ($^{**}P < 0.01$ versus placebo; $n = 5$ per group).

barrier disruption, is observed. This breach in the blood-brain barrier was maximal between 3 and 12 h after injury, with spontaneous resealing observed at 24 h. Administration of Nec-1 at the time of injury significantly reduced Evans blue extravasation at all time points (Figure 5). In contrast, Nec-$1_{inactive}$ did not significantly reduce blood-brain barrier opening at any time point, as compared to placebo-treated mice, suggesting a specific effect of Nec-1.

BBB opening contributes to the development of vasogenic edema; thus, the effect of Nec-1 on edema development was next assessed. As was observed with Evans blue extravasation, Nec-1 reduced brain water content at all time points up to 5 days after ICH. The maximal effect of Nec-1 was noted at 24 h after ICH whereby brain water content was reduced from 80.3 ± 0.2% in placebo-treated ICH mice to 76.8 ± 0.4% following Nec-1 administration ($P < 0.05$ versus placebo) (Figure 6). As was observed with BBB opening, Nec-$1_{inactive}$ was without effect on brain edema development after ICH (82.7 ± 0.7%; $P < 0.05$ versus Nec-1, not significantly different from placebo). No significant differences were observed between groups in the contralateral hemispheres.

3.4. Necrostatin-1 Improves Neurological Outcomes after ICH. In line with a reduction in cell death and reduced edema development, necrostatin-1 improved neurological outcomes after ICH. Specifically, necrostatin-1 significantly improved the outcomes using a 24-point scale across the first 72 h after injury, as compared to either placebo- or Nec-$1_{inactive}$-treated mice after ICH ($P < 0.001$ versus placebo-, Nec-$1_{inactive}$-treated ICH mice) (Figure 7). Mice treated with necrostatin-1 were behaviorally not significantly different from sham-operated mice.

4. Discussion

ICH, the most common form of hemorrhagic stroke, is associated with the highest mortality and the worst long-term neurological outcomes of all stroke subtypes [6]. One-year mortality rates are >60% and of the ~67,000 Americans suffering an ICH annually, <20% recover functional independence after six months [1, 2, 49]. Notably, the incidence of ICH is expected to double over the next several decades due to an aging population and to changes in racial demographics [3]. These data emphasize the devastating nature of ICH and indicate the need for improved treatment options.

Extravasation of erythrocytes creates a space-occupying hematoma within the brain parenchyma [6–9, 50–54]. Hematoma growth continues over the ensuing hours due to rebleeding from the ruptured arteriole, bleeding in surrounding compressed vessels, and/or local clotting defects after vessel rupture [6, 8, 50]. The persistent or recurrent bleeding exacerbates the mass lesion, induces local compression of the microvasculature, and contributes to subsequent neurovascular dysfunction [3, 6–8, 50–53, 55, 56]. Hemolysis promotes spontaneous hematoma resolution; however, the concurrent production of hemoglobin degradation metabolites induces the release of proinflammatory mediators within and around the hematoma core. Along these lines, acute increases in TNF-α within the cerebrospinal fluid and plasma of spontaneous ICH patients correlated with patient mortality [22]. Furthermore, increased expression of

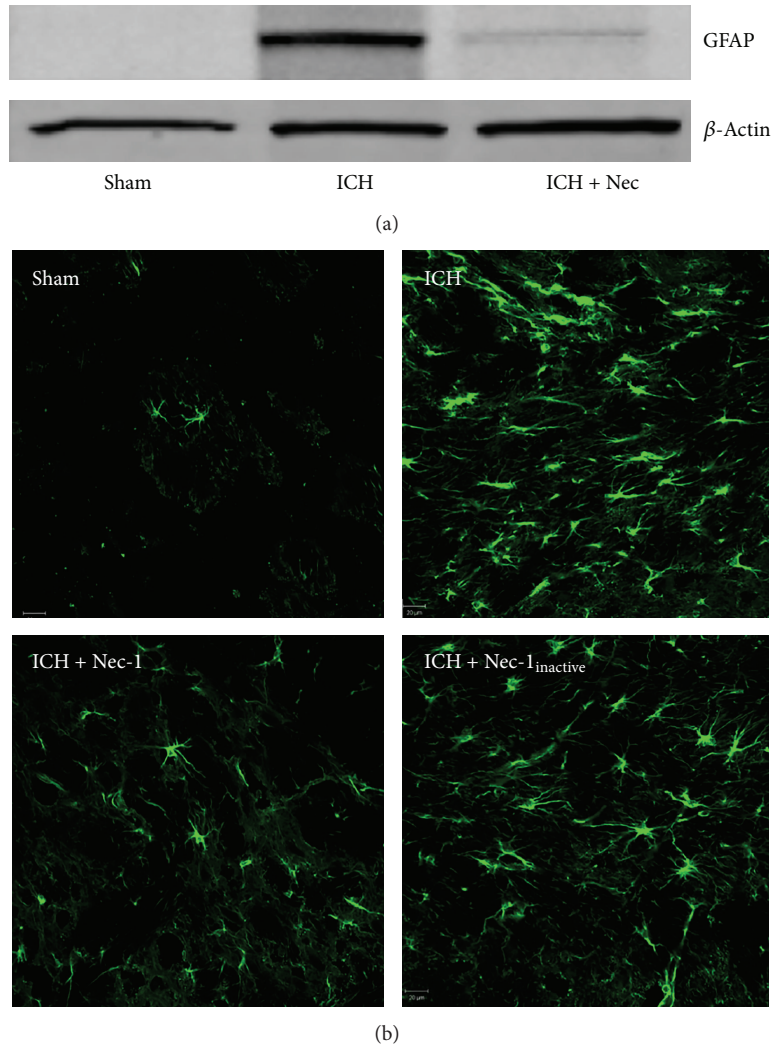

Figure 4: Effect of Nec-1 on ICH-induced reactive gliosis. Reactive astrogliosis was visualized by (a) Western blotting or (b) immunohistochemistry for glial fibrillary acidic protein (GFAP) at 72 h after ICH. GFAP immunoreactivity was increased and exhibited a characteristic stellate morphology after ICH. Administration of Nec-1 significantly reduced these effects whereas Nec-1_{inactive} was without effect. Data are representative of 5 mice per group. Scale bar = 20 μm.

FasL and a corresponding decrease in s-Fas (an inhibitor of Fas activation) were detected in perihematomal brain tissue from ICH patients, as compared to control patients [57]. Although the functional significance of the inflammatory response remains incompletely understood, acute expression of both FasL and TNF-α was associated with cellular injury and with edema formation after ICH [19, 57, 58]. These findings suggest a detrimental role for the early inflammatory response after ICH, yet the precise mechanisms whereby inflammation contributes to poor patient outcomes remain elusive.

Cell death is an important component of neurological injury after ICH, although the form(s) of cell death after ICH remain poorly defined. Features of both apoptotic and necrotic cell death appear within six hours of injury in perihematomal neurons and glia in preclinical ICH models and in postmortem human studies, with peak injury noted at three days [59–62]. Similarly, loss of plasmalemma integrity, a phenotypic hallmark of necrotic cell death, increased over the first three days after collagenase-induced ICH in mice [63], further suggesting a prominent role for necrosis after ICH. In contrast to the view of necrosis as a passive, irreversible form of cell death, necroptosis is a newly described form of programmed necrosis that is induced by FasL and/or TNF-α [64]. As activation of the proinflammatory transcription factor, NFκB, was associated with cell death after ICH, we hypothesized that necroptosis may contribute to neurovascular injury after a brain hemorrhage. To test this possibility, we investigated whether Nec-1, a novel small molecule inhibitor of necroptosis [64], could reduce neurological injury after ICH.

Herein, we identified a novel role for Nec-1 in reducing cell death, attenuating hematoma expansion, limiting blood-brain barrier disruption, and restricting edema development after ICH. Our findings, which are in agreement with a recent report showing Nec-1 on apoptotic and autophagic cell death

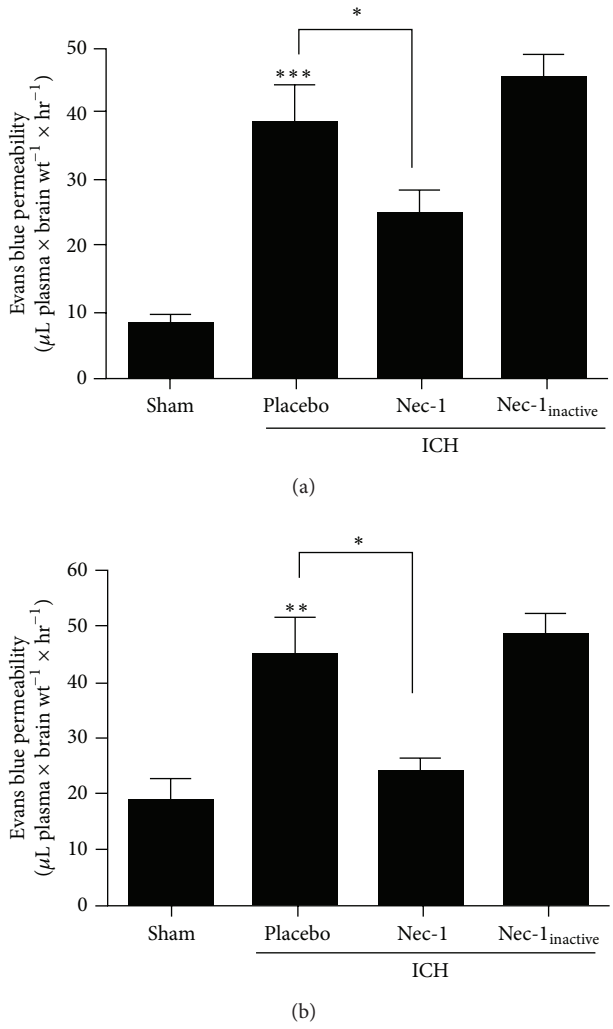

Figure 5: Nec-1 maintains blood-brain barrier integrity after ICH. Mice were administered Nec-1 or Nec-$1_{inactive}$ at the time of collagenase-induced ICH. Evans blue extravasation, a sensitive measure of BBB disruption, was assessed at (a) 3 h or (b) 12 h after ICH. Data are expressed as mean ± SEM and were analyzed by one-way ANOVA followed by Student- Newman-Keuls post hoc test ($^{**}P < 0.01$, $^{***}P < 0.001$, n = 7-8 per group).

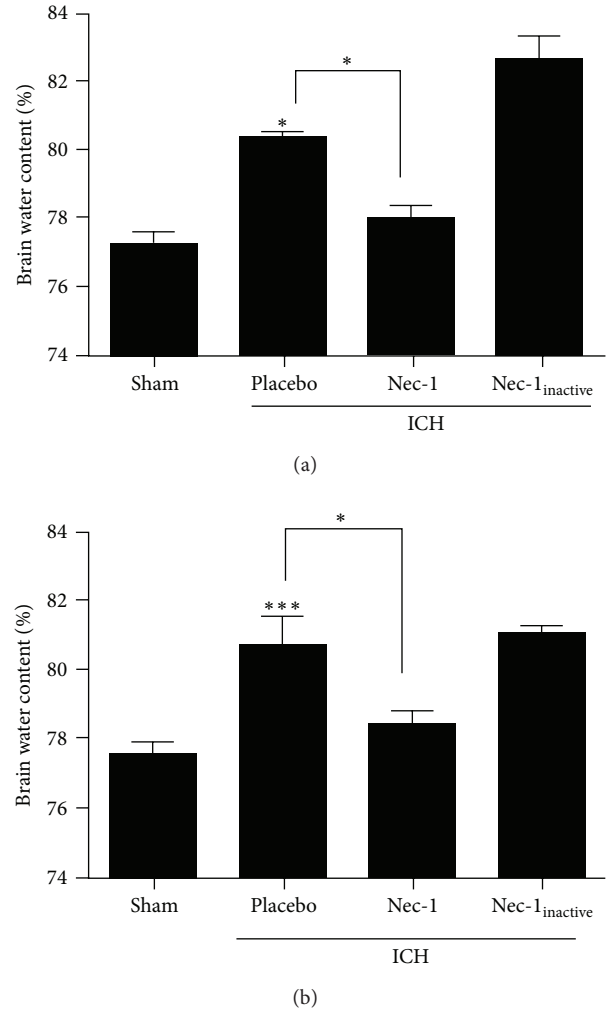

Figure 6: Nec-1 reduced edema development after ICH. Mice were administered Nec-1 or Nec-$1_{inactive}$ at the time of collagenase-induced ICH. Brain water content, a measure of cerebral edema, was assessed in the ipsilateral hemisphere at (a) 24 h or (b) 72 h following ICH. Comparisons within each hemisphere between different treatment groups were done using a one-way ANOVA followed by Student-Newman-Keuls post hoc test ($^{*}P < 0.05$, $^{***}P < 0.001$). Data are expressed as mean ± SEM from 10 mice per group.

after collagenase-induced ICH [65], extend these findings using clinically relevant endpoints and suggest a potential role for targeting cell death pathways after ICH. Although the mechanism(s) whereby Nec-1 limited neurological injury were not explored in this study, it is notable that the biologically inactive, structural analog of Nec-1 did not exert the same protective effects of Nec-1 with respect to BBB opening, edema development, and behavioral outcomes; however, it is noteworthy that Nec-$1_{inactive}$ attenuated hematoma volume to a similar magnitude as compared to Nec-1. Whereas these data suggest that the actions of Nec-1 may be selective rather than due to a nonspecific antioxidant effect, it remains unclear how Nec-$1_{inactive}$ selectively exerted this effect on hematoma volume. Notably, a recent report suggested that Nec-$1_{inactive}$ exerts biological activity on some necroptosis assays and sensitizes mice to lethality during systemic inflammatory response syndrome [66]. These interesting results suggest that caution should be taken in the use of Nec-$1_{inactive}$ as a true biologically inactive control to Nec-1.

Receptor interacting protein 1 (RIP1), the proposed molecular target of Nec-1 [36], is a serine/threonine protein kinase implicated in NFκB activation as well as in the initiation of necroptotic cell death [67]. Inflammatory activation at the time of admission was associated with early neurological deterioration in ICH patients [12] and NFκB activation was sustained over the first several days in a preclinical ICH model [17]. We and others reported that NFκB activation stimulates the expression of inflammatory mediators

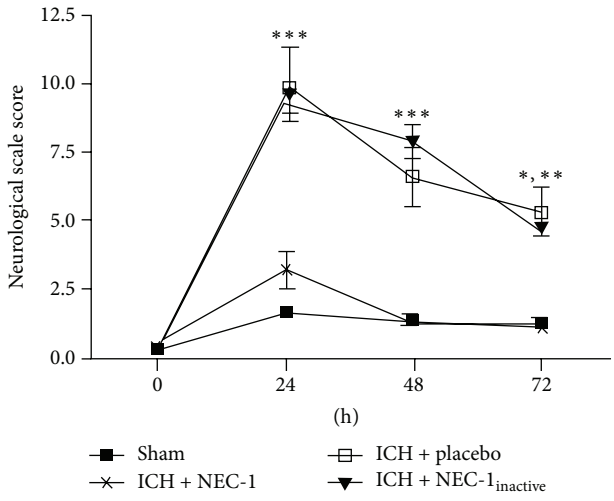

Figure 7: Nec-1 improves neurological outcome after ICH. Mice were administered Nec-1 or Nec-$1_{inactive}$ at the time of collagenase-induced ICH. Neurological outcomes were assessed at 24 h, 48 h, or 72 h following sham or ICH. Data are expressed as mean ± SEM (n = 10/group) and were analyzed using a repeated measures ANOVA followed by Bonferroni's post hoc test ($^{*}P < 0.05$, $^{**}P < 0.01$, $^{***}P < 0.001$).

associated with necroptosis (e.g., TNF-α), induces blood-brain barrier permeability, increases edema development, and exacerbates neurobehavioral deficits after experimental ICH [15, 17, 39]. Furthermore, we reported that the NFκB inhibitor, curcumin, promoted hematoma resolution and improved neurological outcomes after collagenase-induced ICH in mice [39]. Taken together, these results raise the unexplored possibility that RIP1 mediates acute neurological injury after ICH. Future work by our laboratory will characterize this interesting mechanism in further detail.

Nuclear blebbing and karyorrhexis were observed in glial cells within the white matter after intraventricular hemorrhage in preterm infants [68]. Astrocytic loss temporally preceded vascular injury after experimental ICH [28, 62] and focal astrocyte loss increased microvascular damage and induced transient BBB opening [69]. Although the cellular targets of Nec-1 after ICH were beyond the scope of the present study, these findings raise the possibility that the beneficial effects of Nec-1 observed herein may involve, at least in part, maintenance of glial function. Astrocytes are the primary source of the nonenzymatic antioxidant, glutathione, within the brain. We first reported that hemin rapidly depleted intracellular glutathione and induced caspase-independent cell death in murine astrocytes via an inflammatory mechanism [34]. Interestingly, this cellular injury was reversed by Nec-1, suggesting a role for necroptosis after hemorrhagic injury [34]. Our finding is consistent with a subsequent report demonstrating that glutathione depletion enhanced the release of neurotoxic substances, including TNF-α from human astrocytes [70]. Similarly, Nec-1 prevented glutamate-induced glutathione depletion and caspase-independent cytotoxicity in HT-22 cells [71]. Coupled with our recent finding that astrocyte-derived glutathione reduced hemorrhagic injury in cerebral microvessels [72], Nec-1 may improve neurological outcomes by limiting astrocytic dysfunction.

Necroptosis is a novel form of programmed cell death that is initiated by proinflammatory mediators, such as TNF-α. The model of ICH utilized in this study involves the intrastriatal injection of bacterial collagenase. Although this model best recapitulates the spontaneous intracerebral bleeding and evolving hematoma expansion observed in patients, collagenase may induce an exaggerated inflammatory response. Thus, the beneficial effects of Nec-1 may be overestimated. Nonetheless, cells exhibiting both apoptotic and/or necrotic phenotypes characteristic of necroptosis are observed in postmortem human brain sections, suggesting the validity of the protection observed in this study. Another limitation of the present study is that the mechanisms of Nec-1 protection remain undetermined. Although regarded as a highly specific RIP1 inhibitor [36], several *in vitro* studies suggest a possible direct antioxidant role for Nec-1. Furthermore, Nec-1 also may block indoleamine-2,3-dioxygenase (IDO), which catabolizes tryptophan into kynurenine. The inclusion of Nec-$1_{inactive}$ is consistent with a selective effect of Nec-1 as this analogue does not reportedly exhibit antioxidant activity nor does it inhibit mouse IDO [73], although a recent conflicting report suggests that Nec-$1_{inactive}$ may attenuate human IDO activity [66]. Thus, the possibility that some or all of the beneficial actions of Nec-1 are mediated via RIP1-independent mechanisms after ICH cannot be excluded. Future work by our laboratory will further characterize the specific therapeutic role of RIP1 targeting after brain hemorrhage. Regardless of the precise cellular mechanism, these studies suggest a novel protective role for Nec-1 after ICH.

5. Conclusions

The necroptosis inhibitor, Nec-1, reduced neurovascular injury and improved outcomes when administered at the time of injury in a preclinical model of ICH. These data suggest that therapeutic targeting of programmed necrosis may improve patient outcomes after a brain hemorrhage. Future work with more selective necroptosis inhibitors will establish the therapeutic window for improving neurovascular outcomes after ICH, providing a framework for potential clinical translation of these findings.

Conflict of Interests

The authors declare that there is no conflict of interests regarding the publication of this paper.

Acknowledgments

This work was supported by Grants from the National Institute of Health (NS065172, NS075774, and NS084228) and from the American Heart Association (BGIA2300135) to Krishnan M. Dhandapani.

References

[1] M. S. Dennis, J. P. S. Burn, P. A. G. Sandercock, J. M. Bamford, D. T. Wade, and C. P. Warlow, "Long-term survival after first-ever stroke: the Oxfordshire Community Stroke Project," *Stroke*, vol. 24, no. 6, pp. 796–800, 1993.

[2] J. M. Gebel Jr., E. C. Jauch, T. G. Brott et al., "Relative edema volume is a predictor of outcome in patients with hyperacute spontaneous intracerebral hemorrhage," *Stroke*, vol. 33, no. 11, pp. 2636–2641, 2002.

[3] F. Rincon and S. A. Mayer, "Novel therapies for intracerebral hemorrhage," *Current Opinion in Critical Care*, vol. 10, no. 2, pp. 94–100, 2004.

[4] C. Weimar, C. Weber, M. Wagner et al., "Management patterns and health care use after intracerebral hemorrhage: a cost-of-illness study from a societal perspective in Germany," *Cerebrovascular Diseases*, vol. 15, no. 1-2, pp. 29–36, 2003.

[5] M. S. Dennis, "Outcome after brain haemorrhage," *Cerebrovascular Diseases*, vol. 16, supplement 1, pp. 9–13, 2003.

[6] A. I. Qureshi, S. Tuhrim, J. P. Broderick, H. H. Batjer, H. Hondo, and D. F. Hanley, "Spontaneous intracerebral hemorrhage," *The New England Journal of Medicine*, vol. 344, no. 19, pp. 1450–1460, 2001.

[7] G. A. Christoforidis, A. Slivka, Y. Mohammad, C. Karakasis, B. Avutu, and M. Yang, "Size matters: hemorrhage volume as an objective measure to define significant intracranial hemorrhage associated with thrombolysis," *Stroke*, vol. 38, no. 6, pp. 1799–1804, 2007.

[8] M. E. Fewel, B. G. Thompson Jr., and J. T. Hoff, "Spontaneous intracerebral hemorrhage: a review," *Neurosurgical Focus*, vol. 15, no. 4, p. E1, 2003.

[9] P. D. Lyden, A. Shuaib, K. R. Lees et al., "Safety and tolerability of NXY-059 for acute intracerebral hemorrhage: the CHANT trial," *Stroke*, vol. 38, no. 8, pp. 2262–2269, 2007.

[10] A. D. Mendelow, B. A. Gregson, H. M. Fernandes et al., "Early surgery versus initial conservative treatment in patients with spontaneous supratentorial intracerebral haematomas in the International Surgical Trial in Intracerebral Haemorrhage (STICH): a randomised trial," *The Lancet*, vol. 365, no. 9457, pp. 387–397, 2005.

[11] Y. Silva, R. Leira, J. Tejada, J. M. Lainez, J. Castillo, and A. Dávalos, "Molecular signatures of vascular injury are associated with early growth of intracerebral hemorrhage," *Stroke*, vol. 36, no. 1, pp. 86–91, 2005.

[12] R. Leira, A. Dávalos, Y. Silva et al., "Early neurologic deterioration in intracerebral hemorrhage: predictors and associated factors," *Neurology*, vol. 63, no. 3, pp. 461–467, 2004.

[13] T. Doczi, "The pathogenetic and prognostic significance of blood-brain barrier damage at the acute stage of aneurysmal subarachnoid haemorrhage. Clinical and experimental studies," *Acta Neurochirurgica*, vol. 77, no. 3-4, pp. 110–132, 1985.

[14] S. Park, M. Yamaguchi, C. Zhou, J. W. Calvert, J. Tang, and J. H. Zhang, "Neurovascular protection reduces early brain injury after subarachnoid hemorrhage," *Stroke*, vol. 35, no. 10, pp. 2412–2417, 2004.

[15] S. L. Hickenbottom, J. C. Grotta, R. Strong, L. A. Denner, and J. Aronowski, "Nuclear factor-κB and cell death after experimental intracerebral hemorrhage in rats," *Stroke*, vol. 30, no. 11, pp. 2472–2478, 1999.

[16] N. Platt, R. P. da Silva, and S. Gordon, "Recognizing death: the phagocytosis of apoptotic cells," *Trends in Cell Biology*, vol. 8, no. 9, pp. 365–372, 1998.

[17] X. Zhao, Y. Zhang, R. Strong, J. Zhang, J. C. Grotta, and J. Aronowski, "Distinct patterns of intracerebral hemorrhage-induced alterations in NF-κB subunit, iNOS, and COX-2 expression," *Journal of Neurochemistry*, vol. 101, no. 3, pp. 652–663, 2007.

[18] J. S. Kim, S. S. Yoon, Y. H. Kim, and J. S. Ryu, "Serial measurement of interleukin-6, transforming growth factor-β, and S-100 protein in patients with acute stroke," *Stroke*, vol. 27, no. 9, pp. 1553–1557, 1996.

[19] J. Castillo, A. Dávalos, J. Álvarez-Sabín et al., "Molecular signatures of brain injury after intracerebral hemorrhage," *Neurology*, vol. 58, no. 4, pp. 624–629, 2002.

[20] T. Dziedzic, S. Bartus, A. Klimkowicz, M. Motyl, A. Slowik, and A. Szczudlik, "Intracerebral hemorrhage triggers interleukin-6 and interleukin-10 release in blood," *Stroke*, vol. 33, no. 9, pp. 2334–2335, 2002.

[21] C. Woiciechowsky, B. Schöning, J. Cobanov, W. R. Lanksch, H.-D. Volk, and W.-D. Döcke, "Early IL6 plasma concentrations correlate with severity of brain injury and pneumonia in brain-injured patients," *Journal of Trauma*, vol. 52, no. 2, pp. 339–345, 2002.

[22] H.-Y. Fang, W.-J. Ko, and C.-Y. Lin, "Inducible heat shock protein 70, interleukin-18, and tumor necrosis factor alpha correlate with outcomes in spontaneous intracerebral hemorrhage," *Journal of Clinical Neuroscience*, vol. 14, no. 5, pp. 435–441, 2007.

[23] J. Aronowski and C. E. Hall, "New horizons for primary intracerebral hemorrhage treatment: experience from preclinical studies," *Neurological Research*, vol. 27, no. 3, pp. 268–279, 2005.

[24] M. Mayne, W. Ni, H. J. Yan et al., "Antisense oligodeoxynucleotide inhibition of tumor necrosis factor-α expression is neuroprotective after intracerebral hemorrhage," *Stroke*, vol. 32, no. 1, pp. 240–248, 2001.

[25] G. Xi, Y. Hua, R. F. Keep, J. G. Younger, and J. T. Hoff, "Systemic complement depletion diminishes perihematomal brain edema in rats," *Stroke*, vol. 32, no. 1, pp. 162–167, 2001.

[26] A. Lu, Y. Tang, R. Ran, T. L. Ardizzone, K. R. Wagner, and F. R. Sharp, "Brain genomics of intracerebral hemorrhage," *Journal of Cerebral Blood Flow and Metabolism*, vol. 26, no. 2, pp. 230–252, 2006.

[27] K. R. Wagner, S. Beiler, C. Beiler et al., "Delayed profound local brain hypothermia markedly reduces interleukin-1β gene expression and vasogenic edema development in a porcine model of intracerebral hemorrhage," *Acta Neurochirurgica. Supplement*, vol. 96, pp. 177–182, 2006.

[28] J. K. Wasserman, X. Zhu, and L. C. Schlichter, "Evolution of the inflammatory response in the brain following intracerebral hemorrhage and effects of delayed minocycline treatment," *Brain Research*, vol. 1180, no. 1, pp. 140–154, 2007.

[29] G. Kroemer, L. Galluzzi, P. Vandenabeele et al., "Classification of cell death: recommendations of the Nomenclature Committee on Cell Death 2009," *Cell Death and Differentiation*, vol. 16, no. 1, pp. 3–11, 2009.

[30] L. Galluzzi and G. Kroemer, "Necroptosis: a specialized pathway of programmed necrosis," *Cell*, vol. 135, no. 7, pp. 1161–1163, 2008.

[31] J. Hitomi, D. E. Christofferson, A. Ng et al., "Identification of a molecular signaling network that regulates a cellular necrotic cell death pathway," *Cell*, vol. 135, no. 7, pp. 1311–1323, 2008.

[32] C. Kitanaka and Y. Kuchino, "Caspase-independent programmed cell death with necrotic morphology," *Cell Death and Differentiation*, vol. 6, no. 6, pp. 508–515, 1999.

[33] P. B. Letarte, K. Lieberman, K. Nagatani, R. A. Haworth, G. B. Odell, and T. A. Duff, "Hemin: levels in experimental subarachnoid hematoma and effects on dissociated vascular smooth-muscle cells," *Journal of Neurosurgery*, vol. 79, no. 2, pp. 252–255, 1993.

[34] M. D. Laird, C. Wakade, C. H. Alleyne Jr., and K. M. Dhandapani, "Hemin-induced necroptosis involves glutathione depletion in mouse astrocytes," *Free Radical Biology and Medicine*, vol. 45, no. 8, pp. 1103–1114, 2008.

[35] M. A. Kelliher, S. Grimm, Y. Ishida, F. Kuo, B. Z. Stanger, and P. Leder, "The death domain kinase RIP mediates the TNF-induced NF-κB signal," *Immunity*, vol. 8, no. 3, pp. 297–303, 1998.

[36] A. Degterev, J. Hitomi, M. Germscheid et al., "Identification of RIP1 kinase as a specific cellular target of necrostatins," *Nature Chemical Biology*, vol. 4, no. 5, pp. 313–321, 2008.

[37] A. Degterev, Z. Huang, M. Boyce et al., "Chemical inhibitor of nonapoptotic cell death with therapeutic potential for ischemic brain injury," *Nature Chemical Biology*, vol. 1, no. 2, pp. 112–119, 2005.

[38] Z. You, S. I. Savitz, J. Yang et al., "Necrostatin-1 reduces histopathology and improves functional outcome after controlled cortical impact in mice," *Journal of Cerebral Blood Flow and Metabolism*, vol. 28, no. 9, pp. 1564–1573, 2008.

[39] M. D. King, D. J. McCracken, F. M. Wade, S. E. Meiler, C. H. Alleyne Jr., and K. M. Dhandapani, "Attenuation of hematoma size and neurological injury with curcumin following intracerebral hemorrhage in mice: laboratory investigation," *Journal of Neurosurgery*, vol. 115, no. 1, pp. 116–123, 2011.

[40] M. D. King, C. H. Alleyne Jr., and K. M. Dhandapani, "TNF-alpha receptor antagonist, R-7050, improves neurological outcomes following intracerebral hemorrhage in mice," *Neuroscience Letters*, vol. 542, pp. 92–96, 2013.

[41] D. E. Kimbler, J. Shields, N. Yanasak, J. R. Vender, and K. M. Dhandapani, "Activation of P2X7 promotes cerebral edema and neurological injury after traumatic brain injury in mice," *PLoS ONE*, vol. 7, no. 7, Article ID e41229, 2012.

[42] M. D. Laird, S. Sukumari-Ramesh, A. E. B. Swift, S. E. Meiler, J. R. Vender, and K. M. Dhandapani, "Curcumin attenuates cerebral edema following traumatic brain injury in mice: a possible role for aquaporin-4?" *Journal of Neurochemistry*, vol. 113, no. 3, pp. 637–648, 2010.

[43] C. Wakade, M. D. King, M. D. Laird, C. H. Alleyne Jr., and K. M. Dhandapani, "Curcumin attenuates vascular inflammation and cerebral vasospasm after subarachnoid hemorrhage in mice," *Antioxidants and Redox Signaling*, vol. 11, no. 1, pp. 35–45, 2009.

[44] S. Sukumari-Ramesh, C. H. Alleyne Jr., and K. M. Dhandapani, "Astrocyte-specific expression of survivin after intracerebral hemorrhage in mice: a possible role in reactive gliosis?" *Journal of Neurotrauma*, vol. 29, no. 18, pp. 2798–2804, 2012.

[45] G. A. Rosenberg, S. Mun-Bryce, M. Wesley, and M. Kornfeld, "Collagenase-induced intracerebral hemorrhage in rats," *Stroke*, vol. 21, no. 5, pp. 801–807, 1990.

[46] W. Clark, L. Gunion-Rinker, N. Lessov, and K. Hazel, "Citicoline treatment for experimental intracerebral hemorrhage in mice," *Stroke*, vol. 29, no. 10, pp. 2136–2140, 1998.

[47] L. F. Eng and R. S. Ghirnikar, "GFAP and astrogliosis," *Brain Pathology*, vol. 4, no. 3, pp. 229–237, 1994.

[48] M. V. Sofroniew, "Reactive astrocytes in neural repair and protection," *Neuroscientist*, vol. 11, no. 5, pp. 400–407, 2005.

[49] J. Broderick, S. Connolly, E. Feldmann et al., "Guidelines for the management of spontaneous intracerebral hemorrhage in adults: 2007 update: a guideline from the American Heart Association/American Stroke Association Stroke Council, High Blood Pressure Research Council, and the Quality of Care and Outcomes in Research Interdisciplinary Working Group," *Stroke*, vol. 38, no. 6, pp. 2001–2023, 2007.

[50] D. L. Labovitz and R. L. Sacco, "Intracerebral hemorrhage: update," *Current Opinion in Neurology*, vol. 14, no. 1, pp. 103–108, 2001.

[51] J. Wu, Y. Hua, R. F. Keep, T. Nakamura, J. T. Hoff, and G. Xi, "Iron and iron-handling proteins in the brain after intracerebral hemorrhage," *Stroke*, vol. 34, no. 12, pp. 2964–2969, 2003.

[52] D. Davalos, J. Grutzendler, G. Yang et al., "ATP mediates rapid microglial response to local brain injury in vivo," *Nature Neuroscience*, vol. 8, no. 6, pp. 752–758, 2005.

[53] L. P. Wang, F. Li, X. Shen, and J. Z. Tsien, "Conditional knockout of NMDA receptors in dopamine neurons prevents nicotine-conditioned place preference," *PLoS ONE*, vol. 5, no. 1, Article ID e8616, 2010.

[54] S. M. Davis, J. Broderick, M. Hennerici et al., "Hematoma growth is a determinant of mortality and poor outcome after intracerebral hemorrhage," *Neurology*, vol. 66, no. 8, pp. 1175–1181, 2006.

[55] M. R. McLaughlin and D. W. Marion, "Cerebral blood flow and vasoresponsivity within and around cerebral contusions," *Journal of Neurosurgery*, vol. 85, no. 5, pp. 871–876, 1996.

[56] D. G. Nehls, A. D. Mendelow, D. I. Graham, E. J. Sinar, G. M. Teasdale, and R. R. Smith, "Experimental intracerebral hemorrhage: progression of hemodynamic changes after production of a spontaneous mass lesion," *Neurosurgery*, vol. 23, no. 4, pp. 439–444, 1988.

[57] P. Delgado, E. Cuadrado, A. Rosell et al., "Fas system activation in perihematomal areas after spontaneous intracerebral hemorrhage," *Stroke*, vol. 39, no. 6, pp. 1730–1734, 2008.

[58] Y. Hua, J. Wu, R. F. Keep, T. Nakamura, J. T. Hoff, and G. Xi, "Tumor necrosis factor-alpha increases in the brain after intracerebral hemorrhage and thrombin stimulation," *Neurosurgery*, vol. 58, no. 3, pp. 542–550, 2006.

[59] A. P. Nguyen, H. D. Huynh, S. B. Sjovold, and F. Colbourne, "Progressive brain damage and alterations in dendritic arborization after collagenase-induced intracerebral hemorrhage in rats," *Current Neurovascular Research*, vol. 5, no. 3, pp. 171–177, 2008.

[60] K. Matsushita, W. Meng, X. Wang et al., "Evidence for apoptosis after intracerebral hemorrhage in rat striatum," *Journal of Cerebral Blood Flow and Metabolism*, vol. 20, no. 2, pp. 396–404, 2000.

[61] A. I. Qureshi, M. F. Suri, P. T. Ostrow et al., "Apoptosis as a form of cell death in intracerebral hemorrhage," *Neurosurgery*, vol. 52, no. 5, pp. 1041–1047, 2003.

[62] C. Gong, N. Boulis, J. Qian, D. E. Turner, J. T. Hoff, and R. F. Keep, "Intracerebral hemorrhage-induced neuronal death," *Neurosurgery*, vol. 48, no. 4, pp. 875–883, 2001.

[63] X. Zhu, L. Tao, E. Tejima-Mandeville et al., "Plasmalemma permeability and necrotic cell death phenotypes after intracerebral hemorrhage in mice," *Stroke*, vol. 43, no. 2, pp. 524–531, 2012.

[64] D. E. Christofferson and J. Yuan, "Necroptosis as an alternative form of programmed cell death," *Current Opinion in Cell Biology*, vol. 22, no. 2, pp. 263–268, 2010.

[65] P. Chang, W. Dong, M. Zhang et al., "Anti-necroptosis chemical necrostatin-1 can also suppress apoptotic and autophagic pathway to exert neuroprotective effect in mice intracerebral hemorrhage model," *Journal of Molecular Neuroscience*, vol. 52, no. 2, pp. 242–249, 2014.

[66] N. Takahashi, L. Duprez, S. Grootjans et al., "Necrostatin-1 analogues: critical issues on the specificity, activity and in vivo use in experimental disease models," *Cell Death & Disease*, vol. 3, article e437, 2012.

[67] W. Declercq, T. Vanden Berghe, and P. Vandenabeele, "RIP kinases at the crossroads of cell death and survival," *Cell*, vol. 138, no. 2, pp. 229–232, 2009.

[68] S. Chamnanvanakij, L. R. Margraf, D. Burns, and J. M. Perlman, "Apoptosis and white matter injury in preterm infants," *Pediatric and Developmental Pathology*, vol. 5, no. 2, pp. 184–189, 2002.

[69] C. L. Willis, C. C. Nolan, S. N. Reith et al., "Focal astrocyte loss is followed by microvascular damage, with subsequent repair of the blood-brain barrier in the apparent absence of direct astrocytic contact," *Glia*, vol. 45, no. 4, pp. 325–337, 2004.

[70] M. Lee, T. Cho, N. Jantaratnotai, Y. T. Wang, E. McGeer, and P. L. McGeer, "Depletion of GSH in glial cells induces neurotoxicity: relevance to aging and degenerative neurological diseases," *The FASEB Journal*, vol. 24, no. 7, pp. 2533–2545, 2010.

[71] X. Xu, C. C. Chua, J. Kong et al., "Necrostatin-1 protects against glutamate-induced glutathione depletion and caspase-independent cell death in HT-22 cells," *Journal of Neurochemistry*, vol. 103, no. 5, pp. 2004–2014, 2007.

[72] S. Sukumari-Ramesh, M. D. Laird, N. Singh, J. R. Vender, C. H. Alleyne, and K. M. Dhandapani, "Astrocyte-derived glutathione attenuates hemin-induced apoptosis in cerebral microvascular cells," *Glia*, vol. 58, no. 15, pp. 1858–1870, 2010.

[73] A. Degterev, J. L. Maki, and J. Yuan, "Activity and specificity of necrostatin-1, small-molecule inhibitor of RIP1 kinase," *Cell Death and Differentiation*, vol. 20, no. 2, article 366, 2013.

Hindawi Publishing Corporation
International Journal of Cell Biology
Volume 2014, Article ID 152645, 12 pages
http://dx.doi.org/10.1155/2014/152645

Research Article

Changes in the Distribution of the α3 Na^+/K^+ ATPase Subunit in Heterozygous Lurcher Purkinje Cells as a Genetic Model of Chronic Depolarization during Development

Rebecca McFarland,[1,2] Hadi S. Zanjani,[3] Jean Mariani,[3,4] and Michael W. Vogel[1]

[1] *Maryland Psychiatric Research Center, Department of Psychiatry, University of Maryland School of Medicine, P.O. Box 21247, Baltimore, MD 21228, USA*
[2] *Department of Biology, University of Maryland Baltimore County, Baltimore, MD 21201, USA*
[3] *Université Pierre et Marie Curie-P6, UMR7102, 75005 Paris, France*
[4] *Institut de la Longévité, Hôpital Charles Foix, 94205 Ivry-Sur-Seine, France*

Correspondence should be addressed to Michael W. Vogel; vogel.michael1066@gmail.com

Received 9 October 2013; Revised 28 December 2013; Accepted 13 January 2014; Published 27 February 2014

Academic Editor: Alessio D'Alessio

A common assumption of excitotoxic mechanisms in the nervous system is that the ionic imbalance resulting from overstimulation of glutamate receptors and increased Na^+ and Ca^{++} influx overwhelms cellular energy metabolic systems leading to cell death. The goal of this study was to examine how a chronic Na^+ channel leak current in developing Purkinje cells in the heterozygous Lurcher mutant (+/*Lc*) affects the expression and distribution of the α3 subunit of the Na^+/K^+ ATPase pump, a key component of the homeostasis system that maintains ionic equilibrium in neurons. The expression pattern of the catalytic α3 Na^+/K^+ ATPase subunit was analyzed by immunohistochemistry, histochemistry, and Western Blots in wild type (WT) and +/*Lc* cerebella at postnatal days P10, P15, and P25 to determine if there are changes in the distribution of active Na^+/K^+ ATPase subunits in degenerating Purkinje cells. The results suggest that the expression of the catalytic α3 subunit is altered in chronically depolarized +/*Lc* Purkinje cells, although the density of active Na^+/K^+ ATPase pumps is not significantly altered compared with WT in the cerebellar cortex at P15, and then declines from P15 to P25 in the +/*Lc* cerebellum as the +/*Lc* Purkinje cells degenerate.

1. Introduction

The Na^+/K^+ ATPase pump (Na/K pump) in neurons plays a key role in maintaining the transmembrane electrical gradient that is critical for normal function. The mature pump resides in the plasma membrane and exports 3 Na^+ ions for every two K^+ ions it imports at a cost of 1 ATP molecule, resulting in a net outward, hyperpolarizing current [1]. In healthy cerebellar Purkinje cells, increases in the expression levels of the Na/K pump during postnatal development are associated with the gradual hyperpolarization of the Purkinje cell membrane potential [2, 3]. All Na/K pumps contain an alpha (α) and a beta (β) unit, though in some cell types the pump contains an additional FXYD protein [4, 5]. There are at least 4 isoforms of the alpha subunit and 3 isoforms of the beta subunit. The α subunit is the catalytic unit and is responsible for binding of Na^+ and K^+ ions, ATP, and ouabain (an inhibitor). The β subunit plays a crucial role in the structure and maturation of the Na/K pump, including, for example, aiding in the tracking of the α subunit from the ER to the plasma membrane [6]. Cerebellar Purkinje cells exclusively express the α3 and β1 subunits, but some other cerebellar neurons (e.g., basket cells) or structures (e.g., granule cell layer glomeruli) also express the α3 subunit [7]. The FXYD family protein, FXYD1 (Phospholemman), is also expressed in Purkinje cells and the molecular layer of the cerebellum [8], but this protein was not analyzed in this study.

Na/K ATPase activity in neurons may contribute as much as 240 pA to the resting membrane potential and pump activity is increased as a function of neuronal activity [3].

Changes in Na/K pump activity are also associated with the adaptive responses of neurons to hypoxia, ischemia, and cell death [5, 9]. However, whether pump activity is increased or decreased in response to acute models of cellular injury appears to depend on the cell type or injury model [10–13]. There is evidence that Na/K pump activity is directly regulated by a variety of cellular second messenger signaling systems. For example, nitric oxide (NO)/cGMP intracellular signaling can downregulate Na/K pump activity [10]. Conversely, in cerebellar Purkinje cells, carbon monoxide (CO) and glutamate can act through cGMP to promote persistent increases in Na/K pump activity [14]. Under excitotoxic conditions, peroxynitrite and reactive oxygen can react with the Na/K pump to deactivate it [15, 16]. In general, excitotoxic mechanisms in neurons are associated with overstimulation of glutamate receptors resulting in an increased Na^+ and Ca^{++} influx that overwhelms cellular energy metabolic systems leading to cell death [17, 18]. Both increases and decreases in Na/K pump activity may be theoretically associated with neuroprotective or cell-death promoting activities. In chronically depolarized neurons, increased Na/K pump activity could be seen to reduce intracellular Na^+ levels to help restore cellular homeostasis, but the increased demand for ATP could be deleterious. Alternatively, decreased Na/K pump activity in injured cells may allow for increased intracellular Na^+, but the decreased demand for ATP from less active Na/K pumps may be neuroprotective.

A recent study of HEK293 cells expressing $\delta 2$ glutamate receptors (GluRδ2) with the Lurcher mutation, GluR$\delta 2^{Lc}$, found that ectopic expression of the mutant receptor in cultured cells causes a decline in ATP levels [19]. The *Lc* mutation in GluRδ2 turns the receptor into a constitutively open membrane channel that chronically depolarizes the cells expressing the mutant receptor [20]. In the HEK293 *in vitro* studies, the authors speculate that over activation of the Na/K pump in response to the chronic Na^+ leak may consume cellular ATP levels leading to cell death [19, 21]. The purpose of this study is to examine how a chronic Na^+ leak current mediated by the mutant GluR$\delta 2^{Lc}$ receptor in developing Purkinje cells in the heterozygous Lurcher (+/*Lc*) mouse mutant affects the cellular distribution of $\alpha 3$ subunits and active Na/K pumps.

The gene for the GluRδ2 receptor was first identified based on its homology to NMDA and AMPA glutamate receptors, but the receptor does not bind to most glutamate agonists or antagonists, nor does it appear to carry a membrane current under normal circumstances. GluRδ2 is preferentially expressed in cerebellar Purkinje cells, and in the +/*Lc* mutant, cerebellar Purkinje cells become chronically depolarized at the end of the first postnatal week when GluRδ2 receptors are inserted at Purkinje cell-parallel fiber synapses. The majority of +/*Lc* Purkinje cells degenerate during the first month of postnatal life starting at the end of the first week via pathways that have been described as either apoptotic, autophagic, or necrotic [19, 20, 22, 23]. Granule cell death follows as a consequence of the loss of their primary neuron target population, the Purkinje cells: by the end of the second postnatal month, almost all Purkinje cells and 90% of the granule cells have degenerated in the +/*Lc* cerebellum [24]. We have previously hypothesized that before cell death pathways are activated in +/*Lc* Purkinje cells, the chronic depolarization caused by the constitutive cation leak current from the GluR$\delta 2^{Lc}$ channel stresses the neuron's ion exchange and energy production systems [25, 26]. In support of this hypothesis, we have previously shown that cytochrome oxidase activity is dramatically increased in +/*Lc* Purkinje cells through P25 [26] and calcium levels are elevated in +/*Lc* Purkinje cells *in vitro* [27]. In addition, the distal dendrites of +/*Lc* Purkinje cells contain numerous dilated mitochondria, suggesting mitochondrial dysfunction [28]. +/*Lc* Purkinje cells also contain significantly higher levels of nitric oxide synthase (NOS) activity and protein nitration [25]. Stimulation of mitochondrial activity in response to the chronic depolarization is likely to increase the production of reactive oxygen species (ROS) and increases in intracellular Ca^{++} will stimulate NO production. NO and O_2^- free radicals will react to form peroxynitrite, a highly reactive oxidizing agent which can damage and kill cells by tyrosine nitration of critical proteins and membrane lipid peroxidation [29, 30]. The results of this study demonstrate that the expression of the Na/K pump catalytic $\alpha 3$ subunit is increased, or at least more concentrated, in individual +/*Lc* Purkinje cells through P25. However, as +/*Lc* Purkinje cells degenerate by P25, total expression levels of $\alpha 3$ and its 40 kD breakdown product in the +/*Lc* cerebellum declines compared with WT cerebella. The density of active Na/K pumps assayed *ex vivo* is not altered at P15, near the peak of +/*Lc* Purkinje cell death, and decreased at P25 when there are relatively few remaining +/*Lc* Purkinje cells. Our interpretation of the results is that while the expression of the $\alpha 3$ subunit may be increased within individual +/*Lc* Purkinje cells in response to the chronic stress, potential increases in overall ATPase pump activity and ATP consumption due to increased expression of the $\alpha 3$ subunit may be limited by the deactivation and/or degradation of many $\alpha 3$ subunits.

2. Experimental Procedures

2.1. Animals. GluR$\delta 2^{+/Lc}$ mutant and GluR$\delta 2^{+/+}$ wild type (WT) pups were generated by mating B6CBACa A^{w-J}/A-Grid2^{Lc}/J males with WT females (C57BL/6J), both from Jackson Laboratories. All animals were housed in standard conditions (14 hours light, 10 hours dark) in the animal facilities at the Maryland Psychiatric Research Center and provided with food and water *ad libitum*. Males were harem mated with one male per two females. The day of birth was counted as postnatal day 0 (P0). The animal facilities are fully accredited by the American Association for the Accreditation of Laboratory Animal Care (AAALAC) and the studies were conducted in accordance with the Guide for Care and Use of Laboratory Animals provided by the NIH.

Mice were either euthanized by cardiac perfusion with 0.9% saline followed by 4% paraformaldehyde (while deeply anesthetized with Euthasol, >100 μg/g) or by decapitation. Following the perfusions with 4% paraformaldehyde, brains were removed from the skull, postfixed for 2 hours, and then cryoprotected with 20% sucrose in 10 mM phosphate

buffed saline (PBS). At least 48 hours later, the fixed brains were embedded in OCT and frozen in isopentane. Following decapitation, freshly dissected brains were either bisected and frozen in aluminum foil for Na/K pump activity assays or the cerebellum was isolated and frozen in crushed dry ice for Western blot analysis.

2.2. Immunohistochemistry. Fixed, frozen brains were cut at 12 μm on a Leica cryostat, collected directly on slides, and stored at −70°C until stained. For immunofluorescence studies, slides were rinsed in 10 mM PBS, followed by incubation in two changes of 0.1 M glycine for 5 min each. Endogenous fluorescence was reduced by incubating the sections in 50 mM ammonium chloride for 1 hour. The sections were then rinsed three times in 10 mM PBS and then incubated for an hour in blocking solution containing 3% normal goat serum and 0.3%Triton X-100. Sections were then incubated in the primary antibodies overnight at 4°C. Sections were double labeled with either rabbit polyclonal anti-α1 (gift of Dr. M. Blaustein) or rabbit polyclonal anti-α3 Na/K ATPase (Upstate, now Millipore, 1/500: and mouse monoclonal anti-calbindin (Sigma, 1/5000) or rabbit polyclonal anti-activated caspase-3 (R&D, 1/500) and monoclonal mouse anti-α3 Na^+/K^+ ATPase (ABR Affinity BioReagents, Thermo Scientific Pierce Antibodies, 1/250). The sections were rinsed 3 times in PBS and then incubated for 2 hours with fluorescent-labeled secondary antibodies (anti-mouse or anti-rabbit Alexa 594 and Alexa 488, Molecular Probes, 1/200). After incubation, they were rinsed once in 10 mM PBS and incubated with 300 nM DAPI, then rinsed 3 times in 10 mM PBS, once in distilled water, and coverslipped with gel mount. The finished slides were then photographed using either an Olympus FV500 laser scanning confocal microscope or a Zeiss Axioplan fluorescence microscope. Confocal digital images were cropped and adjusted using Adobe Photoshop for color balance and intensity. All immunofluorescence experiments included slides (WT and +/*Lc*) with no 1antibody incubation as a control for nonspecific immunolabeling. The specificity of both the mouse monoclonal (ABR Affinity BioReagents) and the rabbit polyclonal (Upstate/Millipore) anti-α3 antibodies was also tested with Western blots using homogenized cerebellar tissue from WT and +/*Lc* mutant mice (data not shown). The ABR mouse monoclonal antibody labeled a single 110 kD band that represents the unbound, native α3 isoform, while the Upstate rabbit polyclonal antibody labeled two bands, the 110 kD α3 isoform and a 40 kD band that has been shown to be a byproduct of α3 isoform cleavage by calpain activity [31].

For the semiquantitative comparison of Na/K ATPase immunolabeling in WT and +/*Lc* cerebella, digital images of α3 isoform and calbindin immunolabeling of Purkinje cells were taken at 40x on a Zeiss Axioplan with an Olympus DP70 CCD camera within the first two days after staining all of the sections (to avoid uneven fading artifacts). The raw, unprocessed images were then analyzed using Metamorph Version 7.0r1. Threshold and colocalization functions were used to selectively measure the intensity of α3 isoform immunolabeling in areas that colocalized with calbindin-stained Purkinje cells in the same section. At least 3 molecular layer regions per cerebellum were selected from vermal sections in each WT or +/*Lc* cerebella and the mean value calculated for each cerebellum. The number of WT and +/*Lc* cerebella analyzed at each time point was P10, $n = 5$ WT, 4 +/*Lc*; P15, $n = 5$ WT, 5 +/*Lc*; P25, $n = 4$ WT, 5 +/*Lc*. The intensity of the α3 isoform fluorescence signal at P10, P15, and P25 is expressed as a percent change from labeling intensity in control Purkinje cells at P10.

2.2.1. Western Blot Analysis. WT and +/*Lc* cerebella were collected from freshly dissected brains, rapidly frozen in dry ice and stored at −70°C until processed. Each cerebellum was homogenized in a buffer containing 50 mM Tris (pH 8.0), 150 mM NaCl, 5 mM EDTA, 1%SDS, 10 μL/mL Protease inhibitor cocktail (Sigma), 1 mM PMSF, and 1 mM $NaVO_4$. The homogenate was centrifuged at 15,000 rpm for 15 minutes. Protein concentration in the supernatant was measured using a BioRad protein assay kit. Protein extracts were diluted in Laemmli sample buffer with β-mercaptoethanol and denatured at 37°C for 5 min and 10 μg of protein per well was resolved on a Tris-glycine gel. Protein was transferred overnight at 4°C onto a PVDF membrane. The membrane was rinsed with 5% nonfat dry milk dissolved in 1 × TBS. It was then incubated in the anti-α3 Na/K ATPase (ABR, 1/1000 or Upstate, 1/5000), diluted in TBS/0.1% Tween (TBS-T) with 1% milk overnight at 4°C, and then rinsed 3 × 10 min each with PBS-T. The sample membrane was incubated in alkaline phosphatase-conjugated secondary antibody (diluted 1/1000) and the protein was detected using Bio-Rad immun-Star chemiluminescence kit. Film exposed to the chemiluminescent signal was digitized using a light box and Pixera Pro150ES digital camera connected to a Power Macintosh. The optical density of the images was calibrated using a photographic calibration step tablet (Kodak) so that data is collected in the linear range of the O.D. The relative density of the labeled protein bands was determined using densitometric measurements with ImageJ. In all studies, once data from the antigen of interest had been collected, the membrane was stripped and labeled for total protein with India ink as a loading control. The density of α3 isoform protein bands was corrected for the total amount of protein by calculating the ratio of the density of the α3 isoform band and the total protein. Changes in the density of the corrected α3 isoform band were expressed as a percent of the averaged density of the α3 isoform bands from P25 controls within the same gel.

2.3. In Situ Na/K ATPase Activity Assay

Histochemistry. The density of active Na/K pumps was measured in frozen tissue sections using a procedure modified from previously published protocols [32, 33]. WT and +/*Lc* brains were bisected and rapidly frozen in dry ice for 2 min. The brains were then cut the same day in parasagittal sections at 20 μm. A kidney from one of the wild type animals was also frozen and a 20 μm section of kidney was placed on each

slide as a positive control. Two slides with 2 sections per slide from each brain were used in the assay. The sections were fixed for 10 min in 2% paraformaldehyde, rinsed 3 times each in PBS, rinsed twice in 50 mM Tris/100 mM sucrose (pH 7.4), and then rinsed 3 times for 15 min each time in Tris/sucrose buffer. They were then incubated for 20 min at 37°C in a lead citrate mix pH 8.8 of 4mM Potassium Citrate, 4 mM Lead Nitrate, 250 mM Glycine, 25 mM potassium hydroxide, 20% DMSO, 10 mM para-Nitrophenylphosphate (p-NPP), and 2.5 mM Levamisole. Sections were then rinsed in distilled water, rinsed for 10 min in TRIS/sucrose buffer, and rinsed again 2 times in distilled water. Sections were developed for 2 min in 1% ammonium sulfide, rinsed 2 times in distilled water, rinsed for 10 min in PBS on a rocker, rinsed in distilled water, covered in crystal mount, and allowed to dry at room temp. As an assay for ouabain insensitive activity, one slide from each brain was treated with 10 mM Ouabain during the final Tris/sucrose incubation and the lead citrate incubation.

Quantification of Enzyme Activity. Stained slides were photographed at 5x on a Leica DMR microscope with a 24-megapixel Power Phase Scanning camera (Phase 1, Inc.). To decrease variations in background illumination, images of both the sections and adjacent blank areas of slide were photographed. The background images were subtracted from the section images using MatLab. Because of the large number of sections to analyze in each histochemical experiment, digital images were collected over three consecutive days. To calibrate for any potential differences between images taken in different sessions (e.g., changes in light levels), the change in average density of a selected section that was imaged all three days was subtracted from the respective day. Using ImageJ, a systematic random set of points was selected to measure optical densities. The density for the molecular layer and granular cell layers was averaged for each brain from measurements of two sections per brain per experiment. The ouabain-specific activity was calculated by subtracting the density of the ouabain treated tissue from the density of the untreated tissue.

3. Statistical Analyses

Statistical comparisons between experimental and control groups were made using two-way or one-way analysis of variance (ANOVA) and post hoc comparisons were made using Bonferroni/Dunn (Statview 5.01).

4. Results

4.1. Cellular Distribution of α3 Na/K Pump Isoforms in WT and +/Lc Purkinje Cells. A previous study has shown that in an adult mouse cerebellum, the α1 Na/K pump subunit is expressed in granule cells and glomeruli, α2 subunits are expressed in astrocytes, and α3 subunits are expressed in Purkinje cells, basket cell processes, and mossy fiber glomeruli [7]. Since both Purkinje and granule cells degenerate in the +/*Lc* mutant, the α1 and α3 subunits were initially selected for study as the most likely isoforms to show altered expression patterns. A preliminary immunohistochemical survey did not show any evidence of changes in the distribution or intensity of immunolabeling of the α1 subunit (results not shown), but there was evidence of distinct changes in the pattern of immunolabeling for the α3 subunit in the +/*Lc* cerebellum from P10 to P25. Vermal cerebellar sections from at least 4 WT and +/*Lc* cerebella at P10, P15, and P25 were double immunolabeled for calbindin and the α3 subunit using the Upstate rabbit polyclonal antibody that recognizes both the 110 kD full length α3 isoform and the 40 kD byproduct of α3 isoform cleavage in Western blots. In both WT and +/*Lc* cerebella from P10 to P25, the α3 subunits appear to be expressed in Purkinje cells, the molecular layer, and granule cell layer glomeruli in a similar pattern to that described by Peng et al. [7] in the cerebellum of adult rats. α3 expression in WT Purkinje cells is diffusely distributed throughout the dendrites and cell body as shown for P15 WT Purkinje cells in Figures 1(b) and 1(c) (green labeling). In contrast, the immunolabeling for α3 is qualitatively different at all three ages in +/*Lc* Purkinje cells. From P10, the α3 isoform labeling becomes more intense and less diffuse within +/*Lc* Purkinje cells. As shown for P15 +/*Lc* Purkinje cells in Figures 1(e) and 1(f), immunolabeling for the α3 subunit (green) is more punctate and concentrated around the primary dendrites and cell bodies so the labeling appears more intense, though there is some variation between different Purkinje cells. For example, the α3 labeling is particularly intense in the two left most +/*Lc* Purkinje cells in Figures 1(d)–1(f) (white arrows), where the α3 isoform appears to surround the stunted primary Purkinje cell dendrites especially in the lower two-thirds of the molecular layer. α3 immunolabeling is also seen around the Purkinje cell bodies but not as much within the cell body in comparison with WT Purkinje cells. α3 immunolabeling in the granule cell layer glomeruli is indicated by white asterisks in Figures 1(e) and 1(f). While we cannot rule out the possibility that some of the increased α3 immunolabeling in the Purkinje cell and molecular layers in the +/*Lc* cerebellar cortex may be in climbing fibers, it is clear that the intensity and distribution of α3 immunolabeling is altered in the +/*Lc* cerebellar cortex.

+/*Lc* Purkinje cells that appear to be in the final stages of degeneration express activated caspase-3 [34, 35]. To determine if α3 subunit expression persists in dying Purkinje cells, cerebellar sections from P15 and P25 +/*Lc* cerebella were double labeled with antibodies to activated caspase-3 and the α3 isoform and counterstained with DAPI. The distribution of α3 isoform labeling in activated caspase-3 positive +/*Lc* Purkinje cells was examined in cerebellar sections from three +/*Lc* mutants at P15. Confocal images of two such degenerating +/*Lc* Purkinje cells are shown in Figures 2(a) and 2(b), illustrating that +/*Lc* Purkinje cells continue to express the α3 isoform even as they degenerate. The stunted dendrites and cell body of the activated caspase-3 positive (red) +/*Lc* Purkinje cell shown in Figure 2(a) show punctate labeling for α3 (green and yellow) throughout the remaining dendritic tree and cell body. The +/*Lc* Purkinje cell shown in Figure 2(b) appears to be at an advanced stage of degeneration with only a few retracted dendrites remaining

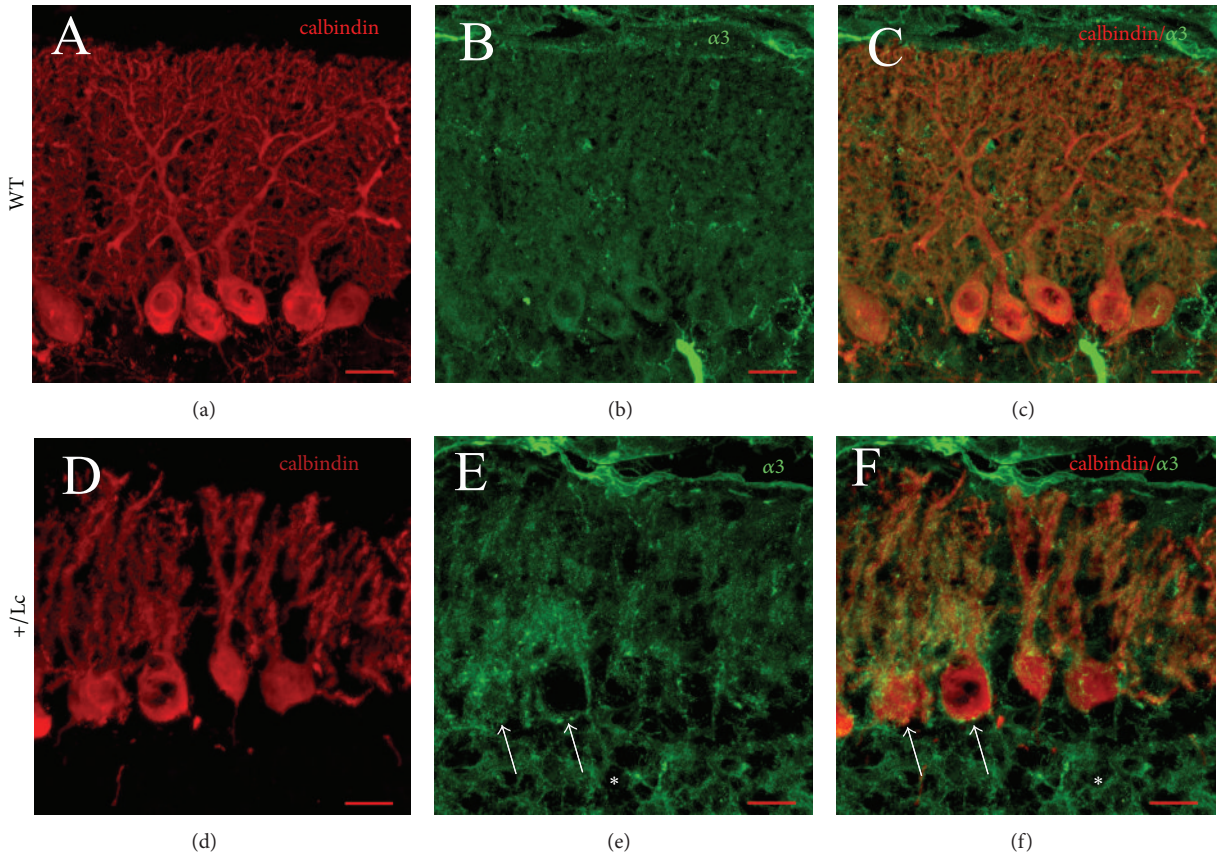

Figure 1: Confocal images of immunohistochemistry for the $\alpha 3$ isoform of Na/K pumps in the cerebellar cortex of wild type (A)–(C) and +/*Lc* mice (D)–(F) at P15. The cerebellar sections in (A)–(F) were double labeled for calbindin (red) and the $\alpha 3$ isoform (green) with overlaid images in (C) and (F). The white arrows in (E) and (F) indicate calbindin labeled +/*Lc* Purkinje cells with particularly intense $\alpha 3$ isoform immunostaining. The asterisks in (E) and (F) indicate $\alpha 3$ isoform labeling in the granule cell layer. Scale bars: 20 μm.

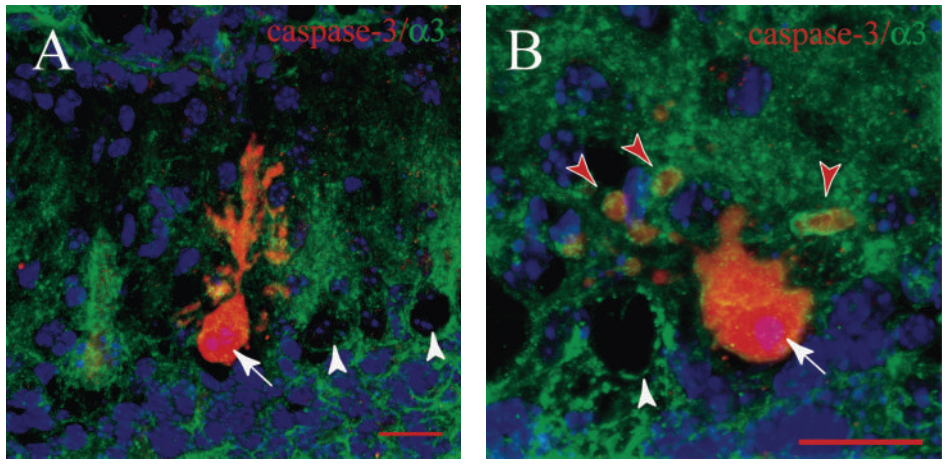

Figure 2: Confocal images of immunohistochemistry for activated caspase-3 (red), the $\alpha 3$ isoform (green), and DAPI (blue) in +/*Lc* cerebellar sections at P15. The white arrows in (a) and (b) indicate degenerating +/*Lc* Purkinje cells that are also immunolabeled for the $\alpha 3$ isoform. The red arrowheads indicate what appear to be the degenerating dendrites of the +/*Lc* Purkinje cell surrounded by $\alpha 3$ immunolabeling. The white arrowheads indicate the cell bodies of +/*Lc* Purkinje cells that have not yet started to express activated caspase-3. The nuclear DAPI labeling is faint and diffuse in the neighboring +/*Lc* Purkinje cells that do not yet express activated caspase-3. The monoclonal mouse anti-$\alpha 3$ isoform specific only for the full 110 kD $\alpha 3$ isoform was used in this case and a similar labeling pattern is observed compared to the rabbit polyclonal $\alpha 3$ antibody. Scale bars: 20 μm.

as detached spherical blebs or tubes (red arrowheads). Yet the remaining parts of the degenerating Purkinje cell dendrites are surrounded by $\alpha 3$ immunolabeling. DAPI labeling (purple) in the nuclei of both activated caspase-3 positive neurons shows the condensation of the nuclei in the degenerating +/*Lc* Purkinje cells (white arrows). Nuclear DAPI labeling is found in the neighboring +/*Lc* Purkinje cells that have not yet begun to express activated caspase-3 (white arrowheads).

The qualitative descriptions of the developmental changes in immunolabeling for the $\alpha 3$ isoform suggest that it is diffusely distributed throughout the Purkinje cell dendritic tree from P10 to P25 in the WT cerebellum. In contrast, in +/*Lc* Purkinje cells, $\alpha 3$ immunolabeling becomes more intense from P10 to P25 with punctate labeling concentrating along the Purkinje cell primary dendrites and cell bodies. As an assay for developmental changes in $\alpha 3$ immunolabeling, the intensity of the $\alpha 3$ (green) fluorescence signal coincident with calbindin labeling in WT and +/*Lc* Purkinje cells was measured using MetaMorph (Figure 3). Two-way ANOVA analysis of the fluorescence intensity measurements indicates that there are significant age- and genotype-dependant effects in $\alpha 3$ subunit immunofluorescence between WT and +/*Lc* Purkinje cells (Figure 3: Age: ANOVA $F_{2,22} = 7.3$, $P = 0.0038$; genotype: ANOVA $F_{1,22} = 7.3$, $P = 0.0128$), but the age x genotype interaction does not reach significance (ANOVA $F_{2,22} = 1.85$, $P = 0.18$). Post hoc analyses of the complete data set suggest that there are significant increases in $\alpha 3$ fluorescence intensity between P10 and P15 and between P10 and P25 and an overall significant difference between fluorescence intensity in +/*Lc* and WT Purkinje cells (Bonferroni/Dunn; $P < 0.0167$). A further exploratory post hoc one-way ANOVA analysis separating the data set by age suggests that while differences between $\alpha 3$ isoform immunofluorescence in +/*Lc* and WT Purkinje cells at P10 and P15 may contribute to the main effect, they are not significantly different when analyzed separately (P10 one-way ANOVA $F_{1,7} = 2.22$, $P = 0.18$; P15 one-way ANOVA $F_{1,8} = 0.48$, $P = 0.5$). However, there is a significant difference between the intensity of $\alpha 3$ isoform immunolabeling in +/*Lc* and WT Purkinje cells at P25 with higher levels in the +/*Lc* Purkinje cells (ANOVA $F_{1,7} = 7.45$, $P < 0.03$).

4.2. Analysis of α3 Isoform Protein Expression Levels. The increase in $\alpha 3$ immunofluorescence in +/*Lc* Purkinje cells from P10–P25 may be due to a variety of reasons, including either a redistribution of existing $\alpha 3$ isoforms or an increase in the expression levels of the $\alpha 3$ isoform. To distinguish between these possibilities, protein extracts of cerebellar tissue were prepared from WT and +/*Lc* cerebella at P10, P15, and P25 and the relative levels of $\alpha 3$ isoform expression were quantified by Western blot (Figure 4). Western blots were performed with both the mouse monoclonal (ABR Affinity BioReagents) and the rabbit polyclonal (Upstate/Millipore) anti-$\alpha 3$ antibodies. The ABR mouse monoclonal antibody labeled a single 110 kD band that represents the unbound, native $\alpha 3$ isoform, while the Upstate rabbit polyclonal antibody labeled two bands, the 110 kD $\alpha 3$ isoform and a 40 kD band that has been shown to be a byproduct of $\alpha 3$ isoform

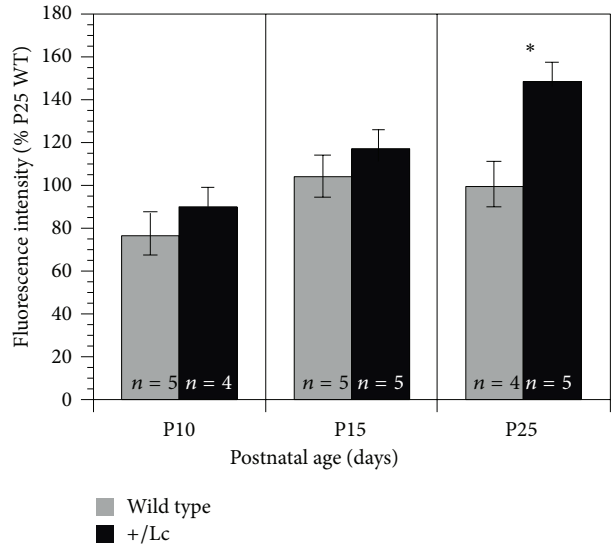

Figure 3: Densitometric measurements of the intensity of immunofluorescent labeling for the $\alpha 3$ subunit in the WT and +/*Lc* cerebellar cortex. The graph illustrates the relative changes in fluorescence intensity relative to the intensity of Purkinje cell immunolabeling in the P25 WT cerebellum (P10, $n = 5$ WT, 4 +/*Lc*; P15, $n = 5$ WT, 5 +/*Lc*; P25, $n = 4$ WT, 5 +/*Lc*).

cleavage by calpain activity [31]. The Upstate rabbit polyclonal 110 kD band showed more background than the ABR mouse monoclonal, so the mouse monoclonal antibody was used to measure $\alpha 3$ isoform levels and the rabbit polyclonal antibody was used to measure levels of the 40 kD $\alpha 3$ isoform calpain degradation product. Representative images of Western blots for the 110 kD $\alpha 3$ isoform are shown for +/*Lc* and WT cerebella at P10, P15, and P25 in Figure 4(a). Figure 4(b) shows representative $\alpha 3$ 40 kD degradation product bands for WT and +/*Lc* cerebella at P10, P15, and P25.

Quantitative changes in the relative optical densities of the 110 kD $\alpha 3$ isoform protein and 40 kD degradation product are shown in the graphs in Figures 4(a) and 4(b), respectively. Two-way ANOVA of the 110 kD protein density data indicates that there is a significant effect of age (ANOVA $F_{2,37} = 10.241$, $P = 0.003$), but there are no significant effects of genotype (ANOVA $F_{1,37} = 1.32$, $P = 0.26$) or age x genotype interactions (ANOVA $F_{2,37} = 1.83$, $P = 0.18$). Post hoc exploratory analyses indicate that in the +/*Lc* and WT cerebella, $\alpha 3$ isoform protein levels at P25 are significantly higher than at P10 and P15 (Bonferroni/Dunn, $P < 0.0167$). A separate one-way ANOVA analysis of the data separated by age indicates that $\alpha 3$ isoform protein levels are only significantly different between WT and +/*Lc* cerebella at P25 (ANOVA $F_{1,12} = 5.18$, $P = 0.042$). The results indicate that $\alpha 3$ isoform levels in the WT and +/*Lc* cerebellum increase with age after P15, but by P25 the increase in $\alpha 3$ levels in +/*Lc* cerebella is not as great as in WT cerebella.

Two-way ANOVA of the 40 kD $\alpha 3$ isoform protein levels (Figure 4(b)) indicates that there are significant effects of age (ANOVA $F_{2.43} = 6.33$, $P = 0.004$), genotype (ANOVA $F_{1,43} = 8.61$, $P = 0.0053$), and age x genotype interactions (ANOVA

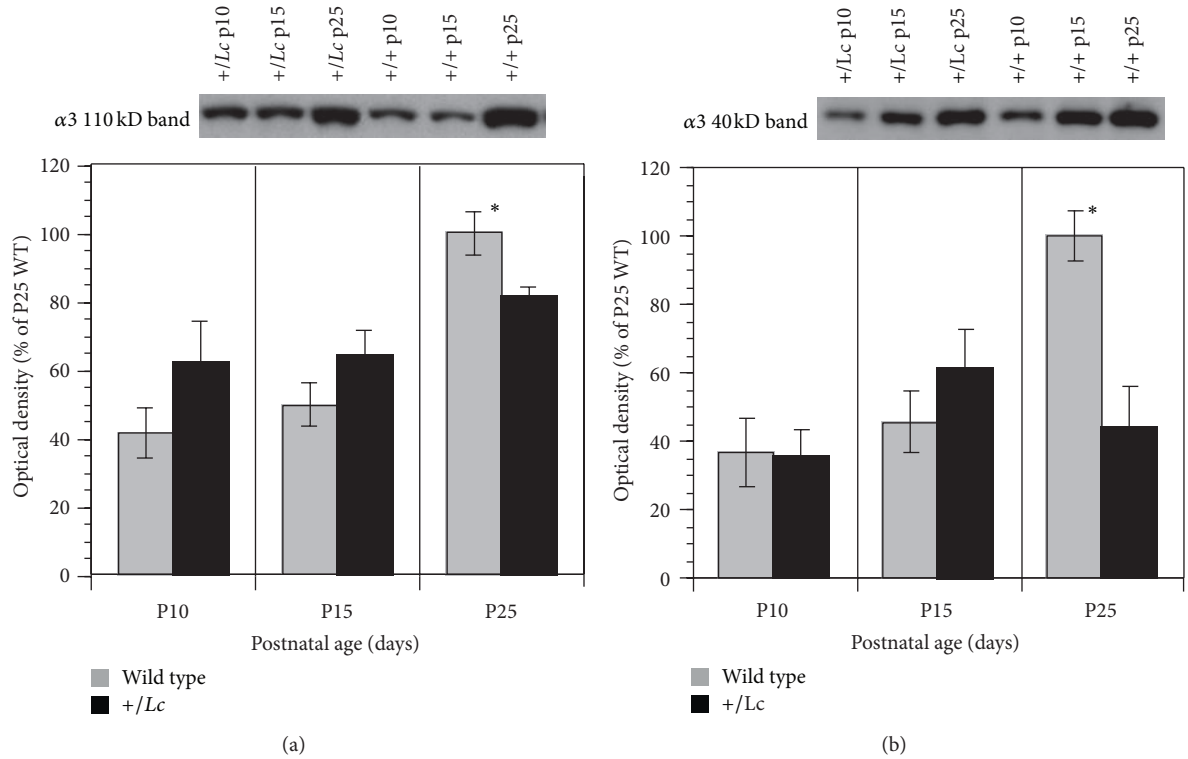

Figure 4: Expression levels of the $\alpha 3$ subunit 110 kD and 40 kD protein bands at P10, P15, and P25 in WT and +/*Lc* cerebella as determined by densitometry of Western blots. Representative Western blots are shown for the $\alpha 3$ 110 kD (a) and 40 kD bands (b) at P10, P15, and P25, along with graphs of the relative density of the bands expressed as a percentage of the mean band intensity for P25 WT cerebella.

$F_{2,42} = 3.8$, $P < 0.028$). Post hoc analyses indicate that group levels for the $\alpha 3$ 40 kD fragment are significantly higher at P25 compared with P10 levels (Bonferroni/Dunn, $P < 0.0167$) but not between P25 and P15 or P15 and P10 (Bonferroni/Dunn, $P > 0.0167$). One-way ANOVA separated by age suggests that the genotype effect is primarily due to a significant difference between the amount of $\alpha 3$ 40 kD fragment at P25 (ANOVA $F_{1,14} = 15.33$, $P = 0.0016$), with significantly lower levels in +/*Lc* cerebella. There are no significant differences between levels of the 40 kD fragment at P10 or P15. The results suggest that by P25 there is a dramatic increase in the 40 kD $\alpha 3$ fragment in WT cerebella, but this age-related increase is not matched in the +/*Lc* cerebella.

4.3. Histochemical Measurements of Active Na/K Pump Density. Since the GluR$\delta 2^{Lc}$ channel mediates an Na^+ leak current we hypothesized that the density of active Na^+/K^+ ATPase pumps would be increased from P10 through P25 in +/*Lc* Purkinje cells in response to increased intracellular Na^+ levels. Furthermore, the changes in the distribution of the catalytic $\alpha 3$ subunit of the Na/K pump also suggest that the distribution and density of pump activity would be altered in +/*Lc* Purkinje cells. To assay changes in the distribution of active Na/K pumps in the +/*Lc* cerebellum, p-NPP was used as a substrate in an *in situ* histochemical assay to detect ouabain-sensitive, potassium-dependent activity of the Na/K pump complex. Representative images of histochemical labeling for Na/K pump activity in WT and +/*Lc* cerebellar cortex at P15 and P25 are shown in Figure 5. The images of both the wild type and +/*Lc* cerebella are taken at the same magnification, but the +/*Lc* cerebella is smaller at P15 and dramatically reduced in size by P25 compared to WT because of ongoing (and by P25, extensive) +/*Lc* Purkinje and granule cell death. Quantitative analysis of *in situ* ouabain-sensitive Na/K pump activity in histological sections of wild type and +/*Lc* cerebellar sections at P15 and P25 shows that the overall density of active Na/K pump in the molecular and granule cell layers is within WT levels at P15 (ML; ANOVA $F_{1,9} = 0.467$, $P > 0.1$; GCL; ANOVA $F_{1,9} = 0.47$, $P > 0.1$) but decreases by P25 in both the +/*Lc* molecular layer (ML: ANOVA $F_{3,16} = 11.9$, $P < 0.003$) and granule cell layer (GCL: ANOVA $F_{3,16} = 19.4$, $P < 0.001$; Figures 5(e) and 5(f)). *In situ* active Na/K pump density is expressed as a percent of WT values at either P15 or P25. Cerebellar slices from WT and +/*Lc* mice at P15 and P25 were processed on separate days so it was not possible to compare densitometric density between P15 and P25.

At P15, significant numbers of +/*Lc* Purkinje cells are still present, so we assume that the Na/K pump activity measurements in the molecular layer reflects pump activity in Purkinje cells dendrites in addition to other cellular elements in the molecular layer. Therefore, at P15 all of the measurements were made in the molecular and granule cell layers of lobes III and IV as representative areas. However, by P25 most +/*Lc* Purkinje cells have degenerated in anterior and central lobules, but approximately 40 to 50% of the +/*Lc* Purkinje

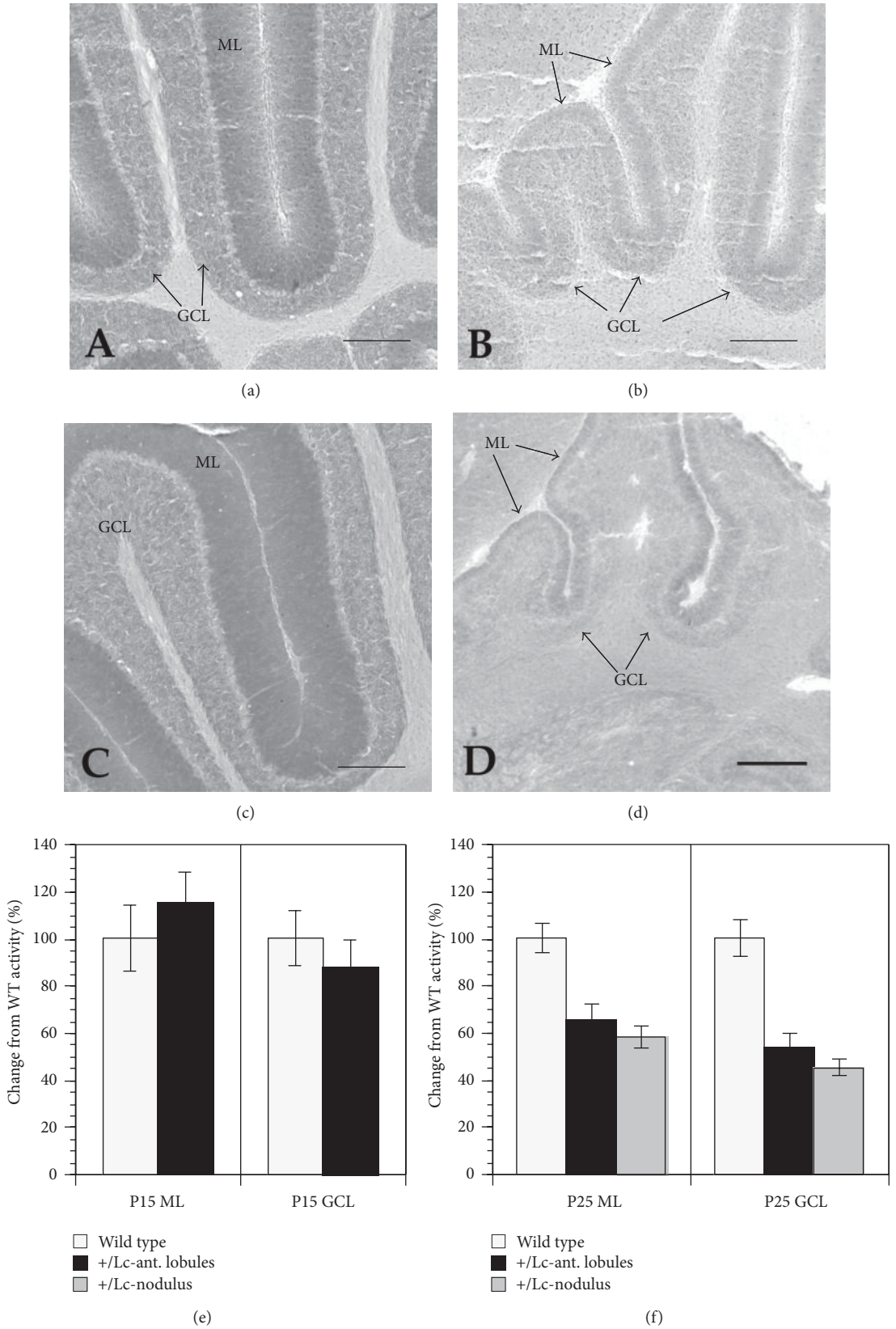

Figure 5: Histochemical assay for ouabain-sensitive Na/K pump activity in P15 (a), (b) and P25 (c), (d) WT and +/*Lc* cerebellar sections. The results of densitometric measurements of the molecular (ML) and granule cell layers (GCL) are expressed as a percent of wild type activity levels either at P15 (e) or P25 (f). At P25, densitometric measurements were made in both anterior lobules of the cerebellum and the nodulus. Scale bars: 200 μm.

cells persist in the nodulus [36]. To determine if there is a difference in Na/K pump activity between cerebellar regions with few Purkinje cells versus regions with surviving Purkinje cells, Na/K pump activity measurements at P25 were made in the molecular and granule cell layers of lobules III and IV versus X (the nodulus) in control and +/*Lc* mutant cerebella (Figure 5(f)). Following the activity measurements, the same sections were stained with cresyl violet to verify the presence of +/*Lc* Purkinje cells. While only a few Purkinje cells were found throughout lobules III and IV, the density of surviving Purkinje cells in the regions of the nodulus analyzed for Na/K pump activity was noticeably higher (data not shown). However, the preferential survival of +/*Lc* Purkinje cells in the nodulus did not appear to affect the overall decline in Na/K pump activity observed at P25 in the +/*Lc* cerebella in both the molecular and granule cell layers.

5. Discussion

The Lurcher mutation in GluRδ2 converts this enigmatic glutamate receptor into a constitutively open cation channel that chronically depolarizes +/*Lc* Purkinje cells as they mature following the first week of postnatal development [20, 22]. The cation leak in +/*Lc* Purkinje cells is thought to initiate excitotoxic cell death pathways [19]. One assumption of excitotoxic mechanisms is that the ionic imbalance resulting from overstimulation of glutamate receptors and the resulting influx of Na^+ and Ca^{++} ions places overwhelming stress on cellular energy metabolism systems [17, 18]. In +/*Lc* Purkinje cells, in particular, mitochondrial cytochrome oxidase activity is significantly increased, possibly in response to increased cellular energy requirements [26]. The goal of this study was to test the hypothesis that Na^+/K^+ ATPase α3 isoform expression and the density of active Na/K pumps are increased in +/*Lc* Purkinje cells. This increase would be consistent with an increased demand for ATP production (and increased cytochrome oxidase activity) to counterbalance the GluR$\delta 2^{Lc}$ Na^+ and Ca^{++} leak current. However, the results indicate that while the expression of the catalytic α3 isoform may be increased in individual +/*Lc* Purkinje cells, the density of active Na/K pumps is not significantly increased above wild type levels in the cerebella of younger +/*Lc* mutants (P10 to P15). Furthermore, by 25, overall expression levels of the α3 isoform and its 40 kD breakdown product are decreased in the +/*Lc* cerebellum compared to WT, along with a decrease in the density of active Na/K pumps. The lower cerebellar expression levels of the α3 isoform and decreased density of active Na/K pumps by P25 in the +/*Lc* cerebellum may simply reflect the substantial loss of +/*Lc* Purkinje and granule cells by this age. While the results indicate that the density of active Na/K pump units are not significantly increased in +/*Lc* Purkinje cells in response to the leak current, it is important to note that in this study we have not analyzed the *in vivo* unit activity of Na/K pumps in living +/*Lc* Purkinje cells.

5.1. Expression of the Na/K Pump α3 Subunit in Depolarized +/Lc Purkinje Cells. In this study, initial immunohistochemical studies of the expression pattern of the primary subunits of the Na/K pump expressed in cerebellar Purkinje cells, the α3, and β1 isoforms suggested that only the expression of the catalytic α3 subunit is altered in the +/*Lc* cerebellar cortex. The change in expression of the α3 isoform in +/*Lc* Purkinje cells was subsequently analyzed by fluorescent immunolabeling to provide information about subunit localization. The significant increase in the intensity of immunofluorescence for the α3 subunit from P10 through P25 (Figure 3) in +/*Lc* Purkinje cells indicates either that there is an increase in the density of the protein or that the localization of the subunit is altered within each +/*Lc* Purkinje cell as their dendrites and cell bodies degenerate. The Western blot data shows that the total cerebellar levels of both the native α3 subunit and its 40 kD cleavage product are not significantly altered from P10 to P15 in the +/*Lc* cerebella compared to WT and their levels do not subsequently increase through P25 as in WT cerebella. While both immunofluorescence and Western blot techniques provide important complementary qualitative and quantitative information about the pattern of protein expression, the results need to be interpreted with caution because of their inherent limitations. The significant increase in the intensity of immunofluorescence for the α3 subunit in +/*Lc* Purkinje cells suggests that there is an increase in the density of the protein within individual Purkinje cells. However, it is not possible to distinguish between the possibilities that there is an increase in the expression of the α3 subunit or that the localization of the subunit is altered as +/*Lc* Purkinje cells fail to differentiate (especially their dendrites) and eventually degenerate. The Western blot data appears to favor the latter hypothesis since the only significant difference in α3 expression is a relative decrease at P25 in +/*Lc* cerebella when 70–90% of the +/*Lc* Purkinje cells and 60% of the granule cells have degenerated [24, 36]. It is also important to consider that +/*Lc* Purkinje cells are degenerating from at least P10 onwards with approximately 50% of the +/*Lc* Purkinje cells missing by P13 to P15 [24]. Given that the intensity of immunolabeling for the subunit within each +/*Lc* Purkinje cell steadily increases from P10 through P25 (Figure 3), it is possible that α3 protein levels may actually steadily increase within individual +/*Lc* Purkinje cells, but the overall expression levels in the cerebellum may not significantly change because of the ongoing loss of +/*Lc* Purkinje cells. Thus, even at P25, α3 subunit expression levels may be significantly increased within the stunted dendritic trees characteristic of +/*Lc* Purkinje cells, but overall cerebellar α3 levels may have declined overall because most Purkinje cells have died by this time.

While the immunohistochemistry and Western blot data are consistent with a change in the density of Na/K pumps within individual Purkinje cells, these results do not indicate how these changes may translate into alterations in pump activity. A previous study of adult acutely dissociated rat thalamic neurons depolarized by exposure to veratridine or monensin found that the resulting Na^+ influx resulted in an increase in Na/K pump density and in the level of phosphorylated pump molecules (implying increased pump activity; [37]). In the chronic Na^+ leak in developing +/*Lc* Purkinje cells in this study, the evidence suggests that the density of active Na/K pumps is not altered in the +/*Lc* cerebellar cortex

until after P15. At P15, there is no significant difference in the density of histochemically measured, ouabain-sensitive active Na/K pumps between the molecular layers of wild type and +/*Lc* cerebella. By P25, there is a significant decrease in the density of molecular layer active Na/K pumps, both in anterior lobules with virtually no Purkinje cells or the nodulus with relatively higher numbers of surviving +/*Lc* Purkinje cells.

The diffuse pattern of Na/K pump activity in the +/*Lc* cerebellar cortex is in stark contrast to the distribution of cytochrome oxidase (COX) histochemical staining at the same ages [26]. Individual +/*Lc* Purkinje cells at P15 and P25 stain darkly for COX, filling the entire Purkinje cell body and dendritic tree. The dramatic increase in COX activity suggests that the mitochondrial respiratory pathway is upregulated to produce more ATP. If the density of active Na/K pumps had been increased in response to the chronic Na^+ influx in +/*Lc* Purkinje cells it seems reasonable to expect that the intensity of the histochemical labeling would have increased along Purkinje cell dendritic membranes. However, the staining pattern for Na/K pump activity remained diffuse in the +/*Lc* cerebellar cortex, with no evidence of discrete patches of labeling corresponding to the patchy labeling for $\alpha 3$ subunit observed in fluorescently labeled sections. The discrepancy between the distribution of $\alpha 3$ subunits detected by immunofluorescence and the pattern of Na/K pump histochemical activity could be due to limitations in the spatial resolution of the histochemical staining or some of the $\alpha 3$ immunolabeling labeling could represent deactivated Na/K pumps, including the 40 kD $\alpha 3$ cleaved isoform. In a mouse model of focal cerebral ischemia, no changes were found in protein or mRNA levels for Na/K pump isoforms [12], but the level of Na/K pump activity was decreased along with a change in ouabain sensitivity, indicating that the decrease in activity was due to intrinsic modifications of the ATPase pump.

There are a number of mechanisms that can reduce or irreversibly block Na/K pump activity. Na/K pump isoforms are routinely recycled by internalization in lysosomes and degradation by lysosomal cathepsin D [31, 38]. However, the membrane bound Na/K pump complex can also be inactivated by the calpain-mediated cleavage of the scaffolding protein, ankyrin, that binds the Na/K pump to the membrane skeleton [39] or by degradation of Na/K pump isoforms themselves [31]. When oxidized, Na/K pump isoforms become more sensitive to intracellular proteinases and activated calpain will cleave the $\alpha 3$ isoform into a 40 kD degradation product [31]. In this study, the amount of the 110 kD native $\alpha 3$ subunit and 40 kD degradation product increases in WT cerebella through P25 suggesting that a significant fraction of the native $\alpha 3$ subunit is oxidized and degraded by calpain in normal cerebellar tissue. Calpain has recently been shown to be active in individual, isolated +/*Lc* Purkinje cells at P14 based on immunolabeling for the 136 kD fragment of α-spectrin cleaved by calpain [19]. In this study, despite the loss of significant numbers of +/*Lc* Purkinje cells at P15, there is no significant reduction in the levels of the 40 kD band in +/*Lc* cerebella until P25, when most Purkinje and granule cells have degenerated. As in the case of the 110 kD native $\alpha 3$ subunit, it is possible that the amount of the 40 kD degradation is increased in individual +/*Lc* Purkinje cells at P15 and P25, but total amounts are within control levels at P15 and significantly decreased at P25 because of the ongoing +/*Lc* Purkinje cell loss. +/*Lc* Purkinje cell degeneration is associated with an increase in oxidative stress, including an increase in mitochondrial cytochrome oxidase activity, which may generate more reactive oxygen species as a byproduct of increased respiratory activity. The results do not indicate that there is a dramatic increase in oxidized forms of the $\alpha 3$ subunit by P15 in the +/*Lc* cerebellum since there is not a significant increase in levels of the 40 kD byproduct, but the results are consistent with sustained proteolysis of the $\alpha 3$ subunit by calpain in +/*Lc* Purkinje cells until most have degenerated.

Na/K pump activity is also regulated by nitric oxide (NO)-cGMP [10] or NO-PKG pathways [40] and inhibited by peroxynitrite through the formation of nitrotyrosine or the modification of cysteine residues [15, 16]. Previous studies of +/*Lc* Purkinje cells have shown that their degeneration is associated with increased expression of neuronal nitric oxide synthase and nitrotyrosine [25]. Since the Na/K pump is sensitive to peroxynitrite and NO, we hypothesize that while the cation leak increases the expression of the catalytic $\alpha 3$ isoform, interactions with peroxynitrite, NO/PKG, and/or NO/cGMP reduce the density of active Na/K pumps. A reduction in the density of active Na/K pumps in +/*Lc* Purkinje cells may contribute to a Na^+ overload in these neurons and exacerbate the cell death process, since increases in intracellular Na^+ have been associated with induction of apoptosis [5, 41].

6. Conclusion

The analysis of the distribution and activity of the Na/K pump in this study of degenerating +/*Lc* Purkinje cells demonstrates that while the expression and/or distribution of the $\alpha 3$ subunit is disrupted in the cerebellar cortex of the +/*Lc* mutant, there is no evidence to suggest that the density of active pumps is increased in response to the constitutive influx of Na^+ ions through the mutant GluR$\delta 2^{Lc}$ channels. We had hypothesized that Na/K pump activity would be stimulated as a homeostatic response to the Na^+ ion influx. The lack of evidence for an increased density of functional Na/K pumps does not rule out the possibility that the activity of individual pumps is increased within each +/*Lc* Purkinje cell, thereby stimulating an increased demand for ATP which would eventually lead to depletion of cellular energy resources. The Na/K pump is estimated to use up to 50% of the ATP produced by neurons [42]. Na^+ is normally the rate-limiting factor in Na/K pump activity [43–45] and elevations in the concentration of Na^+ within +/*Lc* Purkinje cells may increase the activity of individual pumps because of a more complete saturation of its Na^+ binding sites. Thus, while there may be an increased ATP consumption in +/*Lc* Purkinje cells because of the increased activity of individual pumps, this study suggests that any increase in Na/K pump activity and ATP consumption is not due to an

overall increase in the density of active ATPase pumps in chronically depolarized Purkinje cells.

Conflict of Interests

The authors declare that they have no conflict of interests associated with this paper.

Acknowledgments

This work was supported by NIH Grant NS 34309 to Michael W. Vogel. The authors would like to thank Dr. Adam Puche for his assistance with the acquisition and analysis of microscopy data. The authors also thank Carol Armstrong, Michisuke Yuzaki, and Jun Nishiyama for their helpful comments in the preparation of the paper. This paper was prepared while MWV was employed at the University of Maryland School of Medicine. The opinions expressed in this paper are the author's own and do not reflect the view of the National Institutes of Health, the Department of Health and Human Services, or the United States government.

References

[1] R. F. Rakowski, D. C. Gadsby, and P. De Weer, "Stoichiometry and voltage dependence of the sodium pump in voltage-clamped, internally dialyzed squid giant axon," *Journal of General Physiology*, vol. 93, no. 5, pp. 903–941, 1989.

[2] L. R. Molnar, K. A. Thayne, W. W. Fleming, and D. A. Taylor, "The role of the sodium pump in the developmental regulation of membrane electrical properties of cerebellar Purkinje neurons of the rat," *Developmental Brain Research*, vol. 112, no. 2, pp. 287–291, 1999.

[3] S. Genet and R. T. Kado, "Hyperpolarizing current of the Na/K ATPase contributes to the membrane polarization of the Purkinje cell in rat cerebellum," *Pflugers Archiv European Journal of Physiology*, vol. 434, no. 5, pp. 559–567, 1997.

[4] K. Geering, P. Béguin, H. Garty et al., "FXYD proteins: new tissue- and isoform-specific regulators of Na,K-ATPase," *Annals of the New York Academy of Sciences*, vol. 986, pp. 388–394, 2003.

[5] M. I. Panayiotidis, C. D. Bortner, and J. A. Cidlowski, "On the mechanism of ionic regulation of apoptosis: would the Na^+/K^+-ATPase please stand up?" *Acta Physiologica*, vol. 187, no. 1-2, pp. 205–215, 2006.

[6] K. Geering, "Functional roles of Na, K-ATPase subunits," *Current Opinion in Nephrology and Hypertension*, vol. 17, no. 5, pp. 526–532, 2008.

[7] L. Peng, P. Martin-Vasallo, and K. J. Sweadner, "Isoforms of Na,K-ATPase α and β subunits in the rat cerebellum and in granule cell cultures," *Journal of Neuroscience*, vol. 17, no. 10, pp. 3488–3502, 1997.

[8] M. S. Feschenko, C. Donnet, R. K. Wetzel, N. K. Asinovski, L. R. Jones, and K. J. Sweadner, "Phospholemman, a single-span membrane protein, is an accessory protein of Na,K-ATPase in cerebellum and choroid plexus," *Journal of Neuroscience*, vol. 23, no. 6, pp. 2161–2169, 2003.

[9] X. Q. Wang, A. Y. Xiao, C. Sheline et al., "Apoptotic insults impair Na^+, K^+-ATPase activity as a mechanism of neuronal death mediated by concurrent ATP deficiency and oxidant stress," *Journal of Cell Science*, vol. 116, no. 10, pp. 2099–2110, 2003.

[10] D. Z. Ellis, J. Rabe, and K. J. Sweadner, "Global loss of Na,K-ATPase and its nitric oxide-mediated regulation in a transgenic mouse model of amyotrophic lateral sclerosis," *Journal of Neuroscience*, vol. 23, no. 1, pp. 43–51, 2003.

[11] W. C. Golden and L. J. Martin, "Low-dose ouabain protects against excitotoxic apoptosis and up-regulates nuclear Bcl-2 in vivo," *Neuroscience*, vol. 137, no. 1, pp. 133–144, 2006.

[12] I. Jamme, O. Barbey, P. Trouvé et al., "Focal cerebral ischaemia induces a decrease in activity and a shift in ouabain affinity of Na^+, K^+-ATPase isoforms without modifications in mRNA and protein expression," *Brain Research*, vol. 819, no. 1-2, pp. 132–142, 1999.

[13] A. Y. Xiao, X. Q. Wang, A. Yang, and S. P. Yu, "Slight impairment of Na^+,K^+-ATPase synergistically aggravates ceramide- and β-amyloid-induced apoptosis in cortical neurons," *Brain Research*, vol. 955, no. 1-2, pp. 253–259, 2002.

[14] J. A. Nathanson, C. Scavone, C. Scanlon, and M. McKee, "The cellular Na^+ pump as a site of action for carbon monoxide and glutamate: a mechanism for long-term modulation of cellular activity," *Neuron*, vol. 14, no. 4, pp. 781–794, 1995.

[15] W. C. Golden, A. M. Brambrink, R. J. Traystman, D. H. Shaffner, and L. J. Martin, "Nitration of the striatal Na,K-ATPase $\alpha 3$ isoform occurs in normal brain development but is not increased during hypoxia-ischemia in newborn piglets," *Neurochemical Research*, vol. 28, no. 12, pp. 1883–1889, 2003.

[16] M. S. Reifenberger, K. L. Arnett, C. Gatto, and M. A. Milanick, "The reactive nitrogen species peroxynitrite is a potent inhibitor of renal Na-K-ATPase activity," *American Journal of Physiology—Renal Physiology*, vol. 295, no. 4, pp. F1191–F1198, 2008.

[17] A. Mehta, M. Prabhakar, P. Kumar, R. Deshmukh, and P. L. Sharma, "Excitotoxicity: bridge to various triggers in neurodegenerative disorders," *European Journal of Pharmacology*, vol. 698, no. 1–3, pp. 6–18, 2012.

[18] Y. Wang and Z.-H. Qin, "Molecular and cellular mechanisms of excitotoxic neuronal death," *Apoptosis*, vol. 15, no. 11, pp. 1382–1402, 2010.

[19] J. Nishiyama, K. Matsuda, W. Kakegawa et al., "Reevaluation of neurodegeneration in lurcher mice: constitutive ion fluxes cause cell death with, not by, autophagy," *Journal of Neuroscience*, vol. 30, no. 6, pp. 2177–2187, 2010.

[20] J. Zuo, P. L. De Jager, K. A. Takahashi, W. Jiang, D. J. Linden, and N. Heintz, "Neurodegeneration in Lurcher mice caused by mutation in $\delta 2$ glutamate receptor gene," *Nature*, vol. 388, no. 6644, pp. 769–773, 1997.

[21] J. Nishiyama and M. Yuzaki, "Excitotoxicity and autophagy: lurcher may not be a model of "autophagic cell death"," *Autophagy*, vol. 6, no. 4, pp. 568–570, 2010.

[22] F. Selimi, A. M. Lohof, S. Heitz et al., "Lurcher GRID2-induced death and depolarization can Be dissociated in cerebellar Purkinje cells," *Neuron*, vol. 37, no. 5, pp. 813–819, 2003.

[23] M. W. Vogel, J. Caston, M. Yuzaki, and J. Mariani, "The Lurcher mouse: fresh insights from an old mutant," *Brain Research*, vol. 1140, no. 1, pp. 4–18, 2007.

[24] K. W. Caddy and T. J. Biscoe, "Structural and quantitative studies on the normal C3H and Lurcher mutant mouse," *Philosophical transactions of the Royal Society of London B*, vol. 287, no. 1020, pp. 167–201, 1979.

[25] R. McFarland, A. Blokhin, J. Sydnor, J. Mariani, and M. W. Vogel, "Oxidative stress, nitric oxide, and the mechanisms of cell death in Lurcher Purkinje cells," *Developmental Neurobiology*, vol. 67, no. 8, pp. 1032–1046, 2007.

[26] M. W. Vogel, H. Fan, J. Sydnor, and P. Guidetti, "Cytochrome oxidase activity is increased in +/Lc Purkinje cells destined to die," *NeuroReport*, vol. 12, no. 14, pp. 3039–3043, 2001.

[27] H. S. Zanjani, A. M. Lohof, R. McFarland, M. W. Vogel, and J. Mariani, "Enhanced survival of wild-type and Lurcher Purkinje cells in vitro following inhibition of conventional PKCs or stress-activated MAP kinase pathways," *Cerebellum*, vol. 12, no. 3, pp. 377–389, 2012.

[28] N. Dumesnil-Bousez and C. Sotelo, "Early development of the Lurcher cerebellum: purkinje cell alterations and impairment of synaptogenesis," *Journal of Neurocytology*, vol. 21, no. 7, pp. 506–529, 1992.

[29] L.-O. Klotz, P. Schroeder, and H. Sies, "Peroxynitrite signaling: receptor tyrosine kinases and activation of stress-responsive pathways," *Free Radical Biology and Medicine*, vol. 33, no. 6, pp. 737–743, 2002.

[30] M. Minetti, C. Mallozzi, and A. M. M. Di Stasi, "Peroxynitrite activates kinases of the src family and upregulates tyrosine phosphorylation signaling," *Free Radical Biology and Medicine*, vol. 33, no. 6, pp. 744–754, 2002.

[31] N. Zolotarjova, C. Ho, R. L. Mellgren, A. Askari, and W.-H. Huang, "Different sensitivities of native and oxidized forms of Na^+/K^+-ATPase to intracellular proteinases," *Biochimica et Biophysica Acta*, vol. 1192, no. 1, pp. 125–131, 1994.

[32] K. Inomata, H. Mayahara, K. Fujimoto, and K. Ogawa, "Ultrastructural localization of ouabain-sensitive potassium-dependant p-nitrophenylphosphate (Na^+-K^+-ATPase) activity in hte central nervous system of the rat," *Acta Histochemica Cytochemica*, vol. 16, no. 3, pp. 277–285, 1983.

[33] W. C. Golden, A. M. Brambrink, R. J. Traystman, and L. J. Martin, "Failure to sustain recovery of Na,K-ATPase function is a possible mechanism for striatal neurodegeneration in hypoxic-ischemic newborn piglets," *Molecular Brain Research*, vol. 88, no. 1-2, pp. 94–102, 2001.

[34] F. Selimi, M. W. Vogel, and J. Mariani, "Bax inactivation in Lurcher mutants rescues cerebellar granule cells but not Purkinje cells or inferior olivary neurons," *Journal of Neuroscience*, vol. 20, no. 14, pp. 5339–5345, 2000.

[35] M. L. Doughty, P. L. De Jager, S. J. Korsmeyer, and N. Heintz, "Neurodegeneration in Lurcher mice occurs via multiple cell death pathways," *Journal of Neuroscience*, vol. 20, no. 10, pp. 3687–3694, 2000.

[36] C. A. Duffin, R. McFarland, J. R. Sarna, M. W. Vogel, and C. L. Armstrong, "Heat shock protein 25 expression and preferential purkinje cell survival in the lurcher mutant mouse cerebellum," *Journal of Comparative Neurology*, vol. 518, no. 11, pp. 1892–1907, 2010.

[37] V. V. Senatorov, P. K. Stys, and B. Hu, "Regulation of Na^+,K^+-ATPase by persistent sodium accumulation in adult rat thalamic neurones," *Journal of Physiology*, vol. 525, no. 2, pp. 343–353, 2000.

[38] J. S. Cook, E. H. Tate, and C. Shaffer, "Uptake of [3H]ouabain from the cell surface into the lysosomal compartment of HeLa cells," *Journal of Cellular Physiology*, vol. 110, no. 1, pp. 84–92, 1982.

[39] J. Inserte, D. Garcia-Dorado, V. Hernando, and J. Soler-Soler, "Calpain-mediated impairment of Na^+/K^+-ATPase activity during early reperfusion contributes to cell death after myocardial ischemia," *Circulation Research*, vol. 97, no. 5, pp. 465–473, 2005.

[40] D. González-Forero, F. Portillo, L. Gómez, F. Montero, S. Kasparov, and B. Moreno-López, "Inhibition of resting potassium conductances by long-term activation of the NO/cGMP/protein kinase G pathway: a new mechanism regulating neuronal excitability," *Journal of Neuroscience*, vol. 27, no. 23, pp. 6302–6312, 2007.

[41] L. Kiedrowski, "Critical role of sodium in cytosolic [Ca^{2+}] elevations in cultured hippocampal CA1 neurons during anoxic depolarization," *Journal of Neurochemistry*, vol. 100, no. 4, pp. 915–923, 2007.

[42] A. Ames III, "CNS energy metabolism as related to function," *Brain Research Reviews*, vol. 34, no. 1-2, pp. 42–68, 2000.

[43] R. S. Haber, T. A. Pressley, J. N. Loeb, and F. Ismail-Beigi, "Ionic dependence of active Na-K transport: "Clamping" of cellular Na^+ with monensin," *American Journal of Physiology—Renal Fluid and Electrolyte Physiology*, vol. 253, no. 1, pp. F26–F33, 1987.

[44] M. Nakao and D. C. Gadsby, "[Na] and [K] dependence of the Na/K pump current-voltage relationship in guinea pig ventricular myocytes," *Journal of General Physiology*, vol. 94, no. 3, pp. 539–565, 1989.

[45] N. Inoue and H. Matsui, "Activation of a brain type Na pump after glutamate excitation of cerebral neurons," *Brain Research*, vol. 534, no. 1-2, pp. 309–312, 1990.

Hindawi Publishing Corporation
International Journal of Cell Biology
Volume 2014, Article ID 674753, 11 pages
http://dx.doi.org/10.1155/2014/674753

Research Article

The Linker Histone H1.2 Is an Intermediate in the Apoptotic Response to Cytokine Deprivation in T-Effectors

Megha Garg,[1,2] Lakshmi R. Perumalsamy,[1,3] G. V. Shivashankar,[4] and Apurva Sarin[1]

[1] *National Centre for Biological Sciences, Bellary Road, Bangalore, Karnataka 560065, India*
[2] *Department of Biotechnology, Mysore University, Mysore, Karnataka 570005, India*
[3] *Department of Biotechnology, Indian Institute of Technology Madras, Chennai, Tamil Nadu 600036, India*
[4] *Mechanobiology Institute, National University of Singapore, Singapore 117411*

Correspondence should be addressed to Apurva Sarin; sarina@ncbs.res.in

Received 3 November 2013; Revised 3 January 2014; Accepted 5 January 2014; Published 13 February 2014

Academic Editor: Claudia Giampietri

Tissue homeostasis is a dynamic process involving proliferation and the removal of redundant or damaged cells. This is exemplified in the coordinated deletion—triggered by limiting trophic factors/cytokines in the extracellular milieu—of differentiated T cells overproduced during the mammalian immune response. However, mechanisms by which extracellular cues are perceived and transduced as apoptotic triggers remain incompletely understood. T-effectors are dependent on cytokines for survival and undergo apoptosis following cytokine withdrawal. Here we report that leptomycin B (LMB), an inhibitor of nuclear export machinery, protected T-effectors from apoptosis implicating a nuclear intermediate in the apoptotic pathway. Evidence is presented that the linker histone H1.2 localizes to the cytoplasm, by a mechanism sensitive to regulation by LMB, to activate apoptotic signaling culminating in nuclear and mitochondrial damage in T-effectors in response to cytokine deprivation. H1.2 is detected in a complex with the proapoptotic mitochondrial resident Bak and its subcellular localization regulated by Jun-N-terminal kinase (JNK), an intermediate in the apoptotic cascade in T-effectors. These data suggest that metabolic stressors may impinge on H1.2 dynamics favoring its activity at the mitochondrion, thereby functioning as a molecular switch for T-effector apoptosis.

1. Introduction

Cells divide and differentiate to acquire distinct cell fates in multicellular organisms. However, differentiation and proliferation are balanced by the programmed deletion of excess or damaged cells, which is critical for tissue homeostasis. Core elements of the cellular machinery regulating cell death are conserved in different phyla [1] and at least two major pathways regulating apoptosis have been described in mammalian cells. Signaling cascades initiated by ligand-receptor engagements of the TNFR (tumor necrosis factor receptor) superfamily constitute the extrinsic pathway [2]. The intrinsic pathway is activated by metabolic and genotoxic stressors and integrated at the mitochondrion, with members of the Bcl-2 family, which comprise both pro- and antiapoptotic members emerging as dominant regulators of these responses [1, 3, 4]. Cross talk between these two pathways is well documented. Cell-death pathways are variously deployed during development and in adult tissues as seen in the nervous, reproductive, and immune system where cells are overproduced and then removed by apoptosis [5–9]. Competition for limiting nutrients in the extracellular milieu is a widely prevalent mechanism for the regulation of cell number [10–12]. However, mechanisms by which cells perceive changes in their microenvironment are not fully understood.

In this study, we sought to address this question in a well-characterized model system that recapitulates the deletion of differentiated T cells in cell culture. The mature T cell compartment is characterized by dramatic increase in cell number in response to antigen challenge, followed by the eventual elimination of antigen-reactive T-effector cells so generated, a cycle repeated throughout adult life and necessary for

immune functionality [13, 14]. T-effectors generated in the immune response depend on cytokines or trophic factors for nutrient uptake and experiments *in vitro* and *in vivo* model systems indicate that the apoptotic response to nutrient deprivation is mediated by reactive oxygen species- (ROS-) dependent signaling that converges on the mitochondrion [15–18]. While T-cell dependence on cytokines and the ROS-Bcl-2 family signaling axis for survival and apoptosis, respectively, is well established, the cellular machinery that senses and integrates changes in the extracellular milieu remains uncharacterized and forms the focus of this study.

A critical role for nuclear effectors in initiating apoptotic signaling in T-effectors was indicated in our experiments since blocking nuclear export machinery protected cells from apoptosis. Building on a previously described role for the linker histone H1.2 in propagation of apoptotic cascades we followed the spatial dynamics of the linker histone H1.2 isoform in T-effectors. Our experiments show that the nuclear export machinery and JNK activity regulate H1.2 translocation and activity in T-effectors undergoing apoptosis. We provide evidence of H1.2 interaction with the Bcl-2 family proapoptotic protein Bak and propose that H1.2 converges on apoptotic signaling cascades integrated at the mitochondrion. Its role in apoptosis is indicated by the abrogation of apoptotic damage in response to cytokine deprivation following H1.2 ablation in T-effectors. Finally, our experiments implicate the Jun-N-terminal kinase (JNK) in regulating H1.2 dynamics, suggesting a more expansive role for this signaling cascade in tissue homeostasis.

2. Materials and Methods

2.1. Mice. C57BL/6 mice were obtained from The Jackson Laboratory (Maine, USA) and maintained at the Animal Facility at the National Centre for Biological Sciences (NCBS), Bangalore, India. Manipulations involving animals were approved by the Institutional Animal Ethics Committees of NCBS, Bangalore, India, and followed norms specified by the Committee for the Purpose of Control and Supervision of Experiments on Animals (CPCSEA), Government of India.

2.2. Reagents. Antibodies were used at dilutions indicated and procured from the following sources: H1 (1 : 1000) and p38MAPK (1 : 1000) from Santa Cruz (Santa Cruz, CA); AIF (1 : 500) from Chemicon (Billerica, MA); H1.2 (1 : 1000) from Proteintech Europe (Manchester, UK); H3 (1 : 500), H3Ac (1 : 500), and HP1α (1 : 1000) from Upstate Biotechnology (Lake Placid, NY); α-actin (1 : 500) and α-tubulin (1 : 250) from Neomarker (Fremont, CA); and Bak (1 : 1000), Cox-IV (1 : 250), and p-JNK/SAPK (1 : 500) from Cell Signaling Technology (Beverly, MA). The shRNA plasmids to H1.2 and the scrambled control were from Origene Technologies (Rockville, MD). TMRM (tetramethyl rhodamine methyl ester) was obtained from Sigma (St. Louis); Annexin-V AlexaFluor-488 was from Invitrogen (Carlsbad, USA); anacardic acid, leptomycin B, and SP600125 were from Calbiochem (San Diego, CA).

2.3. Generation of T-Effectors. T-cells were isolated from spleens of 6–8-week-old C57BL/6 mice, using mouse IgG coated magnetic (GAMT) beads (NEB, USA) or using CD3+ T cell isolation kits (R&D Systems). T-effectors were generated as described [17]. Briefly, T-cells were stimulated using α-CD3/α-CD28 bound beads (Invitrogen) at 2.0×10^6 cells/mL or in some instances soluble anti-CD3 (500 ng/mL, clone 2C11; R&D Systems) at 2.5×10^6 T cells/mL in cultures spiked with 10^4 splenic adherent cells. T-effectors generated after 48 hours were used for assays or continued in culture with 1 μg/mL cytokine interleukin-2 (R&D Systems) for 24–36 hours. Activation was established by expression of CD69 and CD25 along with the changes in morphology and increased size of T-cells [19].

2.4. Assays of Apoptosis. Assays of cytokine deprivation were performed as described [17]. 0.4×10^6/mL T-effectors were washed thrice in excess medium and phosphate buffered saline (PBS) to remove bound cytokine and then continued in culture with or without IL-7. Apoptosis was assayed at different time points after cytokine deprivation as indicated in the experiments. For assays of subcellular fractionation, cells were typically harvested at 6 hours for the analysis of H1.2 dynamics and at a delayed time point of 8 hours to examine the translocation of AIF. In experiments where H1.2 and AIF translocations were examined together, samples were harvested at the earlier time point of 6 hours.

To assess apoptotic nuclear damage, cells were stained for 3 minutes with the Hoechst-33342 (1 μg/mL) at ambient temperature and nuclear morphology scored in a minimum of 200 cells in each sample, using a fluorescence microscope equipped with a UV filter. For staining with Annexin-V, 0.3×10^6 T-effectors were incubated with Annexin-V ($1 : 60/10^6$ cells) for 15 min at room temperature, washed once with PBS, and analyzed immediately by flow cytometry following the addition of propidium iodide. For the assessment of mitochondrial transmembrane potential, cells were incubated with a 50 nM mitochondria-specific dye, TMRM, in medium for 15 minutes at 37°C, followed by two gentle washes with PBS and immediately analyzed by flow cytometry.

2.5. Retroviral Infections. For packaging murine retroviruses with shRNA plasmids, 1 μg of DNA was cotransfected with 1 μg of pClEco (packaging vector) in HEK293T cells. After 48 hours, the culture supernatant was concentrated and used for infecting T-cells by previously described protocols [17, 20]. Infected T cells were maintained in RPMI complete medium supplemented with 1 μg/mL IL-2, 2 ng/mL IL-7, and 1 μg/mL puromycin for 3 days. Live cells were isolated using Ficoll and continued in culture with IL-2 for 24 hours before being used in cytokine deprivation assays. Protein levels were assessed by Western blot analysis.

2.6. Western Blot Analysis. $0.3–0.5 \times 10^6$ cells were lysed in a SDS lysis buffer (2% SDS, glycerol, bromophenol blue), 1 M DTT, and 1 M Tris—HCl pH 6.8 supplemented with a protease inhibitor cocktail—aprotinin, leupeptin, and pepstatin (2 μg/mL each), 1 mM PMSF, 1 mM NaF, and 1 mM Na_3VO_4

for 10 minutes at 100°C. Using previously established protocols [17, 20], whole cell lysates were resolved by SDS-PAGE and transferred to nitrocellulose membrane (GE Healthcare) and incubated overnight at 4°C with primary antibodies at concentrations recommended by the manufacturers. Membrane was washed thrice with TBS-Tween20 followed by HRP-conjugated secondary antibody (CST, 1 : 1000 dilution) for 1 hour at RT. Membranes were developed either by exposing to X-ray film using an Amersham Hyperprocessor or an ImageQuant LAS 4000 Biomolecular Imager (GE Healthcare).

2.7. Subcellular Fractionation. 10×10^6 T-effectors were used for the subcellular fractionation protocol [21]. Cytoplasmic and nuclear fractions were obtained using the NE-PER nuclear and cytoplasmic extraction kit (Thermo Scientific) following manufacturer's instructions. Equivalent volumes of nuclear and cytoplasmic fractions were boiled in SDS lysis buffer for Western blot analysis.

2.8. Immunoprecipitation. 10×10^6 T-effectors cultured in the absence of cytokine were lysed for 1 hour at 4°C in 1% CHAPS lysis buffer supplemented with protease inhibitors (2 μg/mL aprotinin, leupeptin, pepstatin, 1 mM PMSF, 1 mM NaF, and 1 mM Na_3VO_4). 10 μL antibody was used for precipitating immune complex for 2 hours at 4°C using protein G agarose beads (Pierce Biotechnology) on a rotator. Beads were washed five times with ice-cold PBS at 1700 rpm and then boiled in SDS lysis buffer for 10 min for the Western blot analysis. When the cytoplasmic fraction was used as an input for the IP, 20×10^6 T-cells were subjected to subcellular fractionation as described above and the cytoplasmic fraction obtained was used for immunoprecipitation. True-blot HRP (Ebioscience) has been used for immunoblots of Bak and H1.2.

2.9. Statistical Methods. All graphs show data presented as mean ± SD from a minimum of three independent experiments. Statistical significance was calculated using the two population Student's t-tests, with the following confidence intervals: *99% and **99.9%.

3. Results

3.1. Apoptosis in T-Effectors Is Regulated by Nuclear Events. T-cells proliferate and differentiate in response to antigen, to generate lineage-committed effectors, the bulk of which die, marking termination of the immune response [14]. Key elements of this process can be recapitulated *in vitro*, permitting investigations into the molecular regulation of T-cell apoptosis [16–18, 20, 21]. Using this experimental system we show that cytokine withdrawal from T-effectors triggers apoptotic damage characterized by nuclear fragmentation and externalization of phosphatidylserine (PS) at the cell membrane (Figures 1(a) and 1(b)). Loss of mitochondrial integrity is another feature of cells undergoing apoptotic duress and is reflected in the spatial redistribution of the flavoprotein, AIF (apoptosis inducing factor) [22]. AIF is a mitochondrial intermembrane space resident protein, which is released from mitochondria as a consequence of loss of outer mitochondrial membrane integrity and translocates to the nucleus to mediate DNA damage [21, 23]. In T-cells cultured in cytokine assessed prior to the onset of the deprivation protocol (T0), AIF is detected in the cytoplasmic fraction consistent with its localization to mitochondria (Figure 1(c)). Subcellular fractionation of T-cells following cytokine withdrawal indicated that a substantial signal for AIF is detected in the nuclear fraction (Figure 1(d)). In these assays, we also probed for the distribution of the nuclear heterochromatin binding protein Hp1α and the mitochondrial matrix resident Cox-IV to establish purity of the fractions (Figures 1(c)–1(e)).

Leptomycin B (LMB), a Crm1 inhibitor that blocks nuclear export, substantially reduced apoptotic damage in T-effectors (Figures 1(a) and 1(b)), implicating a nuclear intermediate in the cascade. LMB is typically used at concentrations that range from 0.3 to 10 ng/mL although lower concentrations are also effective at blocking nuclear export [24]. Since 0.3 ng/mL LMB was toxic to T-cells in culture, we tested lower concentrations and found that 0.03 mg/mL or 0.003 ng/mL LMB was well tolerated by T-effectors cultured with cytokine. Since both concentrations also protected from apoptosis with comparable efficacy (not shown), the experiments using the lower concentrations of LMB have been used in the current study. The distribution of AIF in cells cultured without cytokine but in the presence of LMB (Figure 1(e)) was restored to the pattern of live cells (Figure 1(c)), indicating that LMB prevented damage to the mitochondrial outer membrane, a necessary step for the release of AIF. These observations suggested that events in the nucleus influence early, premitochondrial steps of the apoptotic cascade. The linker histone H1.2 has been shown to initiate apoptotic cascades integrated by the mitochondrion, first reported in the context of the DNA damage response in immature T-cells [25]. Activation of H1.2 dependent apoptotic signaling is associated with its displacement from the nucleus. Hence, in subsequent experiments we assessed the cellular distribution and possible involvement of H1.2 in T-effector apoptosis.

3.2. Changes in H1.2 Localization in T-Effectors Undergoing Apoptosis. H1.2 is typically detected in the nucleus as evidenced in the analysis of nuclear and cytoplasmic fractions of cells cultured in conditions that promote survival (Figure 2(a)). In contrast to this distribution, subcellular fractionation of cells following cytokine withdrawal (within 6 hours of the deprivation protocol) was characterized by the appearance of cytoplasmic pools of H1.2 (Figure 2(b)). This positions the translocation of H1.2 at a relatively early time-point in the apoptotic process, well before overt evidence of nuclear damage in experimental conditions. The distribution of the mitochondrial resident protein Cox-IV and the nuclear protein HP1α established purity of the cytoplasmic and nuclear fractions, respectively, in these assays. Consistent with the inhibition of apoptotic nuclear damage, if LMB was included in cytokine-withdrawal conditions, the distribution of H1.2 was restored to the pattern of live cells and only detected in the nucleus (Figure 2(c)). To assess the functional implications of the

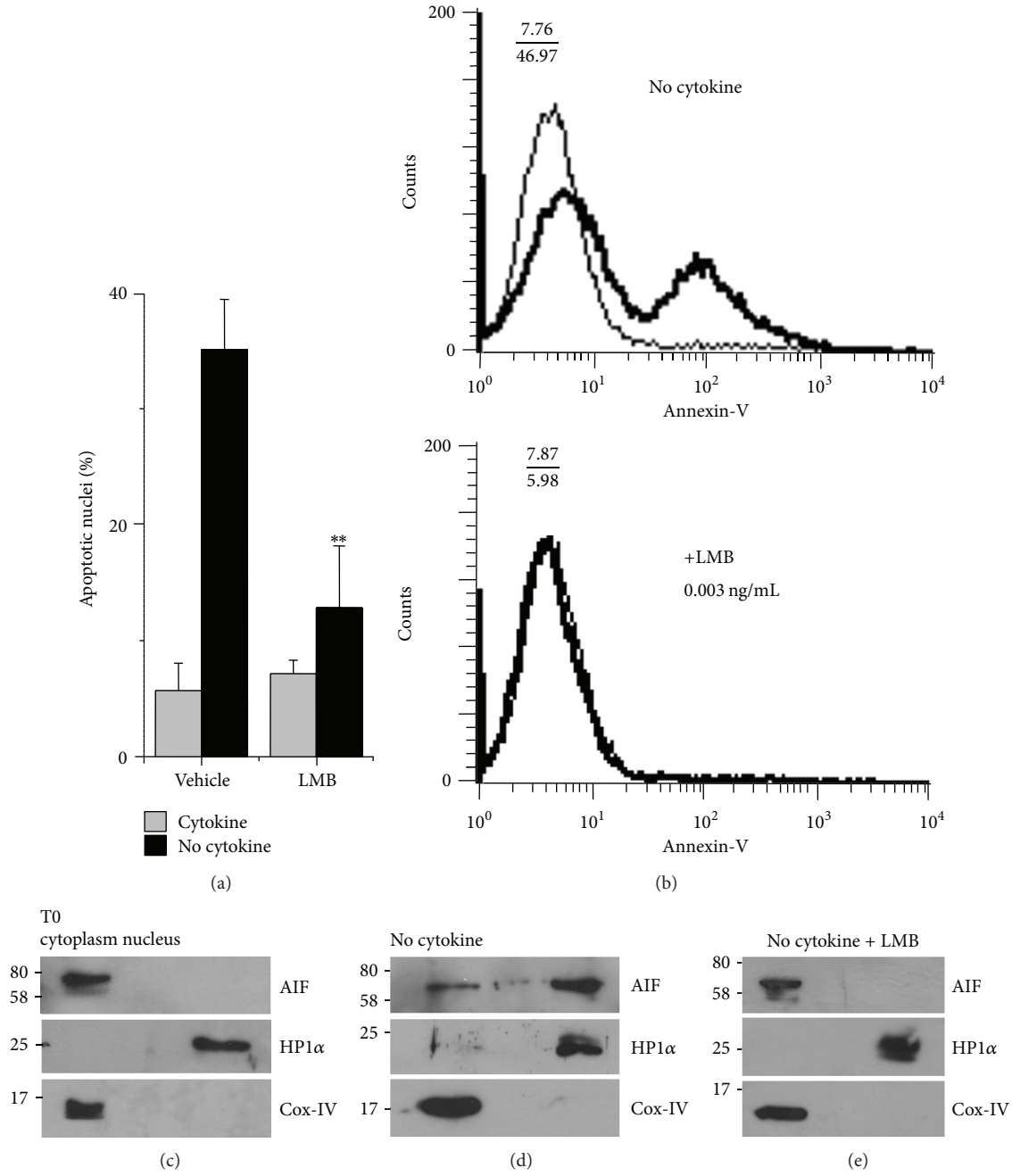

Figure 1: LMB blocks cytokine deprivation induced apoptotic damage in T-effectors. (a)-(b) 0.3×10^6 T-effectors were cultured with or without IL-7 (20 ng/ml) with the addition of vehicle control or LMB (0.003 ng/ml). Apoptotic nuclear damage (a) and Annexin-V binding (b) were scored after 8 and 15 hours, respectively. The dotted lines in (b) indicate cells continued in cytokine. The graph shows mean ± SD from 4 experiments. $^{**}P < 0.001$. (c)–(e) 10×10^6 T-effectors were cultured in the indicated conditions (T0: freshly activated) and 8 hours later cells were fractionated as described in Materials and Methods. Immunoblots of nuclear and cytoplasmic fractions obtained were probed for AIF, HP1α, and Cox-IV. Data are representative of three independent trials.

change in H1.2 localization and elucidate its role, if any, in apoptosis, RNA interference approaches were employed to ablate H1.2 function in T-effectors.

T-effectors were transduced using retroviruses with shRNA to H1.2 or a scrambled control and cultured in puromycin containing medium, as described in materials and Methods, in order to enrich for transfected cells [17]. Efficacy of the shRNA for depletion of H1.2 was established in the NIH3T3 fibroblast cell line (not shown) and as shown demonstrably reduced protein expression in T-effectors (Figure 2(d), inset). T-effectors treated with scrambled or H1.2 shRNA were assessed for their response to cytokine deprivation in the experiments that follow. In contrast to cells transduced with scrambled shRNA, cells with reduced

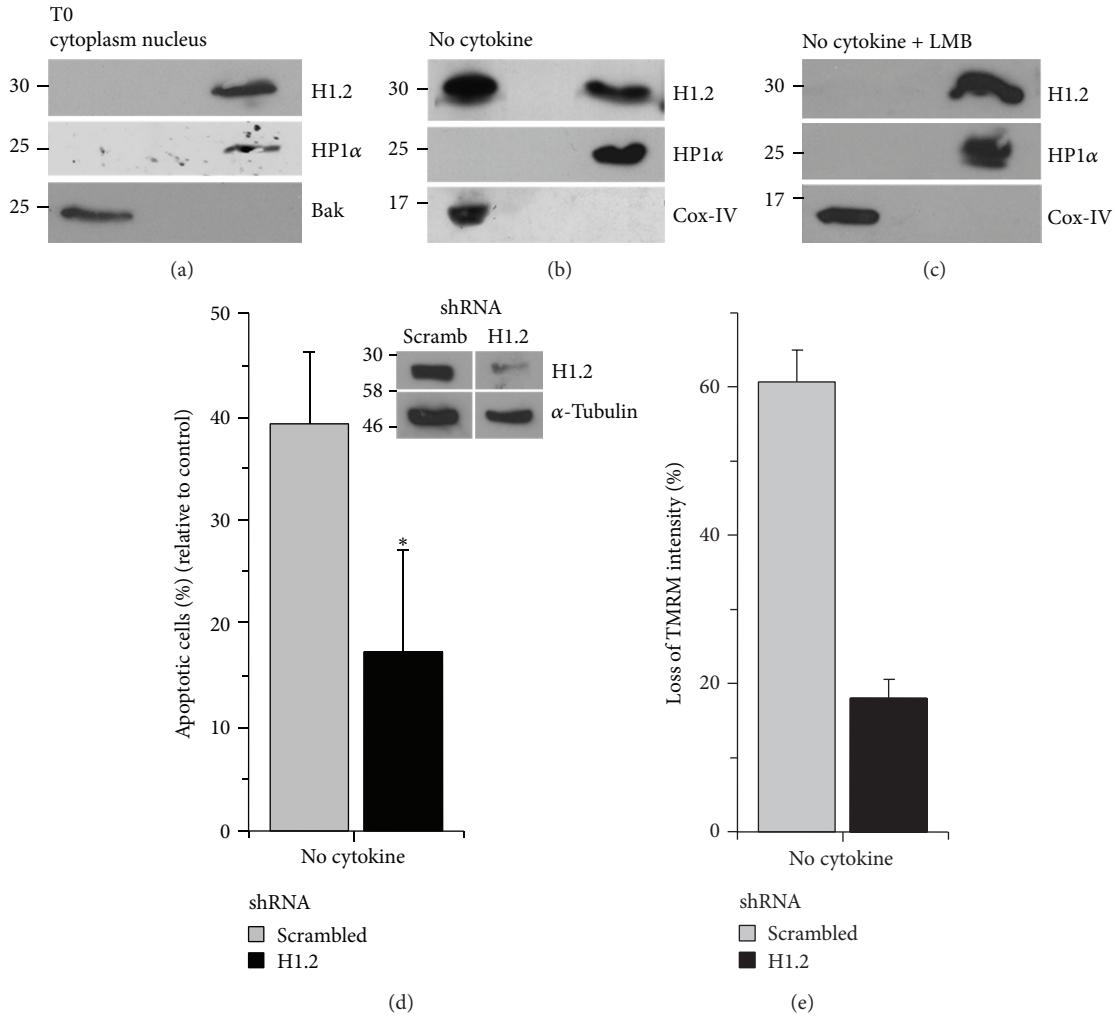

Figure 2: H1.2 is an intermediate in the apoptotic cascade triggered by cytokine deprivation. (a)–(c) 10×10^6 T-effectors were cultured in the indicated conditions (T0: freshly activated) and 6 hours later subject to subcellular fractionation. Immunoblots of nuclear and cytoplasmic fractions were probed for H1.2, HP1α, Bak, or Cox-IV. Data are representative of three independent trials. (d)-(e) T-effectors transduced using retrovirus expressing scrambled control or histone H1.2 shRNA, as described in Materials and Methods, were cultured with or without cytokine for 10 hours. Cells were scored for apoptotic nuclear damage using Hoechst-33342 (d) or mitochondrial transmembrane potential using TMRM (e) as described in Materials and Methods. Graphs show mean ± SD from 5 experiments in (d) and 2 experiments in (e), normalized to cultures with cytokine. Inset: Immunoblot for H1.2 protein and tubulin (parity in loading) in shRNA expressing T-effectors. $^*P < 0.01$.

H1.2 protein levels were protected from nuclear damage triggered by cytokine deprivation (Figure 2(d)). In order to assess if loss of H1.2 also protected from mitochondrial damage we used flow cytometry based analysis of intact cells. Loss of mitochondrial transmembrane potential is a sensitive indicator of damage to the organelle and characteristic of cells undergoing apoptosis. Hence we tested if H1.2 ablation protected T-effectors from mitochondrial damage triggered by cytokine deprivation. In these experiments, changes in mitochondrial activity were assessed by the uptake of the potentiometric dye TMRM. In contrast to cells expressing the control, scrambled shRNA, TMRM intensity was comparable in the presence or absence of cytokine in cells with an ablation of H1.2 consistent with protection from death (Figure 2(e)). This strongly suggests that reduced H1.2 levels protected cells from damage to mitochondria otherwise observed in cells in conditions of cytokine withdrawal. We did not observe deleterious effects of H1.2 depletion in T-effectors continued in culture in cytokine, indicating a specific role for H1.2 in the response to apoptotic stimuli. These data positioned H1.2 translocation and activity at a step controlling events culminating in compromised mitochondrial function and nuclear integrity in the apoptotic cascades in T-effectors.

3.3. H1.2 Associates with Bak in T-Effectors. H1.2 has been reported to localize to the mitochondrion and participate in apoptotic cascades involving the mitochondrial resident protein Bak [25, 26]. The experiments described in the preceding sections indicated that H1.2 activity converged on

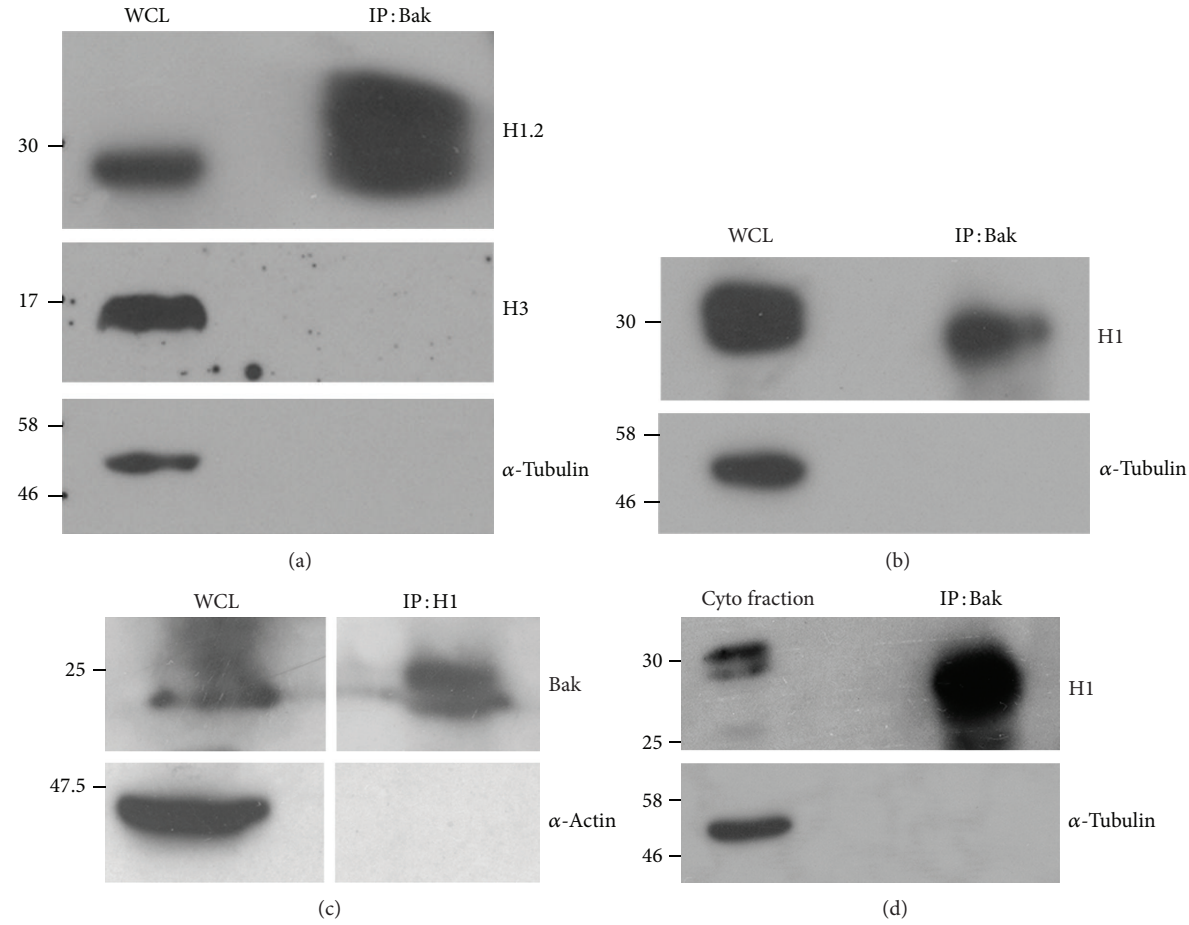

Figure 3: H1.2 immunoprecipitates with the mitochondrial outer-membrane resident Bak in T-effectors. (a)-(b) 10×10^6 T-effectors were cultured without cytokine and 6 hours later immunoprecipitated (IP) with an antibody to Bak. Immunoblots of whole cell lysates (WCL) or the IP were probed with an antibody to H1.2 (a) or a pan H1 antibody (b) and α-Tubulin. (c) Reverse IP with an antibody to H1 in T-effectors cultured as described in (a)-(b) and the immunoblot probed for Bak. Actin is the specificity control. (d) 10×10^6 T-effectors were cultured without cytokine for 6 hours and the cytoplasmic fraction obtained by subcellular fractionation as described in Materials and Methods was used as input for an IP with an antibody to Bak. A representative immunoblot for H1 in the complex IP is shown. α-Tubulin is the specificity control.

mitochondrial function. Hence, we next tested for interactions between Bak and H1.2 in T-effectors under cytokine deprivation. The immune-precipitation (IP) of these proteins as a complex is evidence of a physical association (Figure 3(a)), which was confirmed using antibodies that recognize the H1 family of proteins or with an antibody specific to H1.2 (Figures 3(a) and 3(b)). Although the lysates used as the input for IP analysis are a postnuclear supernatant, we confirmed that core histone H3 was not detected in the immunoprecipitated complex (IP) indicating that nuclear pools of H1.2 were unlikely to be detected in the immunoblots (Figure 3(a)). Mindful of the detergent sensitivities of Bcl-2 family proteins [27], these experiments used the milder detergent CHAPS to generate cell lysates to assess these interactions. The association between Bak and H1.2 in T-cells was also confirmed by reverse immunoprecipitation (Figure 3(c)). In order to rule out possible contamination of the immunoprecipitated complex with nuclear proteins, the cytoplasmic fraction of T-effectors in deprivation (purity ascertained by the exclusion of the nuclear protein HP1α) was used to immunoprecipitate Bak. H1.2 immunoprecipitated in the complex with Bak when the cytoplasmic fraction was used as input as well, confirming that the association is occurring outside the nucleus (Figure 3(d)). The experiments thus far implicate H1.2 as key intermediate in the apoptotic response of T-effectors. In previous work [17], hierarchical interactions involving the Jun-N-terminal kinase (JNK) have been demonstrated to regulate T-effector apoptosis. Therefore, in the experiments that follow we attempted to position H1.2 activity in the context of known premitochondrial intermediates in the apoptotic cascade in T-effectors.

3.4. JNK Activity Regulates H1.2 Dynamics in T-Effectors. ROS-dependent activation of the JNK regulates deprivation-induced apoptosis in T-effectors and apoptotic cascades in other cell types [17, 28]. Hence we asked if JNK inhibited the translocation of H1.2 in T-effectors. To modulate JNK

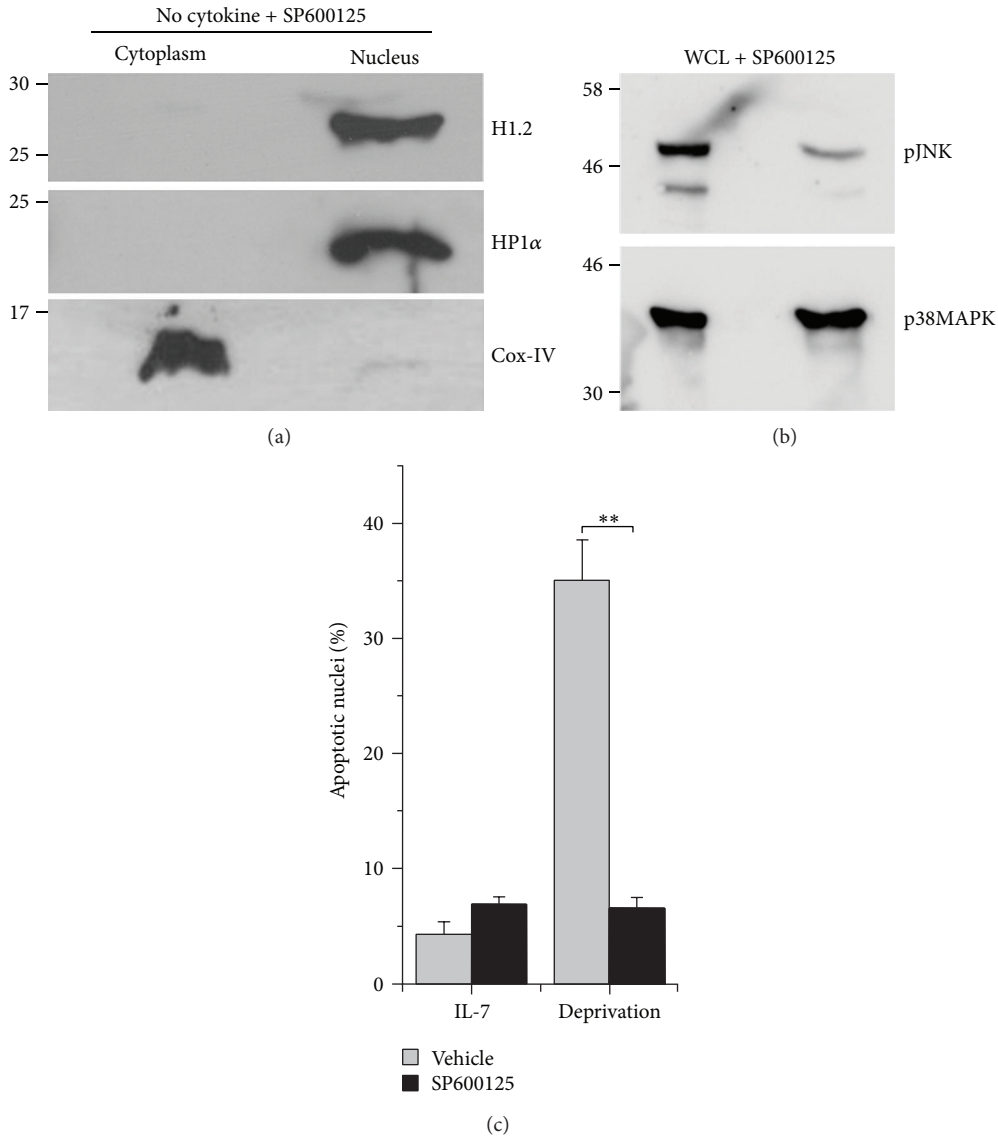

Figure 4: JNK regulates H1.2 displacement in T-effectors. (a) Representative immunoblot of nuclear and cytoplasmic fractions of T-effectors cultured without cytokine +100 nM SP600125 for 6 hours. The immunoblots were probed with antibodies to H1.2, HP1α, and Cox-IV and controlled with fractions generated in previous experiments. Data shown is representative of two independent trials. (b) Representative immunoblot for phosphorylated JNK in T-effectors cultured as described in (a). p38MAPK is the loading control. (c) Apoptotic nuclear damage in T-effectors cultured with and without cytokine (IL-7) in the presence or absence of vehicle control or 100 nM SP600125 for 24 hours. The graph shows the mean ± SD from 3 experiments. $^{**}P < 0.001$.

activity we used the inhibitor, SP610025, demonstrated in earlier experiments to regulate JNK activity in T-effectors [17]. In the analysis of nuclear and cytoplasmic fractions, in cultures where SP610025 was added at the onset of the deprivation protocol, the distribution of H1.2 was comparable to control cells and detected only in the nuclear fraction (Figure 4(a)). Confirming earlier reports and consistent with its effect on the subcellular localization of H1.2, blocking JNK (Figure 4(b)) also protected T-cells from apoptotic damage (Figure 4(c)). Growing evidence of cross talk between signal transduction pathways and the metabolic status of cells, wherein evidence that metabolic stress triggers changes in acetylation and consequently mitochondrial function [29–31], prompted us to assess possible regulation of T-effector apoptosis by cellular acetylation machinery.

3.5. Acetylation Dependence of T-Effector Apoptosis. Mounting evidence of proteins modified by acetylation outside of conventional chromatin targets suggest a broader array and range of cellular processes regulated by this modification [32–34]. As a first approximation, a possible role of acetylation in the activation of the H1.2 mediated apoptotic cascade in T-effectors was tested. Anacardic acid (AA), a broad-spectrum inhibitor of lysine acetyl-transferases protected T-cells from apoptotic damage as seen in assays of nuclear

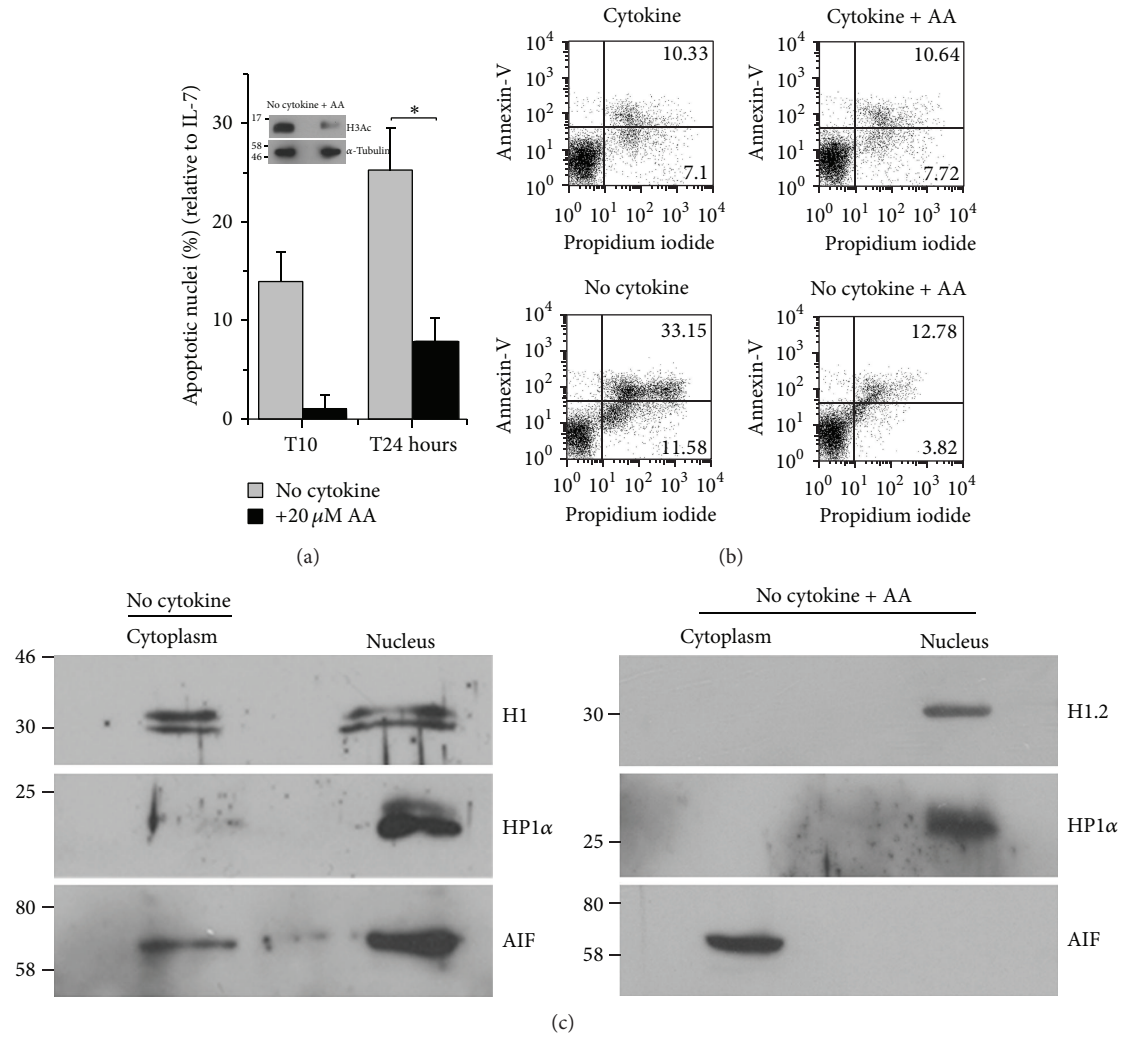

Figure 5: Acetylation dependence of the sub-cellular localization of H1.2 and apoptosis in T-effectors. (a) Apoptotic nuclear damage in T-effectors cultured without cytokine IL-7 (20 ng/ml) and with or without anacardic acid (AA) (20 μM) for indicated time points. The graph shows the mean ± SD from three experiments. Inset: immunoblot for acetylated H3 (H3Ac) and α-tubulin in T-effectors cultured without cytokine (for 6 hours) in the presence or absence of AA. (b) T-effectors cultured for 18 hours in the indicated conditions were stained with propidium iodide (x-axis) and Annexin-V (y-axis) analyzed by flow cytometry. Values in the upper right quadrant, in each plot, indicate dead cells. (c) 10×10^6 T-effectors were cultured without cytokine IL-7 (20 ng/ml) and with or without AA (20 μM) for 6 hours. Immunoblots of nuclear and cytoplasmic fractions were probed for H1 or H1.2, HP1α, and AIF. Data shown is representative of three independent trials.

morphology (Figure 5(a)). To assess if AA delayed rather than inhibited cell death, the uptake of propidium iodide (PI) was also measured in these conditions. After 18 hours in culture without cytokine, the coincident staining with PI and Annexin-V indicated the occurrence of membrane damage, which is in contrast to cells cultured in cytokine (Figure 5(b)). In cells that were cultured with AA, PI and Annexin-V staining was comparable (and low), indicating that AA prevented the loss of membrane integrity (Figure 5(b)). Further, the translocation of H1.2 (and AIF) was inhibited in cells treated with AA relative to the group cultured without cytokine (Figure 5(c)), supporting a possible role for changes in acetylation states as a regulatory step in the apoptotic response in T-effectors. The molecular target(s) of this modification remains to be identified. Experiments discriminating between the possibilities that H1.2 displacement may be a response to acetylation-dependent changes of chromatin organization vis-à-vis effects on histones or by the modulation of nonhistone proteins would provide additional insight into this regulation.

4. Discussion

Competition for limiting nutrients in the extracellular milieu is a widely prevalent mechanism for the regulation of cell number and mechanisms by which cells perceive these changes in their microenvironment continue to be actively investigated. Reduced availability of cell extrinsic growth

factors frequently underlies the coordinated deletion of cells overproduced during development or differentiation. We address this question in a model system that recapitulates the deletion (induced by cytokine withdrawal) of differentiated T-cells in cell culture. We provide evidence that the nucleus functions as a site for integration of extracellular nutritional cues with significant consequences to T-cell survival. This was indicated in the experiments wherein LMB blocked apoptotic damage in T-effectors in response to cytokine deprivation implicating a nuclear intermediate in the signaling cascade. Involvement of nuclear events was confirmed in experiments where, following cytokine withdrawal, we observed that H1.2 was displaced from the nucleus to translocate to the mitochondrion, initiating cascades culminating in cell death. H1.2 translocation from the nucleus has been previously reported in immature thymocytes and chronic lymphocytic leukemic cells in response to genotoxic and nongenotoxic drug treatment [25, 26, 35]. In support of this, we present evidence for H1.2 interactions with the mitochondrial outer-membrane resident, the proapoptotic protein Bak, and its regulation of ensuing damage to mitochondria and the nucleus in T-effectors undergoing apoptosis. These data open up possibilities—not mutually exclusive—of H1.2 associated molecules that regulate apoptotic outcomes or, modifications to H1.2 itself that may be necessary for its activity at the mitochondrion.

A hierarchy of interactions involving Bcl-2 family proteins (Bax and Bak amongst others) and reactive oxygen species are implicated in the apoptotic deletion of T-cells [3, 13–15, 17, 18]. Current understanding of apoptotic signaling positioned molecules with well-characterized functions at the mitochondrion as key intermediates in T-cell apoptosis. Since ablation of H1.2 protected cells from apoptosis in culture, the data suggests an intriguing possibility of amplification or reinforcing loop mediated by H1.2, which converges on the mitochondrion to propagate the apoptotic cascade. We speculated that if signaling resulting from H1.2 and ROS activation converges on a single event/organelle, common regulatory processes might be expected. Earlier work from the laboratory had shown that Jun-N-terminal kinase (JNK) was activated by NADPH-mediated ROS production and regulated mitochondrial damage in the apoptotic response of T-effectors [17]. Supporting the possibility of a hierarchy of interactions, JNK activity controlled the subcellular distribution of H1.2, that is, its liberation from the nucleus following growth factor deprivation. The underlying molecular features and consequences of H1.2 association with Bak remain to be elucidated. Based on the observations in this study we speculate that chromatin may execute a nontranscriptional response to JNK activity to initiate the observed nonnuclear functions of H1.2. This outcome may be linked to the modulation of epigenetic states by JNK activity, which has precedence in other systems [36–38].

The protective effect of AA is consistent with a role for acetylation in the regulation of H1.2 relocation and consequent apoptosis. The possibility that lysine acetyl-transferases form an instructive element in the apoptotic H1.2-dependent cascade suggested by these observations, however, requires more detailed analysis. Our attempts to track T-cell contraction following antigen challenge in mice injected with AA were unsuccessful because of the inhibitory effects of AA on T-cell activation responses *in vivo* (not shown). Genetic manipulations of H1.2 levels in T-cell populations are underway to directly envisage the role of H1.2 pathway in promoting survival of T effectors *in vivo*.

Taken together, the experiments suggest that cytokine inputs necessary for nutrient uptake and consequently survival in T-effectors are integrated in the nucleus. These observations position H1.2 in the molecular coupling of genomic integrity and mitochondrial function, demonstrated here in the programmed deletion of T-effectors. It is tempting to speculate that, since cellular responses to metabolic stressors are conserved across cell types, the pathway described here is likely activated in other cellular contexts involving homeostasis of differentiated cells.

5. Conclusions

Competition for limiting nutrients in the extracellular milieu is a ubiquitous mechanism for the regulation of cell number. Intracellular signaling networks constituting the cellular response to these changes remain an active area of investigation. In this study we provide evidence that events in the nucleus integrate extracellular nutritional cues in T-effector populations and these events are intricately connected to the apoptotic response elicited by nutritional deprivation. Specifically, in response to cytokine withdrawal the linker histone H1.2 is displaced from the nucleus to translocate to the mitochondrion and associate with the mitochondrial resident protein Bak to trigger T-effector apoptosis. Finally, H1.2 dynamics are regulated by JNK signaling and responsive to changes in the acetylation status in T-cells.

Conflict of Interests

The authors have no conflict of interests to declare.

Acknowledgments

The authors acknowledge the Central Imaging and Flow Cytometry Facility (CIFF) and the small animal facility at NCBS. We thank Dr. Nithyakala for assistance with the paper. Megha Garg and Lakshmi R. Perumalsamy were supported by fellowships from the Department of Biotechnology and Council of Scientific and Industrial Research, Government of India, respectively.

References

[1] M. O. Hengartner, "The biochemistry of apoptosis," *Nature*, vol. 407, no. 6805, pp. 770–776, 2000.

[2] A. Ashkenazi and V. M. Dixit, "Death receptors: signaling and modulation," *Science*, vol. 281, no. 5381, pp. 1305–1308, 1998.

[3] J. C. Rathmell, T. Lindsten, W. X. Zong, R. M. Cinalli, and C. B. Thompson, "Deficiency in Bak and Bax perturbs thymic selection and lymphoid homeostasis," *Nature Immunology*, vol. 3, no. 10, pp. 932–939, 2002.

[4] R. J. Youle and A. Strasser, "The BCL-2 protein family: opposing activities that mediate cell death," *Nature Reviews Molecular Cell Biology*, vol. 9, no. 1, pp. 47–59, 2008.

[5] J. Aebischer, R. Sturny, D. Andrieu et al., "Necdin protects embryonic motoneurons from programmed cell death," *PLoS ONE*, vol. 6, no. 9, Article ID e23764, 2011.

[6] L. DiNapoli, J. Batchvarov, and B. Capel, "FGF9 promotes survival of germ cells in the fetal testis," *Development*, vol. 133, no. 8, pp. 1519–1527, 2006.

[7] A. W. Goldrath and M. J. Bevan, "Selecting and maintaining a diverse T-cell repertoire," *Nature*, vol. 402, no. 6759, pp. 255–262, 1999.

[8] J. Yuan and B. A. Yankner, "Apoptosis in the nervous system," *Nature*, vol. 407, no. 6805, pp. 802–809, 2000.

[9] V. Barker, G. Middleton, F. Davey, and A. M. Davies, "TNFα contributes to the death of NGF-dependent neurons during development," *Nature Neuroscience*, vol. 4, no. 12, pp. 1194–1198, 2001.

[10] J. C. Rathmell, M. G. V. Heiden, M. H. Harris, K. A. Frauwirth, and C. B. Thompson, "In the absence of extrinsic signals, nutrient utilization by lymphocytes is insufficient to maintain either cell size or viability," *Molecular Cell*, vol. 6, no. 3, pp. 683–692, 2000.

[11] J. T. Tan, E. Dudl, E. LeRoy et al., "IL-7 is critical for homeostatic proliferation and survival of naïve T cells," *Proceedings of the National Academy of Sciences of the United States of America*, vol. 98, no. 15, pp. 8732–8737, 2001.

[12] M. Lenardo, F. K. Chan, F. Hornung et al., "Mature T lymphocyte apoptosis—immune regulation in a dynamic and unpredictable antigenic environment," *Annual Review of Immunology*, vol. 17, pp. 221–253, 1999.

[13] S. F. Fischer, G. T. Belz, and A. Strasser, "BH3-only protein Puma contributes to death of antigen-specific T cells during shutdown of an immune response to acute viral infection," *Proceedings of the National Academy of Sciences of the United States of America*, vol. 105, no. 8, pp. 3035–3040, 2008.

[14] A. Strasser and M. Pellegrini, "T-lymphocyte death during shutdown of an immune response," *Trends in Immunology*, vol. 25, no. 11, pp. 610–615, 2004.

[15] M. Pellegrini, G. Belz, P. Bouillet, and A. Strasser, "Shutdown of an acute T cell immune response to viral infection is mediated by the proapoptotic Bcl-2 homology 3-only protein Bim," *Proceedings of the National Academy of Sciences of the United States of America*, vol. 100, no. 2, pp. 14175–14180, 2003.

[16] A. T. Vella, S. Dow, T. A. Potter, J. Kappler, and P. Marrack, "Cytokine-induced survival of activated T cells in vitro and in vivo," *Proceedings of the National Academy of Sciences of the United States of America*, vol. 95, no. 7, pp. 3810–3815, 1998.

[17] D. Purushothaman and A. Sarin, "Cytokine-dependent regulation of NADPH oxidase activity and the consequences for activated T cell homeostasis," *Journal of Experimental Medicine*, vol. 206, no. 7, pp. 1515–1523, 2009.

[18] D. A. Hildeman, T. Mitchell, T. K. Teague et al., "Reactive oxygen species regulate activation-induced T cell apoptosis," *Immunity*, vol. 10, no. 6, pp. 735–744, 1999.

[19] S. Gupta, N. Marcel, S. Talwar et al., "Developmental heterogeneity in DNA packaging patterns influences T-cell activation and transmigration," *PLoS ONE*, vol. 7, no. 9, Article ID e43718, 2012.

[20] L. R. Perumalsamy, N. Marcel, S. Kulkarni, F. Radtke, and A. Sarin, "Distinct spatial and molecular features of notch pathway assembly in regulatory T cells," *Science Signaling*, vol. 5, no. 234, article ra53, 2012.

[21] D. Purushothaman, N. Marcel, M. Garg, R. Venkataraman, and A. Sarin, "Apoptotic programs are determined during lineage commitment of CD4+ T effectors: selective regulation of T effector-memory apoptosis by inducible nitric oxide synthase," *Journal of Immunology*, vol. 190, no. 1, pp. 97–105, 2013.

[22] H. K. Lorenzo, S. A. Susin, J. Penninger, and G. Kroemer, "Apoptosis inducing factor (AIF): a phylogenetically old, caspase-independent effector of cell death," *Cell Death and Differentiation*, vol. 6, no. 6, pp. 516–524, 1999.

[23] S. Srivastava, H. Banerjee, A. Chaudhry et al., "Apoptosis-inducing factor regulates death in peripheral T cells," *Journal of Immunology*, vol. 179, no. 2, pp. 797–803, 2007.

[24] H. M. Abkallo, H. Kawano, K. Watanabe, and N. A. Kobayashi, "New cell-based reporter system for sensitive screening of nuclear export inhibitors," *Drug Discoveries and Therapeutics*, vol. 5, no. 6, pp. 286–292, 2011.

[25] A. Konishi, S. Shimizu, J. Hirota et al., "Involvement of histone H1.2 in apoptosis induced by DNA double-strand breaks," *Cell*, vol. 114, no. 6, pp. 673–688, 2003.

[26] H. Okamura, K. Yoshida, B. R. Amorim, and T. Haneji, "Histone H1.2 is translocated to mitochondria and associates with bak in bleomycin-induced apoptotic cells," *Journal of Cellular Biochemistry*, vol. 103, no. 5, pp. 1488–1496, 2008.

[27] Y. T. Hsu and R. J. Youle, "Nonionic detergents induce dimerization among members of the Bcl-2 family," *The Journal of Biological Chemistry*, vol. 272, no. 21, pp. 13829–13834, 1997.

[28] H. Kamata, S. Honda, S. Maeda, L. Chang, H. Hirata, and M. Karin, "Reactive oxygen species promote TNFα-induced death and sustained JNK activation by inhibiting MAP kinase phosphatases," *Cell*, vol. 120, no. 5, pp. 649–661, 2005.

[29] K. L. Guan and Y. Xiong, "Regulation of intermediary metabolism by protein acetylation," *Trends in Biochemical Sciences*, vol. 36, no. 2, pp. 108–116, 2011.

[30] K. E. Wellen and C. B. Thompson, "A two-way street: reciprocal regulation of metabolism and signalling," *Nature Reviews Molecular Cell Biology*, vol. 13, no. 4, pp. 270–276, 2012.

[31] K. E. Wellen, G. Hatzivassiliou, U. M. Sachdeva, T. V. Bui, J. R. Cross, and C. B. Thompson, "ATP-citrate lyase links cellular metabolism to histone acetylation," *Science*, vol. 324, no. 5930, pp. 1076–1080, 2009.

[32] C. Choudhary, C. Kumar, F. Gnad et al., "Lysine acetylation targets protein complexes and co-regulates major cellular functions," *Science*, vol. 325, no. 5942, pp. 834–840, 2009.

[33] T. Kouzarides, "Acetylation: a regulatory modification to rival phosphorylation," *EMBO Journal*, vol. 19, no. 6, pp. 1176–1179, 2000.

[34] S. Spange, T. Wagner, T. Heinzel, and O. H. Krämer, "Acetylation of non-histone proteins modulates cellular signalling at multiple levels," *International Journal of Biochemistry and Cell Biology*, vol. 41, no. 1, pp. 185–198, 2009.

[35] E. Giné, M. Crespo, A. Muntañola et al., "Induction of histone H1.2 cytosolic release in chronic lymphocytic leukemia cells after genotoxic and non-genotoxic treatment," *Haematologica*, vol. 93, no. 1, pp. 75–82, 2008.

[36] V. K. Tiwari, M. B. Stadler, C. Wirbelauer, R. Paro, D. Schübeler, and C. Beisel, "A chromatin-modifying function of JNK during stem cell differentiation," *Nature Genetics*, vol. 44, no. 1, pp. 94–100, 2012.

[37] J. Wu, X. Zhang, H. J. Nauta, Q. Lin, J. Li, and L. Fang, "JNK1 regulates histone acetylation in trigeminal neurons following chemical stimulation," *Biochemical and Biophysical Research Communications*, vol. 376, no. 4, pp. 781–786, 2008.

[38] N. R. Sundaresan, P. Vasudevan, L. Zhong et al., "The sirtuin SIRT6 blocks IGF-Akt signaling and development of cardiac hypertrophy by targeting c-Jun," *Nature Medicine*, vol. 18, no. 11, pp. 1643–1650, 2012.

Hindawi Publishing Corporation
International Journal of Cell Biology
Volume 2014, Article ID 502676, 12 pages
http://dx.doi.org/10.1155/2014/502676

Review Article

The Impact of Autophagy on Cell Death Modalities

Stefan W. Ryter,[1,2] Kenji Mizumura,[1,2] and Augustine M. K. Choi[2]

[1] *Pulmonary and Critical Care Medicine, Brigham and Women's Hospital, Harvard Medical School, 75 Francis Street, Boston, MA 02115, USA*
[2] *Weil Cornell Medical College, 525 East 68th Street, Room M-522, Box 130, New York, NY 10065, USA*

Correspondence should be addressed to Stefan W. Ryter; sryter@partners.org

Received 11 November 2013; Accepted 18 December 2013; Published 4 February 2014

Academic Editor: Claudia Giampietri

Autophagy represents a homeostatic cellular mechanism for the turnover of organelles and proteins, through a lysosome-dependent degradation pathway. During starvation, autophagy facilitates cell survival through the recycling of metabolic precursors. Additionally, autophagy can modulate other vital processes such as programmed cell death (e.g., apoptosis), inflammation, and adaptive immune mechanisms and thereby influence disease pathogenesis. Selective pathways can target distinct cargoes (e.g., mitochondria and proteins) for autophagic degradation. At present, the causal relationship between autophagy and various forms of regulated or nonregulated cell death remains unclear. Autophagy can occur in association with necrosis-like cell death triggered by caspase inhibition. Autophagy and apoptosis have been shown to be coincident or antagonistic, depending on experimental context, and share cross-talk between signal transduction elements. Autophagy may modulate the outcome of other regulated forms of cell death such as necroptosis. Recent advances suggest that autophagy can dampen inflammatory responses, including inflammasome-dependent caspase-1 activation and maturation of proinflammatory cytokines. Autophagy may also act as regulator of caspase-1 dependent cell death (pyroptosis). Strategies aimed at modulating autophagy may lead to therapeutic interventions for diseases in which apoptosis or other forms of regulated cell death may play a cardinal role.

1. Introduction

Macroautophagy (abbreviated as "autophagy") is a genetically regulated and evolutionarily conserved pathway for the degradation of subcellular components [1–5]. This process involves the *de novo* formation of cytoplasmic double membrane-bound vacuoles termed autophagosomes, which sequester cytosolic cargo for delivery to the lysosomes [5, 6]. Autophagic cargoes may include various subcellular targets typified by ubiquitin-modified or long-lived proteins and major cytosolic organelles (e.g., mitochondria and peroxisomes) [7–9]. However, a number of other potential substrates have been identified, including lipids, nucleic acids, reticulocytes, and invading pathogens (e.g., intracellular bacteria, viruses, etc.) [7, 10]. The autophagic pathway proceeds through several defined steps: (i) the initiation phase involving the formation of an isolation membrane or phagophore, (ii) the elongation of the phagophore, (iii) the maturation of an autophagosome with assimilation of a cytosolic cargo, (iv) the fusion of the mature autophagosome to the lysosome, and finally (v) the degradation phase where the contents are digested by lysosomal proteases (e.g., cathepsins) and other hydrolytic enzymes [1–5] (Figure 1). Autophagy has been recognized as an essential function for cell homeostasis and adaptation to environmental stress conditions including nutritional starvation, energy depletion, endoplasmic reticulum stress, oxidative stress, and hypoxia [11–14]. Furthermore, autophagy plays a vital role in innate and adaptive immune mechanisms, including resistance to pathogen infections [10, 15, 16]. The role of autophagy in diseases is an emerging area of investigation, with recent studies indicating that autophagy may exert multifunctional roles in specific diseases, with the potential for both adaptive and maladaptive outcomes. Furthermore, deficiency or absence in autophagic function may also contribute to the pathogenesis of human diseases [2, 12, 17–19].

The occurrence of autophagy in response to environmental stress, most notably starvation, is generally regarded

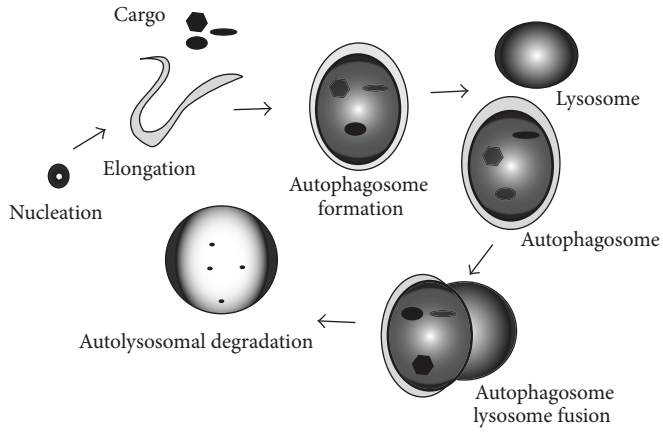

Figure 1: Autophagy pathway. Autophagy is a membrane-dependent pathway that involves a defined series of steps. The pathway is initiated by the autophagosome nucleation step (formation of a preautophagosomal structure leading to an isolation membrane or phagophore). This is followed by autophagosome membrane elongation. The next steps involve the formation of the mature autophagosome, which engulphs cytosol or specific substrates such as mitochondria or ubiquitinated proteins. Subsequently, the autophagosome containing its cargo fuses with the lysosome. In the autolysosome, the autophagosomal cargoes are digested by lysosomal hydrolases and the contents released for metabolic recycling.

as a cell survival mechanism [20–22]. Due to the often coincident appearance of morphological and biochemical markers of autophagy in cells that are dying, the relationship between autophagy and cell death has been both extensively studied and speculated upon [23–26]. Autophagy has previously been classified as a form of programmed cell death, termed "autophagic cell death" to describe a form of caspase-independent necrosis-like cell death associated with accumulation of autophagosomes in cells [27]. This classification is now controversial, and the casual relationship between autophagy and cell death remains unproven [25, 26]. Nevertheless, many studies have pointed to intimate relationships between autophagy and cellular death programs, which are not yet fully understood [28]. Recent studies have also examined potential cross-talk between the signaling pathways that regulate autophagy and those that regulate distinct forms of regulated cell death such as apoptosis [29]. Current advances in these areas will be summarized in this review.

1.1. Modes of Cell Death. The major types of cell death which have been studied most extensively in the context of autophagy research include apoptosis, necrosis, necroptosis, and pyroptosis, as briefly summarized here.

1.1.1. Apoptosis. Apoptosis denotes a regulated form of cell death that requires the coordinated action of proteases and nucleases within an intact plasma membrane. Morphological characteristics of apoptosis include DNA fragmentation, plasma membrane blebbing, cell shrinkage, and cellular decomposition into membrane-bound apoptotic bodies which are removed by phagocytosis [30–33]. The cardinal biochemical features of apoptosis include mitochondrial dysfunction, respiratory chain inhibition, loss of inner mitochondrial membrane potential ($\Delta\Psi_m$), increased mitochondrial membrane permeability, and externalization of phosphatidylserine [30–33]. Apoptosis has a crucial function in the maintenance of tissue homeostasis under physiological conditions and also serves as a component of developmental programs and furthermore may also contribute to disease pathogenesis. Several intracellular signaling pathways may activate apoptosis. The "intrinsic" (mitochondria-dependent) apoptotic pathway represents a major mechanism by which exposure to harmful extracellular stimuli triggers apoptosis. This pathway is dependent on a proteolytic activation cascade for both regulation and execution (i.e., caspases) and subject to regulation by Bcl-2 family proteins. The extrinsic apoptotic pathway, which shares common downstream features with the intrinsic pathway, is defined by its dependence on receptor-ligand (e.g., Fas-Fas ligand) interactions for initiation.

1.1.2. Necrosis. Necrosis is a type of cell death that results from acute, accidental, or nonphysiological injury [30–33]. This type of cell death is associated with cell lysis as the consequence of membrane damage and subsequent leakage of cell constituents into the extracellular space, which may lead to local inflammation and damage to the surrounding tissue. In certain cases, cell swelling or oncosis may precede necrosis [33]. Necrosis and apoptosis differ in morphological features, though the two processes are not necessarily mutually exclusive. Both apoptosis and necrosis can occur in response to treatment with many injurious stimuli, usually in a dose-dependent fashion. Many agents that cause apoptosis at low to moderate doses may ultimately cause necrosis at relatively higher doses. A number of endogenous events can determine the balance between apoptotic and necrotic death. Cellular energy charge (i.e., ATP levels) may represent one such factor that influences cell fate decisions. Whereas ATP is

required for certain steps of caspase activation, rapid decline of cellular ATP levels typically leads to necrotic cell death.

1.1.3. Necroptosis. The existence of necrotic cell death pathways regulated by an intrinsic death program distinct from that of apoptosis has also been proposed. A regulated Fas-dependent but caspase-independent nonapoptotic cell death, termed "*necroptosis*," that resembles necrosis has been described [34, 35]. In this form of regulated necrosis, the ligand binding of death receptors such as the tumor necrosis factor receptor 1 (TNFR1) can promote the formation of a macromolecular complex (necrosome), involving the receptor-interacting protein (RIP) kinase-1 and kinase-3 that initiate necrosis [36, 37]. Increasing evidence affirms the relevance of this mode of cell death in the pathogenesis of various diseases [38–42].

1.1.4. Pyroptosis. Pyroptosis represents a form of cell death that is triggered by proinflammatory signals and which is associated with inflammation [32, 43, 44]. This type of cell death occurs primarily in inflammatory cells such as macrophages and may be triggered by bacterial or pathogen infections. A major feature of pyroptosis is the requirement for caspase-1 activation. Caspase-1 is responsible for the maturation of proinflammatory cytokines such as IL-1β and IL-18 through inflammasome-dependent pathways. Cells undergoing pyroptosis release increased amounts of IL-1β and IL-18. The execution of pyroptosis may also require caspase-7. Cells undergoing pyroptosis share some common features of necrosis. Cell death occurs as a result of membranous pore formation and cytoplasmic swelling and leakage of cytosolic contents. Similar to apoptotic cells, pyroptotic cells may also display DNA fragmentation and nuclear condensation.

1.2. Molecular Regulation of Autophagy. The autophagic pathway is highly regulated by a genetic program. The molecular machinery of autophagic regulation is the subject of recent reviews [45, 46]. Subsequent to their identification in yeast, a number of critical autophagy-related genes (Atg) have been identified whose gene products regulate distinct steps in the induction or progression of autophagy [45, 46].

In brief, the autophagy pathway responds to regulation by nutrient status, including nutrient deficiency (starvation) and loss of energy charge [47]. Starvation induces autophagy through the inhibition of mammalian target of rapamycin (mTOR), which resides in a multiprotein complex, mTORC1 [47]. In response to stimulation by nutrients or growth factors, mTORC1 negatively regulates a macromolecular substrate complex that includes ULK1, ATG13, ATG101, and FIP200 (RB1CC1), which results in autophagy suppression [48–54]. Energy depletion, which stimulates autophagy, inhibits mTORC1, in part through activation of the AMP-dependent protein kinase (AMPK), leading to the activation of ULK1, an important initiating step in autophagy [47, 55, 56].

Autophagy is also coregulated by a multiprotein complex consisting of Beclin 1 (homologue of yeast Atg6), which associates with class III phosphatidylinositol-3-kinase (VPS34) and a number of additional stimulatory or inhibitory coregulatory proteins (e.g., ATG14L, UVRAG, Ambra1, and Rubicon) [57]. In response to proautophagic stimuli, the increased production of phosphatidylinositol-3-phosphate (PI3P) by this complex regulates autophagosome formation [57, 58]. The Beclin 1 complex is subject to negative regulation by the PI3 K/Akt pathway [59] as well by binding interactions with antiapoptotic Bcl-2 family proteins [60]. Following phagophore formation, the elongation of the autophagosome membrane requires the action of two ubiquitin-like conjugation systems: the Atg5-Atg12 conjugation system and the microtubule-associated protein-1 light chain 3 (LC3, Atg8) conjugation system [61, 62]. Atg4B converts the proform of LC3B to its cytosolic free form (LC3-I). In mammals, the conversion of LC3-I (and other Atg8 homologues) to its phosphatidylethanolamine-conjugated and autophagosome-membrane associated form (i.e., LC3-II) is an initiating step in autophagy [63–66].

2. Autophagy in Cellular Homeostasis

Autophagy is now recognized to play multifunctional roles in the maintenance of cellular homeostasis. Once thought to be relatively nonspecific, it is now believed that autophagy is a highly selective process in which distinct cellular mechanisms are employed to identify and target cargo to autophagosomes. Such selective autophagy pathways have been identified for the turnover of mitochondria (mitophagy) and other organelles and the turnover of denatured protein (aggrephagy).

2.1. Cell Survival during Starvation. During starvation (e.g., deprivation of glucose or growth factors or depletion of cellular energy charge) autophagy prolongs cell survival through the degradation and recycling of cellular macromolecules. This process replenishes pools of precursor molecules during nutrient deficiency states [20]. Mice deficient in the autophagy protein Atg5 are susceptible to the lethal effects of starvation [21]. Inhibition of autophagy by Beclin 1 or Atg5 knockdown, or by chemical inhibitors such as 3-methyladenine, can promote apoptosis and caspase-3 activation in starved HeLa cells [22]. These studies have suggested a role for autophagy as a means for prolonging cell survival during starvation.

2.2. Mitophagy. Autophagy performs a cardinal homeostatic function in the removal of damaged or dysfunctional mitochondria, in a selective process referred to as mitophagy [9]. Mitophagy plays an important role in erythrocyte maturation and the maintenance of cellular homeostasis. The increased turnover of mitochondria by mitophagy may occur as a result of chemical or physical stress (e.g., hypoxia) [67]. Mitophagy can regulate mitochondrial number to match metabolic requirements. Mitochondria are removed during erythrocyte maturation by the BH3-only protein, Nix/Bnip3L1. Nix localizes in the outer mitochondrial membrane and directly interacts with mammalian Atg8 homologs through its LIR motif [68]. Damaged or dysfunctional mitochondria are recruited

to the autophagosome for removal by mitophagy through a process regulated by the phosphatase and tensin homolog deleted in chromosome 10 (PTEN)-induced putative kinase 1 (Pink1) and Parkinson protein-2 (Parkin) [9, 69, 70]. Mutations in the corresponding *PINK1* and *PARK2* genes are associated with recessive familial forms of Parkinson's disease [71]. In mice, *PINK1* and *PARK2* deletions are associated with mitochondrial dysfunction [72]. Loss of mitochondrial membrane potential and the increased production of mitochondrial reactive oxygen species (ROS) may provide initiating signals for mitophagy. Pink1, a transmembrane protein, is stabilized on damaged or depolarized mitochondria. Following the decline of mitochondrial membrane potential, which can be caused by chemical stress, Pink1 recruits cytosolic Parkin, an E3 ubiquitin protein ligase, to the mitochondria [69, 70, 73]. Parkin initiates the formation of polyubiquitin chains which identify depolarized mitochondria for degradation. Parkin ubiquitinates mitochondrial outer membrane proteins including porin, mitofusin, and Miro [74, 75]. Ubiquitinated mitochondria are subsequently recognized and targeted to autophagosomes by the autophagic cargo adaptor protein p62 [9, 69, 70].

2.3. Aggrephagy in the Maintenance of Proteostasis. Autophagy can maintain cellular protein homeostasis (proteostasis) by providing a mechanism for the removal of ubiquitinated protein aggregates, in a selective process termed *aggrephagy* [8]. Recent studies suggest that autophagy may provide an alternative pathway to proteolysis in addition to the ubiquitin proteasome system [76–78]. Aggrephagy requires the selective autophagy cargo adaptor p62/SQSTM1 (p62) which can interact with ubiquitinated proteins through a ubiquitin-associated (UBA) domain [76]. Furthermore, p62 can interact with LC3 through its LIR (LC3-interacting region) motif and thereby facilitate the targeting of ubiquitinated proteins to autophagosomes [77]. The selective autophagy adaptor, NBR1 (neighbor of BRCA1 gene 1), promotes the formation of ubiquitin-positive protein aggregates, facilitating their sequestration and removal by aggrephagy [78]. This process involves the 400 kDa, PI3P-binding autophagy-linked FYVE domain protein (ALFY), a p62-interacting protein [79].

2.4. Other Forms of Selective Autophagy. In addition to mitophagy, other forms of organelle-specific or substrate-specific autophagy have been identified and collectively may contribute to the maintenance of cellular integrity under stress. These include the selective autophagic degradation of peroxisomes [80], ribosomes [81], and endoplasmic reticulum fragments [82]. In addition to protein, autophagic processes have been implicated in the degradation of diverse cellular biomolecules, including lipids [83] and RNA [84]. Furthermore, autophagy can degrade exogenously derived substrates, most notably bacteria, virus particles, and other parasites, in a selective process termed "xenophagy" [10, 15, 16]. Although recent studies begin to unravel the role of mitochondrial selective autophagy in cell death pathways, the role of diverse selective autophagy pathways in the modulation of cell death programs remains largely uncharted territory.

3. Autophagy and Apoptosis

Despite a widely accepted role for autophagy in cellular survival, autophagy has also been associated with the regulation of various cell death pathways, most notably apoptosis. Autophagy is a regulated program associated with survival or stress adaptation. However, increased autophagosome formation is often coincident in cells that are dying. Thus, autophagy may represent a failed adaptive mechanism that may have prevented death under milder conditions. Hypothetically, excess activation of autophagy may contribute to apoptotic cell death through unchecked degradative processes [23]. The morphological and biochemical features of autophagy and apoptosis are distinct. Cells undergoing autophagy display an increase in autophagic vesicles (i.e., autophagosomes and autophagolysosomes). While partial chromatin condensation appears in autophagic cells, DNA fragmentation does not occur. The distinctions between autophagy and apoptosis remain incompletely delineated, as the two processes are not always mutually exclusive and may occur simultaneously in the same cell type.

3.1. Cross-Talk between Autophagy and Apoptosis Proteins. Recent studies suggest that factors well known to regulate apoptosis pathways also have the potential to exert regulatory activity on factors that regulate autophagy and *vice-versa* (Figure 2). How these regulatory events, termed "cross-talk", are integrated into a mechanism for the determination of cell fate yet remains incompletely understood.

Antiapoptotic Bcl-2 family proteins, which downregulate apoptosis (i.e., Bcl-2) by antagonizing the activity of proapoptotic proteins, can downregulate autophagy. Beclin 1 interacts with antiapoptotic Bcl-2 family members including Bcl-2 and Bcl-X_L. Binding of these Bcl-2 family proteins to Beclin 1 inhibits autophagy by preventing the association of Beclin 1 with the class III PI3K complex [57, 60]. Recent studies have identified Bcl-B as a novel Beclin 1 binding protein [85]. BNIP3 is a BH3-only protein that can trigger apoptosis by sequestering antiapoptotic Bcl-2 family proteins and promoting Bax/Bad dependent mitochondrial release of proapoptotic mediators. BNIP3 also stimulates mitophagy by disrupting the interaction between Bcl-2 and Beclin 1 [86]. These interactions suggest that autophagy and apoptosis may be coordinately regulated by Bcl-2 family proteins. Experimental evidence also suggests that, once activated, apoptosis effector molecules may suppress autophagy; for example, Beclin 1 may be cleaved and inactivated by caspases during activation of apoptosis [87].

Further studies suggest that certain Atg proteins may play dual roles in autophagy/apoptosis regulation; for example, the autophagic protein Atg5 may affect extrinsic apoptosis pathways through interactions with the Fas-associated death domain (FADD) protein [88]. Atg5 which regulates autophagy can be subject to calpain-dependent cleavage to generate a proapoptotic truncation product (tAtg5). This

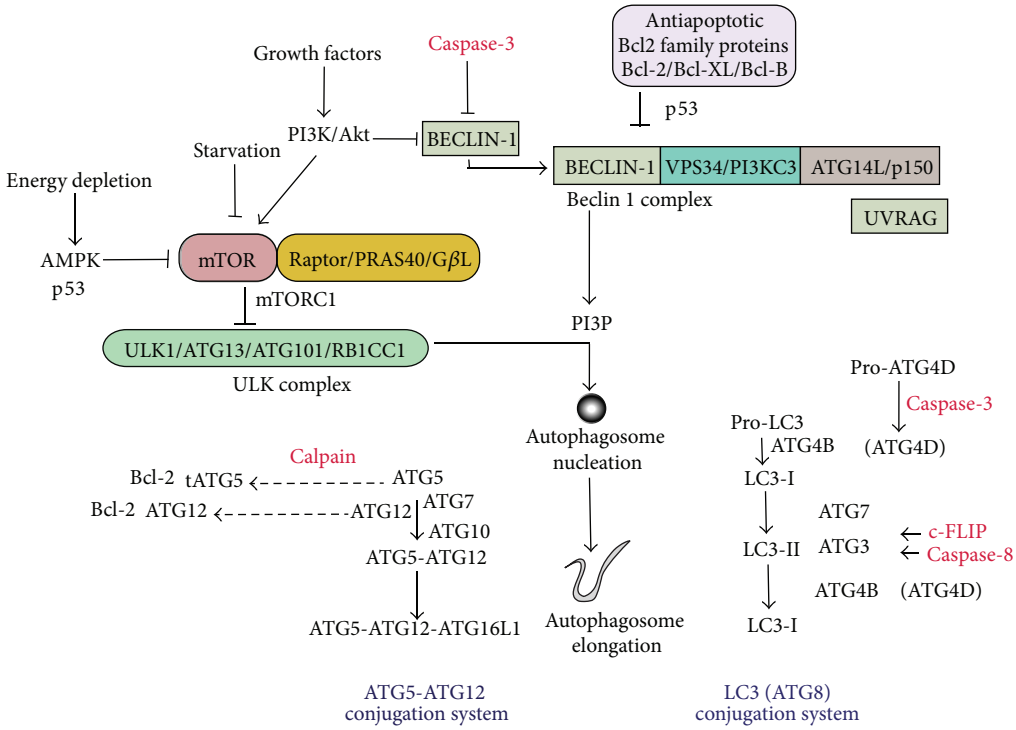

Figure 2: Autophagy is negatively regulated by the phosphatidylinositol 3-kinase (PI3 K)/Akt signaling pathway, which activates mammalian target of rapamycin (mTOR) in response to growth factors and also phosphorylates Beclin 1. The adenosine 5′-monophosphate-activated protein kinase (AMPK) negatively regulates mTOR thereby acting as a positive regulator of autophagy in response to AMP levels. mTOR resides in the mTOR signaling complex (mTORC1), which regulates the mammalian uncoordinated-51-like protein kinase (ULK1) complex, consisting of ULK1, ATG13, ATG101, and RB1CC1. Autophagy is also regulated by the Beclin 1 complex, consisting of Beclin 1, class III phosphatidylinositol-3-kinase (VPS34 or PI3KC3) and ATG14L or UVRAG. Stimulation of the Beclin 1 complex generates phosphatidylinositol-3-phosphate (PI3P), which triggers autophagosomal nucleation. Autophagosome membrane elongation is regulated by ubiquitin-like conjugation systems. ATG12 is conjugated to ATG5 by ATG7 and ATG10 enzymes, which results in the formation of the ATG5-ATG12-ATG16L1 complex. The Atg8 conjugation system involves microtubule-associated protein-1 light chain 3 (LC3, ATG8). LC3 and other Atg8 homologues are modified with the cellular lipid phosphatidylethanolamine. Pro-LC3 is cleaved by ATG4B to generate the LC3-I form. ATG4D may similarly process other Atg8 homologs. Lipid conjugation of LC3-I occurs from the action of ATG7 and ATG3 activities. The conversion of LC3-I (free form) to LC3-II (lipid-conjugated form) is a major step in autophagosome formation. Antiapoptotic Bcl-2 family proteins can interact with the autophagy machinery at the site of Beclin1, resulting in inhibition of autophagy. The tumor suppressor protein p53 and activated caspases potentially interact with the autophagy machinery at the indicated sites. Caspase processing can result in activation of autophagy (e.g., Atg4D) or inhibition of autophagy (e.g., Beclin 1, Atg3). Additionally, Atg12 and a cleavage product of Atg5 can act as proapoptotic mediators by antagonizing antiapoptotic Bcl-2 family proteins.

cleavage product promotes apoptosis by binding to and inhibiting antiapoptotic proteins such as Bcl-X_L [89]. Recent studies also implicate Atg12, the binding partner for Atg5 required for autophagosomal elongation, as an effector of the intrinsic apoptosis pathway [90]. Atg12 may bind to and inactivate antiapoptotic Bcl2 family proteins (e.g., Bcl-2 and Mcl-1), through an interaction involving a BH2 motif, and thereby act as a proapoptotic regulator [90].

Recent advances have identified other regulatory targets for caspase regulation among autophagy related molecules; for example, Atg4D, a member of the Atg4 family of Atg8 processing enzymes, has been identified as a substrate for proapoptotic caspase-3 [91]. Caspase processing of Atg4D results in activation with respect to proautophagic activity. The autophagic protein Atg3 has recently been identified as a caspase-8 substrate, which is cleaved during TNFα-induced apoptosis [92]. The antiapoptotic protein cellular Flice-like inhibitory protein (c-FLIP) can act as a negative regulator of autophagy [93]. The c-FLIP, an endogenous inhibitor of caspase-8 processing and the extrinsic apoptotic pathway, acts to prevent the binding of Atg3 to LC3, which impairs LC3 processing [93].

On the basis of what is known about the molecular cross-talk between autophagy and apoptosis it currently remains unclear whether autophagy and apoptosis are coregulated or mutually exclusive processes. Antiapoptotic (e.g., Bcl-2) as well as proapoptotic (e.g., caspase-3) molecules can down-regulate autophagy by interacting with Beclin 1. Furthermore, other caspase-dependent events have been implicated in anti-autophagy or proautophagy events. For example caspase processing of Atg4D is proautophagy, whereas caspase processing of Beclin 1 is antiautophagy.

The definitive cellular mechanisms that control the decision to embark on each one or both of these pathways in response to specific stimuli remain unclear. Analysis of any single isolated regulatory component (using siRNA knockdown for example) for its potential to cross-regulate autophagy and/or apoptosis will be unlikely to answer these questions. Thus, an integrative approach is needed to understand how the entire molecular machinery of apoptosis and autophagy are coordinated to influence cell fate decisions.

3.2. The Tumor Suppressor p53 Coregulates Autophagy and Apoptosis. The p53 tumor suppressor protein is a well studied regulator of cell cycle progression and apoptosis. p53 modulates the expression of Bcl-2 family proteins (e.g., Bax, Bid) and other apoptosis-related gene targets (e.g., Apaf1). The nuclear form of p53 targets the expression of DRAM (damage regulated autophagic modulator), which can stimulate both autophagy and apoptosis [94]. Alternatively, p53 can induce autophagy through the upregulation of AMPK, which downregulates the mTOR pathway [95]. Recent studies have shown that genetic or pharmacological inhibition of p53 can also activate autophagy and have led to the identification of the cytoplasmic form of p53 as an inhibitor of autophagy [96]. Chemical stimuli known to induce autophagy can promote the proteasomal degradation of p53 [96].

Cellular stimulation with interferon-γ (IFN-γ) induces the deacetylation of p53, leading to suppressed Bmf expression, reduced complex formation between Beclin 1 and Bcl2, and enhanced autophagy [97]. Taken together these studies suggest a complex role of p53 in the regulation of autophagy, with opposing roles for the cytosolic and nuclear forms of p53 [98, 99].

3.3. Autophagy as a Protagonist of Apoptosis. Several recent studies, supported by genetic manipulation of the autophagy program, have revealed that in select toxicological models, autophagy may be associated with the promotion of apoptosis.

In our recent studies we have found that epithelial cells subjected to cigarette smoke extract (CSE) exposure die by activation of the extrinsic apoptosis pathway [100, 101]. CSE-induced cell death involved activation of the Fas-dependent death-inducing signaling complex (DISC) and downstream activation of caspases (-8,-9,-3). Epithelial cells subjected to CSE exposure concurrently responded with increased autophagosome formation and increased processing of LC3B-I to LC3B-II in epithelial cells [100, 101]. Knockdown of autophagy proteins Beclin 1 or LC3B inhibited apoptosis in response to CSE exposure *in vitro*, suggesting that increased autophagy occurred in association with epithelial cell death [100, 101]. Further studies revealed that LC3B may act as a regulatory factor in extrinsic apoptosis in this model [101]. LC3B was found to engage a complex with Fas, the key component of the DISC, in a fashion dependent on the lipid raft protein caveolin-1. CSE exposure caused the rapid dissociation of LC3B from Fas, in association with the activation of apoptosis signaling [101]. In conclusion, these results using genetic knockdown experiments have implicated a proapoptotic role for LC3B, in a specialized model of CSE-induced toxicity, though the relative role of autophagic activity in promoting cell death in this model remains unclear [100, 101].

It should be noted that CSE-induced autophagy may differ from starvation-induced autophagy in that it occurs in the presence of a complex mixture of foreign matter, which may potentially alter the functionality of the autophagy response. Thus, the concept of "toxic autophagy" may involve altered function, which may be dependent not only on whether its activation is physiological or excessive, but also on the nature of foreign substrates (e.g., complex xenobiotics such as tar or virus particles) and their interactions with autophagosomes.

Further examples of coincident autophagy and apoptosis include p53-dependent autophagy through upregulation of DRAM, which is coincidental with upregulation of apoptosis [93]. TNFα can induce autophagy in trophoblasts leading to activation of the intrinsic apoptosis pathway [102]. Knockdown of Atg5 prevented TNFα-dependent activation of proapoptotic caspases in this model [102]. Deletion of Atg5 was also shown to protect cells from prodeath environmental stimuli; however, the authors attributed this resistance to compensatory activation of chaperone-dependent autophagy, rather than inhibition of macroautophagy *per se* [103].

These studies raise an important issue in that genetic knockdown of one specific autophagy-related factor cannot establish whether autophagy was protective or not in any context, as downregulation of the target may potentially affect signaling pathways that are independent of autophagy, or alternatively, promote compensatory mechanisms, such as alternate forms of autophagy.

4. Autophagy, Necrosis, and Necroptosis

4.1. Autophagy Dependent Cell Death during Apoptosis Inhibition. The terms "autophagic cell death" or type II programmed cell death have been previously used to refer to cell death distinct from apoptosis that occurs in association with increases in autophagosome formation and independently of caspases [26]. Many studies that have implicated autophagy as a cell death effector have been performed on apoptosis-compromised or caspase-deficient cells; for example, cells treated with z-VAD-*fmk*, a general inhibitor of caspases, or with caspase-8 and calpain inhibitors, die essentially by a nonapoptotic pathway characterized by dramatic accumulations of autophagic vacuoles [104–107]. Genetic knockdown experiments (e.g., *Beclin 1*) suggest that autophagy contributes to cytotoxicity in these models [104]; however, contrasting studies, also using knockdown of autophagy proteins, have also suggested that autophagy can also protect in the context of nonapoptotic cell death induced by caspase inhibition [108]. In $Bax^{-/-}Bak^{-/-}$ mouse embryonic fibroblasts (MEFs), which cannot activate intrinsic apoptosis, treatment with chemotherapeutic agents results in nonapoptotic necrosis-like cell death accompanied by excessive autophagosome formation [109].

Currently it remains unclear whether the process of autophagy acts as an effector or bystander of caspase-independent necrosis-like cell death, though autophagic proteins likely play an accessory role [25, 26].

4.2. Cross-Talk of Autophagy and Necrosis. Experiments in tumor cells have suggested the possibility of cross-talk between autophagy and necrosis in cells [110]. Autophagy provides a protective function to limit tumor necrosis and inflammation in response to metabolic stress. While autophagy acts to buffer metabolic stress, the combined impairment of apoptosis and autophagy promotes necrotic cell death *in vitro* and *in vivo* [111]. Although it remains to be determined what triggers necrosis in tumor cells, it is likely that insufficient ATP production to maintain plasma-membrane integrity results in metabolic catastrophe and cell lysis [110, 112]. A rapid drop in ATP has been implicated in necrosis [113]. Autophagy integrates a metabolic feedback system to allow sufficient ATP generation to maintain cell viability [114]. Enhanced autophagy by spermidine, a natural polyamine, inhibits loss of membrane integrity and release of chromatin protein high mobility group B1 (HMGB1), a biomarker of necrosis [115].

Necrosis was once described as accidental cell death by extreme physicochemical stress. However, recent consensus agrees that specific genes can regulate necrosis, which is termed necroptosis [35]. The kinases receptor-interacting protein 1 (RIP1) and RIP3 are key signaling molecules in necroptosis. Published studies have suggested that the treatment with zVAD, a caspase inhibitor with broad specificity, induced autophagy and the death of L929 cells; and this death process required RIP1, suggesting that autophagy is involved in necroptosis [107]. In several models, autophagy has been shown to regulate necroptosis [116, 117]. In endothelial cells, inhibition of autophagy rescues palmitic acid-induced necroptosis [118]. On the other hand, a recent study has demonstrated that necrostatin-1 (Nec-1), a specific necroptosis inhibitor, suppressed not only necrosis but also autophagy [119]. These observations suggest that autophagy may be induced by necroptosis [120], raising the possibility that cellular stress during cell death may lead to the induction of autophagy. The molecular mechanism underlying this relationship remains elusive and controversial [121]. It is tempting to speculate that so-called autophagic cell death may involve elements of necroptosis, though further research will be needed to clarify this relationship, as well as the signaling pathways linking autophagy to necroptosis.

5. Autophagy, Inflammasome Activation, and Cross-Talk to Pyroptosis

Recent observations have revealed a relationship between autophagic proteins and inflammasome-associated proinflammatory cytokine maturation in macrophages [122–124]. Inflammasomes are cytosolic multiprotein complexes that constitute a novel inflammatory signaling mechanism and which govern the maturation and secretion of distinct proinflammatory cytokines, such as IL-1β, IL-18, and IL-33 [125]. Cytosolic receptors of the Nod-like receptor (NLR) family (i.e., NLRP3, NLRP1) interact with accessory proteins to form inflammasome complexes. NLRP3 interacts with an adaptor protein [apoptosis-associated speck like protein containing CARD (ASC)], which recruits and activates the procaspase-1 by proteolytic cleavage [125].

Proinflammatory cytokine secretion (IL-1β and IL-18) was enhanced in *atg16l1* or *atg7* deleted macrophages in response to LPS [122]. In contrast, *atg16l1* or *atg7* deficiency did not affect TNF and IFN-β production or NF-κB pathway activation in macrophages stimulated with LPS [122]. Furthermore, *atg16l1* deleted mice displayed increased susceptibility to a murine model of colitis, which could be ameliorated by anti-IL-18 therapy [122]. Increased activation of IL-1β and IL-18 has also been observed in macrophages and monocytes isolated from mice genetically deficient in Beclin 1 and LC3B [123]. Cytokine activation in response to LPS and ATP in wild-type macrophages, as well as the amplification observed in LC3B or Beclin 1 deficient macrophages, required the NLRP3 inflammasome pathway [123, 124]. The mechanism by which autophagy deficiency enhanced NLRP3 inflammasome pathway activation involved mitochondrial dysfunction, including the enhanced production of mitochondrial ROS and increased mitochondrial membrane permeability transition [122, 123]. The pathway to caspase-1 dependent IL-18 secretion in macrophages was inhibited by mitochondrial targeting antioxidants [123]. These experiments suggest that autophagic proteins dampen inflammasome pathway activation by stabilizing mitochondria and/or maintaining mitochondrial quality control through autophagy.

In contrast to negative regulation of autophagy by the inflammasome, a recent study demonstrates that autophagy induction by starvation enhances caspase-1 activation and secretion of IL-1β and IL-18 [126]. Inflammasome-mediated IL-1β secretion utilizes the autophagy-based unconventional secretion pathway [126]. It is possible that a distinct type of autophagy induction might differentially regulate the inflammasome pathway.

Taken together these studies suggest an important role for autophagic proteins in the dampening of proinflammatory responses, which warrants further investigation in models of inflammatory disease.

In addition to confirmed negative regulatory roles of autophagy in inflammasome activation, it has been shown that stimulation of inflammasome pathways can promote autophagosome formation through activation of the GTPase RalB [127]. Furthermore, p62-dependent selective autophagy processes may regulate the turnover and degradation of ubiquitinated inflammasome complexes [127]. Further studies suggest that stimulation of plasminogen activator inhibitor-2 by Toll like receptor activation suppresses NLRP3-dependent cytokines activation by promoting the autophagic degradation of NLRP3 [128]. An important and unanswered question is related to whether inflammasome activation and the generation of inflammasome-associated cytokines exert downstream consequences on autophagic processing.

Pyroptosis is triggered in inflammatory cells in response to excessive inflammation by caspase-1-dependent processes,

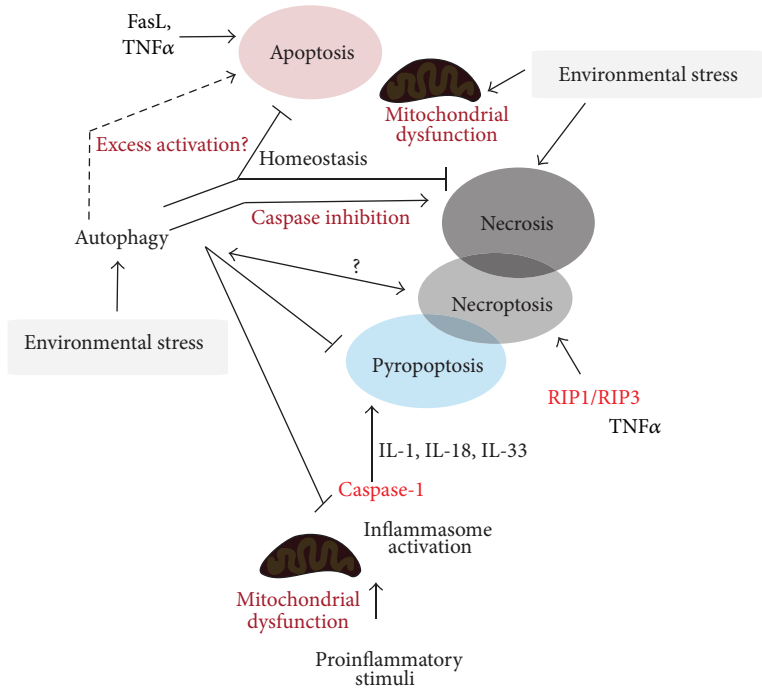

Figure 3: Autophagy has a complex relationship with various modes of cell death, including regulated (e.g., apoptosis, pyroptosis, and necroptosis) and catastrophic (e.g., necrosis) types of cell death. Autophagy has been implicated in association with caspase-independent cell death in apoptosis-compromised cells leading to necrosis and necroptosis. Furthermore, autophagy has been implicated as an inhibitor of both apoptosis and necrosis by preserving cellular functions, removing toxic debris, and maintaining cellular energy charge. Nevertheless, proapoptotic roles of autophagy have also been reported. Proinflammatory stimuli can activate inflammasome-dependent caspase-1 activation leading to proinflammatory cytokines maturation. Excess activation of this pathway can lead to pyroptotic cell death. Mitochondrial dysfunction plays a key role in both apoptosis signaling and the activation of the inflammasome pathway. Autophagy can influence these pathways through modulation of the mitochondrial pool. The relationships between autophagy and necroptosis or pyroptosis require further elucidation.

leading to release of proinflammatory cytokines (e.g., IL-1β, IL-18, and IL-33) from dying cells. Recent studies suggest that macrophages activate autophagy in parallel with inflammasome activation, as a means to delay the onset of pyroptosis [129]. Chemical inhibition of autophagy using 3-methyladenine or inhibition of the Atg4 protease resulted in increased incidence of pyroptotic cell death in activated macrophages [129]. The impact of autophagy modulation on the regulation of pyroptosis, and the relevance of these interactions in *in vivo* models of inflammatory disease and sepsis, warrants further exploration.

6. Conclusions and Therapeutic Implications

Autophagy is generally defined as a cellular program that ensures survival under conditions of stress. The ability of autophagy to clear damaged or denatured subcellular constituents such as aggregated protein (i.e., aggrephagy) as well as to maintain mitochondrial homeostasis (i.e., mitophagy) appears to play important roles in the cytoprotective and homeostatic functions of autophagy [20]. Despite the homeostatic roles, autophagy is now recognized to play complex and incompletely understood roles in cell death programs (Figure 3). Furthermore, there is considerable cross-talk between the molecular regulation of autophagy and other regulated forms of cell death [23–26]. The role of autophagy in diseases is an emerging area of investigation, with recent studies indicating that autophagy may exert multifunctional roles in specific diseases, with the potential for both adaptive and harmful outcomes. Furthermore, deficiency or absence in autophagic function may play a pathogenic role in select human diseases [2, 17–19]. Additional studies are needed to define the dynamic equilibrium between autophagy, apoptosis, regulated necrosis, and other modes of cell death in the context of human disease pathogenesis [121]. Furthermore, additional studies are needed to determine the relevance of autophagic regulation of pyroptosis in inflammatory diseases [130]. An increased understanding of these relationships would be essential in the development of therapeutics targeting the autophagy pathway for the treatment of disease.

Conflict of Interests

The authors declare that there is no conflict of interests regarding the publication of this paper.

Acknowledgment

This work was supported by NIH Grants nos. P01 HL108801 and R01 HL079904 to Augustine M. K. Choi.

References

[1] B. Levine and D. J. Klionsky, "Development by self-digestion: molecular mechanisms and biological functions of autophagy," *Developmental Cell*, vol. 6, no. 4, pp. 463–477, 2004.

[2] N. Mizushima, B. Levine, A. M. Cuervo, and D. J. Klionsky, "Autophagy fights disease through cellular self-digestion," *Nature*, vol. 451, no. 7182, pp. 1069–1075, 2008.

[3] D. J. Klionsky and S. D. Emr, "Autophagy as a regulated pathway of cellular degradation," *Science*, vol. 290, no. 5497, pp. 1717–1721, 2000.

[4] E. L. Eskelinen and P. Saftig, "Autophagy: a lysosomal degradation pathway with a central role in health and disease," *Biochimica et Biophysica Acta*, vol. 1793, no. 4, pp. 664–673, 2009.

[5] B. Ravikumar, S. Sarkar, J. E. Davies et al., "Regulation of mammalian autophagy in physiology and pathophysiology," *Physiological Reviews*, vol. 90, no. 4, pp. 1383–1435, 2010.

[6] A. Kelekar, "Autophagy," *Annals of the New York Academy of Sciences*, vol. 1066, pp. 259–271, 2005.

[7] T. Johansen and T. Lamark, "Selective autophagy mediated by autophagic adapter proteins," *Autophagy*, vol. 7, no. 3, pp. 279–296, 2011.

[8] T. Lamark and T. Johansen, "Aggrephagy: selective disposal of protein aggregates by macroautophagy," *International Journal of Cell Biology*, vol. 2012, Article ID 736905, 21 pages, 2012.

[9] R. J. Youle and D. P. Narendra, "Mechanisms of mitophagy," *Nature Reviews Molecular Cell Biology*, vol. 12, no. 1, pp. 9–14, 2011.

[10] R. Sumpter and B. Levine, "Autophagy and innate immunity: triggering, targeting and tuning," *Seminars in Cell and Developmental Biology*, vol. 21, no. 7, pp. 699–711, 2010.

[11] G. Kroemer, G. Mariño, and B. Levine, "Autophagy and the integrated stress response," *Molecular Cell*, vol. 40, no. 2, pp. 280–293, 2010.

[12] K. Nakahira, S. M. Cloonan, K. Mizumura, A. M. Choi, and S. W. Ryter, "Autophagy: a crucial moderator of redox balance, inflammation, and apoptosis in lung disease," *Antioxidants and Redox Signalling*, 2013.

[13] S. W. Ryter, S. M. Cloonan, and A. M. Choi, "Autophagy: a critical regulator of cellular metabolism and homeostasis," *Molecules and Cells*, vol. 36, no. 1, pp. 7–16, 2013.

[14] S. W. Ryter and A. M. Choi, "Regulation of autophagy in oxygen-dependent cellular stress," *Current Pharmaceutical Design*, vol. 19, no. 15, pp. 2747–2756, 2013.

[15] B. Levine, N. Mizushima, and H. W. Virgin, "Autophagy in immunity and inflammation," *Nature*, vol. 469, no. 7330, pp. 323–335, 2011.

[16] V. Deretic and B. Levine, "Autophagy, immunity, and microbial adaptations," *Cell Host and Microbe*, vol. 5, no. 6, pp. 527–549, 2009.

[17] A. M. Choi, S. W. Ryter, and B. Levine, "Autophagy in human health and disease," *New England Journal of Medicine*, vol. 368, no. 7, pp. 651–662, 2013.

[18] D. C. Rubinsztein, P. Codogno, and B. Levine, "Autophagy modulation as a potential therapeutic target for diverse diseases," *Nature Reviews Drug Discovery*, vol. 11, no. 9, pp. 709–730, 2012.

[19] B. Levine and G. Kroemer, "Autophagy in the pathogenesis of disease," *Cell*, vol. 132, no. 1, pp. 27–42, 2008.

[20] N. Mizushima and M. Komatsu, "Autophagy: renovation of cells and tissues," *Cell*, vol. 147, no. 4, pp. 728–741, 2011.

[21] A. Kuma, M. Hatano, M. Matsui et al., "The role of autophagy during the early neonatal starvation period," *Nature*, vol. 432, no. 7020, pp. 1032–1036, 2004.

[22] P. Boya, R. González-Polo, N. Casares et al., "Inhibition of macroautophagy triggers apoptosis," *Molecular and Cellular Biology*, vol. 25, no. 3, pp. 1025–1040, 2005.

[23] L. Galluzzi, J. M. Vicencio, O. Kepp, E. Tasdemir, M. C. Maiuri, and G. Kroemer, "To die or not to die: that is the autophagic question," *Current Molecular Medicine*, vol. 8, no. 2, pp. 78–91, 2008.

[24] M. C. Maiuri, E. Zalckvar, A. Kimchi, and G. Kroemer, "Self-eating and self-killing: crosstalk between autophagy and apoptosis," *Nature Reviews Molecular Cell Biology*, vol. 8, no. 9, pp. 741–752, 2007.

[25] G. Kroemer and B. Levine, "Autophagic cell death: the story of a misnomer," *Nature Reviews Molecular Cell Biology*, vol. 9, no. 12, pp. 1004–1010, 2008.

[26] H. M. Shen and P. Codogno, "Autophagic cell death: Loch Ness monster or endangered species?" *Autophagy*, vol. 7, no. 5, pp. 457–465, 2011.

[27] S. Shimizu, T. Kanaseki, N. Mizushima et al., "Role of Bcl-2 family proteins in a non-apoptopic programmed cell death dependent on autophagy genes," *Nature Cell Biology*, vol. 6, no. 12, pp. 1221–1228, 2004.

[28] M. V. Jain, A. M. Paczulla, T. Klonisch et al., "Interconnections between apoptotic, autophagic and necrotic pathways: implications for cancer therapy development," *Journal of Cellular and Molecular Medicine*, vol. 17, no. 1, pp. 12–29, 2013.

[29] M. Su, Y. Mei, and S. Sinha, "Role of the crosstalk between autophagy and apoptosis in cancer," *Journal of Oncology*, vol. 2013, Article ID 102735, 14 pages, 2013.

[30] L. Galluzzi, M. C. Maiuri, I. Vitale et al., "Cell death modalities: classification and pathophysiological implications," *Cell Death and Differentiation*, vol. 14, no. 7, pp. 1237–1243, 2007.

[31] G. Kroemer, L. Galluzzi, P. Vandenabeele et al., "Classification of cell death: recommendations of the nomenclature committee on cell death 2009," *Cell Death and Differentiation*, vol. 16, no. 1, pp. 3–11, 2009.

[32] S. L. Fink and B. T. Cookson, "Apoptosis, pyroptosis, and necrosis: mechanistic description of dead and dying eukaryotic cells," *Infection and Immunity*, vol. 73, no. 4, pp. 1907–1916, 2005.

[33] G. Majno and I. Joris, "Apoptosis, oncosis, and necrosis: an overview of cell death," *American Journal of Pathology*, vol. 146, no. 1, pp. 3–15, 1995.

[34] L. Galluzzi and G. Kroemer, "Necroptosis: a specialized pathway of programmed necrosis," *Cell*, vol. 135, no. 7, pp. 1161–1163, 2008.

[35] P. Vandenabeele, L. Galluzzi, T. Vanden Berghe, and G. Kroemer, "Molecular mechanisms of necroptosis: an ordered cellular explosion," *Nature Reviews Molecular Cell Biology*, vol. 11, no. 10, pp. 700–714, 2010.

[36] D. W. Zhang, J. Shao, J. Lin et al., "RIP3, an energy metabolism regulator that switches TNF-induced cell death from apoptosis to necrosis," *Science*, vol. 325, no. 5938, pp. 332–336, 2009.

[37] S. He, L. Wang, L. Miao et al., "Receptor interacting protein kinase-3 determines cellular necrotic response to TNF-α," *Cell*, vol. 137, no. 6, pp. 1100–1111, 2009.

[38] Y. S. Cho, S. Challa, D. Moquin et al., "Phosphorylation-driven assembly of the RIP1-RIP3 complex regulates programmed necrosis and virus-induced inflammation," *Cell*, vol. 137, no. 6, pp. 1112–1123, 2009.

[39] L. Galluzzi, T. Vanden Berghe, N. Vanlangenakker et al., "Programmed necrosis. From molecules to health and disease," *International Review of Cell and Molecular Biology*, vol. 289, pp. 1–35, 2011.

[40] L. Sun, H. Wang, Z. Wang et al., "Mixed lineage kinase domain-like protein mediates necrosis signaling downstream of RIP3 kinase," *Cell*, vol. 148, no. 1-2, pp. 213–227, 2012.

[41] P. S. Welz, A. Wullaert, K. Vlantis et al., "FADD prevents RIP3-mediated epithelial cell necrosis and chronic intestinal inflammation," *Nature*, vol. 477, no. 7364, pp. 330–334, 2011.

[42] C. Günther, E. Martini, N. Wittkopf et al., "Caspase-8 regulates TNF-α-induced epithelial necroptosis and terminal ileitis," *Nature*, vol. 477, no. 7364, pp. 335–339, 2011.

[43] O. Kepp, L. Galluzzi, L. Zitvogel, and G. Kroemer, "Pyroptosis-a cell death modality of its kind?" *European Journal of Immunology*, vol. 40, no. 3, pp. 627–630, 2010.

[44] B. T. Cookson and M. A. Brennan, "Pro-inflammatory programmed cell death," *Trends in Microbiology*, vol. 9, no. 3, pp. 113–114, 2001.

[45] Z. Yang and D. J. Klionsky, "Mammalian autophagy: core molecular machinery and signaling regulation," *Current Opinion in Cell Biology*, vol. 22, no. 2, pp. 124–131, 2010.

[46] C. He and D. J. Klionsky, "Regulation mechanisms and signaling pathways of autophagy," *Annual Review of Genetics*, vol. 43, pp. 67–93, 2009.

[47] C. H. Jung, S. Ro, J. Cao, N. M. Otto, and D.-H. Kim Do-Hyung, "MTOR regulation of autophagy," *FEBS Letters*, vol. 584, no. 7, pp. 1287–1295, 2010.

[48] N. Mizushima, "The role of the Atg1/ULK1 complex in autophagy regulation," *Current Opinion in Cell Biology*, vol. 22, no. 2, pp. 132–139, 2010.

[49] E. Y. Chan, "Regulation and function of uncoordinated-51 like kinase proteins," *Antioxidants & Redox Signaling*, vol. 17, no. 5, pp. 775–785, 2012.

[50] N. Hosokawa, T. Hara, T. Kaizuka et al., "Nutrient-dependent mTORCl association with the ULK1-Atg13-FIP200 complex required for autophagy," *Molecular Biology of the Cell*, vol. 20, no. 7, pp. 1981–1991, 2009.

[51] I. G. Ganley, D. H. Lam, J. Wang, X. Ding, S. Chen, and X. Jiang, "ULK1.ATG13.FIP200 complex mediates mTOR signaling and is essential for autophagy," *Journal of Biological Chemistry*, vol. 284, no. 18, pp. 12297–12305, 2009.

[52] C. H. Jung, C. B. Jun, S. Ro et al., "ULK-Atg13-FIP200 complexes mediate mTOR signaling to the autophagy machinery," *Molecular Biology of the Cell*, vol. 20, no. 7, pp. 1992–2003, 2009.

[53] P. M. Wong, C. Puente, I. G. Ganley, and X. Jiang, "The ULK1 complex: sensing nutrient signals for autophagy activation," *Autophagy*, vol. 9, pp. 124–137, 2013.

[54] T. Hara, A. Takamura, C. Kishi et al., "FIP200, a ULK-interacting protein, is required for autophagosome formation in mammalian cells," *Journal of Cell Biology*, vol. 181, no. 3, pp. 497–510, 2008.

[55] M. M. Mihaylova and R. J. Shaw, "The AMPK signalling pathway coordinates cell growth, autophagy and metabolism," *Nature Cell Biology*, vol. 13, no. 9, pp. 1016–1023, 2011.

[56] J. Kim, M. Kundu, B. Viollet, and K. Guan, "AMPK and mTOR regulate autophagy through direct phosphorylation of Ulk1," *Nature Cell Biology*, vol. 13, no. 2, pp. 132–141, 2011.

[57] C. He and B. Levine, "The Beclin 1 interactome," *Current Opinion in Cell Biology*, vol. 22, no. 2, pp. 140–149, 2010.

[58] E. Itakura, C. Kishi, K. Inoue, and N. Mizushima, "Beclin 1 forms two distinct phosphatidylinositol 3-kinase complexes with mammalian Atg14 and UVRAG," *Molecular Biology of the Cell*, vol. 19, no. 12, pp. 5360–5372, 2008.

[59] R. C. Wang, Y. Wei, Z. An et al., "Akt-mediated regulation of autophagy and tumorigenesis through Beclin 1 phosphorylation," *Science*, vol. 338, no. 6109, pp. 956–959, 2012.

[60] S. Pattingre, A. Tassa, X. Qu et al., "Bcl-2 antiapoptotic proteins inhibit Beclin 1-dependent autophagy," *Cell*, vol. 122, no. 6, pp. 927–939, 2005.

[61] Y. Ohsumi, "Molecular dissection of autophagy: two ubiquitin-like systems," *Nature Reviews Molecular Cell Biology*, vol. 2, no. 3, pp. 211–216, 2001.

[62] I. Tanida, T. Ueno, and E. Kominami, "LC3 conjugation system in mammalian autophagy," *International Journal of Biochemistry and Cell Biology*, vol. 36, no. 12, pp. 2503–2518, 2004.

[63] Y. Kabeya, N. Mizushima, T. Ueno et al., "LC3, a mammalian homologue of yeast Apg8p, is localized in autophagosome membranes after processing," *EMBO Journal*, vol. 19, no. 21, pp. 5720–5728, 2000.

[64] Y. Kabeya, N. Mizushima, A. Yamamoto, S. Oshitani-Okamoto, Y. Ohsumi, and T. Yoshimori, "LC3, GABARAP and GATE16 localize to autophagosomal membrane depending on form-II formation," *Journal of Cell Science*, vol. 117, no. 13, pp. 2805–2812, 2004.

[65] H. He, Y. Dang, F. Dai et al., "Post-translational modifications of three members of the human MAP1LC3 family and detection of a novel type of modification for MAP1LC3B," *Journal of Biological Chemistry*, vol. 278, no. 31, pp. 29278–29287, 2003.

[66] K. Satoo, N. N. Noda, H. Kumeta et al., "The structure of Atg4B-LC3 complex reveals the mechanism of LC3 processing and delipidation during autophagy," *EMBO Journal*, vol. 28, no. 9, pp. 1341–1350, 2009.

[67] H. Zhang, M. Bosch-Marce, L. A. Shimoda et al., "Mitochondrial autophagy is an HIF-1-dependent adaptive metabolic response to hypoxia," *Journal of Biological Chemistry*, vol. 283, no. 16, pp. 10892–10903, 2008.

[68] W. X. Ding, H. M. Ni, M. Li et al., "Nix is critical to two distinct phases of mitophagy, reactive oxygen species-mediated autophagy induction and Parkin-ubiquitin-p62-mediated mitochondrial priming," *Journal of Biological Chemistry*, vol. 285, no. 36, pp. 27879–27890, 2010.

[69] D. Narendra, A. Tanaka, D. Suen, and R. J. Youle, "Parkin is recruited selectively to impaired mitochondria and promotes their autophagy," *Journal of Cell Biology*, vol. 183, no. 5, pp. 795–803, 2008.

[70] S. Geisler, K. M. Holmström, D. Skujat et al., "PINK1/Parkin-mediated mitophagy is dependent on VDAC1 and p62/SQSTM1," *Nature Cell Biology*, vol. 12, no. 2, pp. 119–131, 2010.

[71] H. R. Morris, "Genetics of Parkinson's disease," *Annals of Medicine*, vol. 37, no. 2, pp. 86–96, 2005.

[72] A. Trancikova, E. Tsika, and D. J. Moore, "Mitochondrial dysfunction in genetic animal models of Parkinson's disease," *Antioxidants and Redox Signaling*, vol. 16, no. 9, pp. 896–919, 2012.

[73] C. Vives-Bauza, C. Zhou, Y. Huang et al., "PINK1-dependent recruitment of Parkin to mitochondria in mitophagy," *Proceedings of the National Academy of Sciences of the United States of America*, vol. 107, no. 1, pp. 378–383, 2010.

[74] Y. Chen and G. W. Dorn, "PINK1-phosphorylated mitofusin 2 is a Parkin receptor for culling damaged mitochondria," *Science*, vol. 340, no. 6131, pp. 471–475, 2013.

[75] S. A. Sarraf, M. Raman, V. Guarani-Pereira et al., "Landscape of the PARKIN-dependent ubiquitylome in response to mitochondrial depolarization," *Nature*, vol. 496, no. 7445, pp. 372–376, 2013.

[76] Y. Ichimura and M. Komatsu, "Selective degradation of p62 by autophagy," *Seminars in Immunopathology*, vol. 32, no. 4, pp. 431–436, 2010.

[77] S. Shaid, C. H. Brandts, H. Serve, and I. Dikic, "Ubiquitination and selective autophagy," *Cell Death Differentiation*, vol. 20, no. 1, pp. 21–30, 2013.

[78] V. Kirkin, T. Lamark, Y. Sou et al., "A role for NBR1 in autophagosomal degradation of ubiquitinated substrates," *Molecular Cell*, vol. 33, no. 4, pp. 505–516, 2009.

[79] T. H. Clausen, T. Lamark, P. Isakson et al., "p62/SQSTM1 and ALFY interact to facilitate the formation of p62 bodies/ALIS and their degradation by autophagy," *Autophagy*, vol. 6, no. 3, pp. 330–344, 2010.

[80] E. Deosaran, K. B. Larsen, R. Hua et al., "NBR1 acts as an autophagy receptor for peroxisomes," *Journal of Cell Science*, vol. 126, no. 4, pp. 939–952, 2013.

[81] G. C. MacIntosh and D. C. Bassham, "The connection between ribophagy, autophagy and ribosomal RNA decay," *Autophagy*, vol. 7, no. 6, pp. 662–663, 2011.

[82] E. Cebollero, F. Reggiori, and C. Kraft, "Reticulophagy and ribophagy: regulated degradation of protein production factories," *International Journal of Cell Biology*, vol. 2012, Article ID 182834, 9 pages, 2012.

[83] K. Liu and M. J. Czaja, "Regulation of lipid stores and metabolism by lipophagy," *Cell Death and Differentiation*, vol. 20, no. 1, pp. 3–11, 2013.

[84] Y. Fujiwara, A. Furuta, H. Kikuchi et al., "Discovery of a novel type of autophagy targeting RNA," *Autophagy*, vol. 9, no. 3, pp. 403–409, 2013.

[85] G. Robert, C. Gastaldi, A. Puissant et al., "The anti-apoptotic Bcl-B protein inhibits BECN1-dependent autophagic cell death," *Autophagy*, vol. 8, no. 4, pp. 637–649, 2012.

[86] Y. Zhu, S. Massen, M. Terenzio et al., "Modulation of serines 17 and 24 in the LC3-interacting region of Bnip3 determines pro-survival mitophagy versus apoptosis," *Journal of Biological Chemistry*, vol. 288, no. 2, pp. 1099–1113, 2013.

[87] S. Luo and D. C. Rubinsztein, "Apoptosis blocks Beclin 1-dependent autophagosome synthesis: an effect rescued by Bcl-xL," *Cell Death and Differentiation*, vol. 17, no. 2, pp. 268–277, 2010.

[88] J. O. Pyo, M. Jang, Y. Kwon et al., "Essential roles of Atg5 and FADD in autophagic cell death: dissection of autophagic cell death into vacuole formation and cell death," *Journal of Biological Chemistry*, vol. 280, no. 21, pp. 20722–20729, 2005.

[89] S. Yousefi, R. Perozzo, I. Schmid et al., "Calpain-mediated cleavage of Atg5 switches autophagy to apoptosis," *Nature Cell Biology*, vol. 8, no. 10, pp. 1124–1132, 2006.

[90] A. D. Rubinstein, M. Eisenstein, Y. Ber, S. Bialik, and A. Kimchi, "The autophagy protein atg12 associates with antiapoptotic Bcl-2 family members to promote mitochondrial apoptosis," *Molecular Cell*, vol. 44, no. 5, pp. 698–709, 2011.

[91] V. M. Betin and J. D. Lane, "Caspase cleavage of Atg4D stimulates GABARAP-L1 processing and triggers mitochondrial targeting and apoptosis," *Journal of Cell Science*, vol. 122, no. 14, pp. 2554–2566, 2009.

[92] O. Oral, D. Oz-Arslan, Z. Itah et al., "Cleavage of Atg3 protein by caspase-8 regulates autophagy during receptor-activated cell death," *Apoptosis*, vol. 17, no. 8, pp. 810–820, 2012.

[93] J. S. Lee, Q. Li, J. Lee et al., "FLIP-mediated autophagy regulation in cell death control," *Nature Cell Biology*, vol. 11, no. 11, pp. 1355–1362, 2009.

[94] D. Crighton, S. Wilkinson, J. O'Prey et al., "DRAM, a p53-induced modulator of autophagy, is critical for apoptosis," *Cell*, vol. 126, no. 1, pp. 121–134, 2006.

[95] Z. Feng, H. Zhang, A. J. Levine, and S. Jin, "The coordinate regulation of the p53 and mTOR pathways in cells," *Proceedings of the National Academy of Sciences of the United States of America*, vol. 102, no. 23, pp. 8204–8209, 2005.

[96] E. Tasdemir, M. C. Maiuri, L. Galluzzi et al., "Regulation of autophagy by cytoplasmic p53," *Nature Cell Biology*, vol. 10, no. 6, pp. 676–687, 2008.

[97] A. U. Contreras, Y. Mebratu, M. Delgado et al., "Deacetylation of p53 induces autophagy by suppressing Bmf expression," *Journal of Cell Biology*, vol. 201, no. 3, pp. 427–437, 2013.

[98] E. Tasdemir, M. C. Maiuri, E. Morselli et al., "A dual role of p53 in the control of autophagy," *Autophagy*, vol. 4, no. 6, pp. 810–814, 2008.

[99] B. Levine and J. Abrams, "p53: the Janus of autophagy?" *Nature Cell Biology*, vol. 10, no. 6, pp. 637–639, 2008.

[100] Z. H. Chen, H. P. Kim, F. C. Sciurba et al., "Egr-1 regulates autophagy in cigarette smoke-induced chronic obstructive pulmonary disease," *PLoS ONE*, vol. 3, no. 10, Article ID e3316, 2008.

[101] Z. H. Chen, H. C. Lam, Y. Jin et al., "Autophagy protein microtubule-associated protein 1 light chain-3B (LC3B) activates extrinsic apoptosis during cigarette smoke-induced emphysema," *Proceedings of the National Academy of Sciences of the United States of America*, vol. 107, no. 44, pp. 18880–18885, 2010.

[102] H. H. Cha, J. R. Hwang, H. Y. Kim, S. J. Choi, S. Y. Oh, and C. R. Roh, "Autophagy induced by tumor necrosis factor α mediates intrinsic apoptosis in trophoblastic cells," *Reproductive Sciences*, 2013.

[103] Y. Wang, R. Singh, A. C. Massey et al., "Loss of macroautophagy promotes or prevents fibroblast apoptosis depending on the death stimulus," *Journal of Biological Chemistry*, vol. 283, no. 8, pp. 4766–4777, 2008.

[104] Y. Xu, O. K. Sung, Y. Li, and J. Han, "Autophagy contributes to caspase-independent macrophage cell death," *Journal of Biological Chemistry*, vol. 281, no. 28, pp. 19179–19187, 2006.

[105] L. Yu, F. Wan, S. Dutta et al., "Autophagic programmed cell death by selective catalase degradation," *Proceedings of the National Academy of Sciences of the United States of America*, vol. 103, no. 13, pp. 4952–4957, 2006.

[106] D. T. Madden, L. Egger, and D. E. Bredesen, "A calpain-like protease inhibits autophagic cell death," *Autophagy*, vol. 3, no. 5, pp. 519–522, 2007.

[107] L. Yu, A. Alva, H. Su et al., "Regulation of an ATG7-beclin 1 program of autophaglic cell death by caspase-8," *Science*, vol. 304, no. 5676, pp. 1500–1502, 2004.

[108] Y. T. Wu, H. L. Tan, Q. Huang et al., "Autophagy plays a protective role during zVAD-induced necrotic cell death," *Autophagy*, vol. 4, no. 4, pp. 457–466, 2008.

[109] S. Shimizu, T. Kanaseki, N. Mizushima et al., "Role of Bcl-2 family proteins in a non-apoptopic programmed cell death dependent on autophagy genes," *Nature Cell Biology*, vol. 6, no. 12, pp. 1221–1228, 2004.

[110] R. Mathew, V. Karantza-Wadsworth, and E. White, "Role of autophagy in cancer," *Nature Reviews Cancer*, vol. 7, no. 12, pp. 961–967, 2007.

[111] K. Degenhardt, R. Mathew, B. Beaudoin et al., "Autophagy promotes tumor cell survival and restricts necrosis, inflammation, and tumorigenesis," *Cancer Cell*, vol. 10, no. 1, pp. 51–64, 2006.

[112] S. Jin, R. S. DiPaola, R. Mathew, and E. White, "Metabolic catastrophe as a means to cancer cell death," *Journal of Cell Science*, vol. 120, no. 3, pp. 379–383, 2007.

[113] J. J. Lemasters, A. Nieminen, T. Qian et al., "The mitochondrial permeability transition in cell death: a common mechanism in necrosis, apoptosis and autophagy," *Biochimica et Biophysica Acta*, vol. 1366, no. 1-2, pp. 177–196, 1998.

[114] B. Loos, A. M. Engelbrecht, R. A. Lockshin, D. J. Klionsky, and Z. Zakeri, "The variability of autophagy and cell death susceptibility: unanswered questions," *Autophagy*, vol. 9, no. 9, pp. 1270–1285, 2013.

[115] T. Eisenberg, H. Knauer, A. Schauer et al., "Induction of autophagy by spermidine promotes longevity," *Nature Cell Biology*, vol. 11, no. 11, pp. 1305–1314, 2009.

[116] L. Bonapace, B. C. Bornhauser, M. Schmitz et al., "Induction of autophagy-dependent necroptosis is required for childhood acute lymphoblastic leukemia cells to overcome glucocorticoid resistance," *Journal of Clinical Investigation*, vol. 120, no. 4, pp. 1310–1323, 2010.

[117] B. D. Bell, S. Leverrier, B. M. Weist et al., "FADD and caspase-8 control the outcome of autophagic signaling in proliferating T cells," *Proceedings of the National Academy of Sciences of the United States of America*, vol. 105, no. 43, pp. 16677–16682, 2008.

[118] M. J. Khan, M. Rizwan Alam, M. Waldeck-Weiermair et al., "Inhibition of autophagy rescues palmitic acid-induced necroptosis of endothelial cells," *Journal of Biological Chemistry*, vol. 287, no. 25, pp. 21110–21120, 2012.

[119] Y. Q. Wang, L. Wang, M. Y. Zhang et al., "Necrostatin-1 suppresses autophagy and apoptosis in mice traumatic brain injury model," *Neurochemical Research*, vol. 37, no. 9, pp. 1849–1858, 2012.

[120] J. V. Lu and C. M. Walsh, "Programmed necrosis and autophagy in immune function," *Immunology Reviews*, vol. 249, no. 1, pp. 205–217, 2012.

[121] V. Nikoletopoulou, M. Markaki, K. Palikaras, and N. Tavernarakis, "Crosstalk between apoptosis, necrosis and autophagy," *Biochimica Biophysica Acta*, vol. 1833, no. 12, pp. 3448–3459, 2013.

[122] T. Saitoh, N. Fujita, M. H. Jang et al., "Loss of the autophagy protein Atg16L1 enhances endotoxin-induced IL-1β production," *Nature*, vol. 456, no. 7219, pp. 264–268, 2008.

[123] K. Nakahira, J. A. Haspel, V. A. K. Rathinam et al., "Autophagy proteins regulate innate immune responses by inhibiting the release of mitochondrial DNA mediated by the NALP3 inflammasome," *Nature Immunology*, vol. 12, no. 3, pp. 222–230, 2011.

[124] R. Zhou, A. S. Yazdi, P. Menu, and J. Tschopp, "A role for mitochondria in NLRP3 inflammasome activation," *Nature*, vol. 469, no. 7329, pp. 221–226, 2011.

[125] K. Schroder and J. Tschopp, "The Inflammasomes," *Cell*, vol. 140, no. 6, pp. 821–832, 2010.

[126] N. Dupont, S. Jiang, M. Pilli, W. Ornatowski, D. Bhattacharya, and V. Deretic, "Autophagy-based unconventional secretory pathway for extracellular delivery of IL-1β," *EMBO Journal*, vol. 30, no. 23, pp. 4701–4711, 2011.

[127] C. S. Shi, K. Shenderov, N. N. Huang et al., "Activation of autophagy by inflammatory signals limits IL-1β production by targeting ubiquitinated inflammasomes for destruction," *Nature Immunology*, vol. 13, no. 3, pp. 255–263, 2012.

[128] S. Y. Chuang, C. H. Yang, C. C. Chou, Y. P. Chiang, T. H. Chuang, and L. C. Hsu, "TLR-induced PAI-2 expression suppresses IL-1β processing via increasing autophagy and NLRP3 degradation," *Proceedings of the National Academy of Sciences of the United States of America*, vol. 110, no. 40, pp. 16079–16084, 2013.

[129] B. G. Byrne, J. F. Dubuisson, A. D. Joshi, J. J. Persson, and M. S. Swanson, "Inflammasome components coordinate autophagy and pyroptosis as macrophage responses to infection," *MBio*, vol. 4, no. 1, Article ID e00620, 2013.

[130] K. R. Bortoluci and R. Medzhitov, "Control of infection by pyroptosis and autophagy: role of TLR and NLR," *Cellular and Molecular Life Sciences*, vol. 67, no. 10, pp. 1643–1651, 2010.

Hindawi Publishing Corporation
International Journal of Cell Biology
Volume 2014, Article ID 725928, 13 pages
http://dx.doi.org/10.1155/2014/725928

Research Article

Characterization of NGF, trkA^{NGFR}, and p75^{NTR} in Retina of Mice Lacking Reelin Glycoprotein

Bijorn Omar Balzamino,[1] Filippo Biamonte,[2] Graziana Esposito,[1] Ramona Marino,[3] Francesca Fanelli,[3] Flavio Keller,[3] and Alessandra Micera[1,4]

[1] *IRCCS-G.B. Bietti Foundation, Rome, Italy*
[2] *Institute of Histology and Embryology, School of Medicine "A. Gemelli", Catholic University of the Sacred Heart, Rome, Italy*
[3] *Laboratory of Developmental Neuroscience and Neural Plasticity, University Campus Bio-Medico, Rome, Italy*
[4] *Laboratory of Ophthalmology, IRCCS-G.B. Bietti Foundation, Via Alvaro del Portillo 21, 00128 Rome, Italy*

Correspondence should be addressed to Alessandra Micera; amicera@gmail.com

Received 11 October 2013; Accepted 4 November 2013; Published 30 January 2014

Academic Editor: Alessio D'Alessio

Both Reelin and Nerve Growth Factor (NGF) exert crucial roles in retinal development. Retinogenesis is severely impaired in *E-reeler* mice, a model of Reelin deficiency showing specific Green Fluorescent Protein expression in Rod Bipolar Cells (RBCs). Since no data are available on Reelin and NGF cross-talk, NGF and trkA^{NGFR}/p75^{NTR} expression was investigated in retinas from *E-reeler* versus control mice, by confocal microscopy, Western blotting, and real time PCR analysis. A scattered increase of NGF protein was observed in the Ganglion Cell Layer and more pronounced in the Inner Nuclear Layer (INL). A selective increase of p75^{NTR} was detected in most of RBCs and in other cell subtypes of INL. On the contrary, a slight trend towards a decrease was detected for trkA^{NGFR}, albeit not significant. Confocal data were validated by Western blot and real time PCR. Finally, the decreased trkA^{NGFR}/p75^{NTR} ratio, representative of p75^{NTR} increase, significantly correlated with *E-reeler* versus E-control. These data indicate that NGF-trkA^{NGFR}/p75^{NTR} is affected in *E-reeler* retina and that p75^{NTR} might represent the main NGF receptor involved in the process. This first NGF-trkA^{NGFR}/p75^{NTR} characterization suggests that *E-reeler* might be suitable for exploring Reelin-NGF cross-talk, representing an additional information source in those pathologies characterized by retinal degeneration.

1. Introduction

Reelin and Nerve Growth Factor (NGF) take part in retinogenesis, and their increased levels occur in inflamed/degenerating retina [1–3]. Reelin is a highly conserved extracellular glycoprotein, released by neurons/accessory cells and signals via specific surface receptors belonging to the Apolipoprotein E and the very low density lipoprotein families (ApoER2 and VLDLR) and via adaptor protein Dab1 [4, 5]. Reelin expression peaks during retinogenesis, allowing migration/positioning and differentiation of retinal cells (physiological upregulation), returns to baseline levels in adulthood (physiological downregulation), and increases again following local injury/degeneration (pathological upregulation) [6, 7]. Reelin deprivation causes a macroscopic modification of the retinal structure, with incorrect cells distribution and synaptic circuitry alteration, including a decrease in Rod Bipolar Cells (RBCs) density and an abnormal distribution of their processes in the Inner Nuclear Layer (INL), as well described in the *reeler* model [1, 8].

In the visual system, NGF exerts pleiotropic effects during development and guarantees homeostasis during adulthood [2, 3, 9–11]. NGF appears to exert multiple effects in both the neurons and accessory cells (proliferation, migration, differentiation, cytoskeletal reorganization, survival, apoptosis, etc.) [2, 3, 11]. NGF plays a crucial role during retinogenesis, influencing neuritic outgrowth, survival, and apoptosis, together with other neurotrophins and their related receptors, while in adulthood NGF is involved in several pathophysiological processes (homeostasis, ischemia, glaucoma, etc.) [2, 3, 10, 11]. NGF is produced and used in an autocrine/paracrine fashion by Retinal Ganglion Cells (RGCs), Bipolar and other

retinal cell types (horizontal and amacrine cells, Müller glia) [11]. The biological effects of NGF are directly dependent on the specific binding to two different cell surface receptors, the tyrosine kinase trkA^{NGFR} and the glycoprotein p75^{NTR} [12, 13]. NGF/trkA^{NGFR} promotes the survival and recovery of RGCs, as observed in experimental models and after intraocular injection of NGF [2, 11, 14, 15]. The crucial contribution of the trkA^{NGFR}/p75^{NTR} ratio in the survival of RGCs has been recently envisaged [13, 15]. Previous studies showed an impaired NGF expression in Reelin-deficient mice [16, 17].

In view of all these findings a possible cross-talk between NGF and Reelin during retinal development might be hypothesized, suggesting an abnormal NGF pathway in Reelin-deficient retinas. To address this question, a homozygous *reeler* mice model was developed from founder couples and used to investigate both the biochemical and molecular expression of NGF-trkA^{NGFR}/p75^{NTR}.

2. Materials and Methods

2.1. Ethics Statement. All experiments were performed in compliance with the ARVO Statement for the Use of Animals in Ophthalmic and Vision Research. Animal care procedures were conducted in conformity with the Intramural Committee and Institutional guidelines, in accordance with national and international laws and policies (EEC Council Directive 86/609, OJ L 358, 1, December 12, 1987; NIH Guide for the Care and Use of Laboratory Animals, NIH Publication 85-23, 1985). The experimental protocol was approved by the Ethical Committee of "Tor Vergata" University (Rome, Italy).

2.2. Animals and Genotyping. Founder couples of *reeler* strain (B6C3Fe-a/a-rl; Jackson Laboratories, Bar Harbor, ME, USA), carrying the rl$^{jx-/-}$ mutation in a C57BL/6J background, were purchased from Charles River (Calco, Italy). The colony was housed at animal house facility ("Tor Vergata" University) under standard conditions (12 hrs light/dark cycle, temperature 21 ± 1°C, and relative humidity 60 ± 10%). Both water and food were freely available (Enriched Standard Diet, Mucedola, Settimo Milanese, Italy). To obtain the double-mutant *reeler*-L7-EGFP strain (referred to as *E-reeler* in this study), B6C3Fe-a/a-rl and B6-FVB-Tg (Pcp2-EGFP)2Yuza/J strains (Jackson Laboratories) were crossed and then backcrossed, according to a standard procedure [18]. The offspring from the 8th generation were used as donors that were hemizygotes for the Green Fluorescent Protein (GFP) locus. The B6C3Fe-L7-EGFP mice were used as control (wild-type rl$^{jx+/+}$ genotype; E-control). Since GFP expression is under control of the L7 promoter, high levels of this live cell marker (lacking toxicity) characterize RBCs and allow their easy analysis at confocal microscopy (resistant to bleaching) [19].

For the present study, a total of $n = 62$ eyes (31 mice) were used and grouped as follows: $n = 32$ *E-reeler* eyes (21 ± 1 days; body-weight range: 9–11 g) and $n = 30$ E-control eyes (21 ± 1 days; body-weight range: 12–14 g). In a pilot study, RBCs were quantified at P7, P14, P21, and P35, in order to choose the best time-point for analyses ($n = 3$/time-point; $n = 9$ *E-reeler*, and $n = 3$ E-control).

EGFP expression and *reeler* genotype were assessed as previously reported, with minor modifications [20, 21]. Briefly, 1 μg DNA was extracted from tails and placed in a 10x reaction buffer (100 mM Tris-HCl, pH 8.3, 500 mM KCl, and 15 mM $MgCl_2$) containing 10 mM dNTPs, 20 μM random primers, and 5 U/mL recombinant Taq polymerase (Euroclone, Milan, Italy). DNA amplification was performed in a PTC-100 cycler (MJ Research Inc., Watertown, MA). Specific primers for GFP detection and genotyping studies were synthesized by Invitrogen (Grand Island, USA). Detailed primer sequences, gene accession number and amplification profiles are reported in Table 1(A). DNA products and ladder (100 bps molecular marker; Takara Bio Inc., Shiga, Japan) were separated in 0.8–1.5% agarose gel containing ethidium bromide (0.5 μg/mL; Appligene Oncor). Gels were acquired by the Kodak EDAS 290 imaging system (Kodak, Tokyo, Japan).

2.3. Tissue Sampling. *E-reeler* and E-control mice were deeply anaesthetized by 2 mg/mL ketamine (0.2 mL/10 gr body-weight; Ketavet, Gellini Farmaceutici, Italy) and 0.23 mg/mL medetomidine (0.24 mL/10 gr body-weight; Domitor, Orion Corp., Espoo, Finland) intraperitoneal injection.

For confocal microscopy analysis, mice were perfused through the left ventricle with saline solution (3 min), followed by 4% buffered paraformaldehyde (PFA; 5 min). Enucleated eyes ($n = 10$ eyes for *E-reeler* and $n = 8$ eyes for E-control) were postfixed in the same fixative (48 hrs) and cryoprotected in 10% sucrose (24 hrs).

For molecular and biochemical analysis, mice were sacrificed by cervical dislocation and the retinas were quickly processed for biochemical ($n = 8$ eyes each, for both *E-reeler* and E-control) or molecular ($n = 14$ eyes each, for both *E-reeler* and E-control) analysis. The dissection of retinas from fresh enucleated eyes was carried out under a dissector microscope (SMZ645; Nikon, Tokyo, Japan), equipped with cold-light optic fibers (PL2000 photonic; Axon, Vienna, Austria).

2.4. Immunofluorescence and Digital Analysis. Postfixed and cryoprotected eyes were quickly frozen in dry ice, embedded in OCT medium (TissueTek; Leica, Heidelberg, Germany), and sectioned (CM3050 cryostat; Leica Microsystems, Rijswijk, The Netherlands). Serial sections (7 μm) were placed ($n = 3$ sections/slide, $n = 6$ slides/retina) onto gelatinized slides, preheated to increase tissue attachment, and stored at −20°C. Both antigen retrieval (0.05% trypsin-EDTA solution, 2 min) and blocking/permeabilizing (1% BSA and 0.5% Triton X100 in PBS, 15 min) steps were performed before the addition of specific antibodies: anti-NGF (sc-549), anti-trkA^{NGFR} (sc-118), and anti-p75^{NTR} (sc-6188) antibodies, all from Santa Cruz Biotech (Santa Cruz, CA). A quenching passage was also carried out to minimize PFA background and slightly reduce the higher fluorescent expression of the E-construct. Cy3-conjugated donkey

Table 1: Primers for genotyping (A) and for real time PCR (B) used in the study.

[a]Gene access number	Sequence (For/Rev)	Amplicon	Annealing conditions
	A: genotyping		
[b]Reeler (GM75)	F: 5′-TAA TCT GTC CTC ACT CTG CC-3′	380 bp	55°C, 120 s
[b]Reeler (3W1)	R: 5′-ACA GTT GAC ATA CCT TAA TC-3′	280 bp	
[b]Reeler (3R1)	R: 5′-TGT ATT AAT GTG CAG TGT TG-3′		
[a]GFP 1	F: 5′-CGT AAA CGG CCA CAA GTT CAG-3′	500 bp	65°C, 30 s
[a]GFP 2	R: 5′-ATG CCG TTC TTC TGC TTG TCG-3′		
	B: RT-PCR		
[c]GAPDH	S: 5′-GTGGACCTCATGGCCTACAT-3′	100 bp	53°C, 30 s
BC059110	AS: 5′-GTTGGGATAGGGACTCCTCAC-3′		
[c]trkA	S: 5′-AACAACGGCAACTACAC-3′	137 bp	58°C, 25 s
M23102	AS: 5′-CCTGTTTCTCCGTCCAC-3′		
[c]$p75^{NTR}$	F: 5′-GAGGCACCACCGACAACCTC-3′	131 bp	55°C, 25 s
AF187064	R: 5′-TGCTTGCAGCTGTTCCACCT-3′		
[c]NGF	F: 5′-CTGGCCACACTGAGGTGCAT-3′	120 bp	53°C, 30 s
BC011123	R: 5′-TCCTGCAGGGACATTGCTCTC-3′		

Amplification profiles:
[a]1 cycle at 94°C/5 min, 30 cycles including 94°C/1 min, 55°C/2 min, and 72°C/3 min, and a final cycle at 72°C/10 min.
[b]1 cycle at 94°C/5 min, 35 cycles including 94°C/30 sec, 65°C/30 sec, and 72°C/30 sec, and a final cycle at 72°C/10 min.
[c]1 cycle at 95°C/15 min, 47 cycles of denaturation at 95°C/30 sec, annealing at 55–60°C/25 sec (primer's Tm dependent), and elongation at 72°C/30 sec, fluorescence monitoring at 60–90°C, 0.01°C for 0.3 sec, and final incubation at 72°C/5 min. Single melting curves always verified.

species-specific antibodies (1 : 500–700; Jackson ImmunoResearch Europe Ltd., Suffolk, UK) were used to bind all primary antibodies. Nuclear counterstaining was performed with TOTO3-Iodide (Molecular Probes, Eugene, OR) while GFP expression specifically identified RBCs [19]. Isotypes (negative controls) were carried out in parallel with the omission of primary antibodies and used for appropriate channel series acquisition and related background subtractions. Slides were coverslipped using a glycerol gelatin mounting medium (Sigma-Aldrich, St. Louis, CA). Serial images were acquired by C1 software connected to an inverted microscope (Eclipse TE2000U, Nikon). Digital images (pixel size: 512 × 512 or 1024 × 1024 dpi) were saved, converted into 8-bit TIFF images, and subjected to densitometric analysis (Image J v1.43; NIH-http://rsb.info.nih.gov/ij/). Single integrated optical density (IntDen) was registered for *E-reeler* and E-control retina (n = 5 optic fields/slide/retina; ×40/dry 0.75 DIC M/N2), in terms of specific RBCs density and dendrite length (n = 5 sections/animal). IntDen data were collected: mean values (±SD) were calculated and subjected to statistical analysis. Quantification of RBCs in retinas was performed by evaluating the number of the GFP-expressing RBCs in the INL. A grid of 27 × 18 fields (field size: 25 μm × 27.5 μm) was printed onto a transparent sheet and attached to the screen of a 15′ LCD-display. Three representative regions were analysed as follows: left, right, and across the optic nerve over five consecutive slides/mice/experimental group. Cells outside the region of interest were automatically ignored and the results were averaged as a percentage of positive cells. All counts were performed under blind conditions and presented as mean ± SD.

2.5. Western Blot. Dissected retinas were homogenized in 70 μL modified RIPA Buffer (50 mM Tris-HCl, 150 mM NaCl, 1% Triton-X100, 5 mM EDTA, 100 mM NaF, and 1 mM PMSF; pH 7.5) and briefly sonicated to shrink DNA (VibraCell equipped with microtip; Sonics & Materials, Inc., Newtown, USA) [22]. Total proteins were quantified with the DC protein assay kit (BioRad Laboratories Inc., Hercules, CA), by using the A1000 Spectrophotometer (Nanodrop, Celbio, Milan, Italy). Normalized samples (50 μg) were subjected to 7.5% or 12% SDS-PAGE, under reducing conditions (130 V/frontline; Miniprotean apparatus, Biorad). Electrophoresed proteins were transferred onto Hy-Bond membranes (GE Healthcare, Buckinghamshire, UK), in the presence of 48 mM Tris-Cl (pH 6.8), 39 mM glycine, 0.0037% SDS, and 20% methanol solution (10 V/55 min; semidry condition, Transblotting apparatus, Biorad). Membranes were stained with 0.5% Ponceau S in acetic acid (ICN, Milan, Italy) to verify protein transfer, washed twice in 0.5% Triton X100-Tris buffered saline (TBS: 20 mM Tris-HCl and 150 m NaCl, pH 7.5) for 30 min, and blocked in 0.05% Tween-20 TBS (TW-TBS) containing 5% nonfat dry milk for 1 hr. The membranes were then probed (4°C/18 hrs) with the following primary antibodies: anti-NGF (sc-549), anti-$trkA^{NGFR}$ (sc-118), anti-$p75^{NTR}$ (sc-6188) from Santa Cruz, and anti-Actin (ab-3280) from Abcam (Cambridge, UK). Membranes were washed in TW-TBS and subsequently incubated with POD-conjugated donkey species-specific antibodies (1 : 30000; Jackson ImmunoResearch) for 90 min. Detection of specific signal was performed by using an enhanced Chemi-Luminescent system (West Femto Sensitivity Substrate; Pierce, Rockford, IL). Alternatively, membranes were exposed to Hybond filters in appropriate cassette and developed in appropriate solutions. Both

membranes and filters were acquired by 1D Image Station (Kodak). Data were saved as 8-bit TIFF files and exported to be shown after Adobe Photoshop CS3 assembly (Adobe System, San Jose, CA). Densitometric analysis was performed using the 1D Image software (Kodak) and related Optical Density (OD) values, referred to as normalized samples, were shown in bar plots.

2.6. Real Time PCR Amplification. Dissected retinas were pretreated with Proteinase K (20 mg/mL, 56°C/3 hrs; Finnzyme, Milan, Italy) in modified HIRT buffer (50 mM Tris-Cl, pH 8, 1 mM EDTA, 1% Tween20). Total RNA was extracted 1 : 1 with TRIfast, according to a standard procedure (EuroClone), and resuspended in 10 μL fresh RNase free water (Direct Q5, Millipore Corporation, Billerica, MA). To eliminate any genomic DNA contamination, all total RNA samples were treated with RNase-free DNaseI, according to the supplier's protocol (2 U/μL; AM-1907; Turbo DNA free kit; Ambion Ltd., Huntingdon, Cambridgeshire, UK). Total RNA samples were checked for RNA quantity/purity (>1.8; A280 program, Nanodrop) and for absence of RNA degradation (1% agarose gel analysis). Equivalent amounts of RNA (1 μg) were used as template to generate cDNAs, according to the IMPROM manufacturer's procedure (Promega Corp., Madison, USA), in a one cycler programmable thermocycler (PeqLab Biotech, Erlangen, Germany). The resulting cDNAs were amplified using the SYBR Green PCR core reagent kit (Applied Biosystems, Foster City, CA) in an Opticon2 programmable thermocycler (MJ Research), according to standard procedures [23]. Samples were amplified in duplicate and in parallel with negative controls (either without template or with mRNA as template). Real cycle thresholds (Cts) were recorded during linear amplification and normalized to those of referring genes run in parallel ($nCts = Ct_{target} - Ct_{referring}$). Averages were calculated from these replicates and expressed as normalized Ct or as expression ratio of a normalized target gene (fold changes in log2-scale), according to REST© analysis [24]. Both primer sequence and amplification profile are accurately reported in Table 1(B). The specific primers were designed using Primer3 software (http://www.primer3.com) and synthesized by MWG Biotech (Ebersberg, Germany). GenBank software was used to select the complete mRNA sequence of each gene investigated (http://www.ncbi.nlm.nih.gov/ Genbank; provided by the National Center for Biotechnology Information, Bethesda, MD). Primer specificities were confirmed by single melting curves, monitored during amplification. In random tests, PCR products were separated on 2.5% agarose gel and acquired by 1D Kodak software to verify the presence of a single amplicon.

2.7. Statistical Analysis. All data are shown as mean ± SD (in text) and mean ± SEM (in bar plots). Parametric ANOVA analysis followed by a Tukey-Kramer post hoc comparison was used to estimate differences between groups [25]. The statistical package used was StatView II for PC (Abacus Concepts Inc., Barkley, CA). REST/ANOVA coupled analysis was carried out for molecular comparisons. $trkA^{NGFR}/p75^{NTR}$ ratio was calculated according to the single Cts values recorded during linear amplification and normalized to those of referring genes run in parallel (nCts), where Cts are inversely proportional to mRNA expression [22]. Kendall's rank coefficient (Tau) was also calculated to identify correlation between GFP versus $p75^{NTR}$ and $trkA^{NGFR}$ versus $p75^{NTR}$. A probability of $P < 0.05$ was presumed to reflect statistical significant difference between groups.

3. Results

A preliminary observation of *E-reeler* mice was carried out between P7 and P35 showing ataxia, eating complications (typical of *reeler* mice), and survival difficulties for the majority of animals, in the absence of appropriate handling [1]. Accordingly, the P21 time-point was selected for the following studies of characterization, and only *E-reeler* mice carrying both the *reeler* mutation and EGFP expression were included in the study. The genotyping is shown in Figure 1(a): as depicted in (A), a 500 bp band was observed in *E-reeler* and E-control DNA extracts, as compared to a negative control, confirming the positive EGFP genotyping; as depicted in (B), two DNA fragments were observed in DNA extracts: one corresponding to the wild-type allele (280 bp; WT) and the other to the *reelin* allele (380 bp; Rl). Both bands are visible in the heterozygous mouse, not used in these studies.

According to Oberdick and coworkers procedure, both *E-reeler* and E-control retinas express GFP-specific fluorescence mainly localized in the dendrites, soma, and axon terminals of RBCs, allowing their easy recognition with confocal microscopy [20]. As shown in Figure 1(b) (merge), a decrease in the number (arrows) and dendrite length of RBCs populating the INL, as well as their synaptic buttons (arrowheads) in the GCL, was observed in *E-reeler* retinas. Digital analysis carried out on serial images showed a 27.2% decrease in GFP immunoreactivity in *E-reeler* retina (20899 ± 4663 versus 28727 ± 8134 IntDen, resp., *E-reeler* versus E-control; $P < 0.001$). GFP-bearing RBCs were also counted in serial sections, showing a 27.8% decrease in the *E-reeler* retinas as compared to E-control ones (resp., 209 ± 4 versus 287 ± 81 cells/optic field; $P < 0.001$; Figure 1(c)).

3.1. NGF Expression. In order to understand whether NGF is affected in *E-reeler* retina, serial sections were probed with specific NGF antibody and NGF immunoreactivity was evaluated in the INL and GCL. As shown in Figure 2(a), NGF immunoreactivity was increased in RBCs, as well as in both GCL and other INL cells (arrowheads) of *E-reeler* retina. Therefore, the digital analysis carried out on these sections showed a 13.9% increase of NGF immunofluorescence in *E-reeler* retinas (32705 ± 2197 versus 27756 ± 1124 IntDen, resp., *E-reeler* versus E-control; $P < 0.05$). In line with this result, Western blot and the related OD measurements showed a 37.4% NGF increase (both 12 and 15 kDa bands) in the *E-reeler* ($P < 0.05$; Figure 2(b)). Finally, the molecular analysis of *E-reeler* mRNA extracts did not show a significant effect on NGF mRNA expression ($0.39_{2\,log}$ ratio; 7.21 ± 1.05 versus 7.43 ± 1.89 nCts, resp., *E-reeler* versus E-control; $P > 0.05$).

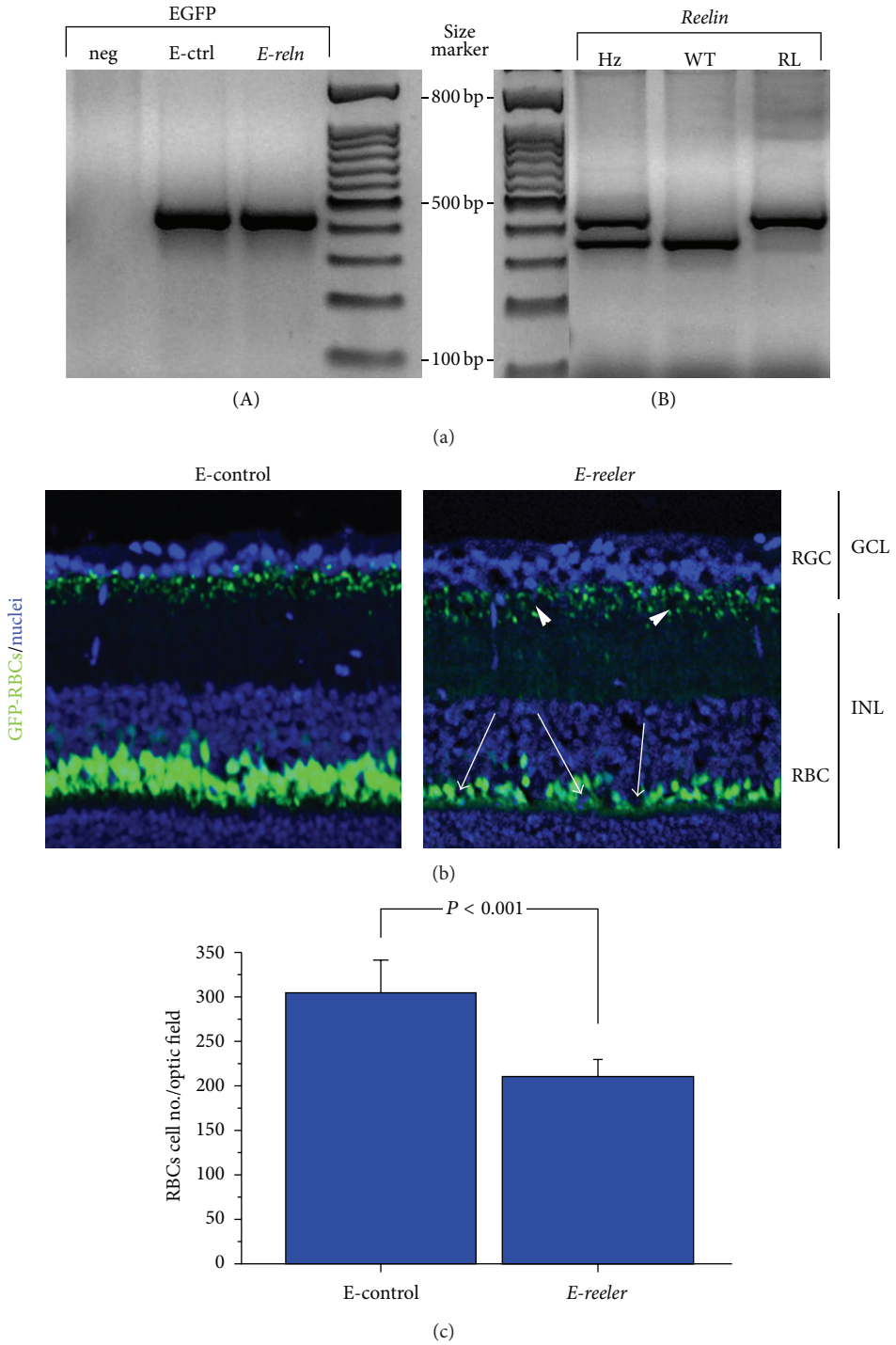

Figure 1: *E-reeler* model. (a) Agarose gel representative of EGFP and *Reelin* gene amplification. (A) EGFP expression in E-control (E-ctrl) and *E-reeler* (*E-reln*) tail genome, with respect to negative control (neg), not expressing GFP linked to L7-EGFP construct; (B) Reelin expression in control (WT), heterozygote (Hz), and *reeler* (Rl). The higher band (380 bps) represents *reeler* status while the lower one (280 bps) represents control rank. (b) Representative confocal microscopy image showing GFP-expressing RBCs (green) and nuclei stained with TOTO3-Iodide (blue). A decrease in the number of RBCs populating the INL is visible in *E-reeler* retina (arrows), as compared to E-control counterpart. Note the reduction of GFP-fluorescence of both the dendrite length and synapses (GFP staining) indicated by arrowheads in the *E-reeler* retinas (×400). (c) Number of GFP-bearing RBCs in *E-reeler* retinas, compared to the E-controls. Note the significant decrease of fluorescent cells ($P < 0.001$). Abbreviations: GFP, Green Fluorescent Protein; RGCs, Retinal Ganglion Cells; INL, Inner Nuclear Layer; RBCs, Rod Bipolar Cells.

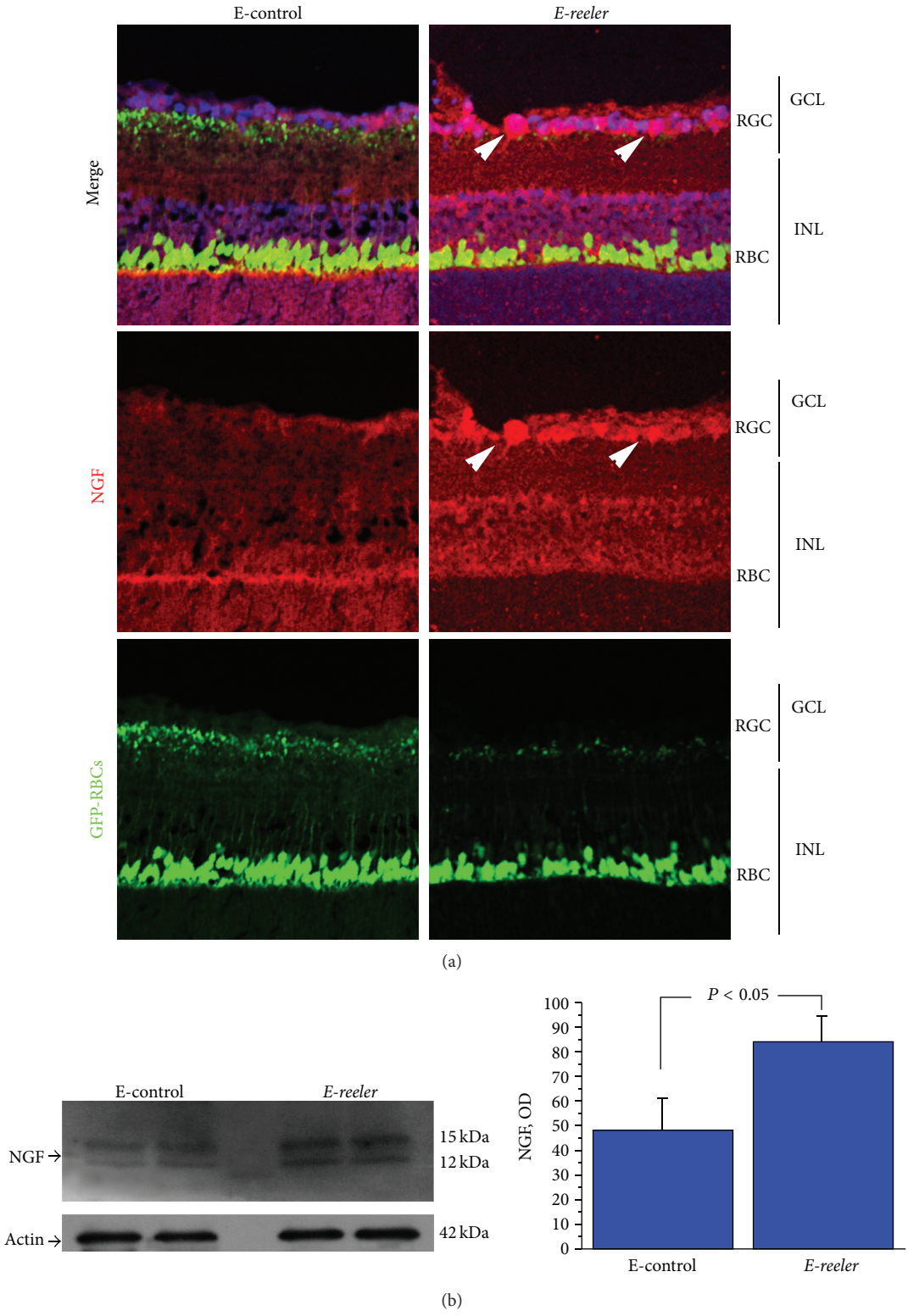

Figure 2: Expression of NGF in *E-reeler* retina. (a) Confocal microscopy showing images of GFP-expressing RBCs (green), NGF immunoreactivity (red), and nuclear staining (blue). As indicated by arrowheads, in the merge and NGF single staining, INL cells strongly immunoreacted with the NGF antibody. Some immunoreactivity was also observed in other structural and accessory cells (×400). (b) Representative 12% SDS-PAGE and relative densitometric analysis of E-control and *E-reeler* retinal extracts probed with the NGF antibody (OD values; $P < 0.05$). The size-marker was run between the two groups. Abbreviations: GCL, Ganglion Cell Layer; INL, Inner Nuclear Layer; RGCs, Retinal Ganglion Cells; RBCs, Rod Bipolar Cells; GFP, Green Fluorescent Protein; OD, Optical Density.

3.2. trkA^{NGFR} Expression. Since trkA^{NGFR} is widely considered the main NGF receptor involved in cell migration, proliferation, and differentiation, trkA^{NGFR} protein expression was investigated by probing both *E-reeler* and E-control retinas. As shown in Figure 3(a), trkA^{NGFR} immunoreactivity was detected in both the INL and GCL of control retinas (merge). A trend towards a 5.64% decrease of trkA^{NGFR} immunoreactivity was quantified in the RGCs of *E-reeler* retinas (22601 ± 2391 versus 23953 ± 1278 IntDen, resp., *E-reeler* versus E-control; $P > 0.05$). Accordingly, Western blot and OD analysis did not show any significant trkA^{NGFR} differences between the *E-reeler* versus the E-control protein extracts (Figure 3(b)). These results were corroborated by molecular analysis ($-0.14_{2\log}$ ratio; 17.04±1.81 versus 16.63± 0.54 nCts, resp., *E-reeler* versus E-control; $P > 0.05$).

3.3. p75^{NTR} Expression. Given that NGF binds to p75^{NTR}, the expression and localization of this glycoprotein were also investigated. In *E-reeler* retinas, p75^{NTR} immunoreactivity increased in RBCs, RGCs, and other INL populating cells, as highlighted by arrows in (Figure 4). Densitometric analysis quantified a 44.7% increase of p75^{NTR} immunoreactivity in the *E-reeler* retina (19587 ± 1916 versus 13539 ± 1368 IntDen, resp., *E-reeler* versus E-control; $P < 0.05$). In line, Western blot analysis coupled to densitometric quantification showed a significant 32.5% increase of p75^{NTR} in *E-reeler* protein extracts ($P < 0.05$; Figure 5(a)). The increased p75^{NTR} protein expression in *E-reeler* retinas was corroborated by real time PCR ($1.69_{2\log}$ ratio; 4.29 ± 1.77 versus 5.73 ± 3.22 nCts; *E-reeler* versus E-control; $P < 0.05$). The decrease of RBCs (GFP$^+$ cells) did not correlate significantly with the increase of p75^{NTR} immunoreactivity (OD), as detected by Kendall rank analysis between the *E-reeler* and E-control values (Tau = −0.308; $P > 0.05$). Interestingly, the trkA^{NGFR}/p75^{NTR} ratio (from nCts values) was decreased in *E-reeler* mice as compared to the E-controls, indicating a shift towards p75^{NTR} expression (Tau = 0.867; $P < 0.01$, Figure 5(b)).

4. Discussion

This study was undertaken to verify the NGF-trkA^{NGFR}/p75^{NTR} expression in retinas from *E-reeler* mice, a Reelin-deprived model showing severe structural and functional changes in the retina, alongside the severe central nervous system alterations. To date, no data are available on the NGF pathway in Reelin deficient retina.

Retinogenesis is driven by a milieu of soluble factors, synergizing to obtain the final well-organized synaptic circuitry [1, 8]. As observed in several experimental models, Reelin and NGF take part actively during retinogenesis and continue all over adulthood, contributing to retina homeostasis (synaptic plasticity) [1, 3, 7, 8]. Structural and functional changes in the retina have been detected in Reelin deficient mice, showing an altered distribution of RBCs (both cell malpositioning and reduced dendrite density) and impaired synaptic circuitry [1]. RGC apoptosis has been quantified upon chemical NGF deprivation, while the recovery of damaged structures and particularly NGF/trkA^{NGFR}-promoted RGC survival were observed upon the intraocular NGF injection, as observed in models of retinal degeneration (ischemia, glaucoma, and diabetes) [11, 26–28].

Since emerging data lead to a possible cross-talk between Reelin and NGF during retinogenesis and tissue remodeling, the well-characterized *reeler*-L7-EGFP model was developed (*E-reeler*) and Reelin-deprived retinas underwent NGF-trkA^{NGFR}/p75^{NTR} confocal microscopy and biomolecular characterization [16, 17]. The morphological analysis of *E-reeler* retina at P7-P35 showed structural changes characterized by altered arrangement and significant decrease of axon/dendrite density of residual RBCs (retina degeneration), in line with previous studies [1, 6, 8]. Ataxia and eating and survival difficulties were observed, and since the survival was highly reduced over P27 in the absence of appropriate management, the P21 was definitely selected for these studies. According to the digital analysis and the conventional cell-counting method, significant reductions in RBCs' soma, dendrites, and axons were quantified in *E-reeler* retina. This observation is in line with previous studies indicating that just RBCs represent the primary target of Reelin defect, even though both RBCs and RGCs express/react to Reelin [1, 5]. Since RBCs carry the signal from the rod photoreceptors to the RGCs (visual function), it is reasonable to hypothesize that RBCs defect might interfere with the physiological activity of RGCs in *E-reeler* retina.

The principal finding of this study is the significant increase of NGF all over *E-reeler* retina, mainly localized in the layers populated by RBCs (INL) and RGCs (GCL). Indeed, NGF immunoreactivity was greatly expressed in accessory/glial cells, representing certainly the main NGF source in the damaged neighbourhood [29–32]. The observation of increased NGF protein, not corroborated by the molecular data, might be explained as possible transcriptional/posttranscriptional regulations (differential regulation, stability, and degradation of mRNA). In line with the well-known NGF pleiotropic effects, this NGF increase might be explained as an endogenous compensatory response to Reelin deficiency, either to limit abnormal/impaired cell distribution or counteract undesired apoptosis [12, 26, 33].

The statement that NGF exerts multiple effects depending on the surface (co)receptor appearance strength suggests the potential contribution of trkA^{NGFR} and/or p75^{NTR} in this model. In the retina, p75^{NTR} privileges Müller glial cells while trkA^{NGFR} is mainly expressed by RGCs [30, 34]. While trkA^{NGFR} tasks in neuronal survival, growth, and synaptic modulation are well established, p75^{NTR} ones are still an open debate due to p75^{NTR}-trkA^{NGFR} coreceptor activity/complexity [15, 33, 35]. p75^{NTR} mediates a widespread range of cellular functions, depending on the cell-to-cell and/or cell-to-factor milieu as well as the repertoire of surface (co)receptors and can signal independently of trkA^{NGFR} [12, 36, 37]. In the nervous system, p75^{NTR} mediates neuronal survival by facilitating trkA^{NGFR} signal, increasing neuronal axon growth and reducing neuronal cell death [37–42]. As a second finding, a significant increase of p75^{NTR} and a trend towards

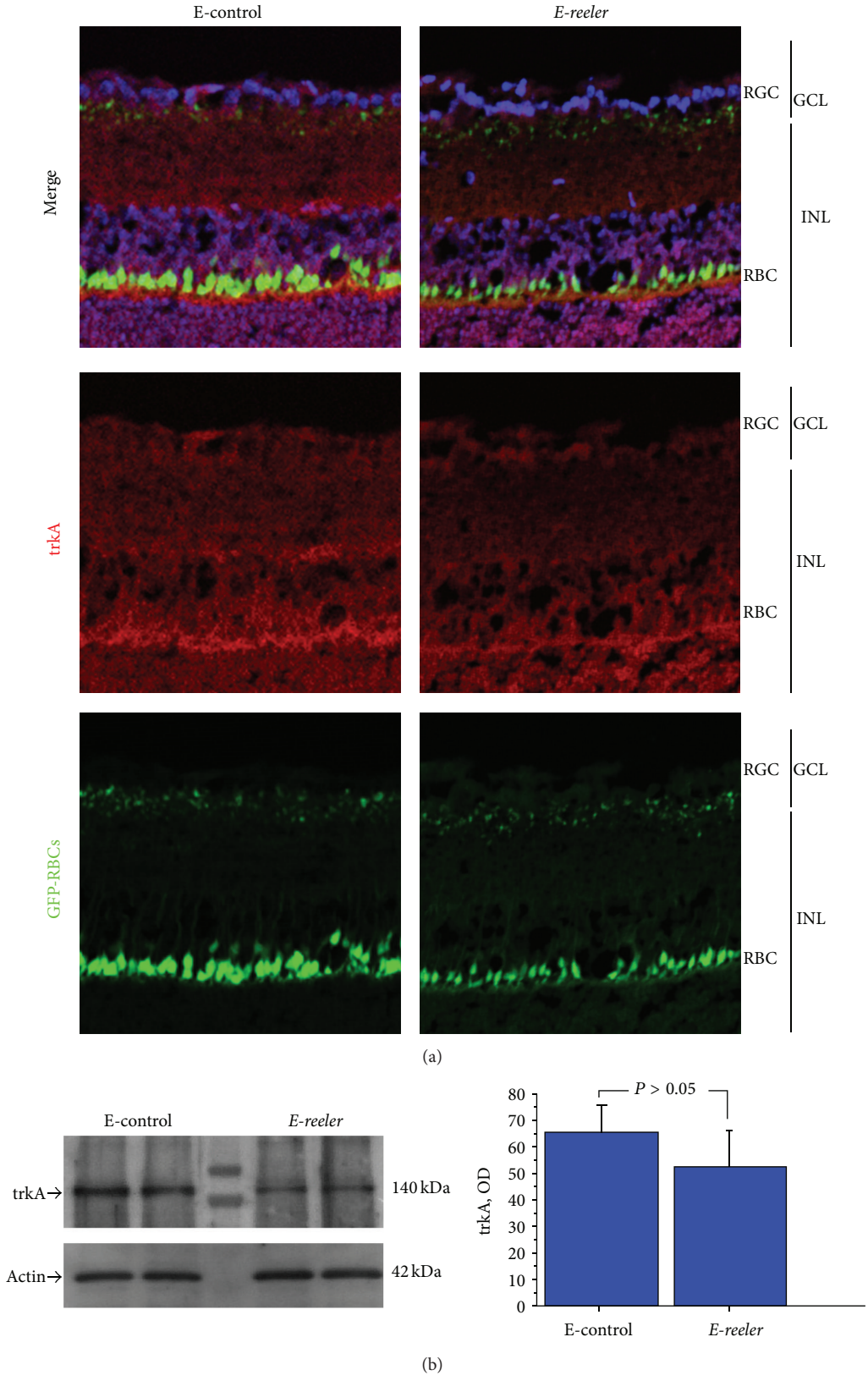

Figure 3: Expression of trkA^{NGFR} in *E-reeler* retina. (a) Confocal microscopy showing images of GFP-expressing RBCs (green), trkA^{NGFR} immunoreactivity (red), and nuclear staining (blue). A weak trkA^{NGFR} immunoreactivity was observed at the RBCs (body and dendrites). trkA^{NGFR} staining was less intense across the INL and in some cells inside the GCL of the *E-reeler* retina (×400). (b) Representative 7.5% SDS-PAGE and relative densitometric analysis of E-control and *E-reeler* retinal extracts probed with the trkA^{NGFR} antibody (OD values; $P > 0.05$). The size-marker was run between the two groups. Abbreviations: GFP, Green Fluorescent Protein; RGC, Retinal Ganglion Cells; GCL, Ganglion Cell Layer; INL, Inner Nuclear Layer; RBCs, Rod Bipolar Cells; OD, Optical Density.

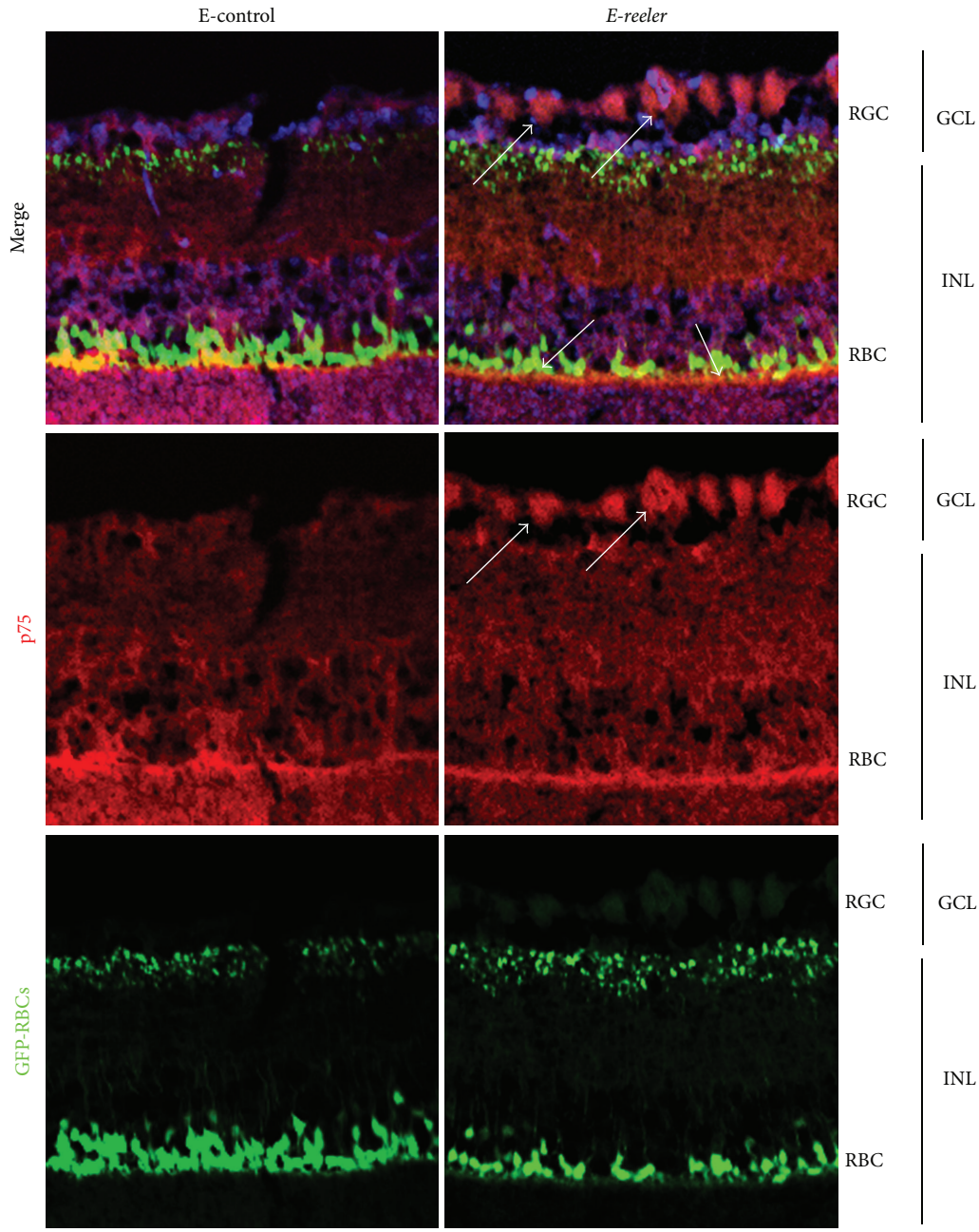

Figure 4: $p75^{NTR}$ localization in *E-reeler* retina. Confocal microscopy showing images of GFP-expressing RBCs (green), $p75^{NTR}$ immunoreactivity (red), and nuclear staining (blue). Arrows point to a noticeable staining of RGCs, RBCs, and accessories/glial cells localized in the GCL/INL of *E-reeler* retina. Note the intense cytoplasmatic $p75^{NTR}$ localization in both RGCs and RBCs. Abbreviations: GFP, Green Fluorescet Protein; GCL, Ganglion Cell Layer; INL, Inner Nuclear Layer; RGCs, Retinal Ganglion Cells; RBCs, Rod Bipolar Cells (×400).

a decrease of $trkA^{NGFR}$ were observed in *E-reeler* retina, as detected by confocal microscopy, Western blot, and real time PCR analysis. Interestingly, $p75^{NTR}$ was mainly localised in RBCs and cells populating the GCL, either RGCs or accessory ones. In particular for GCL, whether $p75^{NTR}$ is expressed by immature/migrating or mature/positioned RGCs during retinogenesis (or in adult retina) remains to be verified, as accessory cells processed tightly surround RGCs [28, 42, 43]. This $p75^{NTR}$ expression would imply that NGF from RGCs and nearby accessory cells might promote the survival of interneurons (and likewise RBCs) via NGF/$p75^{NTR}$-dependent mechanism, favouring a "rescue response" in an autocrine/paracrine fashion [11, 27, 28, 39]. The contribution of $p75^{NTR}$ in the regulation of RBCs survival has been reported in an experiment of exposure to NGF, BDNF, or Neurotrophin 3 [44]. Therefore, the possibility that $p75^{NTR}$ might exert the herein reported actions through other growth factors cannot be excluded [12, 27].

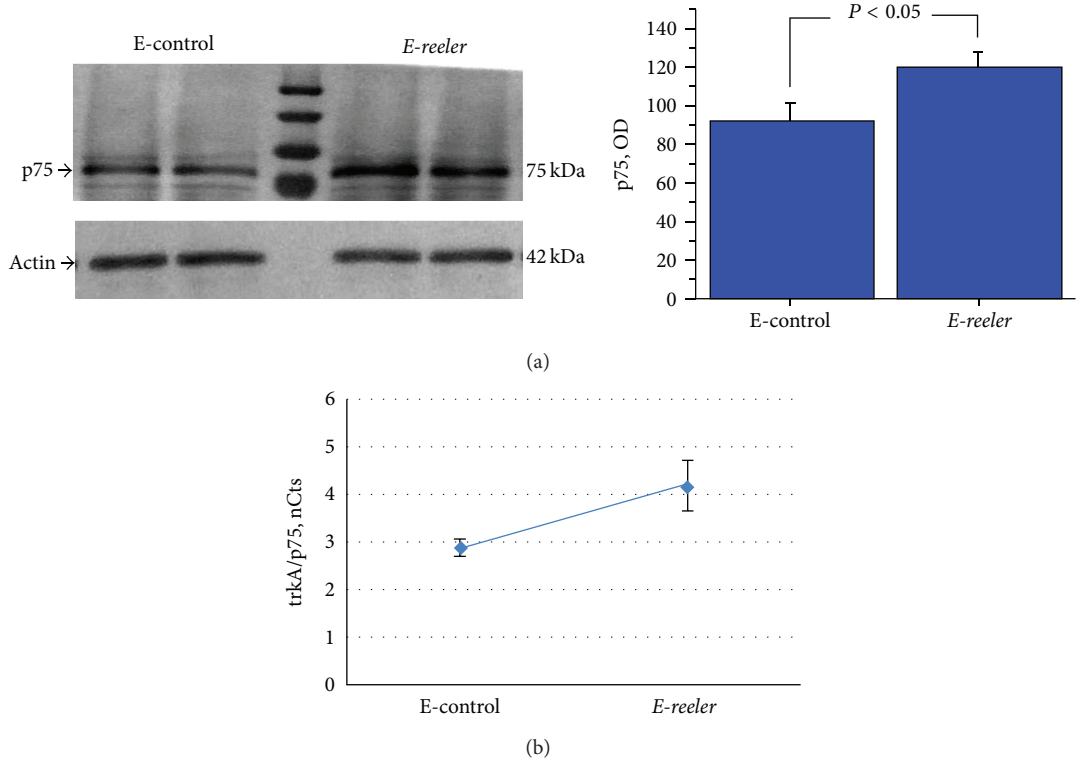

FIGURE 5: $p75^{NTR}$ expression in *E-reeler* retina. (a) Representative 7.5% SDS-PAGE and relative densitometric analysis (OD values; $P < 0.05$), probed with $p75^{NTR}$ antibodies, showing a significant increase of $p75^{NTR}$ in *E-reeler* protein extracts, as compared to the E-control. (b) Scatter plot showing the correlation with the $trkA^{NGFR}/p75^{NTR}$ ratio in the *E-reeler* versus E-control, highlighting a shift towards $p75^{NTR}$ expression (Tau = 0.857; $P < 0.01$).

An attempt for cytoskeleton reorganization might be also prospected for NGF and $p75^{NTR}$ overexpression, since $p75^{NTR}$ is strictly required for appropriate axonal morphology/outgrowth and cell migration [38]. Actin reorganization and cell migration as well as neurite outgrowth are common properties of both NGF and Reelin [1, 4–7, 26, 27]. As reported, the loss of RGCs might be an outcome of the reduced crosstalk with the RBCs (synapses decline) [1]. NGF overexpression in RGCs or accessory/Müller cells might be also viewed as an attempt to stimulate RBC dendrites/arbors elongation, to (re)establish synaptic connections, or to provide a gradient for new dendrites [45–48]. As a support, $p75^{NTR}$ binds both pro/mature forms of NGF and other neurotrophins (NTs, BDNF, NT3, and NT5), takes part in retrograde axonal transport of NTs (as survival or apoptotic factor), and works as a shuttle molecule for BDNF and NT4 (RBC survival NTs) [44, 49]. As reported, NGF pathway contributes to the cytoskeleton reorganization, at least in structural cells as myofibroblasts [50].

By the way, the selective shift toward $p75^{NTR}$ expression does not exclude the potential contribution of $trkA^{NGFR}$ signalling. As reported, $p75^{NTR}$ acts as neuroprotective molecule, and $trkA^{NGFR}$ might work as a death receptor [43, 51]. Upon NGF exposure, both homo- and heterodimerizations of membrane bound $trkA^{NGFR}$ and $p75^{NTR}$ occur on receptive cells, and the ultimate signalling response is the result of some predominant cascade pathways [12, 13]. The dogma "$trkA^{NGFR}$ mediates survival while $p75^{NTR}$ triggers apoptosis" is strictly dependent on the cell type, microenvironment, and $trkA^{NGFR}/p75^{NTR}$ surface-expression ratio [12, 15]. In line with our finding, a possible role of $trkA^{NGFR}/p75^{NTR}$ ratio in determining the fate of RBCs and RGCs might be prospected, as supported by studies on degeneration rescue [11, 14, 15]. Therefore the $p75^{NTR}$ increase in RGCs and RBCs might also be interpreted as a proapoptotic effect. Studies aimed at verifying/quantifying apoptosis of RGC and/or RBC are actually under investigation.

As widely reported, a milieu of soluble factors synergize to allow for the correct position and functional activity of the RGCs, amacrine cells, RBCs, horizontal cells, Müller glial cells, and rod/cone photoreceptors during retinogenesis [8, 52]. The possibility that upon Reelin deprivation other factors (cytokines and growth and angiogenic factors) might be upregulated to offset or facilitate the entire process cannot be excluded. Beside NGF, several other factors (such as BDNF, NT4, and GDNF) have been reported to increase RGC survival and regeneration [44, 53]. These activities might be direct or indirect as observed for NGF-$p75^{NTR}$-induced TNF-α and TGF-β activities in developing retina [54].

Any attempt to comprehend the mechanism underlying the pathogenesis of some retinal disorders represents a step forward in ophthalmology field characterized by

severe, invalidating, and life-threatening diseases (glaucoma, ischemia, retinopathies, etc.). One of the major challenges of current eye-disease research is to develop models that mimic eyes pathologies, useful tools for studying cell-to-cell and cell-to-mediator mechanisms and providing the basis for novel therapeutic approaches to offset retinal degeneration. Despite recent advances, a clear comprehension of the mechanism underlying retinopathies is still needed and might require the understanding of some "missing" aspects during retinogenesis. For several decades, the *reeler* mutant has been used as a model for studying neurological disorders [1, 16]. In line with recent and the herein presented data, we propose *E-reeler* mice as a good "retinal disease" model to explore the cross-talk between NGF and Reelin [16, 17]. Growing data indicate that NGF provides a potential approach in the treatment of retinopathies, characterized by RGCs death and following optic nerve degeneration [2, 3, 10, 11]. Studies are underway to discriminate $p75^{NTR}$-induced cell rescue or apoptosis and characterize the proNGF/NGF expression. These studies will contribute to better understanding of the relationship between NGF and Reelin in the retina under normal and pathological conditions.

Conflict of Interests

The authors declare that there is no conflict of interests regarding the publication of this paper.

Acknowledgments

This work was partially supported by the Italian Minister of Health to IRCCS-Bietti and the Italian Ministry of Education to UCBM (PRIN 2009P9CE2R). The authors are grateful to Professor Marco Centofanti, Glaucoma Research Unit ("Tor Vergata" University, Rome, Italy), for suggestions during the preparation of the paper. The study was partially presented at the annual meeting of the Association for Research in Vision and Ophthalmology, Fort Lauderdale, FL, May 2012 (E-Abstract).

References

[1] D. S. Rice, S. Nusinowitz, A. M. Azimi, A. Martínez, E. Soriano, and T. Curran, "The Reelin pathway modulates the structure and fof retinal synaptic circuitry," *Neuron*, vol. 31, no. 6, pp. 929–941, 2001.

[2] G. Carmignoto, M. C. Comelli, P. Candeo et al., "Expression of NGF receptor and NGF receptor mRNA in the developing and adult rat retina," *Experimental Neurology*, vol. 111, no. 3, pp. 302–311, 1991.

[3] N. Berardi and L. Maffei, "From visual experience to visual function: roles of neurotrophins," *Journal of Neurobiology*, vol. 41, no. 1, pp. 119–126, 1999.

[4] E. Förster, H. H. Bock, J. Herz, X. Chai, M. Frotscher, and S. Zhao, "Emerging topics in Reelin function," *European Journal of Neuroscience*, vol. 31, no. 9, pp. 1511–1518, 2010.

[5] J. H. Trotter, M. Klein, U. K. Jinwal et al., "ApoER2 function in the establishment and maintenance of retinal synaptic connectivity," *Journal of Neuroscience*, vol. 31, no. 40, pp. 14413–14423, 2011.

[6] G. D'Arcangelo, "The role of the Reelin pathway in cortical development," *Symposia of the Society for Experimental Biology*, no. 53, pp. 59–73, 2001.

[7] J. S. Pulido, I. Sugaya, J. Comstock, and K. Sugaya, "Reelin expression is upregulated following ocular tissue injury," *Graefe's Archive for Clinical and Experimental Ophthalmology*, vol. 245, no. 6, pp. 889–893, 2007.

[8] M. Frotscher, "Role for Reelin in stabilizing cortical architecture," *Trends in Neurosciences*, vol. 33, no. 9, pp. 407–414, 2010.

[9] R. Levi-Montalcini, "The nerve growth factor 35 years later," *Science*, vol. 237, no. 4819, pp. 1154–1162, 1987.

[10] M. V. Sofroniew, C. L. Howe, and W. C. Mobley, "Nerve growth factor signaling, neuroprotection, and neural repair," *Annual Review of Neuroscience*, vol. 24, pp. 1217–1281, 2001.

[11] G. Carmignoto, L. Maffei, P. Candeo, R. Canella, and C. Comelli, "Effect of NGF on the survival of rat retinal ganglion cells following optic nerve section," *Journal of Neuroscience*, vol. 9, no. 4, pp. 1263–1272, 1989.

[12] A. Micera, A. Lambiase, B. Stampachiacchiere, S. Bonini, S. Bonini, and F. Levi-Schaffer, "Nerve growth factor and tissue repair remodeling: $trkA^{NGFR}$ and $p75^{NTR}$, two receptors one fate," *Cytokine and Growth Factor Reviews*, vol. 18, no. 3-4, pp. 245–256, 2007.

[13] M. V. Chao and B. L. Hempstead, "p75 and Trk: a two-receptor system," *Trends in Neurosciences*, vol. 18, no. 7, pp. 321–326, 1995.

[14] V. Colafrancesco, M. Coassin, S. Rossi, and L. Aloe, "Effect of eye NGF administration on two animal models of retinal ganglion cells degeneration," *Annali dell'Istituto Superiore di Sanita*, vol. 47, no. 3, pp. 284–289, 2011.

[15] Y. Bai, P. Dergham, H. Nedev et al., "Chronic and acute models of retinal neurodegeneration TrkA activity are neuroprotective whereas $p75^{NTR}$ activity is neurotoxic through a paracrine mechanism," *The Journal of Biological Chemistry*, vol. 285, no. 50, pp. 39392–39400, 2010.

[16] K. Matsui, S. Furukawa, H. Shibasaki, and T. Kikuchi, "Reduction of nerve growth factor level in the brain of genetically ataxic mice (weaver, reeler)," *FEBS Letters*, vol. 276, no. 1-2, pp. 78–80, 1990.

[17] A. M. Betancourt, S. C. Burgess, and R. L. Carr, "Effect of developmental exposure to chlorpyrifos on the expression of neurotrophin growth factors and cell-specific markers in neonatal rat brain," *Toxicological Sciences*, vol. 92, no. 2, pp. 500–506, 2006.

[18] L. Silver, *Mouse Genetics Concepts and Application*, Oxford University Press, New York, NY, USA, 1995.

[19] M. Tomomura, D. S. Rice, J. I. Morgan, and M. Yuzaki, "Purification of Purkinje cells by fluorescence-activated cell sorting from transgenic mice that express green fluorescent protein," *European Journal of Neuroscience*, vol. 14, no. 1, pp. 57–63, 2001.

[20] J. Oberdick, R. J. Smeyne, J. R. Mann, S. Zackson, and J. I. Morgan, "A promoter that drives transgene expression in cerebellar Purkinje and retinal bipolar neurons," *Science*, vol. 248, no. 4952, pp. 223–226, 1990.

[21] G. D'Arcangelo, G. G. Miao, and T. Curran, "Detection of the reelin breakpoint in reeler mice," *Molecular Brain Research*, vol. 39, no. 1-2, pp. 234–236, 1996.

[22] M. Coassin, A. Lambiase, V. Sposato, A. Micera, S. Bonini, and L. Aloe, "Retinal p75 and bax overexpression is associated with

retinal ganglion cells apoptosis in a rat model of glaucoma," *Graefe's Archive for Clinical and Experimental Ophthalmology*, vol. 246, no. 12, pp. 1743–1749, 2008.

[23] A. Micera, I. Puxeddu, A. Lambiase et al., "The pro-fibrogenic effect of nerve growth factor on conjunctival fibroblasts is mediated by transforming growth factor-β," *Clinical and Experimental Allergy*, vol. 35, no. 5, pp. 650–656, 2005.

[24] M. W. Pfaffl, "A new mathematical model for relative quantification in real-time RT-PCR," *Nucleic Acids Research*, vol. 29, no. 9, article e45, 2001.

[25] R. R. Wilcox, "Understanding the practical advantages of modern ANOVA methods," *Journal of Clinical Child and Adolescent Psychology*, vol. 31, no. 3, pp. 399–412, 2002.

[26] X. Sun, X. Xu, F. Wang et al., "Effects of nerve growth factor for retinal cell survival in experimental retinal detachment," *Current Eye Research*, vol. 32, no. 9, pp. 765–772, 2007.

[27] A. Lambiase, M. Centofanti, A. Micera et al., "Nerve growth factor (NGF) reduces and NGF antibody exacerbates retinal damage induced in rabbit by experimental ocular hypertension," *Graefe's Archive for Clinical and Experimental Ophthalmology*, vol. 235, no. 12, pp. 780–785, 1997.

[28] C. Harada, T. Harada, K. Nakamura, Y. Sakai, K. Tanaka, and L. F. Parada, "Effect of p75NTR on the regulation of naturally occurring cell death and retinal ganglion cell number in the mouse eye," *Developmental Biology*, vol. 290, no. 1, pp. 57–65, 2006.

[29] Y. S. Kim, D. H. Jo, H. Lee, J. H. Kim, K. W. Kim, and J. H. Kim, "Nerve growth factor-mediated vascular endothelial growth factor expression of astrocyte in retinal vascular development," *Biochemical and Biophysical Research Communications*, vol. 431, no. 4, pp. 740–745, 2013.

[30] F. Lebrun-Julien, B. Morquette, A. Douillette, H. U. Saragovi, and A. Di Polo, "Inhibition of $p75^{NTR}$ in glia potentiates TrkA-mediated survival of injured retinal ganglion cells," *Molecular and Cellular Neuroscience*, vol. 40, no. 4, pp. 410–420, 2009.

[31] R. A. de Melo Reis, M. E. C. Cabral-da-Silva, F. G. de Mello, and J. S. H. Taylor, "Müller glia factors induce survival and neuritogenesis of peripheral and central neurons," *Brain Research*, vol. 1205, pp. 1–11, 2008.

[32] M. Karlsson, R. Mayordomo, L. F. Reichardt, S. Catsicas, H. J. Karten, and F. Hallböök, "Nerve growth factor is expressed by postmitotic avian retinal horizontal cells and supports their survival during development in an autocrine mode of action," *Development*, vol. 128, no. 4, pp. 471–479, 2001.

[33] M. Rydén, B. Hempstead, and C. F. Ibáñez, "Differential modulation of neuron survival during development by nerve growth factor binding to the p75 neurotrophin receptor," *The Journal of Biological Chemistry*, vol. 272, no. 26, pp. 16322–16328, 1997.

[34] S. O. Yoon, P. Casaccia-Bonnefil, B. Carter, and M. V. Chao, "Competitive signaling between TrkA and p75 nerve growth factor receptors determines cell survival," *Journal of Neuroscience*, vol. 18, no. 9, pp. 3273–3281, 1998.

[35] P. A. Barker and E. M. Shooter, "Disruption of NGF binding to the low affinity neurotrophin receptor p75(LNTR) reduces NGF binding to TrkA on PC12 cells," *Neuron*, vol. 13, no. 1, pp. 203–215, 1994.

[36] D. Esposito, P. Patel, R. M. Stephens et al., "The cytoplasmic and transmembrane domains of the p75 and Trk A receptors regulate high affinity binding to nerve growth factor," *The Journal of Biological Chemistry*, vol. 276, no. 35, pp. 32687–32695, 2001.

[37] G. L. Barrett and P. F. Bartlett, "The p75 nerve growth factor receptor mediates survival or death depending on the stage of sensory neuron development," *Proceedings of the National Academy of Sciences of the United States of America*, vol. 91, no. 14, pp. 6501–6505, 1994.

[38] K. Lee, K. Bachman, S. Landis, and R. Jaenisch, "Dependence on p75 for innervation of some sympathetic targets," *Science*, vol. 263, no. 5152, pp. 1447–1449, 1994.

[39] C. A. Bentley and K. F. Lee, "p75 is important for axon growth and Schwann cell migration during development," *Journal of Neuroscience*, vol. 20, no. 20, pp. 7706–7715, 2000.

[40] R. T. Dobrowsky and B. D. Carter, "p75 neurotrophin receptor signaling: mechanisms for neurotrophic modulation of cell stress?" *Journal of Neuroscience Research*, vol. 61, no. 3, pp. 237–243, 2000.

[41] T. Yamashita, K. L. Tucker, and Y. A. Barde, "Neurotrophin binding to the p75 receptor modulates Rho activity and axonal outgrowth," *Neuron*, vol. 24, no. 3, pp. 585–593, 1999.

[42] M. F. DeFreitas, P. S. McQuillen, and C. J. Shatz, "A novel $p75^{NTR}$ signaling pathway promotes survival, not death, of immunopurified neocortical subplate neurons," *Journal of Neuroscience*, vol. 21, no. 14, pp. 5121–5129, 2001.

[43] B. Hu, H. K. Yip, and K. F. So, "Expression of p75 neurotrophin receptor in the injured and regenerating rat retina," *NeuroReport*, vol. 10, no. 6, pp. 1293–1297, 1999.

[44] A. Bosco and R. Linden, "BDNF and NT-4 differentially modulate neurite outgrowth in developing retinal ganglion cells," *Journal of Neuroscience Research*, vol. 57, no. 6, pp. 759–769, 1999.

[45] R. S. Aloyz, S. X. Bamji, C. D. Pozniak et al., "P53 is essential for developmental neuron death as regulated by the TrkA and p75 neurotrophin receptors," *Journal of Cell Biology*, vol. 143, no. 6, pp. 1691–1703, 1998.

[46] A. Cohen, G. M. Bray, and A. J. Aguayo, "Neurotrophin-4/5 (NT-4/5) increases adult rat retinal ganglion cell survival and neurite outgrowth in vitro," *Journal of Neurobiology*, vol. 25, no. 8, pp. 953–959, 1994.

[47] Y. J. Chang, C. M. Hsu, C. H. Lin, M. S. Lu, and L. Chen, "Electrical stimulation promotes nerve growth factor-induced neurite outgrowth and signaling," *Biochimica Et Biophysica Acta*, vol. 1830, no. 8, pp. 4130–4136, 2013.

[48] C. Radtke, H. O. Rennekampff, K. Reimers, P. M. Vogt, and J. D. Kocsis, "Paracrine loop of keratinocyte proliferation and directed neuritic outgrowth in a neuroepithelial coculture," *Annals of Plastic Surgery*, vol. 70, no. 2, pp. 162–167, 2013.

[49] B. D. Carter and G. R. Lewint, "Neurotrophins live or let die: does p75(NTR) decide?" *Neuron*, vol. 18, no. 2, pp. 187–190, 1997.

[50] A. Micera, I. Puxeddu, B. O. Balzamino, S. Bonini, and F. Levi-Schaffer, "Chronic nerve growth factor exposure increases apoptosis in a model of in vitro induced conjunctival myofibroblasts," *PLoS ONE*, vol. 7, no. 10, Article ID e47316, 2012.

[51] E. M. Wexler, O. Berkovich, and S. Nawy, "Role of the low-affinity NGF receptor (p75) in survival of retinal bipolar cells," *Visual Neuroscience*, vol. 15, no. 2, pp. 211–218, 1998.

[52] C. L. Cepko, C. P. Austin, X. Yang, M. Alexiades, and D. Ezzeddine, "Cell fate determination in the vertebrate retina," *Proceedings of the National Academy of Sciences of the United States of America*, vol. 93, no. 2, pp. 589–595, 1996.

[53] Q. Yan, J. Wang, C. R. Matheson, and J. L. Urich, "Glial cell line-derived neurotrophic factor (GDNF) promotes the survival of axotomized retinal ganglion cells in adult rats: comparison

to and combination with brain-derived neurotrophic factor (BDNF)," *Journal of Neurobiology*, vol. 38, no. 3, pp. 382–390, 1999.

[54] F. Lebrun-Julien, M. J. Bertrand, O. de Backer et al., "ProNGF induces TNFα-dependent death of retinal ganglion cells through a $p75^{NTR}$ non-cell-autonomous signaling pathway," *Proceedings of the National Academy of Sciences of the United States of America*, vol. 107, no. 8, pp. 3817–3822, 2010.

Hindawi Publishing Corporation
International Journal of Cell Biology
Volume 2014, Article ID 473857, 7 pages
http://dx.doi.org/10.1155/2014/473857

Review Article

LncRNAs: New Players in Apoptosis Control

Marianna Nicoletta Rossi[1] and Fabrizio Antonangeli[2]

[1] *Pasteur Institute-Fondazione Cenci Bolognetti, Department of Cellular Biotechnologies and Hematology, Sapienza University of Rome, Viale Regina Elena 324, 00161 Rome, Italy*
[2] *Pasteur Institute-Fondazione Cenci Bolognetti, Department of Molecular Medicine, Sapienza University of Rome, Viale Regina Elena 291, 00161 Rome, Italy*

Correspondence should be addressed to Fabrizio Antonangeli; fabrizio.antonangeli@uniroma1.it

Received 11 October 2013; Accepted 22 November 2013; Published 30 January 2014

Academic Editor: Claudia Giampietri

The discovery that the mammalian genome is largely transcribed and that almost half of the polyadenylated RNAs is composed of noncoding RNAs has attracted the attention of the scientific community. Growing amount of data suggests that long noncoding RNAs (lncRNAs) are a new class of regulators involved not only in physiological processes, such as imprinting and differentiation, but also in cancer progression and neurodegeneration. Apoptosis is a well regulated type of programmed cell death necessary for correct organ development and tissue homeostasis. Indeed, cancer cells often show an inhibition of the apoptotic pathways and it is now emerging that overexpression or downregulation of different lncRNAs in specific types of tumors sensitize cancer cells to apoptotic stimuli. In this review we summarize the latest studies on lncRNAs and apoptosis with major attention to those performed in cancer cells and in healthy cells upon differentiation. We discuss the new perspectives of using lncRNAs as targets of anticancer drugs. Finally, considering that lncRNA levels have been reported to have a correlation with specific cancer types, we argue the possibility of using lncRNAs as tumor biomarkers.

1. Introduction

Apoptosis is the most common type of programmed cell death by which the body eliminates damaged or exceeding cells without local inflammation. Thus, functional apoptotic pathways are essential for organ development and tissue homeostasis. DNA damage or growth factor's withdrawal can induce apoptosis through the socalled intrinsic pathway by the release of cytochrome c and other proteins from the intermembranous space of mitochondria [1]. Alternatively, the socalled extrinsic apoptotic pathway is triggered by the activation of specific death receptors on the cellular membrane [2]. Accordingly, deregulation of apoptosis is implicated in a wide range of diseases. Low rate of apoptosis can promote the survival and accumulation of abnormal cells, leading to cancer development or autoimmune disease [3, 4]. On the other hand, increased levels of apoptosis are associated with neurodegenerative diseases, characterized by progressive neuronal death, or with acute pathologies such as cardiac ischemia [5, 6]. During last years, much effort has been spent to study and possibly control apoptosis in pathological conditions. To this aim it is of fundamental importance to understand the molecular pathways and cellular stimuli that regulate and trigger apoptosis.

Genomic studies conducted in the past decades highlighted the presence of a large amount of DNA that is transcribed but not translated, leading to the formation of RNAs that do not code for proteins (noncoding RNAs) [7–9]. Some of these RNAs are associated with the translational machinery, such as ribosomal and transfer RNAs, but for many others a key role in the regulation of cell fate has been demonstrated [10, 11]. This class of regulatory RNAs includes not only the well-known microRNAs (miRNAs) but also an heterogenous group of socalled long noncoding RNAs (lncRNAs).

LncRNAs can be very different in size, ranging from 340 nucleotides of 7SK to 118 kb of Airn. They can be transcribed by RNA polymerase II or III, they can be either spliced or

not, and localized either in the nucleus or in the cytoplasm. On the basis of the position of their genes they can be divided in long intergenic noncoding RNAs (lincRNAs) and in antisense RNAs (asRNAs) if they are transcribed from the minus strand of an open reading frame (for a review on lncRNA classification see [12]).

Regarding their functions, many nuclear lncRNAs are directly involved in gene expression control and several mechanisms of action have been demonstrated so far. Some lncRNAs act as downregulators of gene expression recruiting gene silencing complexes such as PRC1 and PRC2 to the promoters of target genes. This mechanism of action has been described for the well-known regulator of imprinting Xist that remains tethered to its site of transcription [13] and for HOTAIR that instead acts in *trans* [14]. Other lncRNAs, such as GAS5, act as decoy precluding the access of regulatory proteins to DNA [15]. Some lncRNAs modify the activity of DNA binding proteins changing the expression of target genes (e.g., CCND1) [16]. In the cytoplasm, lncRNAs have been described to modulate mRNA stability, for example, by duplexing with the 3′ UTRs [17], or to act as miRNA decoy, as it has been demonstrated for lincMD1 that sponges miRNA-133 and miRNA-135 during muscle differentiation [18].

Through those different mechanisms of action, lncRNAs are involved in the regulation of different aspects of both cell physiology and pathology, such as imprinting [19], maintenance of pluripotency [20], and cancer [21]. Indeed, the emerging view from recent studies and transcriptome analysis is that lncRNAs are often deregulated in cancer cells compared to normal cells, thus suggesting to exploit lncRNAs as potential cancer markers. Furthermore, their modulation (overexpression or downregulation according to the specific lncRNA) in cancer cells often induces apoptosis or sensitizes cells to apoptotic treatments, suggesting that lncRNAs can be considered, at least for some cancer types, as therapeutic targets. This review focuses on the role of lncRNAs in the apoptosis processes with particular attention to the studies performed on cancer cell lines and tissues.

2. Regulation of the Tumor Suppressor Genes *PTEN* and *p53* by lncRNAs

PTEN and *p53* are two of the most studied tumor suppressor genes and both of them have well described antiproliferative and proapoptotic activity [22, 23]. PTEN is able to induce apoptosis through the AKT/PI3 K pathway [24] and is epigenetically silenced in several cancers [25]. In 2010, Poliseno and colleagues demonstrated that PTEN mRNA is regulated by PTEN pseudogene1 (PTENpg1), a lncRNA that sequesters numerous PTEN-targeting miRNAs by acting as miRNA sponge [26]. Moreover, Johnsson and colleagues demonstrated the presence of two antisense transcripts from the *PTENpg1* gene, adding another level of complexity to the transcriptional and posttranscriptional regulation of PTEN [27]. In detail, one antisense transcript, the isoform α (PTENpg1 asRNAα) directly binds PTEN promoter and represses the transcription of the gene (Figure 1(a)), while the isoform β stabilizes and facilitates the export in the cytoplasm of PTENpg1, enhancing its role of miRNA sponge and thus increasing PTEN mRNA stability and translation (Figure 1(b)). Accordingly, suppression of PTENpg1 asRNAα sensitizes cells to the DNA damaging agent doxorubicin. This mechanism results in both transcriptional and posttranscriptional regulation of PTEN by its pseudogene.

p53 is a well-known tumor suppressor that regulates many cellular processes including DNA repair, cell cycle progression, and apoptosis [22]. Consistently with its importance, p53 expression is subjected to different levels of regulation: transcriptional, posttranscriptional, and translational. It was recently demonstrated another level of regulation for p53 by lincRNA-RoR (RoR) [28]. In particular, after DNA damage stimuli, ectopic overexpression of RoR was shown to downregulate p53 accumulation leading to decreased levels of apoptosis, as evaluated by TUNEL assay. The authors claim that RoR acts on newly synthesized p53 interacting with the RNA binding protein hnRNP I (Figure 1(c)). In addition, the authors also demonstrated a regulative feedback loop as p53 induces the transcription of RoR (Figure 1(c)).

3. LncRNAs Involved in Apoptosis of Cancer Cells

Several recent studies described an altered expression pattern of specific lncRNAs in cancer cells when compared with normal cells and tissues. Some of them reported lncRNAs being negative regulators of apoptosis in different types of tumors (Table 1). For example, AFAP1-AS1, a lncRNA derived from the antisense strand of the *AFAP1* coding gene locus, was shown to be hypomethylated and upregulated in esophageal adenocarcinoma tissues and cell lines [29]. Its silencing by small interfering RNA (siRNA) was reported to induce apoptosis in the esophageal adenocarcinoma OE-33 cell line, considering both annexin V flow cytometry assay and caspase-3 cleavage by Western blot. Cell cycle analysis was also performed after siRNA treatment revealing that knockdown of AFAP1-AS1 induces G2/M-phase arrest. Taken together these findings suggest that AFAP1-AS1 can modulate both proliferation and programmed cell death in esophageal cancer cells.

Similar findings were reported by Khaitan and colleagues in melanoma cells [30]. Melanoma is the most common skin cancer and the authors reported the upregulation of the lncRNA SPRY4-IT1 in melanoma cells in comparison to melanocytes and keratinocytes. SPRY4-IT1 is transcribed from the second intron of the *SPRY4* gene and the two transcripts share similar expression profile, suggesting they may either be transcribed independently from the same promoter or, alternatively, they may be transcribed as a single transcript with SPRY4-IT1 then being processed from the intron of SPRY4. The effects of SPRY4-IT1 knockdown on cell death was investigated in the melanoma cell line WM1552C. The authors showed an increase of annexin V positive cells, while no differences were observed in propidium iodide-positive cells, indicating that the knockdown of SPRY4-IT1 induces cell death primarily through apoptosis and not necrosis. Interestingly, the main subcellular localization of

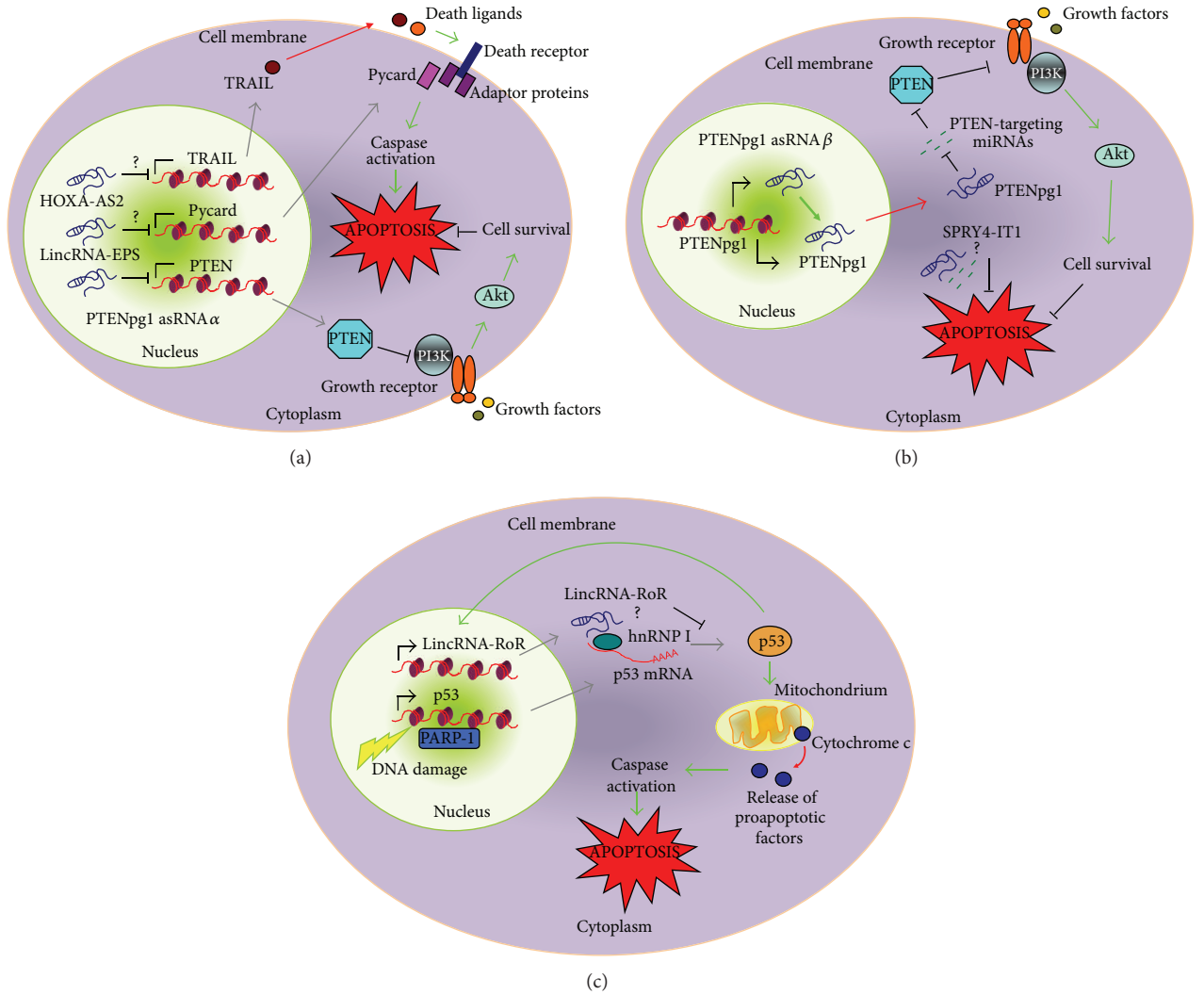

Figure 1: Schematic view of the different mechanisms through which lncRNAs can modulate apoptosis. (a) Transcriptional inhibition, as reported for PTENpg1 asRNA and proposed for HOXA-AS2 and LincRNA-EPS towards *PTEN*, *TRAIL*, and *Pycard* genes, respectively. (b) miRNA sponge. PTENpg1 can function as decoy for PTEN mRNA-targeting miRNAs; similar mechanism has been supposed for SPRY4-IT1. (c) Inhibition of mRNA translation. LincRNA-RoR has been hypothesized to interact with the mRNA binding protein hnRNP1 modulating the translation of p53 mRNA. L-bar arrows indicate gene transcription; T-bar arrows indicate negative regulation; green arrows indicate positive regulation; red arrows indicate release/translocation; grey arrows indicate mRNA translocation/translation; and ? indicates a supposed mechanism.

SPRY4-IT1 was reported to be cytoplasmic and on the basis of its localization the authors speculate that SPRY4-IT1 could function as a sponge for proteins or RNAs as reported for other cytoplasmic lncRNAs (see Section 1) (Figure 1(b)).

In prostate cancer cell lines and tissues, Cui and colleagues reported the overexpression of the lncRNA PlncRNA-1 [31]. Upregulated genes in cancer cells often play a role in tumor survival and progression and accordingly the knockdown of PlncRNA-1 by siRNA was shown to induce apoptosis in LNCaP cells, as observed by increased cleavage of PARP-1, a key component of the DNA damage response.

Notably, Zhao and colleagues demonstrated a mechanism through which the lncRNA HOXA-AS2 inhibits apoptosis in a model of promyelocytic leukemia [32]. *HOXA-AS2* gene is located between *HOXA3* and *HOXA4* genes on the antisense strand. Its transcript is expressed in human peripheral blood neutrophils and in NB4 cells, a human promyelocytic leukemia cell line derived from a patient with acute promyelocytic leukemia. NB4 cells treated with all *trans* retinoic acid (ATRA) are prone to undergo apoptosis through caspase activation. Interestingly, the authors found that ATRA-treated NB4 cells increased HOXA-AS2 expression. Performing HOXA-AS2 knockdown by short hairpin RNA (shRNA) they showed an increase in ATRA-induced apoptosis measured by annexin V binding and by activity and cleavage of caspase-3, caspase-8 and caspase-9. The involvement of the intrinsic apoptotic pathway was confirmed by the increased levels of BAX, the well-known proapoptotic protein of the BCL2 family. More remarkably, they discovered an increase in TRAIL (TNF-related

Table 1: LncRNAs involved in the regulation of apoptosis in cancer cells.

LncRNA	Cancer cell line	Apoptotic effect	Reference
AFAP1-AS1	Esophageal adenocarcinoma OE-33	−	[29]
SPRY4-IT1	Melanoma WM1552C	−	[30]
PlncRNA-1	Prostate cancer LNCaP	−	[31]
HOXA-AS2	Promyelocytic leukemia NB4	−	[32]
uc002mbe.2	Hepatocellular carcinoma Huh7	+	[33]
GAS5	Prostate cancer PC-3	+	[34]

+: indicates proapoptotic effect; −: indicates antiapoptotic effect.

apoptosis-inducing ligand) protein and mRNA expression after ATRA treatment in HOXA-AS2 knockdown cells. It is known that ATRA-induced cell death in NB4 cells is linked to paracrine production of TRAIL [35]. This suggests the involvement also of the extrinsic apoptotic pathway. Indeed caspase-8 activation is due, at least in part, to the paracrine effects of TRAIL, as TRAIL-neutralizing antibody partially blocks caspase-8 cleavage. These results indicate that the lncRNA HOXA-AS2 negatively regulates ATRA-induced TRAIL production and the authors suggest that HOXA-AS2 may directly affect the transcription of the TRAIL gene (Figure 1(a)).

Other authors have reported examples of lncRNAs with proapoptotic effects in different cancer cells (Table 1). Expression levels of the lncRNA uc002mbe.2 were found lower in human hepatocellular carcinoma (HCC) cells compared to normal human hepatocytes and adjacent noncancerous tissues [33]. The expression levels were rapidly restored, within hours, upon treatment with the histone deacetylase inhibitor trichostatin A (TSA) and positively correlated with the apoptotic effect of TSA on HCC cells. Accordingly, uc002mbe.2 knockdown by siRNA reduced TSA-induced apoptosis as revealed by TUNEL assay [33]. Thus, at least in HCC cells, uc002mbe.2 is involved in the TSA-induced apoptosis.

Finally, in prostate cancer cell lines, Pickard and colleagues reported a lncRNA transcribed from the growth arrest-specific 5 (*GAS5*) gene locus able to mediate apoptosis in UV-C irradiated 22RV1 or PC-3 cells [34]. Again, cell death, evaluated by TUNEL assay, was increased in cells transfected with GAS5 constructs and attenuated following downmodulation of GAS5 expression.

4. LncRNAs Involved in Apoptosis during Development and Differentiation

Beside the cited paper that have investigated the role of lncRNAs in modulating apoptosis in cancer cells, there are also a couple of papers describing lncRNAs as apoptosis regulator during cellular differentiation and organ development. Hu and colleagues reported lncRNA-mediated antiapoptotic activity in murine erythroid terminal differentiation [36]. Using murine foetal liver cells as model of erythropoiesis, the authors characterized an erythroid specific lincRNA called LincRNA-EPS (for LincRNA erythroid prosurvival). LincRNA-EPS was found to be highly induced in terminally differentiating erythroblasts considering the developmental markers CD71 and Ter119. Loss of function studies by shRNA revealed that inhibition of LincRNA-EPS induction resulted in apoptosis (evaluated by annexin V staining, caspase-3 activity and TUNEL assay) and arrest of proliferation of erythroid progenitors. Conversely, LincRNA-EPS ectopic expression by retroviral transduction was able to prevent apoptosis in erythroid cells starved for erythropoietin (Epo), an essential prosurvival and differentiating cytokine of the erythropoiesis system, even if it did not restore the terminal differentiation, as determined by the levels of haemoglobin. These findings and the timing of LincRNA-EPS induction are in agreement with an Epo-derived survival mechanism mediated by LincRNA-EPS. Remarkably, microarray analysis after LincRNA-EPS overexpression highlighted the repression of many proapoptotic genes, such as *Bad, Bax, Caspase-2* and *-6, Fadd, Pycard*, and with *Pycard* being the most affected. Pycard plays its role in apoptosis as adaptor protein for caspase activation and several evidences were shown to suggest Pycard as direct target of LincRNA-EPS. Pycard expression during normal erythropoiesis is inversely correlated with that of LincRNA-EPS. Pycard overexpression results in similar phenotypes on erythroid terminal differentiation as inhibition of LincRNA-EPS induction. Pycard knockdown mimics the antiapoptotic phenotype conferred by LincRNA-EPS ectopic expression in Epo-deprived erythroid cells. Finally, overexpression of Pycard suppresses the antiapoptotic phenotype mediated by ectopic expression of LincRNA-EPS. Considering the nuclear localization of LincRNA-EPS, Hu et al. conclude that the antiapoptotic ability of LincRNA-EPS is mediated through repressing the transcription of Pycard and perhaps through the epigenetic control of other genes involved in cell apoptosis (Figure 1(a)).

Finally, studying the fragile X syndrome, Khalil and colleagues identified a new 2.4 kb lncRNA that was named FMR4 [37]. Fragile X syndrome, the most common cause of inherited mental retardation, is caused by the expansion of CGG trinucleotide repeats in the 5′ UTR of the fragile X mental retardation 1 gene (*FMR1*) [38, 39]. The expansion of CGG repeats above 200 leads to the repression or silencing of *FMR1* and consequently to the absence of the fragile X mental retardation protein (FMRP). LncRNA FMR4, that is located upstream and likely shares a bidirectional promoter with *FMR1*, becomes silenced too as a result of the CGG expansion in the 5′ UTR of *FMR1* in fragile X syndrome. The authors analyzed the expression pattern of FMR4 in adult

and foetal tissues finding FMR4 widely expressed, especially in the kidney and heart during embryonic development. The authors hypothesize that the foetal cardiac expression of FMR4 may be of functional relevance considering the fact that many patients with fragile X syndrome exhibit heart defects such as dilation of the aortic root and mitral valve prolapse [40]. Furthermore, they described that FMR4 regulate cell proliferation in HEK-293T cells. Knockdown of FMR4 resulted in cell cycle arrest and induction of apoptosis, while the overexpression of FMR4 led to an increase in cell proliferation, indicating that FMR4 has an antiapoptotic function in human cells.

5. LncRNAs as Therapeutic Targets and Biomarkers

As reported above, some lncRNAs and probably others that will be identified in the next years are involved in promoting or inhibiting apoptosis. This finding is of great relevance for the design of new drugs for the treatment of cancer and degenerative diseases. Targeting lncRNAs is challenging because it can potentially open a new field in drug development as they are completely different from proteins in both conformation and mechanism of action. Indeed, often they act as transcriptional repressors and so targeting a lncRNA can lead to the upregulation of tumour suppressors, growth factors, transcription factors and genes that are deficient in various genetic diseases, while the majority of currently available drugs exhibit an inhibitory mechanism of action. On the other hand, lncRNAs are particular appealing as drug targets because, once developed, the right technology for the delivery of their modulator can be applied with minor modifications to many lncRNAs. For example, H19 is a lncRNA with oncogenic properties, upregulated in a wide range of tumors. A plasmid carrying diphtheria toxin under the control of the H19 regulatory sequence has been developed to target cells overexpressing H19. Intratumoral injection of the plasmid was successfully applied in patients with bladder, ovarian, and pancreatic cancers to reduce tumor size [41]. Moreover, it was recently published an *in vivo* study in which targeting the asRNA BDNF-AS the authors obtained an increase in the levels of brain derived neural factor (BDNF) in mouse brain [42]. In this study they used single-stranded oligonucleotides named antago-NATs to target the asRNA. Antago-NATs can act by blocking the interactions of asRNA (or NAT: natural antisense transcript) with effector proteins and/or by causing RNAase H-mediated degradation of the antisense transcript. The authors used 16mer antago-NAT oligonucleotides with phosphorothioate-modified backbones and three locked nucleic acid (LNA) substitutions at each end to protect the molecules against exonuclease cleavage and increase affinity to the RNA target. Indeed, antago-NATs seem to be capable of inducing locus-specific upregulation as the expression of unrelated control genes, even neighbouring genes, seems to be unaffected.

Despite these examples, many problems still need to be solved for an extensive use of lncRNAs inhibitors in clinical studies such as off-target toxicity, delivery of oligonucleotides and lifetime administration [43].

Interestingly, lncRNAs often present an aberrant expression pattern in cancer cells, arising the question if they can be used as biomarker for diagnosis. The use of lncRNAs in diagnostics has intrinsic advantages over protein-coding RNAs because measurement of their expression directly represents the levels of the active molecule. In contrast, mRNA levels are only indirectly indicative of the levels of the functional product, the encoded protein. Furthermore, lncRNA levels may have a higher correlation with particular cancer types and thus be more useful as diagnostic tools. A recent analysis combined the expression profiles of more than 10 thousand lncRNAs with 1 thousand of tumors from 4 different cancer types with the aim to identify new biomarkers and potential drug targets. The authors identified and validated two new lncRNAs that drive prostate cancer progression [44]. LncRNAs are often stable in human serum and thus measuring either marker RNAs (e.g., by qPCR) or the entire transcriptome (e.g., RNA-seq) may allow the noninvasive generation of reliable and actionable clinical indicators [45]. For example, the lncRNA prostate cancer gene 3 (PCA3) is highly associated with prostate cancer and is routinely used to indicate prostate cancer risk from urine samples [46].

6. Conclusions

The world of lncRNAs has just started to be disclosed and only for a few of them the mechanisms of action are already known. Growing amount of evidences point out that lncRNAs are implicated in the control of apoptosis but their molecular roles in the apoptotic pathways are still largely unknown. Thus, it is now of primary importance not only to continue in identifying new lncRNAs involved in apoptosis but also to deepen the knowledge of mechanisms by which each lncRNA regulates apoptosis as well as other cellular processes. LncRNAs are now emerging as new master regulators of cell fate in response to stimuli and stress conditions and, as highlighted in this review, the outcome between cell proliferation and cell death is due, at least in certain types of cancer cells, to the expression levels of tissue-specific lncRNAs. Furthermore, lncRNA levels may have a correlation with particular cancer types and thus can be useful diagnostic tools as tumor biomarkers. The idea of targeting lncRNAs to modulate apoptosis in cancer cells is now opening a challenging field in drug discovery.

Conflict of Interests

The authors declare that there is no conflict of interests regarding the publication of this paper.

Acknowledgments

The authors gratefully thank Doctor Francesca Di Rosa for critical reading of the paper.Marianna Nicoletta Rossi

was supported by a fellowship from the Pasteur Institute-Fondazione Cenci Bolognetti. Fabrizio Antonangeli was supported by a Grant from MIUR-FIRB "Futuro In Ricerca."

References

[1] M. D'Amelio, E. Tino, and F. Cecconi, "The apoptosome: emerging insights and new potential targets for drug design," *Pharmaceutical Research*, vol. 25, no. 4, pp. 740–751, 2008.

[2] M. E. Guicciardi and G. J. Gores, "Life and death by death receptors," *FASEB Journal*, vol. 23, no. 6, pp. 1625–1637, 2009.

[3] T. G. Cotter, "Apoptosis and cancer: the genesis of a research field," *Nature Reviews Cancer*, vol. 9, no. 7, pp. 501–507, 2009.

[4] A. Giovannetti, M. Pierdominici, A. Di Iorio et al., "Apoptosis in the homeostasis of the immune system and in human immune mediated diseases," *Current Pharmaceutical Design*, vol. 14, no. 3, pp. 253–268, 2008.

[5] M. Clarke, M. Bennett, and T. Littlewood, "Cell death in the cardiovascular system," *Heart*, vol. 93, no. 6, pp. 659–664, 2007.

[6] E. M. Ribe, E. Serrano-Saiz, N. Akpan, and C. M. Troy, "Mechanisms of neuronal death in disease: defining the models and the players," *Biochemical Journal*, vol. 415, no. 2, pp. 165–182, 2008.

[7] P. Bertone, V. Stolc, T. E. Royce et al., "Global identification of human transcribed sequences with genome tiling arrays," *Science*, vol. 306, no. 5705, pp. 2242–2246, 2004.

[8] E. Birney, J. A. Stamatoyannopoulos, A. Dutta et al., "Identification and analysis of functional elements in 1% of the human genome by the ENCODE pilot project," *Nature*, vol. 447, no. 7146, pp. 799–816, 2007.

[9] P. Carninci, T. Kasukawa, S. Katayama et al., "The transcriptional landscape of the mammalian genome," *Science*, vol. 309, no. 5740, pp. 1559–1563, 2005.

[10] P. P. Amaral, M. E. Dinger, T. R. Mercer, and J. S. Mattick, "The eukaryotic genome as an RNA machine," *Science*, vol. 319, no. 5871, pp. 1787–1789, 2008.

[11] C. P. Ponting, P. L. Oliver, and W. Reik, "Evolution and functions of long noncoding RNAs," *Cell*, vol. 136, no. 4, pp. 629–641, 2009.

[12] L. Ma, V. B. Bajic, and Z. Zhang, "On the classification of long non-coding RNAs," *RNA Biology*, vol. 10, no. 6, pp. 925–933, 2013.

[13] C. J. Brown, A. Ballabio, J. L. Rupert et al., "A gene from the region of the human X inactivation centre is expressed exclusively from the inactive X chromosome," *Nature*, vol. 349, no. 6304, pp. 38–44, 1991.

[14] J. L. Rinn, M. Kertesz, J. K. Wang et al., "Functional demarcation of active and silent chromatin domains in human HOX Loci by noncoding RNAs," *Cell*, vol. 129, no. 7, pp. 1311–1323, 2007.

[15] T. Kino, D. E. Hurt, T. Ichijo, N. Nader, and G. P. Chrousos, "Noncoding RNA Gas5 is a growth arrest- and starvation-associated repressor of the glucocorticoid receptor," *Science Signaling*, vol. 3, no. 107, p. ra8, 2010.

[16] X. Wang, S. Arai, X. Song et al., "Induced ncRNAs allosterically modify RNA-binding proteins in cis to inhibit transcription," *Nature*, vol. 454, no. 7200, pp. 126–130, 2008.

[17] C. Gong and L. E. Maquat, "LncRNAs transactivate STAU1-mediated mRNA decay by duplexing with 39 UTRs via Alu eleme," *Nature*, vol. 470, no. 7333, pp. 284–290, 2011.

[18] M. Cesana, D. Cacchiarelli, I. Legnini et al., "A long noncoding RNA controls muscle differentiation by functioning as a competing endogenous RNA," *Cell*, vol. 147, no. 2, pp. 358–369, 2011.

[19] F. Sleutels, R. Zwart, and D. P. Barlow, "The non-coding Air RNA is required for silencing autosomal imprinted genes," *Nature*, vol. 415, no. 6873, pp. 810–813, 2002.

[20] S. Loewer, M. N. Cabili, M. Guttman et al., "Large intergenic non-coding RNA-RoR modulates reprogramming of human induced pluripotent stem cells," *Nature Genetics*, vol. 42, no. 12, pp. 1113–1117, 2010.

[21] M. T. Qiu, J. W. Hu, R. Yin, and L. Xu, "Long noncoding RNA: an emerging paradigm of cancer research," *Tumor Biology*, vol. 34, no. 2, pp. 613–620, 2013.

[22] A. J. Levine and M. Oren, "The first 30 years of p53: growing ever more complex," *Nature Reviews Cancer*, vol. 9, no. 10, pp. 749–758, 2009.

[23] K. M. Yamada and M. Araki, "Tumor suppressor PTEN: modulator of cell signaling, growth, migration and apoptosis," *Journal of Cell Science*, vol. 114, no. 13, pp. 2375–2382, 2001.

[24] L. P. Weng, O. Gimm, J. B. Kum et al., "Transient ectopic expression of PTEN in thyroid cancer cell lines induces cell cycle arrest and cell type-dependent cell death," *Human Molecular Genetics*, vol. 10, no. 3, pp. 251–258, 2001.

[25] M. Xing, "Genetic alterations in the phosphatidylinositol-3 kinase/Akt pathway in thyroid cancer," *Thyroid*, vol. 20, no. 7, pp. 697–706, 2010.

[26] L. Poliseno, L. Salmena, J. Zhang, B. Carver, W. J. Haveman, and P. P. Pandolfi, "A coding-independent function of gene and pseudogene mRNAs regulates tumour biology," *Nature*, vol. 465, no. 7301, pp. 1033–1038, 2010.

[27] P. Johnsson, A. Ackley, L. Vidarsdottir et al., "A pseudogene long-noncoding-RNA network regulates PTEN transcription and translation in human cells," *Nature Structural & Molecular Biology*, vol. 20, no. 4, pp. 440–446, 2013.

[28] A. Zhang, N. Zhou, J. Huang et al., "The human long non-coding RNA-RoR is a p53 repressor in response to DNA damage," *Cell Research*, vol. 23, no. 3, pp. 340–350, 2013.

[29] W. Wu, T. D. Bhagat, X. Yang et al., "Hypomethylation of non-coding DNA regions and overexpression of the long noncoding RNA, AFAP1-AS1, in Barrett's esophagus and esophageal adenocarcinoma," *Gastroenterology*, vol. 144, no. 5, pp. 956–966, 2013.

[30] D. Khaitan, M. E. Dinger, J. Mazar et al., "The melanoma-upregulated long noncoding RNA SPRY4-IT1 modulates apoptosis and invasion," *Cancer Research*, vol. 71, no. 11, pp. 3852–3862, 2011.

[31] Z. Cui, S. Ren, J. Lu et al., "The prostate cancer-up-regulated long noncoding RNA PlncRNA-1 modulates apoptosis and proliferation through reciprocal regulation of androgen receptor," *Urologic Oncology*, vol. 31, no. 7, pp. 1117–1123, 2013.

[32] H. Zhao, X. Zhang, J. B. Frazao, A. Condino-Neto, and P. E. Newburger, "HOX antisense lincRNA HOXA-AS2 is an apoptosis repressor in all Trans retinoic acid treated NB4 promyelocytic leukemia cells," *Journal of Cellular Biochemistry*, vol. 114, no. 10, pp. 2375–2383, 2013.

[33] H. Yang, Y. Zhong, H. Xie et al., "Induction of the liver cancer-down-regulated long noncoding RNA uc002mbe. 2 mediates trichostatin-induced apoptosis of liver cancer cells," *Biochemical Pharmacology*, vol. 85, no. 12, pp. 1761–1769, 2013.

[34] M. R. Pickard, M. Mourtada-Maarabouni, and G. T. Williams, "Long non-coding RNA GAS5 regulates apoptosis in prostate cancer cell lines," *Biochimica et Biophysica Acta*, vol. 1832, no. 10, pp. 1613–1623, 2013.

[35] L. Altucci, A. Rossin, W. Raffelsberger, A. Reitmair, C. Chomienne, and H. Gronemeyer, "Retinoic acid-induced apoptosis

in leukemia cells is mediated by paracrine action of tumor-selective death ligand TRAIL," *Nature Medicine*, vol. 7, no. 6, pp. 680–686, 2001.

[36] W. Hu, B. Yuan, J. Flygare, and H. F. Lodish, "Long noncoding RNA-mediated anti-apoptotic activity in murine erythroid terminal differentiation," *Genes and Development*, vol. 25, no. 24, pp. 2573–2578, 2011.

[37] A. M. Khalil, M. A. Faghihi, F. Modarresi, S. P. Brothers, and C. Wahlestedt, "A novel RNA transcript with antiapoptotic function is silenced in fragile X syndrome," *PLoS ONE*, vol. 3, no. 1, Article ID e1486, 2008.

[38] B. A. Oostra and P. Chiurazzi, "The fragile X gene and its function," *Clinical Genetics*, vol. 60, no. 6, pp. 399–408, 2001.

[39] A. J. Verkerk, M. Pieretti, J. S. Sutcliffe et al., "Identification of a gene (FMR-1) containing a CGG repeat coincident with a breakpoint cluster region exhibiting length variation in fragile X syndrome," *Cell*, vol. 65, no. 5, pp. 905–914, 1991.

[40] N. Sreeram, C. Wren, M. Bhate, P. Robertson, and S. Hunter, "Cardiac abnormalities in the fragile X syndrome," *British Heart Journal*, vol. 61, no. 3, pp. 289–291, 1989.

[41] M. C. Smaldone and B. J. Davies, "BC-819, a plasmid comprising the H19 gene regulatory sequences and diphtheria toxin A, for the potential targeted therapy of cancers," *Current Opinion in Molecular Therapeutics*, vol. 12, no. 5, pp. 607–616, 2010.

[42] F. Modarresi, M. A. Faghihi, M. A. Lopez-Toledano et al., "Inhibition of natural antisense transcripts in vivo results in gene-specific transcriptional upregulation," *Nature Biotechnology*, vol. 30, no. 5, pp. 453–459, 2012.

[43] C. Wahlestedt, "Targeting long non-coding RNA to therapeutically upregulate gene expression," *Nature Reviews Drug Discovery*, vol. 12, no. 6, pp. 433–446, 2013.

[44] Z. Du, T. Fei, R. G. Verhaak et al., "Integrative genomic analyses reveal clinically relevant long noncoding RNAs in human cancer," *Nature Structural & Molecular Biology*, vol. 20, no. 7, pp. 908–913, 2013.

[45] Y. K. Tong and Y. M. D. Lo, "Plasma epigenetic markers for cancer detection and prenatal diagnosis," *Frontiers in Bioscience*, vol. 11, no. 2, pp. 2647–2656, 2006.

[46] A. de la Taille, "Progensa PCA3 test for prostate cancer detection," *Expert Review of Molecular Diagnostics*, vol. 7, no. 5, pp. 491–497, 2007.

Hindawi Publishing Corporation
International Journal of Cell Biology
Volume 2014, Article ID 490275, 6 pages
http://dx.doi.org/10.1155/2014/490275

Review Article

Necroptosis: Molecular Signalling and Translational Implications

Claudia Giampietri, Donatella Starace, Simonetta Petrungaro, Antonio Filippini, and Elio Ziparo

Department of Anatomical, Histological, Forensic and Orthopaedic Sciences, Section of Histology and Medical Embryology, Sapienza University of Rome, Via Scarpa 14, 00161 Rome, Italy

Correspondence should be addressed to Claudia Giampietri; claudia.giampietri@uniroma1.it

Received 10 October 2013; Revised 11 December 2013; Accepted 16 December 2013; Published 23 January 2014

Academic Editor: Alessio Paone

Necroptosis is a form of programmed necrosis whose molecular players are partially shared with apoptotic cell death. Here we summarize what is known about molecular signalling of necroptosis, particularly focusing on fine tuning of FLIP and IAP proteins in the apoptosis/necroptosis balance. We also emphasize necroptosis involvement in physiological and pathological conditions, particularly in the regulation of immune homeostasis.

1. Introduction

In 1998 Vandenabeele's group demonstrated that murine L929 fibrosarcoma cells treated with the pan-caspase inhibitor zVAD-FMK rapidly die in a necrotic way after tumor necrosis factor (TNF) incubation, indicating a possible involvement of caspases in protection against TNF-induced necrosis [1]. Additional works then described this particular form of cell death having many hallmarks of cellular necrosis and induced by death receptor stimulation [2, 3]. Further studies performed by introducing the cowpox virus serpin and caspase-8 inhibitor CrmA in the cells, confirmed that caspase-8 inhibition leads to this form of cell death [4]. Remarkably, while necrosis has been believed in the past to be a passive and accidental form of cell death, it is now considered a finely regulated process [5]. For such a reason it is called necroptosis or programmed necrosis. Necroptosis is characterized by cell swelling, mitochondria dysfunction, plasma membrane permeabilization, and release of cytoplasmic content to the extracellular space. This form of cell death is also associated with high mitochondrial reactive oxygen species (ROS) production and unlike apoptosis it does not involve DNA fragmentation [6].

2. Necroptosis Activation and Signalling

Necroptosis can be activated by members of the tumor necrosis factor (TNF) family (through TNFR1, TNFR2, TRAILR1, and TRAILR2), Fas ligand, toll-like receptors, lipopolysaccharides (LPS), and genotoxic stress [2, 7–9]. Also different kinds of physical-chemical stress stimuli can initiate necroptosis, including anticancer drugs, ionizing radiation, photodynamic therapy, glutamate, and calcium overload [10].

Under conditions that are insufficient to trigger apoptosis, TNFα activates TNFR1 and in turn induces the recruitment of receptor-interacting protein 1 (RIP1) kinase and other proteins to form complex I. Subsequently, these proteins dissociate from TNFR1 and RIP1 can be found in the cytosol in complex IIb, which includes RIP1, receptor-interacting protein 3 (RIP3) kinase, caspase-8 and FADD. The formation of complex IIb leads to necroptosis [11]. Complex I also includes TRADD which is important in mediating the recruitment of RIP1 kinase to TNFR1 via its death domain (DD) [12].

Necroptosis has been shown to be generally dependent on RIP3, which is activated following phosphorylation by the serine/threonine kinase RIP1 [13]. RIP3 is thought to

induce a switch in cell's metabolism, leading to the increase of mitochondrial ROS production that culminates in cell death [14, 15]. The complex RIP1/RIP3 within the so-called necrosome is therefore crucial for the induction of necroptosis. Experiments carried out by multiple experimental approaches have clarified that RIP1 and RIP3 are indeed necessary for necroptosis execution [13, 15, 16]. The RIP1 kinase activity is required for necrosome formation since necrostatin, which allosterically blocks the kinase activity of RIP1, abolishes the assembly of the RIP1-RIP3 complex [13, 16]. While RIP1 involvement has been identified in both apoptosis and necroptosis, RIP3 appears to participate solely in necroptosis. RIP1 and RIP3 have been shown to assemble only in the absence of functional caspase-8, indicating that this enzyme acts as a necrosome inhibitor. Interestingly, caspase-8 has also been shown to cleave, and presumably inactivate, both RIP1 and RIP3 thus acting as a negative regulator of this pathway also through this mechanism. When caspase-8 inactivates RIP1 and RIP3 by proteolytic cleavage, a proapoptotic caspase activation instead of a pronecrotic cascade is triggered [17–19]. Recently the activity of the NAD-dependent deacetylating enzyme SIRT2 has been found to be implicated in the RIP1-mediated recruitment of RIP3 and the necrosome formation [20]. Also the adapter proteins FADD and NEMO appear to be crucial for TNF-alpha-induced necroptosis [21].

The mixed lineage kinase domain like protein (MLKL) has been shown to be an important substrate of RIP3 likely targeting functional downstream targets on cellular organelles such as mitochondria and/or lysosomes [22]. MLKL is phosphorylated by RIP3 at the threonine 357 and serine 358 residues, and these phosphorylation events are critical for necroptosis. In fact blocking MLKL activity leads to necroptosis inhibition. Although the entire molecular mechanism of necroptosis execution is not completely clear these findings implicate MLKL as a key mediator of necroptosis signalling downstream of RIP3 kinase [23].

A schematic overview of major signal transduction pathways induced by various stimuli and ultimately leading to necroptosis can be found in Figure 1 of the review article by Kaczmarek et al. [24].

3. Flip and Necroptosis

Flip molecules have been originally described as regulators of caspase-8-mediated apoptosis [25] although they are involved in additional functions such as autophagy modulation, proliferative control, cardiac hypertrophy regulation, and Akt/Gsk3β activity modulation [26–30]. Different studies indicate that Flip, FADD, and caspase-8 are required for normal embryonic development since their ablation is lethal around E10.5 with similar vascular defects [31–33] suggesting that these proteins display also important non-apoptotic functions during development. Recent evidence indicates that FADD and caspase-8 deficiency can be rescued by RIP3 and RIP1 deletion. Furthermore the lethal effects of Flip deletion are rescued by concurrent ablation of FADD and RIP3. These data suggested that FADD/caspase-8/Flip may negatively regulate RIP1 and RIP3 [34, 35]. More in detail the apoptotic platform constituted by FADD, caspase-8, and Flip has been hypothesized to negatively control necroptosis during development. Although the molecular complex driving necroptosis during development is not completely clear, results obtained *in vitro* confirmed that a caspase-8/Flip heterodimer can inhibit RIP signalling to necroptosis [36]. Furthermore, the embryonic lethality in mice lacking caspase-8, Flip, or the adaptor molecule FADD has been associated with massive necroptosis of endothelial and hematopoietic cells and can be rescued by RIP deletion [37].

Indeed, literature data show that Flip role is quite complex. Flip expression in fact prevents apoptosis that is a caspase-dependent and RIP3-independent cell death. At the same time Flip can inhibit RIP3-dependent necrotic cell death in a caspase-8-dependent manner [36]. In particular caspase-8/Flip heterodimer may prevent the stable association of FADD, RIP1, and RIP3, thereby inhibiting necrotic death. These results support the hypothesis that the main nonapoptotic function of caspase-8 is to suppress RIP3-dependent necrosis during development, likely acting in complex with Flip. The precise mechanism by which the catalytic activity of the caspase-8-Flip complex is engaged to prevent RIP3-dependent necroptosis without triggering apoptosis is not presently known; some additional details are reported below.

4. IAPs and Necroptosis

Members of the inhibitors of apoptosis (IAP) protein family are E3 ubiquitin ligases and are well known caspases regulators, characterized by baculoviral IAP repeat domains [38]. During the intrinsic pathway of apoptosis Smac/Diablo is released from mitochondria to cytosol thus removing the inhibition imposed by the IAPs resulting in apoptotic death. Smac protein in fact induces in the cytosol IAP1 and IAP2 autodegradation, allowing the formation of a caspase-8-activating complex containing both RIP1 and caspase-8 [39]. Several mammalian IAPs may utilize ubiquitination to regulate their own stability. It has been recently found that autophagy activation resulted in c-IAP1 and c-IAP2 degradation thus contributing to necroptosis induction [40]. Remarkably, in the absence of IAPs and under conditions where caspases are blocked, necroptosis can be stimulated via RIP1 and its downstream kinase [16]. It has been demonstrated that genotoxic stress or TLR3 stimulation through poly(I:C), a synthetic homologue of virus-derived double stranded DNA, induces IAPs depletion leading to spontaneous aggregation of RIP1 and caspase-8. Such event occurs independently of death receptor stimulation and leads to the formation of "ripoptosome" [41]. The term "ripoptosome" refers to a cell death inducing platform containing RIP1 and most likely RIP3 and regulated by both Flip and IAP proteins (cIAP1, cIAP2, and XIAP). Flip long isoform ($Flip_L$) knockdown is able to enhance ripoptosome aggregation thus sensitizing cells to etoposide or TLR3-mediated cell death. IAP proteins are able to inactivate ripoptosome

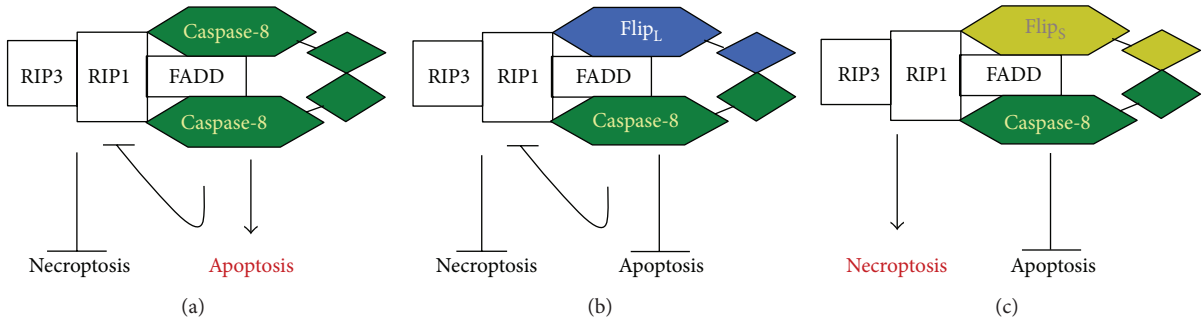

Figure 1: (a) Dimerization of caspase-8 drives apoptosis initiation without triggering necroptosis. (b) c-Flip$_L$/caspase-8 heterodimer, by leading to reduced caspase-8 activity, can induce neither apoptosis nor necroptosis. (c) c-Flip$_S$/caspase-8 heterodimer, by inhibiting caspase-8, leads to necroptosis induction.

likely inducing proteasomal degradation of RIP1. The role played by ripoptosome is complex since, depending on the cell type, it can stimulate caspase-8-mediated apoptosis or caspase-independent necroptosis [35]. Data from Feoktistova and collaborators demonstrate that in the absence of IAPs (achieved by a IAP antagonist) Flip isoforms levels in the ripoptosome directly control the balance between caspase-dependent apoptosis and RIP-dependent necroptosis [41]. As shown in Figure 1, when Flip proteins are lacking, procaspase-8 homodimers within the ripoptosome lead to caspase-8 activation thus initiating apoptosis. Conversely, in the presence of Flip$_L$, caspase-8/Flip$_L$ heterodimers may induce RIP cleavage thus leading to ripoptosome disassembly and necroptosis inhibition. Conversely the short Flip isoform (Flip$_S$) differently from the long Flip isoform (Flip$_L$) promotes RIP3-dependent necroptosis. The caspase-8/Flip$_S$ heterodimers lack proteolytic activity necessary for RIP1 degradation thus leading to necroptosis induction via RIP1 and RIP3 [41].

5. Necroptosis in Physiology and Pathology

Necroptosis occurs physiologically during development as well as in adult life. Chondrocytes die by necroptosis in human growth plate during bones longitudinal growth [42]. Furthermore, necroptosis may represent an alternative form of death which can substitute apoptosis when caspase activation is blocked. It has been demonstrated that interdigital cells and thymocytes obtained from mice lacking the caspase activator Apaf1 undergo necroptosis instead of apoptosis [43]. Importantly, also in keratinocytes, caspase-8 ablation leads to enhanced necroptosis [44]. It has been hypothesized that an ancestral cell death resembling necrosis was overcome by more recent and more complex processes like autophagy and apoptosis that carry the selective advantage to better contribute to the elimination of cell bodies and organelles [45]. This hypothesis may explain at least in part why, although the ancestral form of cell death is often hidden by other cell death forms, it resumes as a back-up mechanism when the other pathways are blocked.

Necroptosis regulation plays a key role also in the context of immune homeostasis. In fact, whereas the role of apoptosis has been clearly defined in the generation of self-tolerant lymphocytes involved in the establishment of central tolerance, more recently, necroptosis has been implicated in the regulation of T cells proliferation. Previous studies showed that caspase-8, the key molecule mediating apoptosis in response to activation of death receptors, such as Fas [46], also has important nonapoptotic functions [47], as antigen-induced proliferation of T cells required for peripheral T cell homeostasis and T cell survival in response to activation stimuli [48]. In agreement, the specific deletion of caspase-8 in the T cell lineage leads to immunodeficiency associated with impaired T cell homeostasis, T cell lymphopenia, defective T cells proliferation after stimulation with mitogens or antigens, and impaired responses to viral infection [48]. Remarkably, the deficit in T cell expansion caused by loss of caspase-8 was associated with decrease in cell viability but not with apoptosis since no DNA fragmentation was detected. This expansion defect in caspase-8-deficient T cells was rescued by necrostatin or a knockdown of RIP1 [49, 50]. Moreover, it has been later demonstrated that the loss of RIP3 is able to rescue the defective T cell proliferation of casp8−/− mice [36, 49, 51], demonstrating that necroptosis also in T cells is regulated by caspase-8. It is generally accepted that caspase-8 may suppress necroptosis through cleavage and consequent inhibition of RIP1 and RIP3 [17, 19]; it is therefore possible to hypothesize that in physiological conditions caspase-8 is active in suppressing T cells necroptosis, whereas, in pathological conditions, such as viral infection, caspase-8 may be inactivated and consequently T cells may die via necroptosis [49]. Several studies investigated the interaction between key molecules involved in the regulation of necroptosis in T cells. It has been demonstrated that the conditional deletion of FADD, which directly binds to RIP1, leads to impaired lymphocyte proliferation [52–54]. The relationship linking FADD and RIP1 has been more deeply analyzed by Zhang and collaborators [55] demonstrating that levels of RIP1 were increased in FADD−/− embryos in association with necroptosis. By crossing null alleles of RIP1 into FADD−/− mice, normal proliferation of FADD−/− T cells was restored. Moreover, the developmental defect of RIP1−/−

lymphocytes was partially corrected by FADD deletion. These data have a dual importance indicating that both apoptosis and necroptosis during T cell development are regulated by the FADD-RIP1 axis. Interestingly, defects in T cells described in FADD−/− mice resemble analogous defects detected in caspase-8−/− mice [31, 32, 56], again confirming the role of caspase-8, and FADD in the control of RIP1-mediated necroptosis in T cells. Another study disclosing the importance of the interplay between apoptotic and necroptotic pathways in T cells has been recently published by Bohgaki et al. [57] demonstrating that the inactivation of caspase-8 in T cells by increasing necroptosis, suppresses autoimmunity caused by Bim deficiency. Bim (Bcl-2-interacting mediator of cell death) is a proapoptotic BH3-only protein belonging to the Bcl-2 protein family, involved in mediating the intrinsic apoptosis pathway [58]. Previous studies demonstrated that the loss of Bim induces autoimmunity due to impaired apoptosis of T cells [59]. Interestingly, Bohgaki and collaborators [57] demonstrated that inactivation of caspase-8 in Bim−/− T cells increases their spontaneous and activation-induced necroptosis thus leading to elimination of Bim−/− T cells. Thus, loss of caspase-8 determines necroptosis of Bim−/− T cells which balances the low apoptotic rate due to Bim deficiency of single mutant Bim−/− T cells. Thus caspase-8 loss in T cells appears to have antagonizing effects on autoimmunity associated with Bim deficiency, suggesting a role for necroptosis in the suppression of autoimmunity. In agreement, the inhibition of the necroptotic process by means of the necroptosis inhibitor necrostatin fully rescued the survival and proliferation of casp8−/− and Bim−/− T cells [57]. Altogether, these data indicate that apoptosis and necroptosis must be tightly regulated in order to maintain immune homeostasis.

Necroptosis has been also associated with different pathological conditions such as ischemia in brain and myocardial tissues, infections [13, 60], neurodegenerative diseases, pancreatitis [16], photoreceptor cell loss [61], and ischaemia-reperfusion damage [62]. Necroptosis may be induced by pathogens (both bacteria and viruses). Recognition of pathogens through pattern-recognition receptors (PRRs) is the first line of defense against infections and some PRRs may initiate necroptosis [24] through RIP1 and/or RIP3 activity [63–65]. Cytomegalovirus infection has been shown to induce RIP3-dependent but RIP1-independent necroptosis thus indicating RIP3 as the main kinase controlling cellular necrotic pathways in such viral pathogenesis [60]. Necroptosis of intestinal epithelial cells seems to be implicated in the pathogenesis of inflammatory bowel diseases. In such pathologies the death receptor 3 (DR3) signalling results in expansion of the Treg pool with concomitant and transient inhibition of Treg suppressive function [66]. It has been demonstrated that mechanisms preventing RIP3-mediated epithelial cell death are crucial for maintaining intestinal homeostasis [67]. Importantly, high levels of RIP3 and increased necroptosis in the ileum of Crohn's disease patients have been found, suggesting a role for necroptosis in the etiopathogenesis of this disease.

There is increasing evidence that necroptosis can be impaired during tumorigenesis. Chronic lymphocytic leukemia cells have been reported to have defects in components involved in necroptosis regulation such as RIP3 and the deubiquitination cylindromatosis (CYLD), an enzyme directly regulating RIP1 ubiquitination [68]. CYLD mutations have been found in epidermal cancer cells [69]. In non-Hodgkin lymphoma, polymorphisms in the RIP3 gene were identified correlating with increased risk to develop the tumor [6]. Necroptosis undoubtedly represents an important process for enhancing tumor cell sensitivity to anticancer treatments and therefore its potentiation may represent an important therapeutic opportunity to kill tumor cells, particularly those resistant to apoptosis. Although apoptotic resistance is a formidable strategy adopted by cancer cells against chemotherapy, cancer cells can be intrinsically susceptible to necroptosis and therefore its induction may represent a valuable tool to counteract their apoptosis resistance [70, 71].

In conclusion necroptosis is emerging as an important process closely interconnected with apoptosis and represents a promising field for innovative therapeutic approaches.

Conflict of Interests

The authors declare that there is no conflict of interests regarding the publication of this paper.

Authors' Contribution

Antonio Filippini and Elio Ziparo equally contributed to this work.

Acknowledgments

Work in the Authors' laboratory is supported by PRIN 2010-2011 and Fondazione Roma grants to Elio Ziparo.

References

[1] D. Vercammen, R. Beyaert, G. Denecker et al., "Inhibition of caspases increases the sensitivity of L929 cells to necrosis mediated by tumor necrosis factor," *The Journal of Experimental Medicine*, vol. 187, no. 9, pp. 1477–1485, 1998.

[2] N. Holler, R. Zaru, O. Micheau et al., "Fas triggers an alternative, caspase-8-independent cell death pathway using the kinase RIP as effector molecule," *Nature Immunology*, vol. 1, no. 6, pp. 489–495, 2000.

[3] A. Kawahara, Y. Ohsawa, H. Matsumura, Y. Uchiyama, and S. Nagata, "Caspase-independent cell killing by Fas-associated protein with death domain," *Journal of Cell Biology*, vol. 143, no. 5, pp. 1353–1360, 1998.

[4] B. J. van Raam and G. S. Salvesen, "Proliferative versus apoptotic functions of caspase-8: Hetero or homo: the caspase-8 dimer controls cell fate," *Biochimica et Biophysica Acta*, vol. 1824, no. 1, pp. 113–122, 2012.

[5] N. Festjens, T. Vanden Berghe, and P. Vandenabeele, "Necrosis, a well-orchestrated form of cell demise: signalling cascades, important mediators and concomitant immune response," *Biochimica et Biophysica Acta*, vol. 1757, no. 9-10, pp. 1371–1387, 2006.

[6] W. Wu, P. Liu, and J. Li, "Necroptosis: an emerging form of programmed cell death," *Critical Reviews in Oncology/Hematology*, vol. 82, pp. 249–258, 2012.

[7] F. K.-M. Chan, J. Shisler, J. G. Bixby et al., "A role for tumor necrosis factor receptor-2 and receptor-interacting protein in programmed necrosis and antiviral responses," *The Journal of Biological Chemistry*, vol. 278, no. 51, pp. 51613–51621, 2003.

[8] H. Matsumura, Y. Shimizu, Y. Ohsawa, A. Kawahara, Y. Uchiyama, and S. Nagata, "Necrotic death pathway in Fas receptor signaling," *Journal of Cell Biology*, vol. 151, no. 6, pp. 1247–1256, 2000.

[9] D. Vercammen, G. Brouckaert, G. Denecker et al., "Dual signaling of the Fas receptor: initiation of both apoptotic and necrotic cell death pathways," *The Journal of Experimental Medicine*, vol. 188, no. 5, pp. 919–930, 1998.

[10] S. Fulda, "The mechanism of necroptosis in normal and cancer cells," *Cancer Biology & Therapy*, vol. 14, no. 11, pp. 999–1004, 2013.

[11] D. E. Christofferson and J. Yuan, "Necroptosis as an alternative form of programmed cell death," *Current Opinion in Cell Biology*, vol. 22, no. 2, pp. 263–268, 2010.

[12] D. M. Moujalled, W. D. Cook, T. Okamoto et al., "TNF can activate RIPK3 and cause programmed necrosis in the absence of RIPK1," *Cell Death & Disease*, vol. 4, article e465, 2013.

[13] Y. S. Cho, S. Challa, D. Moquin et al., "Phosphorylation-driven assembly of the RIP1-RIP3 complex regulates programmed necrosis and virus-induced inflammation," *Cell*, vol. 137, no. 6, pp. 1112–1123, 2009.

[14] N. Vanlangenakker, T. Vanden Berghe, P. Bogaert et al., "cIAP1 and TAK1 protect cells from TNF-induced necrosis by preventing RIP1/RIP3-dependent reactive oxygen species production," *Cell Death and Differentiation*, vol. 18, no. 4, pp. 656–665, 2011.

[15] D.-W. Zhang, J. Shao, J. Lin et al., "RIP3, an energy metabolism regulator that switches TNF-induced cell death from apoptosis to necrosis," *Science*, vol. 325, no. 5938, pp. 332–336, 2009.

[16] S. He, L. Wang, L. Miao et al., "Receptor interacting protein kinase-3 determines cellular necrotic response to TNF-alpha," *Cell*, vol. 137, no. 6, pp. 1100–1111, 2009.

[17] S. Feng, Y. Yang, Y. Mei et al., "Cleavage of RIP3 inactivates its caspase-independent apoptosis pathway by removal of kinase domain," *Cellular Signalling*, vol. 19, no. 10, pp. 2056–2067, 2007.

[18] Y. Lin, A. Devin, A. Cook et al., "The death domain kinase RIP is essential for TRAIL (Apo2L)-induced activation of IκB kinase and c-Jun N-terminal kinase," *Molecular and Cellular Biology*, vol. 20, no. 18, pp. 6638–6645, 2000.

[19] F. Martinon, N. Holler, C. Richard, and J. Tschopp, "Activation of a pro-apoptotic amplification loop through inhibition of NF-κB-dependent survival signals by caspase-mediated inactivation of RIP," *FEBS Letters*, vol. 468, no. 2-3, pp. 134–136, 2000.

[20] N. Narayan, I. H. Lee, R. Borenstein et al., "The NAD-dependent deacetylase SIRT2 is required for programmed necrosis," *Nature*, vol. 492, pp. 199–204, 2012.

[21] K. M. Irrinki, K. Mallilankaraman, R. J. Thapa et al., "Requirement of FADD, NEMO, and BAX/BAK for aberrant mitochondrial function in tumor necrosis factor alpha-induced necrosis," *Molecular and Cellular Biology*, vol. 31, no. 18, pp. 3745–3758, 2011.

[22] L. Sun, H. Wang, Z. Wang et al., "Mixed lineage kinase domain-like protein mediates necrosis signaling downstream of RIP3 kinase," *Cell*, vol. 148, no. 1-2, pp. 213–227, 2012.

[23] J. M. Murphy, P. E. Czabotar, J. M. Hildebrand et al., "The pseudokinase MLKL mediates necroptosis via a molecular switch mechanism," *Immunity*, vol. 39, pp. 443–453, 2013.

[24] A. Kaczmarek, P. Vandenabeele, and D. V. Krysko, "Necroptosis: the release of damage-associated molecular patterns and its physiological relevance," *Immunity*, vol. 38, pp. 209–223, 2013.

[25] M. Irmler, M. Thome, M. Hahne et al., "Inhibition of death receptor signals by cellular FLIP," *Nature*, vol. 388, no. 6638, pp. 190–195, 1997.

[26] C. Giampietri, S. Petrungaro, M. Musumeci et al., "c-Flip overexpression reduces cardiac hypertrophy in response to pressure overload," *Journal of Hypertension*, vol. 26, no. 5, pp. 1008–1016, 2008.

[27] C. Giampietri, S. Petrungaro, P. Coluccia et al., "c-Flip overexpression affects satellite cell proliferation and promotes skeletal muscle aging," *Cell Death and Disease*, vol. 1, no. 4, article e38, 2010.

[28] C. Giampietri, S. Petrungaro, F. Padula et al., "Autophagy modulators sensitize prostate epithelial cancer cell lines to TNF-alpha-dependent," *Apoptosis*, vol. 17, no. 11, pp. 1210–1222, 2012.

[29] C. Giampietri, S. Petrungaro, A. Facchiano, A. Filippini, and E. Ziparo, "Therapeutic implications of autophagy modulation in prostate cancer," *Journal of Endocrinological Investigation*, vol. 35, no. 10, p. 945, 2012.

[30] C. Quintavalle, M. Incoronato, L. Puca et al., "C-FLIPL enhances anti-apoptotic Akt functions by modulation of Gsk3B activity," *Cell Death and Differentiation*, vol. 17, no. 12, pp. 1908–1916, 2010.

[31] E. E. Varfolomeev, M. Schuchmann, V. Luria et al., "Targeted disruption of the mouse Caspase 8 gene ablates cell death induction by the TNF receptors, Fas/Apo1, and DR3 and is lethal prenatally," *Immunity*, vol. 9, no. 2, pp. 267–276, 1998.

[32] W.-C. Yeh, J. L. de la Pompa, M. E. McCurrach et al., "FADD: essential for embryo development and signaling from some, but not all, inducers of apoptosis," *Science*, vol. 279, no. 5358, pp. 1954–1958, 1998.

[33] W.-C. Yeh, A. Itie, A. J. Elia et al., "Requirement for Casper (c-FLIP) in regulation of death receptor-induced apoptosis and embryonic development," *Immunity*, vol. 12, no. 6, pp. 633–642, 2000.

[34] C. Dillon, A. Oberst, R. Weinlich et al., "Survival function of the FADD-CASPASE-8-cFLIPL complex," *Cell Reports*, vol. 1, pp. 401–407, 2012.

[35] T. Tenev, K. Bianchi, M. Darding et al., "The Ripoptosome, a signaling platform that assembles in response to genotoxic stress and loss of IAPs," *Molecular Cell*, vol. 43, no. 3, pp. 432–448, 2011.

[36] A. Oberst, C. P. Dillon, R. Weinlich et al., "Catalytic activity of the caspase-8-FLIP L complex inhibits RIPK3-dependent necrosis," *Nature*, vol. 471, no. 7338, pp. 363–367, 2011.

[37] N. Vanlangenakker, T. Vanden Berghe, and P. Vandenabeele, "Many stimuli pull the necrotic trigger, an overview," *Cell Death and Differentiation*, vol. 19, no. 1, pp. 75–86, 2012.

[38] S. M. Srinivasula and J. D. Ashwell, "IAPs: what's in a name?" *Molecular Cell*, vol. 30, no. 2, pp. 123–135, 2008.

[39] L. Wang, F. Du, and X. Wang, "TNF-alpha induces two distinct caspase-8 activation pathways," *Cell*, vol. 133, no. 4, pp. 693–703, 2008.

[40] W. He, Q. Wang, B. Srinivasan et al., "A JNK-mediated autophagy pathway that triggers c-IAP degradation and necroptosis for anticancer chemotherapy," *Oncogene*, 2013.

[41] M. Feoktistova, P. Geserick, B. Kellert et al., "CIAPs block Ripoptosome formation, a RIP1/caspase-8 containing intracellular cell death complex differentially regulated by cFLIP isoforms," *Molecular Cell*, vol. 43, no. 3, pp. 449–463, 2011.

[42] H. I. Roach and N. M. P. Clarke, "Physiological cell death of chondrocytes in vivo is not confined to apoptosis: new observations on the mammalian growth plate," *Journal of Bone and Joint Surgery B*, vol. 82, no. 4, pp. 601–613, 2000.

[43] M. Chautan, G. Chazal, F. Cecconi, P. Gruss, and P. Golstein, "Interdigital cell death can occur through a necrotic and caspase-independent pathway," *Current Biology*, vol. 9, no. 17, pp. 967–970, 1999.

[44] M. C. Bonnet, D. Preukschat, P.-S. Welz et al., "The adaptor protein FADD protects epidermal keratinocytes from necroptosis in vivo and prevents skin inflammation," *Immunity*, vol. 35, no. 4, pp. 572–582, 2011.

[45] P. Golstein and G. Kroemer, "Redundant cell death mechanisms as relics and backups," *Cell Death and Differentiation*, vol. 12, supplement 2, pp. 1490–1496, 2005.

[46] N. S. Wilson, V. Dixit, and A. Ashkenazi, "Death receptor signal transducers: nodes of coordination in immune signaling networks," *Nature Immunology*, vol. 10, no. 4, pp. 348–355, 2009.

[47] T.-B. Kang, T. Ben-Moshe, E. E. Varfolomeev et al., "Caspase-8 serves both apoptotic and nonapoptotic roles," *Journal of Immunology*, vol. 173, no. 5, pp. 2976–2984, 2004.

[48] L. Salmena, B. Lemmers, A. Hakem et al., "Essential role for caspase 8 in T-cell homeostasis and T-cell-mediated immunity," *Genes and Development*, vol. 17, no. 7, pp. 883–895, 2003.

[49] I. L. Ch'en, J. S. Tsau, J. D. Molkentin, M. Komatsu, and S. M. Hedrick, "Mechanisms of necroptosis in T cells," *The Journal of Experimental Medicine*, vol. 208, no. 4, pp. 633–641, 2011.

[50] A. Degterev, J. Hitomi, M. Germscheid et al., "Identification of RIP1 kinase as a specific cellular target of necrostatins," *Nature Chemical Biology*, vol. 4, no. 5, pp. 313–321, 2008.

[51] W. J. Kaiser, J. W. Upton, A. B. Long et al., "RIP3 mediates the embryonic lethality of caspase-8-deficient mice," *Nature*, vol. 471, no. 7338, pp. 368–372, 2011.

[52] H. Z. Imtiyaz, S. Rosenberg, Y. Zhang et al., "The Fas-associated death domain protein is required in apoptosis and TLR-induced proliferative responses in B cells," *Journal of Immunology*, vol. 176, no. 11, pp. 6852–6861, 2006.

[53] S. L. Osborn, G. Diehl, S.-J. Han et al., "Fas-associated death domain (FADD) is a negative regulator of T-cell receptor-mediated necroptosis," *Proceedings of the National Academy of Sciences of the United States of America*, vol. 107, no. 29, pp. 13034–13039, 2010.

[54] Y. Zhang, S. Rosenberg, H. Wang, H. Z. Imtiyaz, Y.-J. Hou, and J. Zhang, "Conditional Fas-associated death domain protein (FADD): GFP knockout mice reveal FADD is dispensable in thymic development but essential in peripheral T cell homeostasis," *Journal of Immunology*, vol. 175, no. 5, pp. 3033–3044, 2005.

[55] H. Zhang, X. Zhou, T. McQuade, J. Li, F. K. Chan, and J. Zhang, "Functional complementation between FADD and RIP1 in embryos and lymphocytes," *Nature*, vol. 471, pp. 373–376, 2011.

[56] J. Zhang, D. Cado, A. Chen, N. H. Kabra, and A. Winoto, "Fas-mediated apoptosis and activation-induced T-cell proliferation are defective in mice lacking FADD/Mort1," *Nature*, vol. 392, no. 6673, pp. 296–300, 1998.

[57] T. Bohgaki, J. Mozo, L. Salmena et al., "Caspase-8 inactivation in T cells increases necroptosis and suppresses autoimmunity in Bim-/- mice," *Journal of Cell Biology*, vol. 195, no. 2, pp. 277–291, 2011.

[58] A. Strasser, "The role of BH3-only proteins in the immune system," *Nature Reviews Immunology*, vol. 5, no. 3, pp. 189–200, 2005.

[59] P. Bouillet, D. Metcalf, and D. C. S. Huang, "Proapoptotic Bcl-2 relative Bim required for certain apoptotic responses, leukocyte homeostasis, and to preclude autoimmunity," *Science*, vol. 286, no. 5445, pp. 1735–1738, 1999.

[60] J. W. Upton, W. J. Kaiser, and E. S. Mocarski, "Virus inhibition of RIP3-dependent necrosis," *Cell Host and Microbe*, vol. 7, no. 4, pp. 302–313, 2010.

[61] G. Trichonas, A. Manola, Y. Morizane et al., "A novel nonradioactive method to evaluate vascular barrier breakdown and leakage," *Investigative Ophthalmology and Visual Science*, vol. 51, no. 3, pp. 1677–1682, 2010.

[62] C. C. T. Smith, S. M. Davidson, S. Y. Lim, J. C. Simpkin, J. S. Hothersall, and D. M. Yellon, "Necrostatin: a potentially novel cardioprotective agent?" *Cardiovascular Drugs and Therapy*, vol. 21, no. 4, pp. 227–233, 2007.

[63] M. François, V. Le Cabec, M.-A. Dupont, P. J. Sansonetti, and I. Maridonneau-Parini, "Induction of necrosis in human neutrophils by Shigella flexneri requires type III secretion, IpaB and IpaC invasins, and actin polymerization," *Infection and Immunity*, vol. 68, no. 3, pp. 1289–1296, 2000.

[64] J. F. Koterski, M. Nahvi, M. M. Venkatesan, and B. Haimovich, "Virulent Shigella flexneri causes damage to mitochondria and triggers necrosis in infected human monocyte-derived macrophages," *Infection and Immunity*, vol. 73, no. 1, pp. 504–513, 2005.

[65] Y. Ma, V. Temkin, H. Liu, and R. M. Pope, "NF-κB protects macrophages from lipopolysaccharide-induced cell death: the role of caspase 8 and receptor-interacting protein," *The Journal of Biological Chemistry*, vol. 280, no. 51, pp. 41827–41834, 2005.

[66] G. Bamias, L. G. Jia, and F. Cominelli, "The tumor necrosis factor-like cytokine 1A/death receptor 3 cytokine system in intestinal inflammation," *Current Opinion in Gastroenterology*, vol. 29, pp. 597–602, 2013.

[67] P.-S. Welz, A. Wullaert, K. Vlantis et al., "FADD prevents RIP3-mediated epithelial cell necrosis and chronic intestinal inflammation," *Nature*, vol. 477, no. 7364, pp. 330–334, 2011.

[68] P. Liu, B. Xu, W. Shen et al., "Dysregulation of TNFα-induced necroptotic signaling in chronic lymphocytic leukemia: suppression of CYLD gene by LEF1," *Leukemia*, vol. 26, pp. 1293–1300, 2012.

[69] J. P. Alameda, R. Moreno-Maldonado, M. Navarro et al., "An inactivating CYLD mutation promotes skin tumor progression by conferring enhanced proliferative, survival and angiogenic properties to epidermal cancer cells," *Oncogene*, vol. 29, no. 50, pp. 6522–6532, 2010.

[70] W. Han, L. Li, S. Qiu et al., "Shikonin circumvents cancer drug resistance by induction of a necroptotic death," *Molecular Cancer Therapeutics*, vol. 6, no. 5, pp. 1641–1649, 2007.

[71] M. Wu, Z. Jiang, H. Duan et al., "Deoxypodophyllotoxin triggers necroptosis in human non-small cell lung cancer NCI-H460 cells," *Biomedicine & Pharmacotherapy*, vol. 67, pp. 701–706, 2013.

Hindawi Publishing Corporation
International Journal of Cell Biology
Volume 2014, Article ID 135908, 7 pages
http://dx.doi.org/10.1155/2014/135908

Research Article

Lithium Improves Survival of PC12 Pheochromocytoma Cells in High-Density Cultures and after Exposure to Toxic Compounds

Cinzia Fabrizi,[1] Stefania De Vito,[1] Francesca Somma,[1] Elena Pompili,[1] Angela Catizone,[1] Stefano Leone,[2] Paola Lenzi,[3] Francesco Fornai,[3,4] and Lorenzo Fumagalli[1]

[1] *Department of Anatomy, Histology, Forensic Medicine and Orthopedics, Sapienza University, Via A. Borelli 50, 00161 Rome, Italy*
[2] *Department of Science, Roma Tre University, Rome, Italy*
[3] *Department of Human Morphology and Applied Biology, University of Pisa, Pisa, Italy*
[4] *I.R.C.C.S. Neuromed, Pozzilli, Italy*

Correspondence should be addressed to Cinzia Fabrizi; cinzia.fabrizi@uniroma1.it

Received 11 October 2013; Accepted 20 November 2013; Published 20 January 2014

Academic Editor: Claudia Giampietri

Autophagy is an evolutionary conserved mechanism that allows for the degradation of long-lived proteins and entire organelles which are driven to lysosomes for digestion. Different kinds of stressful conditions such as starvation are able to induce autophagy. Lithium and rapamycin are potent autophagy inducers with different molecular targets. Lithium stimulates autophagy by decreasing the intracellular myo-inositol-1,4,5-triphosphate levels, while rapamycin acts through the inhibition of the mammalian target of rapamycin (mTOR). The correlation between autophagy and cell death is still a matter of debate especially in transformed cells. In fact, the execution of autophagy can protect cells from death by promptly removing damaged organelles such as mitochondria. Nevertheless, an excessive use of the autophagic machinery can drive cells to death via a sort of self-cannibalism. Our data show that lithium (used within its therapeutic window) stimulates the overgrowth of the rat Pheochromocytoma cell line PC12. Besides, lithium and rapamycin protect PC12 cells from toxic compounds such as thapsigargin and trimethyltin. Taken together these data indicate that pharmacological activation of autophagy allows for the survival of Pheochromocytoma cells in stressful conditions such as high-density cultures and exposure to toxins.

1. Introduction

Pheochromocytoma is a rare neuroendocrine tumour derived from chromaffin cells of the adrenal gland. Surgical resection of the tumour is the treatment of choice and usually results in cure of the hypertension related to the excessive release of catecholamines. Approximately, 17% of these tumours are malignant and treatment for metastatic disease includes surgical resection and chemotherapy with nonspecific agents which indiscriminately target dividing cells [1].

A previous report indicates a possible novel strategy for treatment of Pheochromocytomas and paragangliomas showing that lithium determines a net reduction of the growth in culture of the rat Pheochromocytoma cell line PC12 [2].

Lithium is already therapeutically widely used as a mood stabilizer in the treatment of bipolar disorders and in human patients levels of lithium in the serum are kept in the range of 0.4–1.2 mM [3]. Due to its diverse molecular targets, the action of lithium may be complex and the interpretation of its effects in biological systems is often controversial.

In fact, lithium is a monovalent cation with different cellular targets depending on its concentration. At 0.5–1 mM it acts mainly as an inhibitor of inositol monophosphatase (IMPase) (Ki 0.8 mM) leading to free inositol depletion and activating autophagy [4]. Autophagy is a catabolic pathway which delivers cellular components to lysosomes for digestion. First step is the engulfment of cytoplasmic material or entire organelles in autophagosomes which later on fuse with lysosomes to form autophagolysosomes. LC3 (microtubule-associated protein light chain 3) is localized in

autophagosome membrane and is a widely applied marker for autophagy [5].

Conversely, when used at high doses lithium inhibits the glycogen synthase kinase-3 (GSK3) (Ki 1.5–2 mM) and reduces cellular proliferation and autophagy [6]. Two paralogs of GSK3 exist (GSK3α and GSK3β) usually referred to as isoforms because of their similar sequences and functions although they are derived from different genes [7]. These ubiquitously expressed serine/threonine kinases modulate a large number of cellular functions and their activity is inhibited by the phosphorylation of serine-21 in GSK3α and serine-9 in GSK3β.

Our data show that lithium if used in the range which corresponds to its therapeutic window (0.5–1 mM) favors the proliferation and survival of the rat Pheochromocytoma cell line PC12. Consistently with an activation of the autophagic pathway, 0.5 mM lithium induces the appearance of many autophagic vacuoles whereas the phosphorylation/inactivation of GSK3α/β was observed only at a higher lithium concentration (2 mM).

2. Materials and Methods

2.1. Cell Cultures and Treatments. PC12 rat pheochromocytoma cells (ECACC) were cultured in RPMI1640 and DMEM/F12 (1 : 1) supplemented with 5% foetal bovine serum, 10% horse serum, and 1% penicillin-streptomycin. Cells were incubated at 37°C in a humidified 5% CO_2 atmosphere and medium was changed every three days.

PC12 cells were plated onto poly-L-ornithine-treated glass coverslips in 24 w plates (for fluorescence microscopy) or directly in 6-well or 96-well plates (for western blot analysis and assessment of neurotoxicity, resp.). PC12 cells were treated with LiCl (0.5, 1, 2 mM; Sigma) alone or in combination with thapsigargin (100 nM) or trimethyltin (TMT) (10 μM; Heraeus, Karlsruhe, Germany). As for lithium treatment, rapamycin (400 nM; Sigma) was used alone or with TMT (1, 5, 10 μM).

2.2. Proliferation Curve. PC12 cells were plated onto T25 culture flasks (5×10^5 cells/mL) in 5 mL growth medium without antibiotics. Every 24 hours cells were resuspended in phosphate buffer and stained with Trypan blue. After 3 days of culture further 5 mL of growth medium was added. Viable cells were counted in triplicate by a hemocytometer.

2.3. Assessment of Cell Death. The DNA fragmentation of the apoptotic PC12 cells was detected using the terminal deoxynucleotidyl transferase-mediated biotinylated UTP nick end labeling (TUNEL) kit (In situ Cell Death Detection Kit, Roche). The cells were cultured on coverslips for 24 hours and at the end of the drug treatment fixed in 4% paraformaldehyde in phosphate buffer (pH 7.4) at room temperature for 15 min and then incubated with a permeabilizing solution (0.1% Triton X-100) for 10 min at 4°C. The cells were incubated with the TUNEL reaction mixture for 60 min at 37°C and visualized by inverted fluorescence microscopy (Eclipse E600, Nikon Instruments SpA, Italy). TUNEL-positive nuclei were counted in ten nonoverlapping fields per coverslip and then converted to percentage by comparing TUNEL-positive counts with the total cell nuclei as determined by DAPI (4′,6′-diamino-2-phenylindole) counterstaining.

Cell death was also evaluated by measuring the release of lactate dehydrogenase (LDH) in the culture medium by the Cytotoxicity Detection Kit (Roche, Mannheim, Germany) according to manufacturer's protocols.

2.4. Electron Microscopy. PC12 cells were treated with 0.5 mM lithium for 24 hours and then processed for electron microscopy. After washing with phosphate buffer 0.1 M (pH 7.4) samples were fixed in 0.1% glutaraldehyde and 2% paraformaldehyde in phosphate buffer 0.1 M (pH 7.4) for 1.30 hour at 4°C. After washing with phosphate buffer 0.1 M (pH 7.4) samples were postfixed in 1% OsO_4 for 1 hour at 4°C and dehydrated in decreased series of ethanol and embedded in Epoxy resin. Ultrathin sections (40–50 nm) were cut at ultramicrotome. Sections were contrasted with uranyl acetate (saturated solution in methanol) and lead citrate and examined using a Jeol JEM SX 100 electron microscope (Jeol, Tokyo, Japan).

2.5. Detection of Autophagic Vacuoles by Immunofluorescence. PC12 cells were treated for 24 hours with 0.5 mM lithium and then fixed in 4% paraformaldehyde in phosphate buffer (pH 7.4) 1 hour at room temperature. After washings nonspecific antibody binding sites were blocked with 10% donkey serum (Sigma) and then cells were incubated for 1 hour at room temperature with a rabbit anti-LC3B antibody (Sigma) and binding of the primary antibody visualized by a secondary donkey Cy3-labelled-anti-rabbit-IgG (Jackson ImmunoResearch Laboratories). Immunolocalization was analyzed using a Leica confocal microscope (Laser Scanning TCS SP2) (Leica Microsystems, Wetzlar, Germany) equipped with Ar/ArKr and HeNe lasers. The images were scanned under a 40X oil immersion objective with electronic zoom of 2X and 4X. In order to perform a quantitative analysis, spatial series through the z-axis each composed of 9-10 optical sections with a step size of 2 μm were performed and maximal amplitude of fluorescence was evaluated as described by [8] utilizing the Leica confocal software. No significant fluorescent signal was detected with the secondary antibody alone.

2.6. Western Blotting. Treated and untreated cells were lysed in RIPA buffer containing protease and phosphatase inhibitors (Protease Inhibitor Cocktail and Phosphatase Inhibitor Cocktail 2, Sigma). Samples were clarified by centrifugation at 1000 rpm for 5 min. Equivalent amount of protein (10 μg) from each sample was electrophoretically resolved on 12.5% precast SDS-polyacrylamide gels (Excel-Gel, GE Healthcare Biosciences) using horizontal apparatus (Pharmacia Biotech, Uppsala, Sweden). Then, separated proteins were electrotransferred onto nitrocellulose membranes (Schleicher & Schuell) by a semidry system (Novablot, Pharmacia Biotech). Membranes were blocked with 5% BSA

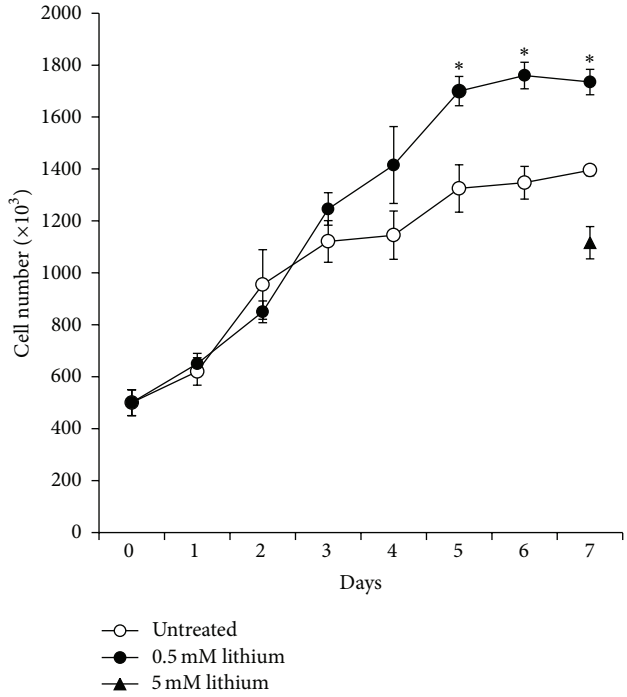

Figure 1: Proliferation curve of PC12 cells treated with lithium. Cells were treated with 0.5 mM lithium for 7 days and counted every day with the Trypan blue exclusion method. Counts obtained with 5 mM lithium at 7 days are shown as reference. Averages ± SEM of three independent experiments. ANOVA with Bonferroni's-corrected t-test. $^{*}P < 0.01$ versus untreated control.

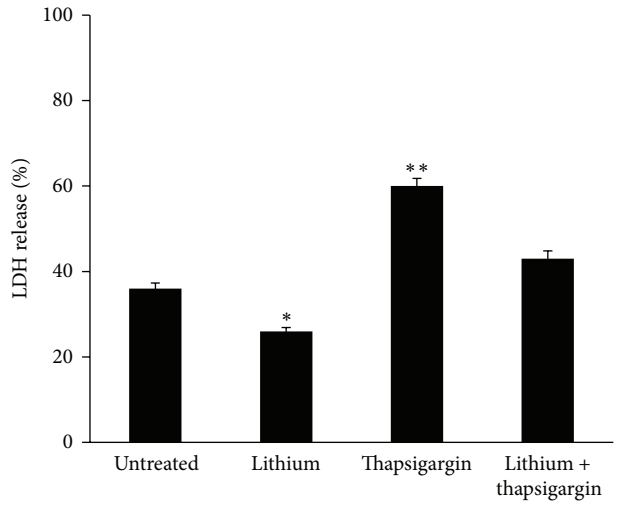

Figure 2: LDH release in the culture medium of PC12 cells treated for 24 hours with 100 nM thapsigargin alone or in combination with 0.5 mM lithium. Lithium treatment significantly reduces the thapsigargin-induced LDH release; a low but significant decrease in LDH release is observed in cultures treated with lithium alone with respect to the untreated control. Averages ± SEM of three independent experiments. ANOVA with Bonferroni's-corrected t-test. $^{*}P < 0.01$, $^{**}P < 0.001$ versus untreated control.

in PBS and then were incubated (overnight at 4°C) with the following monoclonal antibodies: GSK3α/β (Sigma), phospho-GSK3α/β (Ser 21/9) (cell signalling). After extensive washing with PBS containing 0.1% tween-20 (TBST), blots were incubated with 1 : 2000 dilution of HRP-conjugated secondary antibody (Amersham Biosciences) for 1 hour at room temperature. Immunopositive bands were detected with a chemiluminescence's detection system (GE Healthcare Biosciences). To check for equal loading of the gel, membranes were stripped and reprobed with mouse anti-β-actin antibody (1 : 20000, Sigma). Densitometric analysis was performed with the Quantity One software (BioRad Laboratories).

2.7. Statistics. Statistical analyses were conducted using GraphPad Prism version 4.00 software. Data are expressed as averages ± SEM. Comparisons were analysed using one-way ANOVA with Bonferroni-corrected t-test. All experiments were performed at least three times.

3. Results

As aforementioned, a previous report indicates lithium as a possible novel treatment for pheocromocytomas and paragangliomas [2]. Since lithium concentrations used in that study were beyond its potential therapeutic use, we decided to check the effect of lithium administration at the concentration measured in sera of lithium-treated patients. Similarly to Kappes and colleagues [2], we tested lithium administration in the rat Pheochromocytoma cell line PC12 which is widely used for toxicity studies. We noticed that after 5 days of culture 0.5 mM lithium increases PC12 cell number with respect to the untreated control, with this effect remaining stable up to 7 days of culture (Figure 1). A similar proliferation curve was obtained doubling the concentration of lithium to 1 mM while when PC12 cells were seeded at low density (2×10^5/mL) neither 0.5 mM nor 1 mM lithium modified cell number with respect to control (not shown). Interestingly, no significant differences between treated and untreated cultures were observed before the proliferation curve reaches the plateau. BrdU incorporation analyses performed during the same period of time indicated a similar rate of DNA synthesis in untreated and lithium-treated cultures (not shown). Consistently with previously published results [2], lithium used at the concentration of 5 mM reduced cell number in PC12 cell cultures (Figure 1).

In order to check if lithium at 0.5 mM was effective in inhibiting PC12 cell death, we administered this cation in combination with two different toxic molecules, thapsigargin and trimethyltin (TMT). As shown in Figure 2, lithium was able to almost completely rescue PC12 cells from thapsigargin-induced cell death. Similarly, lithium protected PC12 cells from TMT-induced apoptosis measured by TUNEL at 24 hours (Figure 3(a)). At 24 hours of TMT treatment PC12 cells seem to die mainly by apoptosis since the release of LDH in the culture medium remained similar to control (not shown). The release of LDH measured at 48 hours after TMT administration, which comprehends both

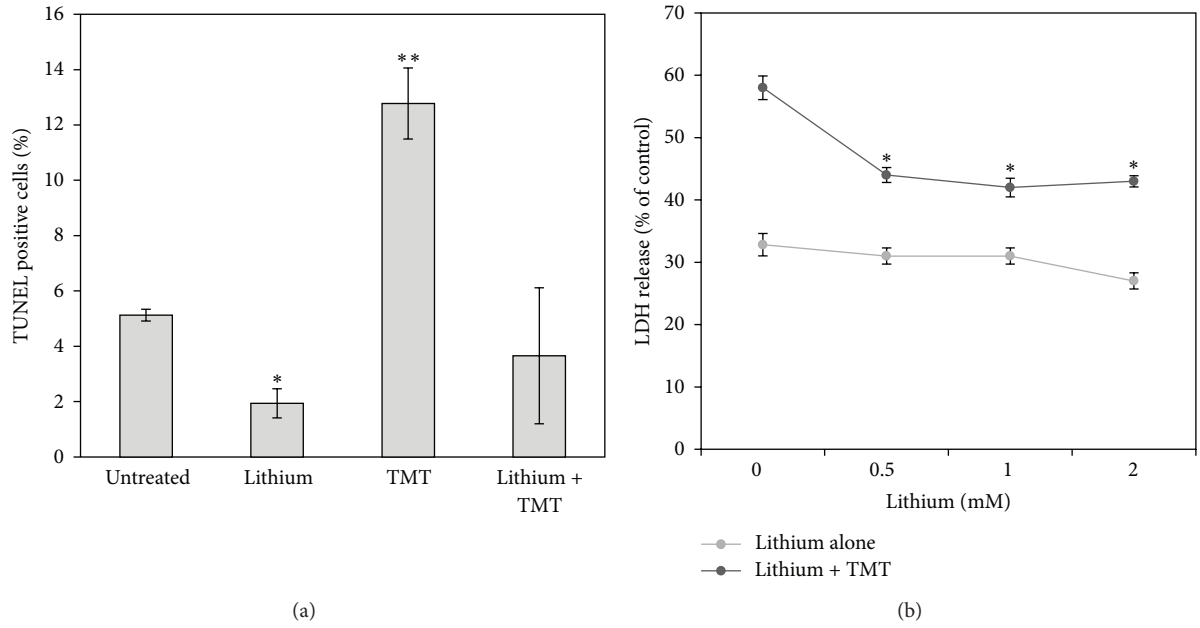

Figure 3: Detection of TUNEL-positive cells (a) and release of LDH (b) in the culture medium of PC12 cells treated for 24 and 48 hours, respectively, with 10 μM TMT alone or in combination with 0.5 mM lithium. Lithium treatment completely reverses TMT-induced apoptosis (a); a significant inhibition of LDH release is observed in PC12 cells treated with doses of lithium ranging from 0.5 to 2 mM with respect to cultures treated with TMT alone. Averages ± SEM of three independent experiments. ANOVA with Bonferroni's-corrected t-test. $^{*}P < 0.01$, $^{**}P < 0.001$ versus untreated control.

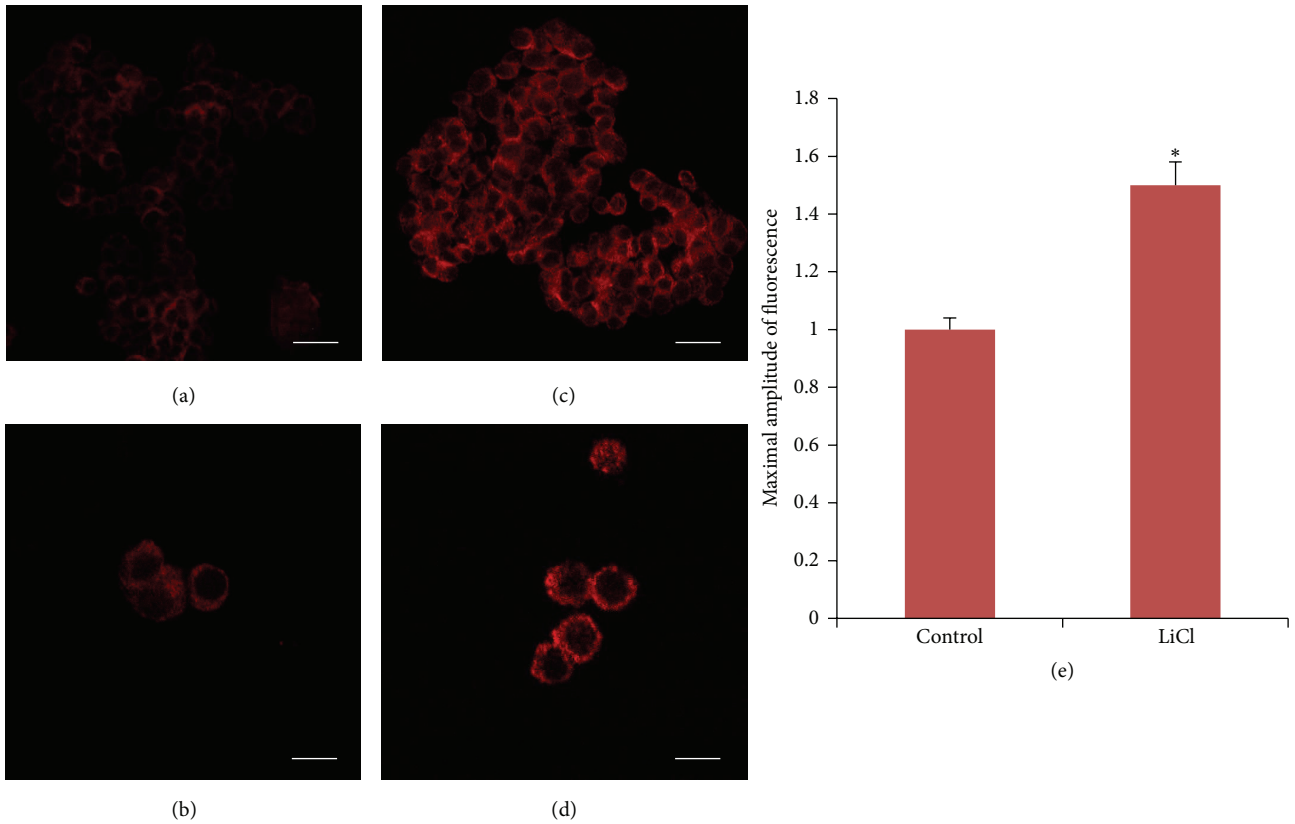

Figure 4: Confocal microscopy of LC3B distribution in PC12 cells after treatment for 24 hours with 0.5 mM lithium. Left panel: representative image of control ((a), (b)) and lithium-treated samples ((c), (d)). Scale bars = 20 μm ((a), (c)); 40 μm ((b), (d)). (e): quantitative analysis. The data represent the mean ± SE of maximal amplitude of fluorescence. $^{*}P < 0.001$ versus control.

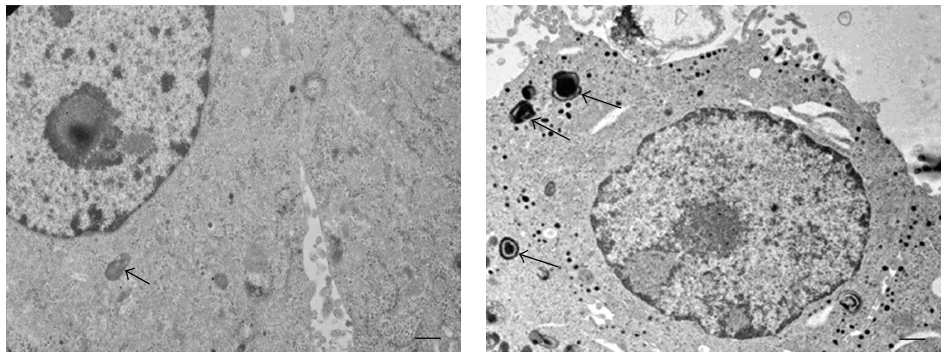

(a) (b)

Figure 5: Ultrastructural analysis of lithium-treated PC12 cells. Membrane-delimited vacuoles in the cytoplasm with the characteristic features of autophagic vacuoles (arrows) are present in untreated cells (a) and more numerous in lithium-treated sample (b). Scale bars = (a): 1 μm; (b): 0.4 μm.

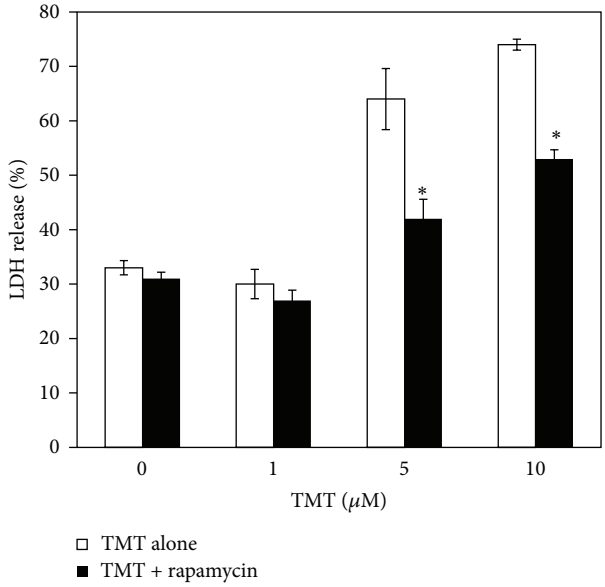

Figure 6: Rapamycin protects PC12 cultures from TMT toxicity. Rapamycin (400 nM) limits the release of LDH in the culture medium following 5–10 μM TMT exposure and its effect lasts up to 72 hours. ANOVA with Bonferroni's-corrected t-test. $^*P < 0.01$ versus TMT alone.

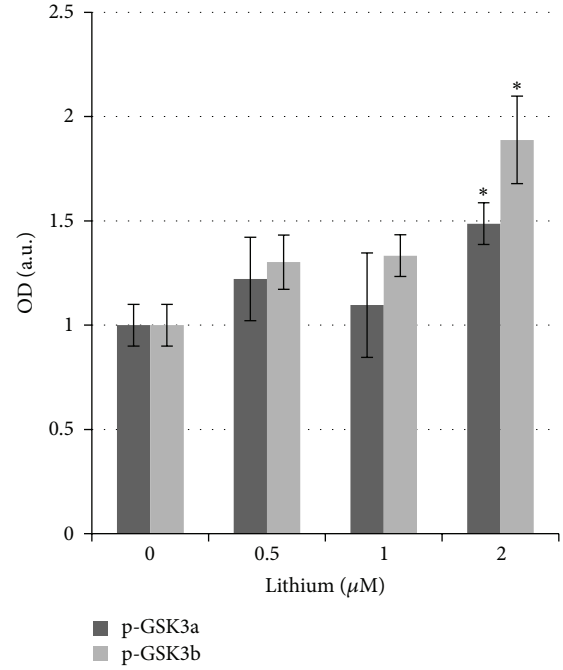

Figure 7: Analysis of the level of GSK3 phosphorylation in PC12 cells treated with lithium (0.5, 1, 2 mM) for 48 hours. Quantification data of western blot analysis of the phosphorylation of GSK3α Ser^{21} and GSK3β Ser^{9}. Averages ± SEM of three independent experiments. ANOVA with Bonferroni's-corrected t-test. $^*P < 0.01$ versus untreated cells.

necrosis and late apoptosis, was also reduced by lithium (Figure 3(b)).

Since lithium is known to be able to activate the autophagic pathway in different cellular systems, we checked the presence of autophagic vesicles in lithium-treated PC12 cells.

The expression of the autophagosome marker LC3B was evaluated by means of confocal microscopy in the control and lithium-treated samples. In lithium-treated PC12 the fluorescence intensity of LC3B was more evident and the mean value of the maximal amplitude of fluorescence was significantly increased (approximately 50%) with respect to the control (Figure 4).

Many autophagic vesicles were also detected by electron microscopy in lithium-treated cultures (Figure 5).

Besides, another known autophagy inducer such as rapamycin similarly to lithium was effective in reducing TMT neurotoxicity (Figure 6) confirming that a prompt activation of the autophagic machinery can protect PC12 from cell death.

We also checked in our cultures the phosphorylation of GSK3 which is a well-known lithium target. The phosphorylation/inactivation of GSK3 resulted to be unchanged

after treatment with 0.5 mM lithium, while at 2 mM a statistically significant increase in the phosphorylation of both the GSK3α and GSK3β isoforms was measured with respect to the untreated control (Figure 7).

4. Discussion

How the autophagic pathway can be involved in the progression of cancer is still a matter of controversy. In fact, autophagy has been reported to participate in both tumour suppression and tumour maintenance (for a recent review see [9]). On the one hand, loss of genes which govern the autophagic machinery such as beclin1 is observed in various cancers [10]. On the other hand, autophagy by limiting oxidative stress and supplying metabolic substrates can promote tumour growth and maintenance [11, 12].

One way to reconcile these apparently conflicting results is to speculate that the correct execution of autophagy prevents the initial phase of tumourigenesis while later on in the progression of cancer the same autophagic machinery can be used by transformed cells to survive in adverse growth conditions which are present inside a solid tumour due to the limited blood supply.

In this connection, our data support this interpretation indicating autophagy as a prosurvival mechanism for tumour cells growing in a stressful environment, such as an overpopulated culture.

As mentioned before, lithium has been proposed for the treatment of Pheochromocytomas and paragangliomas [2]. These authors demonstrated that this cation can block the proliferation of PC12 cells in culture. The minimum dose of lithium showing this antiproliferative effect is 5 mM and thus far beyond its potential therapeutic use. In fact, lithium has a narrow therapeutic window and well-known adverse effects. Serum levels of lithium ranging from 0.4 to 1.2 mM are effective in the treatment of bipolar disorders and show minor side effects [3]. Conversely, prolonged exposures to serum levels of 2 mM lithium lead to renal and liver damage and permanent neurological impairment is observed with plasma levels above 2.5 mM [13].

When we used lithium in a range of concentration corresponding to 0.5–1 mM we observed a completely different result with respect to Kappes and colleagues [2]. In fact, PC12 cells in the presence of 0.5 mM lithium grow as the untreated control during the first 3 days of culture showing a similar exponential phase. Afterwards, in lithium-treated PC12 cells a higher cellular number was reached with respect to control at 5 days and maintained up to 7 days during the stationary phase. These results are not consistent with a direct mitogenic activity of lithium. In particular, lithium seemed to favor the growth of PC12 cells just in high-density cultures which likely grow in stressful conditions due to shortage of nutrients and accumulation of catabolites.

Besides, our data indicate that lithium at 0.5 mM exerts a neuroprotective action in PC12 cells treated with two toxic molecules (thapsigargin and TMT) which act with different mechanisms. Thapsigargin is a potent inhibitor of the Ca2+-ATPase in the endoplasmic reticulum [14] and our results are in agreement with a previous report which indicates that lithium can revert thapsigargin toxicity in a range of concentration from 0.5 to 4 mM [15]. TMT is another molecule highly toxic for PC12 cells determining a strong loss of the mitochondrial membrane potential correlated with an increased expression of bax/bcl-2 ratio [16]. TMT toxicity relates to the expression of stannin, a highly conserved protein mainly localized within mitochondria [17]. We show here that in PC12 cultures the addiction of lithium reduces the percentage of TUNEL-positive apoptotic nuclei completely rescuing PC12 from TMT toxicity. Lithium administration also limits the release of LDH in the culture medium which is observed during necrotic cell death and in the late stages of apoptosis. In agreement with data reported here, our previous results indicate that lithium (0.5–2 mM) protects hippocampal and cortical primary neurons from TMT-induced cell death [18]. Moreover, 1.2 mM lithium was also shown to reverse the effect of morphine on the mRNA expression of bax and bcl-2 in PC12 cells [19].

Lithium is a cation with a complex mechanism of action. Its main molecular targets are IMPase and GSK3. For the former the reported Ki is 0.8 mM [4] while for the latter it corresponds to 1.5–2 mM [6]. Thus, it is very likely that completely different biological effect of the same molecule (lithium) can be observed just changing its concentration. In this study we show the appearance of numerous autophagic vesicles in PC12 cells after treatment with 0.5 mM lithium while at this low concentration of lithium the phosphorylation/inactivation of GSK3 was not observed. Besides, lithium neuroprotection with respect to TMT toxicity can be mimicked by a known autophagy inducer such as rapamycin. Nevertheless, the neuroprotective effect of lithium observed in our culture system can also be related to an increased synthesis and release of trophic factors. In fact, long-term lithium chronic treatment has been demonstrated to enhance BDNF and NT-3 expression in vivo [20, 21].

We conclude that lithium when used at low doses (0.5 mM) can protect PC12 cells from toxic molecules and can also allow the overgrow of these cells in high-density cultures. Thus, caution should be taken for the clinical use of this cation in tumour bearing patients.

Conflict of Interests

The authors declare that there is no conflict of interests regarding the publication of this paper.

Acknowledgments

These studies were supported by Grants awarded by PRIN 2008 and The Sapienza University of Rome (Ricerche Universitarie 2010-11) to LF.

References

[1] C. Jimenez, E. Rohren, M. A. Habra, T. Rich, P. Jimenez, and M. Ayala-Ramirez E, "Baudin, current and future treatments for malignant pheochromocytoma and sympathetic paraganglioma," *Current Oncology Report*, vol. 15, no. 4, pp. 356–371, 2013.

[2] A. Kappes, A. Vaccaro, M. Kunnimalaiyaan, and H. Chen, "Lithium ions: a novel treatment for pheochromocytomas and paragangliomas," *Surgery*, vol. 141, no. 2, pp. 161–165, 2007.

[3] W. E. Severus, N. Kleindienst, F. Seemüller, S. Frangou, H. J. Möller, and W. Greil, "What is the optimal serum lithium level in the long-term treatment of bipolar disorder—a review?" *Bipolar Disorders*, vol. 10, no. 2, pp. 231–237, 2008.

[4] S. Sarkar and D. C. Rubinsztein, "Inositol and IP3 levels regulate autophagy: biology and therapeutic speculations," *Autophagy*, vol. 2, no. 2, pp. 132–134, 2006.

[5] J. Lee, S. Giordano, and J. Zhang, "Autophagy, mitochondria and oxidative stress: cross-talk and redox signalling," *Biochemical Journal*, vol. 441, no. 2, pp. 523–540, 2012.

[6] M. K. Rowe, C. Wiest, and D.-M. Chuang, "GSK-3 is a viable potential target for therapeutic intervention in bipolar disorder," *Neuroscience and Biobehavioral Reviews*, vol. 31, no. 6, pp. 920–931, 2007.

[7] O. Kaidanovich-Beilin and J. R. Woodgett, "GSK-3: functional insights from cell biology and animal models," *Frontiers in Molecular Neuroscience*, vol. 4, article 40, 2011.

[8] A. Catizone, G. Ricci, and M. Galdieri, "Hepatocyte growth factor modulates Sertoli-Sertoli tight junction dynamics," *Journal of Cellular Physiology*, vol. 216, no. 1, pp. 253–260, 2008.

[9] S. Z. Lu and D. D. Harrison-Findik, "Autophagy and cancer," *World Journal of Biological Chemistry*, vol. 4, no. 3, pp. 64–70, 2013.

[10] C. Liang and J. U. Jung, "Autophagy genes as tumor suppressors," *Current Opinion in Cell Biology*, vol. 22, no. 2, pp. 226–233, 2010.

[11] A. C. Kimmelman, "The dynamic nature of autophagy in cancer," *Genes and Development*, vol. 25, no. 19, pp. 1999–2010, 2011.

[12] R. Scherz-Shouval and Z. Elazar, "Regulation of autophagy by ROS: physiology and pathology," *Trends in Biochemical Sciences*, vol. 36, no. 1, pp. 30–38, 2011.

[13] S. Nassir Ghaemi, D. J. Hsu, F. Soldani, and F. K. Goodwin, "Antidepressants in bipolar disorder: the case for caution," *Bipolar Disorders*, vol. 5, no. 6, pp. 421–433, 2003.

[14] O. Thastrup, P. J. Cullen, B. K. Drobak, M. R. Hanley, and A. P. Dawson, "Thapsigargin, a tumor promoter, discharges intracellular Ca^{2+} stores by specific inhibition of the endoplasmic reticulum Ca^{2+}-ATPase," *Proceedings of the National Academy of Sciences of the United States of America*, vol. 87, no. 7, pp. 2466–2470, 1990.

[15] T. Hiroi, H. Wei, C. Hough, P. Leeds, and D.-M. Chuang, "Protracted lithium treatment protects against the ER stress elicited by thapsigargin in rat PC12 cells: roles of intracellular calcium, GRP78 and Bcl-2," *Pharmacogenomics Journal*, vol. 5, no. 2, pp. 102–111, 2005.

[16] F. Misiti, F. Orsini, M. E. Clementi, W. Lattanzi, B. Giardina, and F. Michetti, "Mitochondrial oxygen consumption inhibition importance for TMT-dependent cell death in undifferentiated PC12 cells," *Neurochemistry International*, vol. 52, no. 6, pp. 1092–1099, 2008.

[17] M. L. Billingsley, J. Yun, B. E. Reese, C. E. Davidson, B. A. Buck-Koehntop, and G. Veglia, "Functional and structural properties of stannin: roles in cellular growth, selective toxicity, and mitochondrial responses to injury," *Journal of Cellular Biochemistry*, vol. 98, no. 2, pp. 243–250, 2006.

[18] C. Fabrizi, F. Somma, E. Pompili et al., "Role of autophagy inhibitors and inducers in modulating the toxicity of trimethyltin in neuronal cell cultures," *Journal of Neural Transmission*, pp. 1–11, 2012.

[19] M. Sahebgharani, M. Nejati, Z. Sepehrizadeh et al., "Lithium chloride protects PC12 pheochromocytoma cell line from morphine-induced apoptosis," *Archives of Iranian Medicine*, vol. 11, no. 6, pp. 639–648, 2008.

[20] B. N. Frey, A. C. Andreazza, K. M. M. Ceresér et al., "Effects of mood stabilizers on hippocampus BDNF levels in an animal model of mania," *Life Sciences*, vol. 79, no. 3, pp. 281–286, 2006.

[21] J. C. Walz, B. N. Frey, A. C. Andreazza et al., "Effects of lithium and valproate on serum and hippocampal neurotrophin-3 levels in an animal model of mania," *Journal of Psychiatric Research*, vol. 42, no. 5, pp. 416–421, 2008.

Hindawi Publishing Corporation
International Journal of Cell Biology
Volume 2013, Article ID 297537, 15 pages
http://dx.doi.org/10.1155/2013/297537

Research Article

Modulation of Vascular Cell Function by Bim Expression

Margaret E. Morrison,[1] Tammy L. Palenski,[2] Nasim Jamali,[2] Nader Sheibani,[2,3] and Christine M. Sorenson[1,3]

[1] *Department of Pediatrics, University of Wisconsin School of Medicine and Public Health, 600 Highland Avenue, H4/444 CSC, Madison, WI 53792-4108, USA*
[2] *Department of Ophthalmology and Visual Sciences, University of Wisconsin School of Medicine and Public Health, Madison, WI 53792, USA*
[3] *McPherson Eye Research Institute, University of Wisconsin School of Medicine and Public Health, Madison, WI 53792, USA*

Correspondence should be addressed to Christine M. Sorenson; cmsorenson@pediatrics.wisc.edu

Received 24 July 2013; Accepted 4 September 2013

Academic Editor: Claudia Giampietri

Apoptosis of vascular cells, including pericytes and endothelial cells, contributes to disease pathogenesis in which vascular rarefaction plays a central role. Bim is a proapoptotic protein that modulates not only apoptosis but also cellular functions such as migration and extracellular matrix (ECM) protein expression. Endothelial cells and pericytes each make a unique contribution to vascular formation and function although the details require further delineation. Here we set out to determine the cell autonomous impact of Bim expression on retinal endothelial cell and pericyte function using cells prepared from Bim deficient ($Bim^{-/-}$) mice. $Bim^{-/-}$ endothelial cells displayed an increased production of ECM proteins, proliferation, migration, adhesion, and VEGF expression but, a decreased eNOS expression and nitric oxide production. In contrast, pericyte proliferation decreased in the absence of Bim while migration, adhesion, and VEGF expression were increased. In addition, we demonstrated that the coculturing of either wild-type or $Bim^{-/-}$ endothelial cells with $Bim^{-/-}$ pericytes diminished their capillary morphogenesis. Thus, our data further emphasizes the importance of vascular cell autonomous regulatory mechanisms in modulation of vascular function.

1. Background

Apoptosis facilitates the removal of unwanted cells during development and maintains tissue homeostasis. Bcl-2 family members influence apoptosis in either a positive or a negative fashion. Family members are classically grouped into three subclasses including one that inhibits apoptosis, a second that induces apoptosis and a third contains that family members, such as Bim, that only have a BH3 domain that binds antiapoptotic family members to promote apoptosis [1]. Bcl-2 exerts opposing effects with regards to apoptosis compared with Bim, consistent with their opposing effects on cell adhesion and migration [2]. The removal of a single allele of Bim is sufficient to prevent the degenerative disorders caused by Bcl-2 deficiency [3, 4]. Bim expression is also essential for apoptosis of a wide range of growth factor deprived cells [5], including endothelial cells and pericytes [6]. Therefore, improper modulation of apoptosis could impact the development and/or the pathogenesis of many diseases including diabetic retinopathy.

Murine retinal vascular development proceeds after birth and is complete by postnatal day 21 (P21). Remodeling and pruning of the retinal vasculature continue until P42 [7, 8]. Pro- and anti-apoptotic factors regulate apoptosis during retinal vascular development, remodeling, and regression [8–10]. Bim influences not only apoptosis but also cell adhesion, migration, and extracellular matrix (ECM) protein expression. The ability of Bim to impact both apoptosis and the ECM milieu is integral to its role during retinal vessel remodeling, and regression. However, whether Bim expression impacts retinal endothelial cell and pericyte function in a similar manner remains to be determined.

Our previous studies demonstrated that Bim modulates retinal vascular development, remodeling, and regression

[11]. Bim deficient ($Bim^{-/-}$) mice demonstrated precocious formation of the retinal vascular plexus, increased vascular density, and attenuated hyaloid vessel regression. Loss of Bim expression also protected the retinal vasculature from hyperoxia-mediated vessel obliteration and neovascularization during oxygen induced ischemic retinopathy (OIR) [11]. These studies indicated that Bim expression is essential for retinal vascular remodeling but did not implicate a specific vascular cell type. Thus, understanding the role Bim plays in modulating endothelial cell and pericyte function will give us further insight into how aberrant regulation of retinal vessel development and remodeling can be avoided to preserve vision.

Endothelial cells and pericytes play specialized roles in the retina during the development and maintenance of the vasculature. Pericyte coverage of vascular sprouts stabilizes the vessels while endothelial cells provide the inner lining of the blood vessel [12, 13]. Retinal endothelial cell and pericyte dysfunction can lead to retinal vascular rarefaction and subsequent vision loss as the one that occurs in diabetic retinopathy. Here, we assessed whether the loss of the proapoptotic protein Bim differentially impacts the retinal endothelial cell and pericyte function. We observed an increased VEGF expression, ECM protein production, cell migration, proliferation, and adhesion in $Bim^{-/-}$ retinal endothelial cells compared with wild-type cells. Although the decreased endothelial nitric oxide synthase (eNOS) expression corresponded with decreased nitric oxide (NO) production in $Bim^{-/-}$ retinal endothelial cells, capillary morphogenesis was similar to that observed in wild-type retinal endothelial cells. In contrast to $Bim^{-/-}$ retinal endothelial cells, $Bim^{-/-}$ pericytes displayed decreased proliferation compared with their wild-type counterpart. $Bim^{-/-}$ pericytes also demonstrated increased migration, adhesion, and VEGF expression. Coculturing wild-type or $Bim^{-/-}$ retinal endothelial cells with $Bim^{-/-}$ pericytes diminished capillary morphogenesis. The data presented here demonstrate that the deletion of Bim differentially impacts retinal endothelial cell and pericyte function, perhaps through the modulation of response to their microenvironment.

2. Results

2.1. $Bim^{-/-}$ Retinal Endothelial Cells and Pericytes Demonstrate Aberrant Proliferation. To further investigate the role Bim plays in retinal vascular function, we isolated retinal endothelial cells and pericytes from wild-type and $Bim^{-/-}$ mice as previously described [2, 14–17]. We first examined retinal endothelial cell and pericyte morphology and their expression of cell specific markers to confirm that these cells maintain their endothelial cell and pericyte characteristics. $Bim^{-/-}$ retinal endothelial cells displayed a slightly elongated morphology compared to wild-type cells when plated on gelatin-coated plates (Figure 1(a)). The morphology of wild-type and $Bim^{-/-}$ retinal pericytes was similar (Figure 1(b)). Wild-type and $Bim^{-/-}$ retinal endothelial cells expressed the endothelial cell markers VE-cadherin and PECAM-1 (Figure 1(c)). Retinal pericytes expressed the pericyte markers platelet derived growth factor-receptor β (PDGFRβ) and neuroglia proteoglycan 2 (NG2) (Figure 1(d)).

Next we examined the rate of retinal endothelial cell and pericyte apoptosis and proliferation. Wild-type and $Bim^{-/-}$ retinal endothelial cells and pericytes were incubated with staurosporine to induce apoptosis. Although the basal levels of apoptosis were similar, upon incubation with staurosporine for 24 h, $Bim^{-/-}$ endothelial cells and pericytes demonstrated less apoptosis compared to wild-type cells (Figures 2(a) and 2(b)). Next cell proliferation was examined by counting the number of cells every other day for 2 weeks. Figure 2(c) shows that $Bim^{-/-}$ retinal endothelial cells proliferated at a faster rate than their wild-type counterpart. In contrast, $Bim^{-/-}$ pericytes demonstrated a reduced rate of proliferation compared to their wild-type counterpart (Figure 2(d)).

2.2. Loss of Bim Expression Enhances Retinal Endothelial Cell and Pericyte Migration. An appropriate rate of migration is essential for optimal capillary morphogenesis. Here we examined cell migration characteristics using scratch wound and transwell migration assays. A confluent monolayer of wild-type and $Bim^{-/-}$ endothelial cells (Figure 3(a)) and pericytes (Figure 3(b)) was wounded, and 5-fluorouracil (5-FU) was added to prevent cell proliferation. Both Bim deficient retinal endothelial cells and pericytes migrated faster than their wild-type counterparts (Figures 3(a) and 3(b)). A quantitative assessment of the scratch wound data for endothelial cells and pericytes is shown in Figures 3(c) and 3(d), respectively. Enhanced migration of $Bim^{-/-}$ endothelial cells and pericytes was also observed using a transwell migration assay as shown in Figures 3(e) and 3(f), respectively. Thus, the lack of Bim expression enhances the migration of retinal vascular cells.

2.3. $Bim^{-/-}$ Retinal Vascular Cells Were More Adherent. Changes in migration of $Bim^{-/-}$ retinal vascular cells could be due to altered cell adhesion. We next examined the ability of wild-type and $Bim^{-/-}$ endothelial cells (Figure 4(a)) and pericytes (Figure 4(b)) to adhere to fibronectin, collagen I, collagen IV, and vitronectin. Bim deficient endothelial cells and pericytes displayed increased adhesion to all of these matrices compared to their wild-type counterpart.

Changes in cell migration and adhesion could be the result of aberrant integrin expression. Next we analyzed the integrin expression on the surface of retinal endothelial cells and pericytes by FACScan analysis (Figures 5(a) and 5(b)). Wild-type and $Bim^{-/-}$ endothelial cells expressed similar levels of $\alpha 5$, $\alpha v\beta 3$, and $\beta 1$ integrins on their surface while wild-type and $Bim^{-/-}$ retinal pericytes expressed similar levels of $\alpha 2$, $\alpha v\beta 3$, $\beta 1$, and $\beta 3$ integrins. Thus, the increased adhesion noted in $Bim^{-/-}$ retinal vascular cells may be independent of significant changes in the integrin expression and may be due to alterations in the affinity and/or avidity of these integrins.

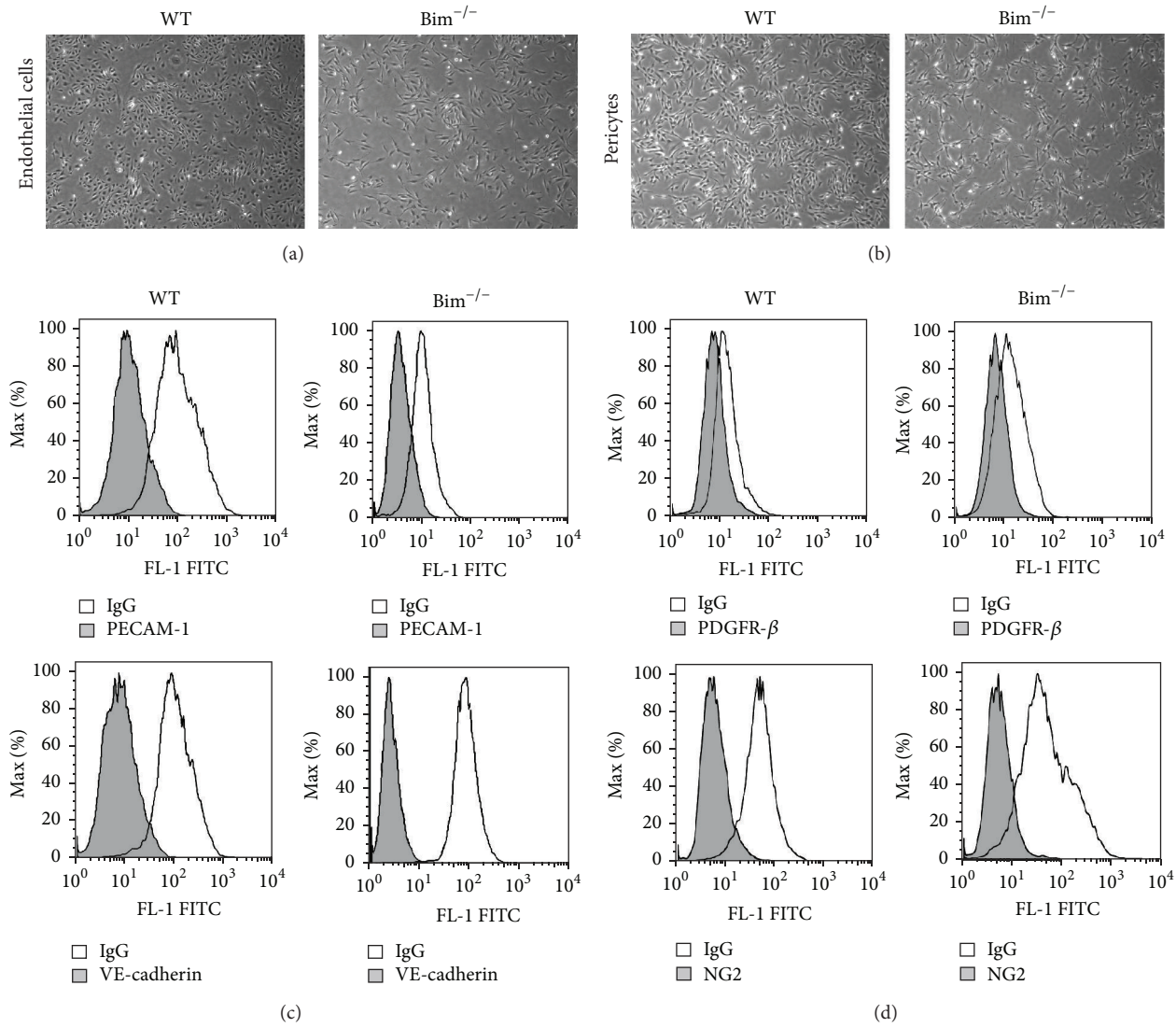

Figure 1: Wild-type and Bim$^{-/-}$ cells morphology. Wild-type and Bim$^{-/-}$ retinal endothelial cells (panel (a)) and pericytes (panel (b)) were cultured on gelatin or uncoated plates, respectively. Cells were photographed using a phase microscope in digital format at low magnification (×40). In panel (c), retinal endothelial cells prepared from wild-type and Bim$^{-/-}$ mice were examined for the expression of PECAM-1 and VE-cadherin FACScan analysis. In panel (d), retinal pericytes from wild-type and Bim$^{-/-}$ mice were examined for the expression of NG2 and PDGFR-β by FACScan analysis. The shaded areas show staining in the presence of control IgG.

2.4. Increased Tenascin C and Osteopontin Expression in Bim$^{-/-}$ Retinal Endothelial Cells. Modulating the ECM milieu can influence vascular cell functions including cell adhesion and migration. To examine whether the lack of Bim expression differentially impacts retinal endothelial cell or pericyte ECM expression, serum-free conditioned medium from these retinal vascular cells was evaluated by Western blot analysis. Retinal endothelial cells from Bim$^{-/-}$ mice displayed an increased expression of tenascin C, osteopontin, fibronectin, and TSP1 compared to their wild-type counterpart (Figure 6(a)). In contrast, Bim$^{-/-}$ retinal pericytes displayed similar levels of tenascin C, fibronectin, but an increased TSP1 and a decreased osteopontin expression (Figure 6(b)).

2.5. Decreased p-eNOS Expression in Bim$^{-/-}$ Retinal Endothelial Cells. The activation of eNOS and Akt1 by VEGF promotes angiogenesis [18–20]. In the absence of Bim, VEGF expression was dramatically increased in retinal endothelial cells and pericytes (Figures 7(a) and 7(b)). However, in Bim$^{-/-}$ retinal endothelial cells, the increased VEGF expression did not affect Akt, phospho-Akt, or HSP90 expression (Figure 7(c)). Bim$^{-/-}$ retinal endothelial cells also demonstrated nearly undetectable eNOS expression (Figure 7(c))

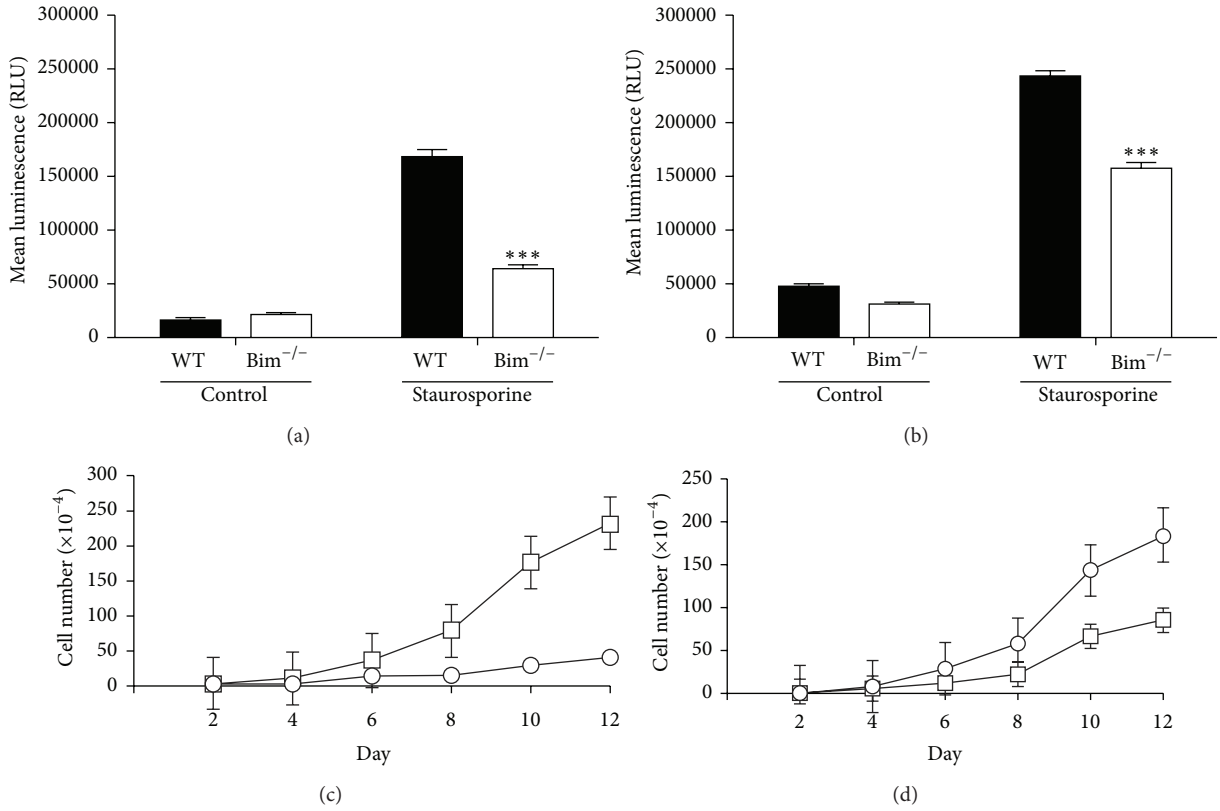

FIGURE 2: Modulation of proliferation in $Bim^{-/-}$ cells. Wild-type and $Bim^{-/-}$ retinal endothelial cells (panel (a)) and pericytes (panel (b)) were incubated with 10 nM staurosporine for 24 hours. Apoptosis was determined using a Caspase-Glo 3/7 assay. Wild-type and $Bim^{-/-}$ retinal endothelial cells (panel (c)) and pericytes (panel (d)) were monitored for their growth rate over a two-week time frame for wild-type (○) and $Bim^{-/-}$ (□) cells. These experiments were repeated twice with similar results ($^{***}P < 0.001$).

which corresponded with a 25-fold decrease in NO production (Figure 7(d)). Thus, VEGF activation of eNOS through the activation of Akt is uncoupled in the absence of Bim.

2.6. $Bim^{-/-}$ Pericytes Disrupt Retinal Endothelial Cell Capillary Morphogenesis. Capillary morphogenesis is fundamental in vascular development and remodeling in which pericytes play a major role. The ability of pericytes to migrate and produce survival factors is central to their recruitment along the developing endothelium. However, pericytes typically do not undergo any substantial morphogenesis in Matrigel [21]. In the retina, endothelial cells and pericytes function together to facilitate retinal vascularization. Here, we evaluated the ability of pericytes from wild-type and $Bim^{-/-}$ mice to impact retinal endothelial cell capillary morphogenesis.

Wild-type and $Bim^{-/-}$ endothelial cells demonstrated a similar number of branch points in Matrigel (Figures 8(a)–8(c)). However, $Bim^{-/-}$ endothelial cells formed rather stunted capillary-like tubes compared with wild-type cells (Figures 8(a)–8(c)). Next, we cocultured wild-type retinal endothelial cells with either wild-type or $Bim^{-/-}$ pericytes. Wild-type retinal endothelial cells cocultured with wild-type pericytes demonstrated an improved tubular network compared to wild-type endothelial cells alone (Figures 8(a)–8(c)). In contrast, wild-type retinal endothelial cells cocultured with $Bim^{-/-}$ pericytes demonstrated diminished capillary morphogenesis. $Bim^{-/-}$ endothelial cells cocultured with wild-type pericytes demonstrated enhanced capillary morphogenesis while cocultures of $Bim^{-/-}$ endothelial cells and pericytes demonstrated diminished capillary morphogenesis (Figures 8(a) and 8(c)). Thus, coculturing of retinal endothelial cells with $Bim^{-/-}$ pericytes resulted in diminished endothelial cell capillary morphogenesis.

$Bim^{-/-}$ pericytes demonstrated increased VEGF levels compared to their wild-type counterpart. Next, we addressed whether an increased VEGF expression contributed to the inability of wild-type endothelial cells to undergo capillary morphogenesis when cocultured with $Bim^{-/-}$ pericytes. VEGFR-1 (Flt-1) has a higher affinity for VEGF compared to VEGFR-2 and can compete for VEGF binding to VEGFR-2 and its activation. Thus, the soluble form of Flt-1 can act as a trap for VEGF and prevent its signaling. Here, we used sFlt-1 FC chimera to demonstrate that the negative impact of $Bim^{-/-}$ pericytes on capillary morphogenesis of retinal endothelial cells is driven by the production of excess VEGF. The sFlt1 was added to wild-type endothelial cell and $Bim^{-/-}$ pericyte coculture experiments, and capillary morphogenesis was monitored (Figure 8(d)). As shown

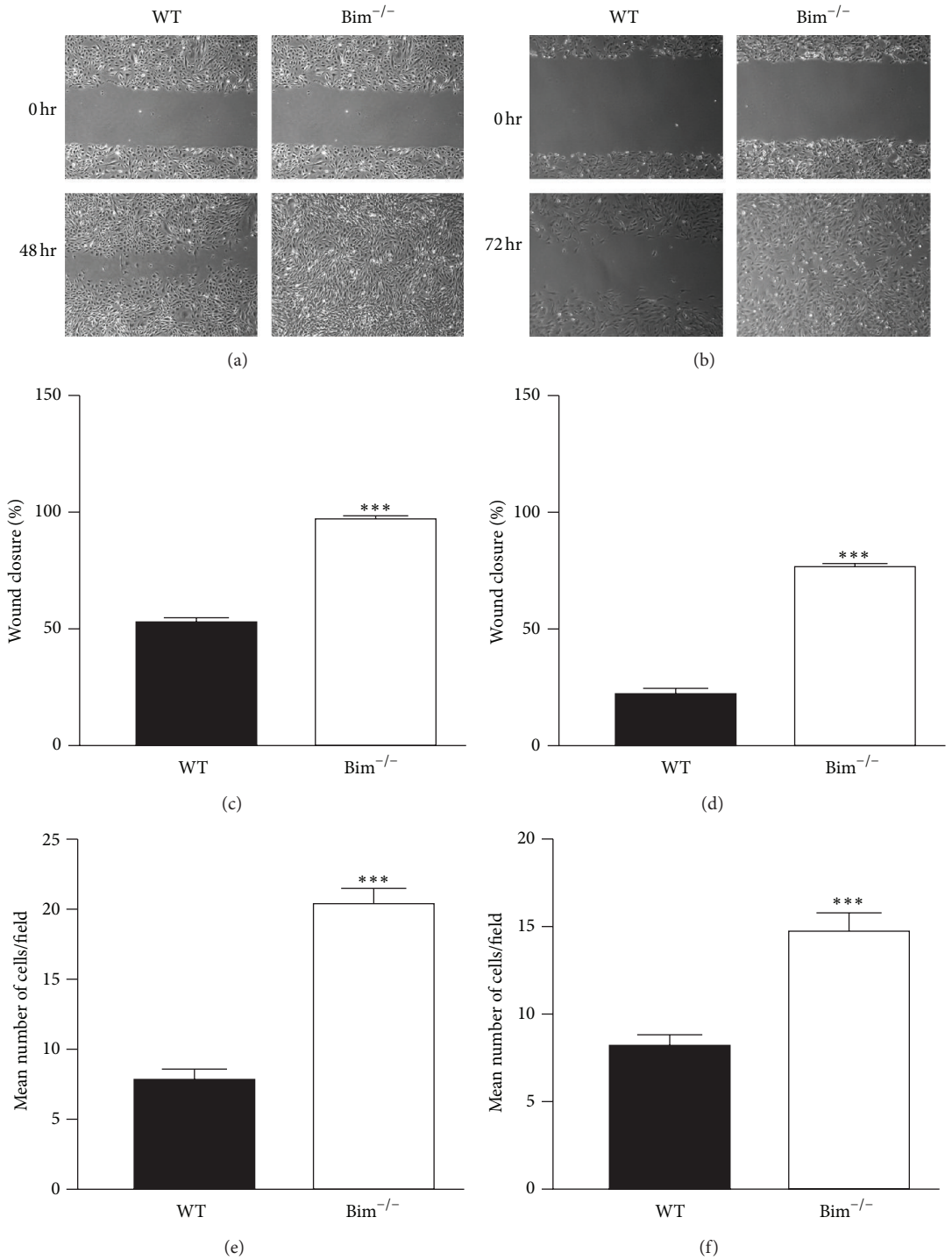

Figure 3: $Bim^{-/-}$ retinal endothelial cells and pericytes demonstrate increased migration. Cell migration was determined by the scratch wounding of retinal endothelial cells (panel (a)) or pericytes (panel (b)) monolayers, and wound closure was monitored using a phase microscope in digital format at low magnification (×40). A representative experiment is shown here. Please note that wild-type vascular cells migrate slower than $Bim^{-/-}$ cells. The quantitative assessment of the data is shown in panels (c) and (d). Transwell assays were performed with wild-type and $Bim^{-/-}$ retinal endothelial cells (panel (e)) and pericytes (panel (f)). These experiments were repeated twice with similar results ($^{***}P < 0.001$).

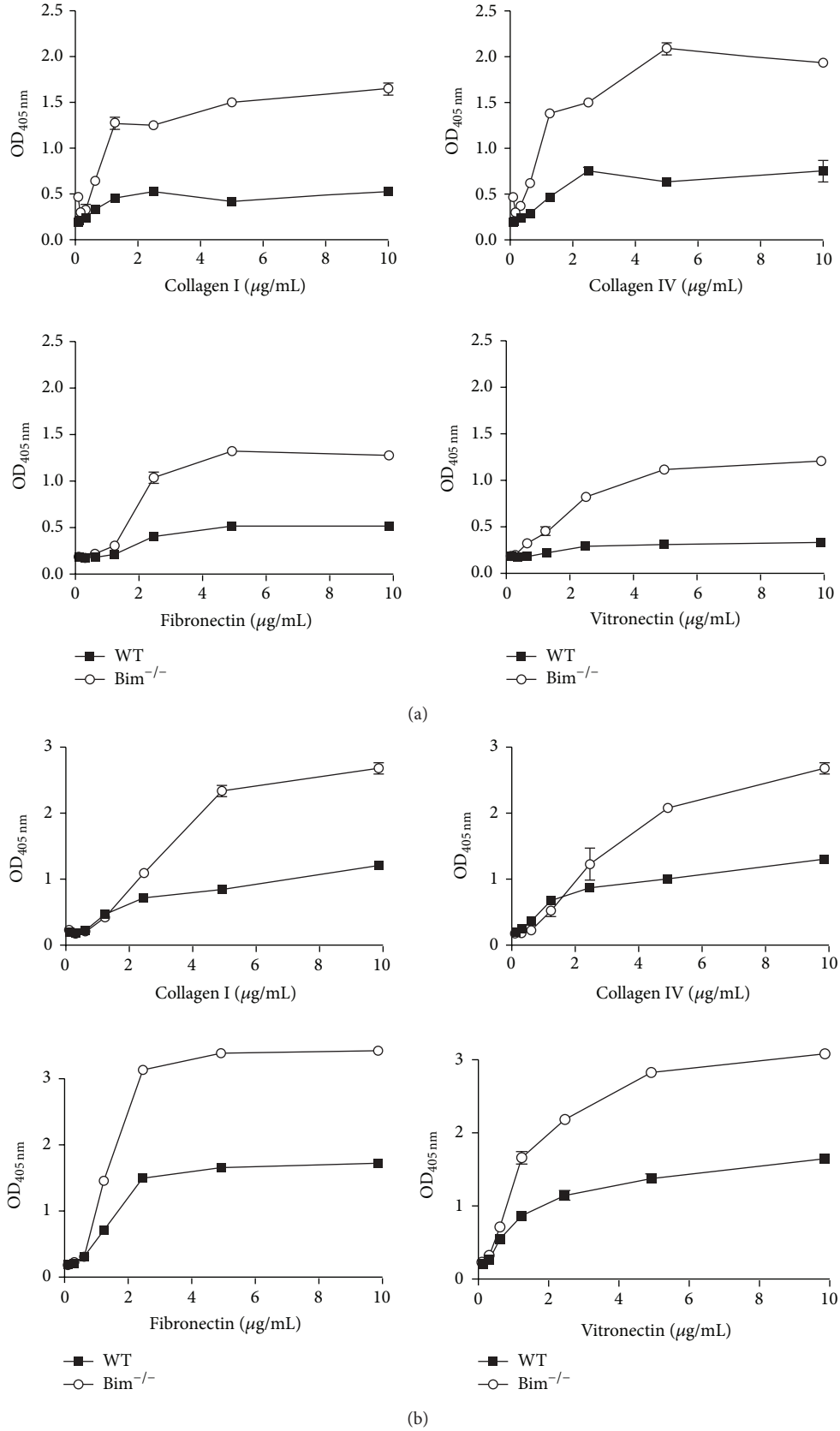

Figure 4: $Bim^{-/-}$ endothelial cells and pericytes were more adherent. The adhesion of retinal wild-type (■) and $Bim^{-/-}$ (○) endothelial cells (panel (a)) and pericytes (panel (b)) to fibronectin, vitronectin, collagen type I, or collagen IV was determined as described in Section 5. Please note that $Bim^{-/-}$ vascular cells had increased adherence. These experiments were repeated twice with similar results.

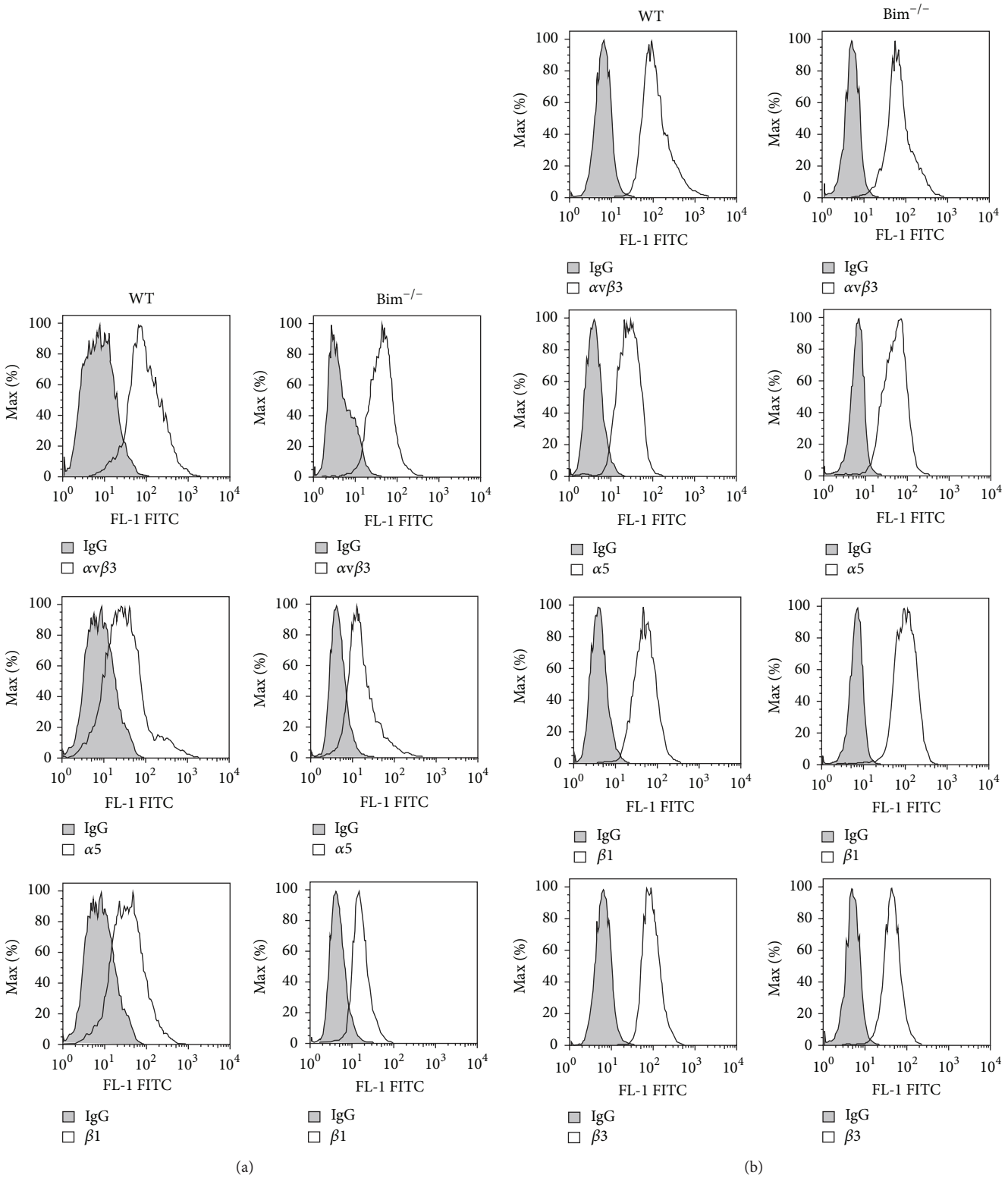

Figure 5: Wild-type and Bim$^{-/-}$ retinal vascular cells had similar integrin expression. Expression of various integrins was determined in wild-type and Bim$^{-/-}$ endothelial cells (panel (a)) and pericytes (panel (b)) using FACScan analysis as described in Section 5. The shaded graphs show staining in the presence of control IgG. These experiments were repeated twice with similar results.

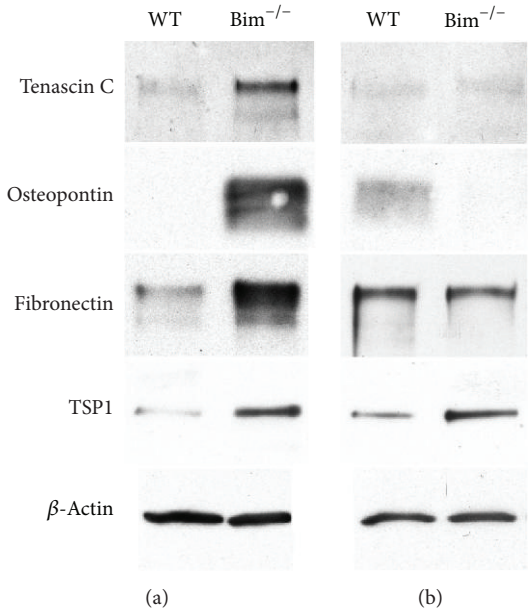

Figure 6: Altered expression of ECM proteins in $Bim^{-/-}$ retinal cells. Wild-type and $Bim^{-/-}$ retinal endothelial cells (panel (a)) and pericytes (panel (b)) were grown for 2 days in serum-free medium. The medium was harvested, clarified, and Western-blotted for extracellular matrix proteins as noted. The expression of β-actin from total cell lysates was used as a loading control. These experiments were repeated twice with similar results.

above, coculture of wild-type endothelial cells with $Bim^{-/-}$ pericytes demonstrated decreased numbers of branch points compared to wild-type endothelial cells alone. The addition of sFlt1 to wild-type endothelial and $Bim^{-/-}$ pericyte coculture experiments significantly restored branching morphogenesis in Matrigel. The addition of control IgG to wild-type endothelial cell and $Bim^{-/-}$ pericyte coculture experiments did not impact the number of branch points (Figures 8(d) and 8(e)). Therefore, enhanced VEGF expression contributes to the decreased capillary morphogenesis of endothelial cells cocultured with $Bim^{-/-}$ pericytes.

3. Discussion

Aberrant modulation of apoptosis has a reoccurring theme in many diseases that result in blindness. The regression of the hyaloid vasculature is an apoptosis-driven process in which Bim expression plays a central role [11]. Failure of the hyaloid vasculature to regress is a common congenital ocular malformation that can lead to blindness [22]. Improper modulation of apoptosis can also contribute to retinal vascular rarefaction and/or neovascularization, observed during retinopathy of prematurity and diabetic retinopathy. Thus, understanding how apoptosis is modulated in retinal vascular cells, including endothelial cells and pericytes, will further our understanding of normal and abnormal retinal vascularization and vascular cell autonomous functions.

The retina has the highest numbers of pericytes covering its blood vessels compared to other tissues [23]. The appropriate interaction of pericytes with each other and endothelial cells is important for vessel maturation and stabilization. Altered pericyte migration or adhesion may disrupt or enhance these interactions leading to vasculopathies or increased vascular stabilization. Here, we show that pericyte migration and adhesion are enhanced in the absence of Bim perhaps as a result of their increased VEGF expression. Increased pericyte migration may lead to greater pericyte coverage of the retinal vasculature, which may contribute to the precocious formation of the deep vascular plexus and protection from hyperoxia-mediated vessel obliteration that we previously observed [11].

Maturation of the retinal vasculature involves remodeling and pruning of vessels into an organized branched network of vessels to meet the demand of the tissue. Modulation of apoptosis by Bcl-2 family members facilitates retinal vascular remodeling and regression [11, 24]. Bim expression is required for retinal capillary pruning, hyaloid vessel regression, and hyperoxia-induced retinal vessel obliteration [11]. Here, we have extended these findings to delineate the role Bim plays in retinal endothelial cell and pericyte function. We show that in addition to enhanced migration, retinal pericytes from $Bim^{-/-}$ mice were resistant to an apoptotic challenge and demonstrated an increased adhesion to extracellular matrices. Extracellular matrix protein expression by pericytes was only modestly impacted by the loss of Bim expression. Perhaps an increased pericyte adhesion in the absence of Bim enhances pericyte survival and coverage of retinal vessels. This may explain the resistance of the retinal vasculature of $Bim^{-/-}$ mice to developmental pruning or excessive pruning in response to hyperoxia. Therefore, modulating pericyte adhesion and migratory properties may be essential for retinal vascular pruning.

VEGF expression is thought to be a key player in maintaining endothelial cell homeostasis. Since VEGF withdrawal can lead to endothelial cell apoptosis, determining how VEGF levels can be modulated by expression of Bcl-2 family members may aid in our understanding of normal and aberrant retinal vascularization and pruning. Here, we show that Bim deficiency increases VEGF levels in both endothelial cells and pericytes. Pericytes act as an angiogenic soup, producing 7-fold higher VEGF levels than their endothelial cell counterpart (Figure 7). In the absence of Bim, VEGF expression in retinal endothelial cells increased to nearly twice that observed in wild-type pericytes. Unfortunately, VEGF can also inhibit blood vessel maturation and ablate pericyte coverage of nascent sprouts causing vessel destabilization [25]. The increased VEGF produced by $Bim^{-/-}$ pericytes may result in the diminished capillary morphogenesis observed when cocultured with either wild-type or $Bim^{-/-}$ endothelial cells. Greenberg et al. [25] have also defined VEGF as an inhibitor of neovascularization which is consistent with the inability of $Bim^{-/-}$ mice to undergo neovascularization following hyperoxia-induced ischemia [11]. However, retinal development in these mice proceeds quite well with precocious formation of the retinal vascular plexus and increased

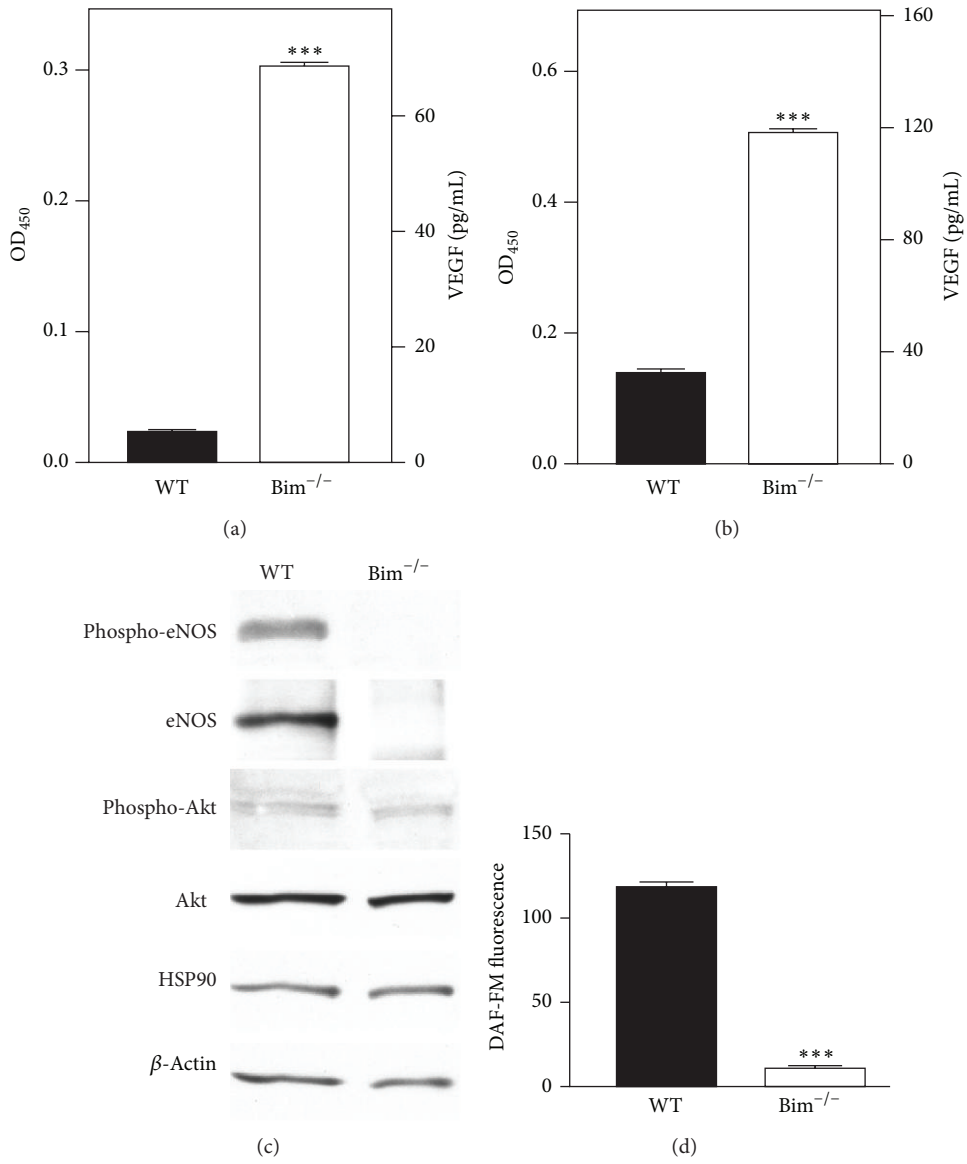

Figure 7: Decreased eNOS and increased VEGF expressions in $Bim^{-/-}$ vascular cells. In panels (a) and (b), an immunoassay was used to determine VEGF levels (pg/mL) in retinal endothelial cells (a) and pericytes (b) from wild-type and $Bim^{-/-}$ mice. Protein lysates (20 μg) from wild-type and $Bim^{-/-}$ retinal endothelial cells were analyzed by Western blot analysis for the expression of phospho-eNOS, eNOS, HSP90, phospho-Akt, and Akt (panel (c)). β-Actin expression was assessed as a loading control (panel (c)). In panel (d), the intracellular NO production was determined as analyzed by DAF-FM fluorescence for retinal endothelial cells. Please note that the increased VEGF expression was independent of eNOS expression in $Bim^{-/-}$ endothelial cells ($^{***}P < 0.001$).

vascular density in contrast to what has been previously shown in fibrosarcomas [11, 25]. Thus, the ability of Bim to impact cell survival may be, in part, through the modulation of VEGF expression.

Phosphorylation of eNOS can mediate the proangiogenic activity of VEGF. Here, we show an increased VEGF expression but a decreased eNOS expression in $Bim^{-/-}$ retinal endothelial cells, consistent with our previous studies in $Bim^{-/-}$ kidney and lung endothelial cells [2]. Moreover, our recent studies further support a reciprocal relationship between VEGF and eNOS expressions in endothelial cells [26]. Our previous studies demonstrated that knocking down eNOS expression in kidney endothelial cells from diabetic mice not only decreased VEGF expression but also restored migration and capillary morphogenesis [26]. Thus, local regulation of Bim expression may play a central role in vascular pruning through modulating eNOS and VEGF expressions.

4. Conclusions

Our previous studies demonstrated an inability of the retinas from $Bim^{-/-}$ mice to undergo retinal vascular pruning

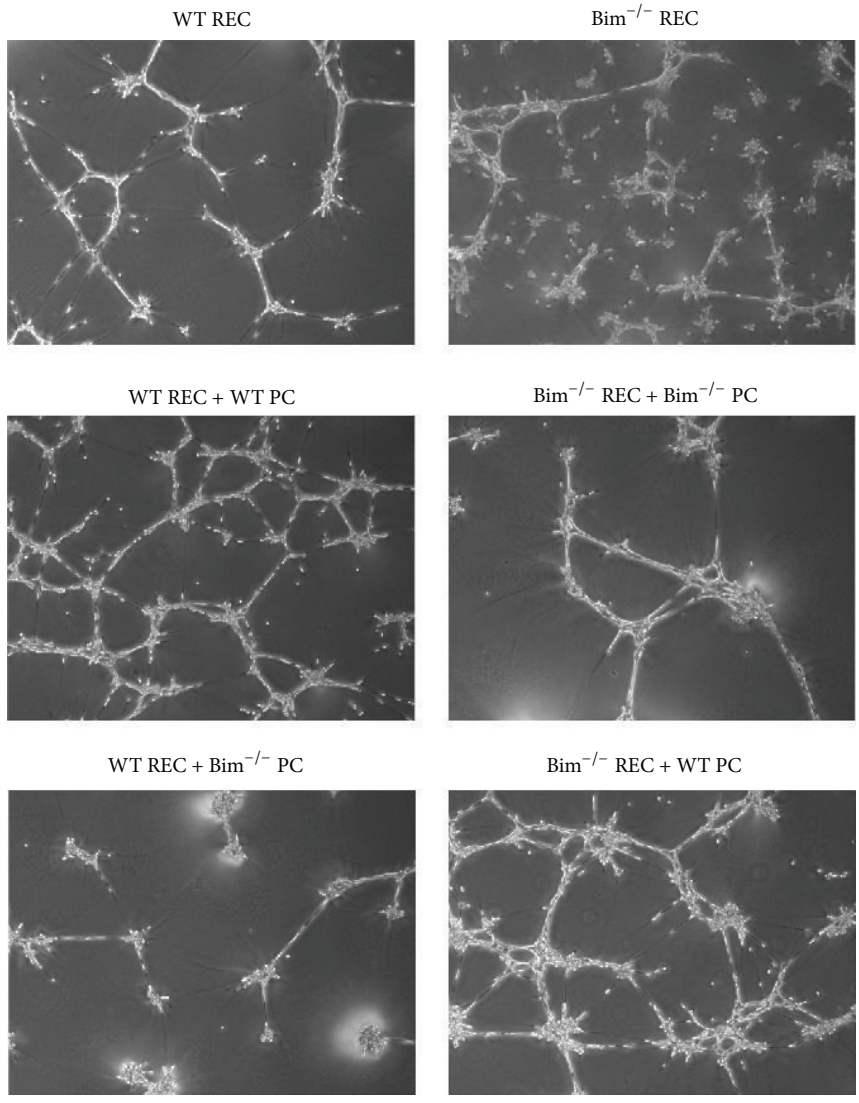

Figure 8: Continued.

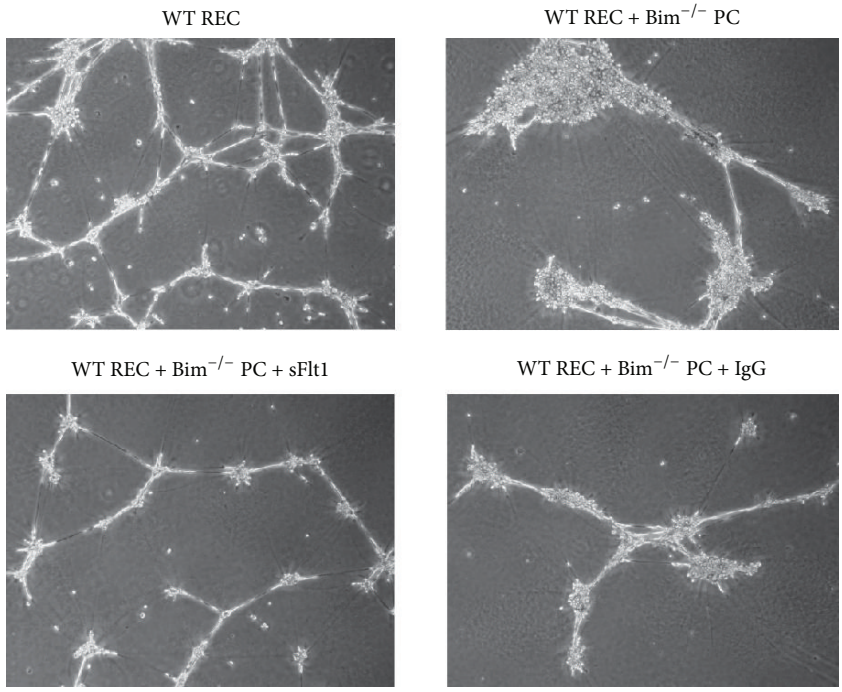

(d)

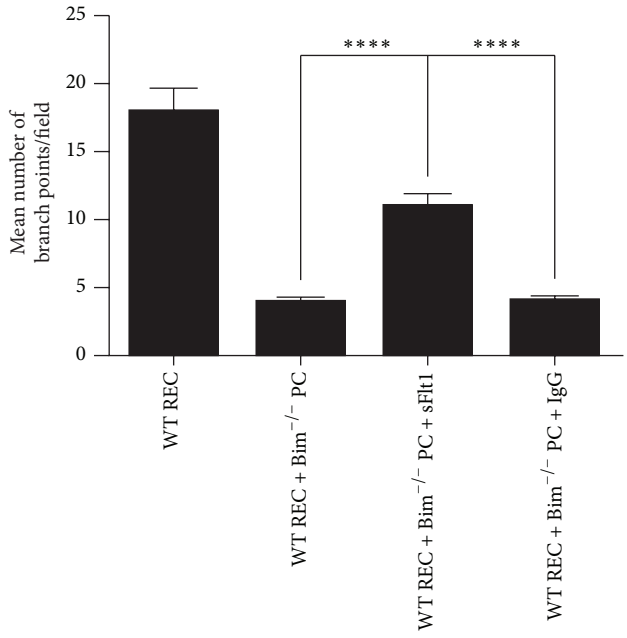

(e)

FIGURE 8: Bim$^{-/-}$ pericytes diminished capillary morphogenesis of retinal endothelial cells. Wild-type (WT) and Bim$^{-/-}$ retinal endothelial cells (REC) were plated alone or with wild-type or Bim$^{-/-}$ pericytes (PC) in Matrigel and photographed in digital format (panel (a)). The quantitative assessment of the data is shown in panels (b) and (c). In panel (d), wild-type retinal endothelial cells were plated alone or with Bim$^{-/-}$ pericytes in the presence or absence of sFlt1 or IgG control (10 μg/mL) and photographed. Panel (e) is the quantitative assessment of the data in panel (d). The data are the mean number of branch points per field (×40) ± SD. These experiments were repeated at least twice with similar results ($^{***}P < 0.001$; $^{****}P < 0.0001$).

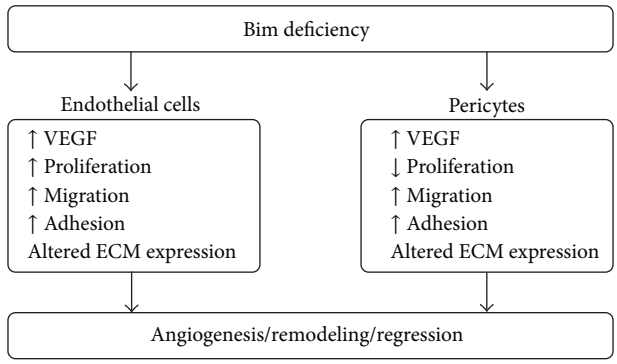

Figure 9: A summary of the modulation of VEGF expression, proliferation, migration, adhesion, and ECM expression in Bim deficient endothelial cells and pericytes.

leading to increased retinal cellularity and capillary loops [11]. These mice were also resistant to hyperoxia-mediated vessel obliteration and neovascularization during OIR, as well as a hyaloid vessel regression. Thus, Bim expression may modulate retinal vascular pruning by localized changes in retinal vascular cell adhesion, migration, and VEGF expression (Figure 9) thereby, either protecting or inducing pruning by localized apoptosis.

5. Methods

5.1. Experimental Animals and Cell Cultures. The mice used for these studies were maintained and treated in accordance with our protocol approved by the University of Wisconsin Animal Care and Use Committee. Immortomice expressing a temperature-sensitive SV40 large T antigen were obtained from Charles River Laboratories (Wilmington, MA, USA). $Bim^{-/-}$ mice (Jackson Laboratory, Bar Harbor, ME, USA) were crossed with Immortomice and screened as previously described [2, 17]. To isolate retinal endothelial cells, retinas from approximately four- to five-week-old wild type and $Bim^{-/-}$ Immortomice were dissected out aseptically and placed in serum-free Dulbecco's Modified Eagle Medium (DMEM) containing penicillin/streptomycin (Sigma, St. Louis, MO, USA). The retinas were pooled together, rinsed with DMEM, minced into small pieces in a 60 mm tissue culture dish using sterilized razor blades, and digested in 5 mL of collagenase type I (1 mg/mL in serum-free DMEM; Worthington, Lakewood, NJ, USA) for 30–45 minutes at 37°C. Following digestion, DMEM containing 10% fetal bovine serum (FBS) was added and cells were pelleted. The cellular digests were then filtered through a double layer of sterile 40 μm nylon mesh (Sefar America Inc., Hanover Park, IL, USA), centrifuged at 400 ×g for 10 min to pellet cells, and then washed twice with DMEM containing 10% FBS. The cells were resuspended in 1.5 mL medium (DMEM with 10% FBS) and incubated with sheep anti-rat magnetic beads precoated with anti-PECAM-1 antibody (MEC13.3, BD Biosciences, Bedford, MA, USA) as described previously [27]. After affinity binding, magnetic beads were washed six times with DMEM containing 10% FBS. Bound cells in endothelial cell growth medium were plated into a single well of a 24-well plate precoated with 2 μg/mL of human fibronectin (BD Biosciences). Endothelial cells were grown in DMEM containing 10% FBS, 2 mM L-glutamine, 2 mM sodium pyruvate, 20 mM HEPES, 1% nonessential amino acids, 100 μg/mL streptomycin, 100 U/mL penicillin, heparin at 55 U/mL (Sigma, St. Louis, MO, USA), endothelial growth supplement 100 μg/mL (Sigma, St. Louis, MO, USA), and murine recombinant interferon-γ (R&D, Minneapolis, MN, USA) at 44 units/mL. Cells were maintained at 33°C with 5% CO_2. Cells were progressively passed to larger plates, maintained, and propagated in 1% gelatin-coated 60 mm dishes. Retinal endothelial cells were positive for B4-lectin (a mouse endothelial cell specific lectin) and expressed PECAM-1 and VE-cadherin as previously described [2, 14].

Pericytes were isolated from mouse retina by collecting retinas from one litter (6-7 pups, 4 weeks old) using a dissecting microscope. Retinas (12 to 14) were rinsed with serum-free Dulbecco's Modified Eagle's Medium (Sigma), pooled in a 60 mm dish, minced, and digested for 45 min with collagenase type II (1 mg/mL; Worthington, Lakewood, NJ, USA) with 0.1% bovine serum albumin (BSA) in serum-free DMEM at 37°C. Cells were rinsed in DMEM containing 10% fetal bovine serum (FBS) and centrifuged for 5 min at 400 ×g. Digested tissue was resuspended in 4 mL of DMEM containing 10% FBS, 2 mM L-glutamine, 100 μg/mL streptomycin, 100 U/mL penicillin, and the murine recombinant interferon-γ (R&D, Minneapolis, MN, USA) at 44 U/mL. Cells, tissue, and medium were evenly divided into 4 wells of a 24-well tissue culture plate and maintained at 33°C with 5% CO_2. Cells were progressively passed to larger plates, maintained, and propagated in 60 mm dishes [21]. The experiments described here were performed with two separate isolations of cells with similar results.

5.2. Cell Apoptosis Assays. Apoptosis was determined by measuring caspase activation using a Caspase-Glo 3/7-assay kit as recommended by the supplier (Promega, Madison, WI, USA). The assay provides caspase-3/7 DEVD-aminoluciferin substrate and the caspase 3/7 activity is detected by luminescent signal. For the assay, cells were plated at 8×10^3 per well of a 96-well plate. As an oxidative or apoptotic stimulus, cells were incubated with 10 nM staurosporine (Invitrogen),

in growth medium for 24 h at 33°C. Caspase activity was detected using a luminescent microplate reader (Victa2 1420 Multilabel Counter, PerkinElmer, Waltham, MA, USA). All samples were prepared in triplicate and repeated twice with similar results [15].

5.3. Scratch Wound Assay. Cells (4×10^5) were plated in 60 mm tissue culture dishes and allowed to reach confluence (2-3 days). After aspirating the medium, cell layers were wounded using a 1 mL micropipette tip. Plates were then rinsed with PBS, fed with growth medium containing 100 ng/mL of 5-fluorouracil (5-FU), to rule out potential contribution of differences in cell proliferation. The wounds were observed and photographed every 24 hours for up to 72 hours. The distance migrated was determined as a percent of total distance for quantitative assessments as described previously [2]. These experiments were repeated at least twice with two different isolations with similar results.

5.4. Capillary Morphogenesis in Matrigel. Matrigel (10 mg/mL; BD Biosciences) was applied at 0.5 mL/well of a 6-well tissue culture dish and incubated at 37°C for at least 30 minutes to harden. Cells were removed using trypsin-EDTA, washed with growth medium once, and resuspended at 1×10^5 cells per mL in serum-free growth medium. For coculture experiments, retinal endothelial cells and pericytes were used at a 1 : 1 ratio as we previously described [28]. Cells (2 mL) were gently added to the Matrigel coated plates, incubated at 37°C, monitored at ~18 h, and photographed using a Nikon microscope equipped with a digital camera. In some cases, 10 μg/mL of control IgG or sFlt1-FC chimera (R&D Systems) was added to the coculture experiments. For a quantitative assessment of the data the mean number of branch points in 8 fields (×40) was determined. A longer incubation of the cells did not result in further branching morphogenesis [27].

5.5. Cell Adhesion Assays. Cell adhesion to various extracellular matrix proteins was performed as previously described [9]. Varying concentrations of fibronectin, human type I and IV collagen, and vitronectin (BD Biosciences) prepared in TBS with $Ca^{2+}Mg^{2+}$ (2 mM each; TBS with $Ca^{2+}Mg^{2+}$) were coated on 96-well plates (50 μL per well; Nunc MaxiSorp plates, Fisher Scientific) overnight at 4°C. Plates were then rinsed four times with TBS with $Ca^{2+}Mg^{2+}$ and blocked with 200 μL of 1% BSA prepared in TBS with $Ca^{2+}Mg^{2+}$ for at least 1 h at room temperature. Cells were removed using 1.5 mL dissociation solution, washed once with TBS, and resuspended at 5×10^5 cells/mL in HEPES-buffered saline (25 mM HEPES, pH 7.60, 150 mM NaCl, and 4 mg/mL BSA). After blocking, plates were rinsed with TBS $Ca^{2+}Mg^{2+}$ once, 50 μL of cell suspension was added to each well containing 50 μL of TBS with $Ca^{2+}Mg^{2+}$, and the cells were allowed to adhere for 90 min at 37°C in a humidified incubator. Nonadherent cells were removed by gently washing the plate four times with 200 μL of TBS with $Ca^{2+}Mg^{2+}$ until no cells were left in wells coated with BSA. The number of adherent cells in each well was quantified by measuring the levels of intracellular acid phosphatase. Cells were lysed in 100 μL of lysis buffer (50 mM sodium acetate pH 5.0, 1% Triton X-100, and 4 mg/mL p-nitrophenyl phosphate) and incubated at 4°C overnight. The reaction was neutralized by adding 50 μL of 1 M NaOH, and the absorbance was determined at 405 nm using a microplate reader (Thermomax, Molecular Devices). All samples were prepared in triplicate, and the experiments were repeated at least three times with similar results.

5.6. Western Blot Analysis. Cells were plated at 4×10^5 in 60 mm dishes coated with 1% gelatin (endothelial cells) or uncoated (pericytes) and allowed to reach nearly 90% confluence in 2 days. The cells were then rinsed once with serum-free medium and incubated with serum-free DMEM for 48 hours. Then, conditioned medium (2 mL) was collected and clarified by centrifugation. The 45 μL of the sample was mixed with appropriate volume of 6X SDS buffer and analyzed by SDS-PAGE (4–20% Tris glycine gel; Invitrogen, Carlsbad, CA). In some cases, total protein lysates were prepared from these cells in a modified RIPA buffer (142.5 mM KCl, 5 mM $MgCl_2$, 10 mM HEPES, pH 7.4, 2 mM orthovanadate and 2 mM sodium difluoride, 1% Nonidet P-40, and a complete protease inhibitor cocktail (Roche, Mannheim, Germany)). The proteins were transferred to a nitrocellulose membrane, and the membrane was incubated with an antifibronectin (Sigma), a rabbit anti-chicken tenascin-C polyclonal antibody (Thermo Scientific; Pierce, Rockford, IL, USA), anti-TSP1 monoclonal antibody (Clone A6.1, Neo Marker, Fremont, CA, USA), antiosteopontin (R&D, Minneapolis, MN), anti-β-actin (Thermo Scientific; Pierce, USA), anti-HSP90 (Cell Signaling Technology), anti-Akt (Cell Signaling) antiphospho-Akt (Cell Signaling), antiphospho-eNOS (Cell Signaling), and anti-eNOS (SC-654; Santa Cruz Technology, Santa Cruz, CA). Membranes were washed, incubated with horseradish-peroxidase-conjugated secondary antibody (1 : 5000, Jackson ImmunoResearch Laboratories, West Grove, PA) for 1 hour at room temperature, and the protein was visualized according to the chemiluminescent procedure (Chemiluminescence reagent; GE Biosciences) [2, 14].

5.7. Flow Cytometry. Flow cytometry was performed as previously described [14]. The cells were washed once with PBS containing 0.04% EDTA and incubated with 2 mL of dissociation solution (Sigma) to remove the cells from the plate. The cells (10^6) were washed with TBS, blocked in TBS containing 1% goat serum on ice for 20 minutes, and incubated with the appropriate dilution of primary antibody, anti-PECAM-1 (BD Pharmingen), antivascular endothelial (VE)-cadherin (Alexis Biochemical, San Diego, CA), anti-β1 (Millipore), anti-α5 (MAB1949; Millipore), anti-α2 (Chemicon), anti-β3 (MAB1957; Millipore), anti-$\alpha v\beta$3 (MAB1976Z; Millipore), control IgG (Jackson), rabbit anti-NG2 (AB5320; Millipore, Temecula, CA), and rat anti-mouse PDGFRβ (eBiosciences, San Diego, CA). For antibodies that required cell permeabilization, cells were removed, washed with PBS, fixed with 2% paraformaldehyde on ice for 30 min, washed

with PBS, and resuspended in PBS containing 0.1% Triton-X-100 and 0.1% BSA containing appropriate dilution of primary antibody. The cells were washed with TBS containing 1% BSA and then incubated with the appropriate FITC-conjugated secondary antibody (Jackson ImmunoResearch, West Grove, PA) for 30 min on ice. After the incubation, the cells were washed twice with TBS containing 1% BSA and resuspended in 0.5 mL of TBS containing 1% BSA. Analysis was performed on a FACScan caliber flow cytometer (Becton-Dickinson, Franklin Lakes, NJ).

5.8. Transwell Assay. Transwell filters (Corning, Acton, MA) were coated with 2 μg/mL fibronectin in PBS and incubated overnight at 4°C. The bottom of the transwell was rinsed with PBS and blocked with 2% BSA in PBS for 1 h at room temperature. The transwell was rinsed with PBS, and 500 μL serum-free DMEM was added to the bottom of each well, and 1×10^5 cells in 100 μL of serum-free medium were added to the top of the transwell membrane. Following 4 hours in a 33°C tissue culture incubator, the cells and medium were aspirated and the upper side of the membrane was wiped with a cotton swab. The cells that migrated through the membrane were fixed with 4% paraformaldehyde, stained with hematoxylin-eosin, and mounted on a slide. Ten-high power fields (×200) of cells were counted for each condition and the average and standard error of the means were determined. All samples were prepared in duplicate, and the experiment was repeated at least three times with similar results.

5.9. VEGF Analysis. VEGF protein levels produced by vascular cells were determined using a Mouse VEGF Immunoassay kit (R&D Systems, Minneapolis, MN). Cells were plated at 6×10^5 cells on 60 mm tissue culture dishes and allowed to reach approximately 90% confluence. The cells were then rinsed once with serum-free DMEM and were grown in serum-free medium for 2 days. Conditioned medium was centrifuged at 400 ×g for 5 min to remove cell debris, and 50 μL was used in the VEGF Immunoassay. The assay was performed in triplicate as recommended by the manufacturer and was normalized to the number of cells. The amount of VEGF was determined using a standard curve generated with known amounts of VEGF in the same experiment. The assay was repeated twice using two different isolations of endothelial cells with similar results.

5.10. Nitric Oxide Analysis. Cells were plated in black wall clear bottom Microtest 96-well plates (BD #35 3948; 1×10^4 cells in 100 μL). The next morning the medium was changed to endothelial cell or pericyte medium containing 30 μM DAF-FM diacetate (Invitrogen; D-23842) and 5 μg/mL of CellTracker Red (Invitrogen; C34552). Following a 40 min incubation at 33°C, fresh medium was placed on the cells and the incubation continued for 20 min. The wells were washed with TBS and the cells in each well were resuspended in 100 μL of TBS. Absorbance was read at 495/515 nm using a fluorescence plate reader [2]. These experiments were performed in triplicate and repeated twice with similar results.

5.11. Statistical Analysis. Statistical differences between groups were evaluated with an unpaired t-test (two-tailed). Mean ± standard deviations are shown. P values <0.05 were considered significant.

Conflict of Interests

The authors declare that they have no conflict of interests.

Authors' Contribution

Margaret Morrison, Tammy L. Palenski, and Nasim Jamali performed experiments and analyzed data. Margaret Morrison, Tammy L. Palenski, Nasim Jamali, Nader Sheibani, and Christine Sorenson conceived and designed the experiments. Christine Sorenson and Nader Sheibani prepared the paper.

Acknowledgments

This work was supported by Grants from the University of Wisconsin Department of Pediatrics Research and Development Fund (Christine M. Sorenson). Christine M. Sorenson was funded, in part, by EY 023024 from the National Institutes of Health and the Retina Research Foundation. Nader Sheibani is supported by NIH Grants EY016995, EY018179, and RC4 EY 021357, P30 CA014520 UW Paul P. Carbone Cancer Center Support Grant, P30 EY016665, and an Unrestricted Departmental Award from Research to Prevent Blindness. Nader Sheibani is a recipient of a Research Award from American Diabetes Association (1-10-BS-160) and Retina Research Foundation. Tammy L. Palenski is a recipient of a Kirschstein-NRSA Fellowship Award (F31 EY021091) and NIH Grant T32 ES007015. Margaret E. Morrison is a recipient of a Senior Thesis Grant from the College of Letters and Science at the University of Wisconsin-Madison. The authors wish to thank Robert Gordon for his assistance with the graphics and SunYoung Park for the VEGF analysis.

References

[1] R. J. Youle and A. Strasser, "The BCL-2 protein family: opposing activities that mediate cell death," *Nature Reviews Molecular Cell Biology*, vol. 9, no. 1, pp. 47–59, 2008.

[2] C. Grutzmacher, S. Park, T. L. Elmergreen et al., "Opposing effects of bim and bcl-2 on lung endothelial cell migration," *The American Journal of Physiology—Lung Cellular and Molecular Physiology*, vol. 299, no. 5, pp. L607–L620, 2010.

[3] P. Bouillet, M. Robati, M. Bath, and A. Strasser, "Polycystic kidney disease prevented by transgenic RNA interference," *Cell Death and Differentiation*, vol. 12, no. 7, pp. 831–833, 2005.

[4] P. Bouillet, S. Cory, L. C. Zhang, A. Strasser, and J. M. Adams, "Degenerative disorders caused by Bcl-2 deficiency prevented by loss of its BH3-only antagonist bim," *Developmental Cell*, vol. 1, no. 5, pp. 645–653, 2001.

[5] P. Bouillet, D. Metcalf, D. C. Huang et al., "Proapoptotic Bcl-2 relative Bim required for certain apoptotic responses, leukocyte homeostasis, and to preclude autoimmunity," *Science*, vol. 286, no. 5445, pp. 1735–1738, 1999.

[6] R. Ley, K. E. Ewings, K. Hadfield, and S. J. Cook, "Regulatory phosphorylation of Bim: sorting out the ERK from the JNK," *Cell Death and Differentiation*, vol. 12, no. 8, pp. 1008–1014, 2005.

[7] M. Fruttiger, "Development of the retinal vasculature," *Angiogenesis*, vol. 10, no. 2, pp. 77–88, 2007.

[8] S. Wang, Z. Wu, C. M. Sorenson, J. Lawler, and N. Sheibani, "Thrombospondin-1-deficient mice exhibit increased vascular density during retinal vascular development and are less sensitive to hyperoxia-mediated vessel obliteration," *Developmental Dynamics*, vol. 228, no. 4, pp. 630–642, 2003.

[9] M. J. Pollman, L. Naumovski, and G. H. Gibbons, "Endothelial cell apoptosis in capillary network remodeling," *Journal of Cellular Physiology*, vol. 178, no. 3, pp. 359–370, 1999.

[10] K. Walsh, R. C. Smith, and H. S. Kim, "Vascular cell apoptosis in remodeling, restenosis, and plaque rupture," *Circulation Research*, vol. 87, no. 3, pp. 184–188, 2000.

[11] S. Wang, S. Park, P. Fei, and C. M. Sorenson, "Bim is responsible for the inherent sensitivity of the developing retinal vasculature to hyperoxia," *Developmental Biology*, vol. 349, no. 2, pp. 296–309, 2011.

[12] P. Carmeliet, "Angiogenesis in life, disease and medicine," *Nature*, vol. 438, no. 7070, pp. 932–936, 2005.

[13] J. Andrae, R. Gallini, and C. Betsholtz, "Role of platelet-derived growth factors in physiology and medicine," *Genes and Development*, vol. 22, no. 10, pp. 1276–1312, 2008.

[14] S. Kondo, E. A. Scheef, N. Sheibani, and C. M. Sorenson, "PECAM-1 isoform-specific regulation of kidney endothelial cell migration and capillary morphogenesis," *The American Journal of Physiology—Cell Physiology*, vol. 292, no. 6, pp. C2070–C2083, 2007.

[15] N. Sheibani, E. A. Scheef, T. A. Dimaio, Y. Wang, S. Kondo, and C. M. Sorenson, "Bcl-2 expression modulates cell adhesion and migration promoting branching of ureteric bud cells," *Journal of Cellular Physiology*, vol. 210, no. 3, pp. 616–625, 2007.

[16] S. Kondo, Y. Tang, E. A. Scheef, N. Sheibani, and C. M. Sorenson, "Attenuation of retinal endothelial cell migration and capillary morphogenesis in the absence of bcl-2," *The American Journal of Physiology—Cell Physiology*, vol. 294, no. 6, pp. C1521–C1530, 2008.

[17] J. Ziehr, N. Sheibani, and C. M. Sorenson, "Alterations in cell-adhesive and migratory properties of proximal tubule and collecting duct cells from bcl-2 -/- mice," *The American Journal of Physiology—Renal Physiology*, vol. 287, no. 6, pp. F1154–F1163, 2004.

[18] A. Józkowicz, J. Dulak, A. Nigisch et al., "Involvement of nitric oxide in angiogenic activities of vascular endothelial growth factor isoforms," *Growth Factors*, vol. 22, no. 1, pp. 19–28, 2004.

[19] D. Fukumura, T. Gohongi, A. Kadambi et al., "Predominant role of endothelial nitric oxide synthase in vascular endothelial growth factor-induced angiogenesis and vascular permeability," *Proceedings of the National Academy of Sciences of the United States of America*, vol. 98, no. 5, pp. 2604–2609, 2001.

[20] M. G. Blanes, M. Oubaha, Y. Rautureau, and J. Gratton, "Phosphorylation of tyrosine 801 of vascular endothelial growth factor receptor-2 is necessary for Akt-dependent endothelial nitric-oxide synthase activation and nitric oxide release from endothelial cells," *Journal of Biological Chemistry*, vol. 282, no. 14, pp. 10660–10669, 2007.

[21] E. A. Scheef, C. M. Sorenson, and N. Sheibani, "Attenuation of proliferation and migration of retinal pericytes in the absence of thrombospondin-1," *The American Journal of Physiology—Cell Physiology*, vol. 296, no. 4, pp. C724–C734, 2009.

[22] M. Saint-Geniez and P. A. D'Amore, "Development and pathology of the hyaloid, choroidal and retinal vasculature," *International Journal of Developmental Biology*, vol. 48, no. 8-9, pp. 1045–1058, 2004.

[23] M. R. Hayden, Y. Yang, J. Habibi, S. V. Bagree, and J. R. Sowers, "Pericytopathy: oxidative stress and impaired cellular longevity in the pancreas and skeletal muscle in metabolic syndrome and type 2 diabetes," *Oxidative Medicine and Cellular Longevity*, vol. 3, no. 5, pp. 290–303, 2010.

[24] S. Wang, C. M. Sorenson, and N. Sheibani, "Attenuation of retinal vascular development and neovascularization during oxygen-induced ischemic retinopathy in Bcl-2-/- mice," *Developmental Biology*, vol. 279, no. 1, pp. 205–219, 2005.

[25] J. I. Greenberg, D. J. Shields, S. G. Barillas et al., "A role for VEGF as a negative regulator of pericyte function and vessel maturation," *Nature*, vol. 456, no. 7223, pp. 809–813, 2008.

[26] C. Grutzmacher, S. Park, Y. Zhao, M. E. Morrison, N. Sheibani, and C. M. Sorenson, "Aberrant production of extracellular matrix proteins and dysfunction in kidney endothelial cells with a short duration of diabetes," *The American Journal of Physiology—Renal Physiology*, vol. 304, no. 1, pp. F19–F30, 2013.

[27] X. Su, C. M. Sorenson, and N. Sheibani, "Isolation and characterization of murine retinal endothelial cells," *Molecular Vision*, vol. 9, pp. 171–178, 2003.

[28] T. L. Palenski, C. M. Sorenson, C. R. Jefcoate, and N. Sheibani, "Lack of Cyp1b1 promotes the proliferative and migratory phenotype of perivascular supporting cells," *Laboratory Investigation*, vol. 93, no. 6, pp. 646–662, 2013.